

**Investigating the Mechanism of
Self-Incompatibility in *Papaver rhoeas* and
Functional Transfer of *Papaver*
S-Determinants to *Arabidopsis thaliana***

by

SABINA VATOVEC

A thesis submitted to
The University of Birmingham
for the degree of
DOCTOR OF PHILOSOPHY

School of Biosciences
The University of Birmingham
January 2012

UNIVERSITY OF
BIRMINGHAM

University of Birmingham Research Archive

e-theses repository

This unpublished thesis/dissertation is copyright of the author and/or third parties. The intellectual property rights of the author or third parties in respect of this work are as defined by The Copyright Designs and Patents Act 1988 or as modified by any successor legislation.

Any use made of information contained in this thesis/dissertation must be in accordance with that legislation and must be properly acknowledged. Further distribution or reproduction in any format is prohibited without the permission of the copyright holder.

ABSTRACT

Flowering plants have evolved complex genetic mechanisms of self-incompatibility (SI) to overcome the problem of self-fertilization. SI is a cell-cell recognition system where the interaction of genetically linked pollen and pistil *S*-determinants prevents self-fertilization.

In *Papaver rhoeas*, the pistil *S*-determinant is PrsS, a secreted protein of around 15 kDa. The pollen determinant, PrpS, encodes a novel transmembrane protein of around 20 kDa. Upon the interaction of incompatible PrsS and PrpS variants, the SI response is triggered, activating a signalling network. Rapid increases in cytosolic free calcium ($[Ca^{2+}]_i$) are followed by changes to the actin cytoskeleton and activation of a DEVDases, resulting in programmed cell death (PCD).

Within this thesis, three inter-related studies are described. Initially, we investigated the role of the ubiquitin-proteasomal system during SI in *Papaver*, the second study focused on the PrpS protein. Thirdly, we also created transgenic *Arabidopsis thaliana* lines expressing PrpS and PrsS, in order to investigate if the *Papaver* SI system might be functionally transferable to other plant species. We have demonstrated that PrpS binds the PrsS in an *S*-specific manner, while the functional analysis “*in vitro*” revealed that PrpS expressed in *A.thaliana* is functional and that just PrpS and PrsS are sufficient for a fully functional SI response in *A.thaliana* pollen.

I dedicate this thesis to my dearest:

my parents Tatjana and Lojze Vatovec and to my partner Miha Zakotnik

ACKNOWLEDGEMENTS

I would like to thank my supervisor Noni Franklin-Tong for the opportunity to do the PhD project and for all the guidance, support and counsel throughout my PhD.

I would also like to express my gratitude to the other members, staff and PIs of the labs on the second floor, past and present, who encouraged me, helped me on many different levels, gave me the confidence and great scientific example, and provided stimulating, challenging and yet relaxed and enjoyable working environment: Barend de Graaf, Candida Nibau, Maurice Bosch, Natalie Poulter, Eugenio Sanchez-Moran, Ruth Perry, Chris Franklin, Richard Tudor, Katie Wilkins, Javier-Andres Juarez-Diaz, Karen Staples, Steve Price, Huawen Zou, Juyou Wu, Andrew Beacham, Kim Osman, Sarah Smith, Adriana Machlicova, Younosse Saidi, Laura Moody. I would also like to thank my great students Kreepa, Fuz, Tom, Sebastien and Steph, as I learned a lot through teaching. I am also thankful to other horticultural staff, past from the Elms laboratories, especially dear Bill, and new from the Winterbourne botanical gardens. I would also like to acknowledge Ari Sadanandom for providing the PUB and POB antibodies. My project was funded by the Biotechnological and Biological Sciences Research Council (BBSRC), and living expenses were covered by an Ad Futura scholarship from Slovenia.

My gratitude is extended to all the good friends that I had in Birmingham, who also provided invaluable moral and social support as well as practical scientific, statistical or thesis-editing advice: Stephen Dove, Alex Bevan, Adrian Hunt, Walter del Pozzo, Stephanie Dumon, Emille Dasse, Lenka Cerna, Maria Barilla, Giacomo Volpe, Natalia Lopez, Sal Adrwish, Hiroto Kitaguchi, Antonio Perreca, Ludovico Carbone, Iryna Kepyck, Elisavet Vasilopoulou, Kai Tollner, Peter Chong, Mayumi Fuchi and great divers from BSAC25.

My gratitude is also extended to my dearest friend Marjetka Alfirević, for being a great friend, for giving me statistical advice, moral support through countless internet chats and for making me the happiest “adopted auntie” with her beautiful daughter Mila.

Finally and most importantly, I would like to thank my love Miha and my extended family in Slovenia, who all believed in me from the start. You have been the best support throughout my thesis and a pillar on which I could lean on when I needed you the most. Thank you! Hvala!

TABLE OF CONTENTS

1 INTRODUCTION	1
1.1 PLANT SEXUAL REPRODUCTION	2
1.1.1 Pollen-pistil interactions: Pollination and fertilization.....	3
1.1.2 Pollen tube	7
1.2 PROGRAMMED CELL DEATH (PCD)	10
1.2.1 Plant caspase-like proteases	13
1.2.2 Hypersensitive response (HR-) induced PCD.....	16
1.2.3 Self-incompatibility induced PCD in incompatible <i>Papaver</i> , <i>Pyrus</i> and <i>Olea</i> pollen....	19
1.3 RECEPTORS AND CELL SIGNALLING	20
1.3.1 Plant receptors	21
1.3.1.1 Plant receptor-like kinases.....	23
1.3.1.1.1 LRR-RLKs.....	25
1.3.1.1.2 SRK-RLKs.....	25
1.3.1.1.3 Other RLKs.....	26
1.3.1.2 G-protein coupled receptor.....	27
1.3.1.3 PrpS receptor in <i>Papaver rhoeas</i>	28
1.4 SELF-INCOMPATIBILITY	28
1.4.1 Sporophytic SI in the Brassicaceae	31
1.4.2 S-RNase based gametophytic SI	34
1.4.3 Gametophytic SI in <i>Papaveraceae</i>	37
1.4.3.1 Pistil S-determinant.....	38
1.4.3.2 Pollen S-determinant.....	39
1.4.3.3 Mechanism of SI in <i>Papaver</i>	40
1.4.3.3.1 Role of Ca ²⁺ in the SI response.....	41
1.4.3.3.2 Role of soluble inorganic pyrophosphatases in poppy SI.....	42
1.4.3.3.3 Role of MAPK in poppy SI.....	43
1.4.3.3.4 Role of actin in poppy SI.....	44
1.4.3.3.5 Programmed cell death triggered by poppy SI.....	46
1.4.3.3.6 Role of ROS in <i>Papaver</i> SI.....	47
1.5 Arabidopsis thaliana AS A MODEL FOR SELF INCOMPATIBILITY	48
1.6 THE UBIQUITIN-26S PROTEASOME SYSTEM	49
1.6.1 The 26S Proteasome	53
1.6.2 Ubiquitination and self-incompatibility	55
1.7 SUMMARY AND OBJECTIVE	57
2 Materials and Methods	59
2.1 Plant material: Papaver rhoeas	60
2.1.1 <i>Papaver</i> plant cultivation	60
2.1.2 Determination of <i>Papaver S</i> -genotype	60
2.1.3 Collection of <i>Papaver</i> pollen	60
2.1.4 <i>Papaver</i> pollen tube growth <i>in vitro</i>	62
2.1.5 Production of <i>Papaver</i> seeds.....	62
2.2 Plant material: Arabidopsis thaliana	63
2.2.1 <i>A.thaliana</i> cultivation	63
2.2.2 <i>A.thaliana</i> plant conditions.....	64
2.2.3 Collection and germination of <i>A.thaliana</i> pollen	65
2.2.4 Collection of <i>A.thaliana</i> seeds.....	66
2.3 Experiments	66
2.3.1 Production of recombinant PrsS proteins.....	66

2.3.2	Treatments of pollen tubes	68
2.3.3	Pollen protein extraction	69
2.3.4	Bradford Assay	70
2.3.5	SDS-Polyacrylamide gel electrophoresis (SDS-PAGE)	71
2.3.5.1	Preparation of SDS-PAGE.....	71
2.3.5.2	Protein staining on the polyacrylamide gel.....	71
2.3.6	Western blot	71
2.3.6.1	Protein transfer.....	71
2.3.6.2	Protein immunodetection.....	72
2.3.6.2.1	Enhanced chemiluminescence detection.....	73
2.3.6.2.2	Light intensity evaluation of western blots (ECL detection).....	74
2.3.6.2.3	Alkaline phosphatase detection.....	74
2.3.6.3	Modified western blot for detection of membrane proteins.....	74
2.3.7	Slot-blot binding assay	75
2.3.8	Purification of antibodies using Immobilised <i>E.coli</i> lysate kit	77
2.3.9	Pollen tube length measurement.....	78
2.3.10	Programmed cell death – caspase-like activity assay.....	78
2.3.11	Cell Death.....	79
2.3.11.1	Cell death - viability test.....	79
2.3.11.2	Pretreatment with tetrapeptide inhibitor Ac-DEVD-CHO.....	80
2.3.12	Actin labelling	80
2.3.13	Leaf mesophyll protoplast production.....	82
2.3.14	PCR screening for the presence of inserts in transgenic plants.....	83
2.3.15	DNA analysis by agarose gel electrophoresis	85
2.3.16	Semi-quantitative RT-PCR.....	85
2.3.16.1	RNA extraction.....	85
2.3.16.2	RNA analysis by agarose gel electrophoresis.....	86
2.3.16.3	DNase treatment of RNA.....	87
2.3.16.4	cDNA synthesis by RT-PCR.....	87

3	Investigation of the possible involvement of the ubiquitin-proteasomal pathway during SI in <i>Papaver</i> pollen.....	89
3.1	INTRODUCTION	90
3.2	RESULTS	95
3.2.1	The proteasome inhibitor MG132 affects pollen germination and tube growth	95
3.2.2	Effect of inhibition of proteasomal activity on pollen tube growth	97
3.2.3	Effect of inhibition of proteasomal activity on pollen tube viability	99
3.2.4	Proteasomal degradation and PCD in incompatible poppy pollen.....	100
3.2.5	Effect of proteasomal inhibition by MG132 on the ubiquitination levels in incompatible pollen tubes	102
3.2.6	Proteasomal degradation acts upstream or in parallel with caspase-3-like activity	104
3.2.7	Caspase-3 inhibitor decreases ubiquitination	105
3.2.8	Involvement of an E3 ligases in <i>Papaver</i> SI	107
3.3	DISCUSSION.....	109
4	Investigation of the interaction between PrpS and PrsS.....	124
4.1	INTRODUCTION	125
4.2	RESULTS: The S-specific interaction of PrpS and PrsS.....	127
4.2.1	Analysis of predicted structure of PrpS.....	127
4.2.2	Binding assays.....	133
4.3	DISCUSSION.....	139

5	Functional analysis <i>in vitro</i> of the <i>Arabidopsis thaliana</i> expressing <i>Papaver rhoeas</i> PrpS₁ and PrpS₃	141
5.1	INTRODUCTION	142
5.2	RESULTS	147
5.2.1	Characterization of <i>A.thaliana</i> expressing <i>Papaver</i> SI system	147
5.2.1.1	PrpS expressing <i>A.thaliana</i> lines	148
5.2.2	<i>In vitro</i> functional analysis of <i>Papaver</i> SI determinants in transgenic <i>Arabidopsis thaliana in vitro</i>	158
5.2.2.1	<i>S</i> -specific inhibition of transgenic <i>A.thaliana</i> pollen tube growth	159
5.2.2.2	PrpS-PrsS interaction stimulates formation of punctate actin foci in transgenic <i>A.thaliana</i> pollen	164
5.2.2.3	Evidence for PCD in the <i>A.thaliana</i> transgenic pollen upon SI challenge	168
5.2.2.3.1	Pollen viability is decreased in an <i>S</i> -specific manner upon interaction between PrpS-GFP expressing <i>A.thaliana</i> pollen and recombinant stigmatic PrsS	168
5.2.2.3.2	Decrease of pollen viability involving DEVDase activity	172
5.2.2.4	PCD in <i>A.thaliana</i> transgenic pollen expressing PrpS-GFP	176
5.2.3	<i>A.thaliana</i> mesophyll protoplasts expressing PrpS ₁	181
5.3	DISCUSSION	184
5.3.1	Alterations to the actin cytoskeleton	184
5.3.2	Decrease of viability involving DEVDase activity	187
5.3.3	PCD in <i>A.thaliana</i> transgenic pollen	189
6	Functional analysis <i>in vivo</i> of transgenic <i>A.thaliana</i> expressing <i>Papaver S</i>-determinants, PrsS and PrpS	192
6.1	INTRODUCTION	193
6.2	RESULTS	196
6.2.1	Characterization of <i>A.thaliana</i> expressing <i>Papaver</i> PrsS determinants	197
6.2.2	<i>S</i> ₁ -locus expressing <i>A.thaliana</i> line	201
6.2.3	<i>Papaver</i> pollen growth in the presence of stigmatic extract of <i>A.thaliana</i> expressing PrsS ₁ and PrsS ₃	204
6.2.4	<i>Papaver</i> SI <i>in vivo</i> in transgenic <i>A.thaliana</i>	209
6.2.4.1	Pollination assays in transgenic <i>A.thaliana</i> expressing <i>Papaver</i> PrsS and PrpS	209
6.2.4.2	Seed set analysis in transgenic <i>A.thaliana</i> expressing <i>Papaver</i> PrsS and PrpS	214
6.2.4.3	Seed set and silique length of F ₁ progeny from incompatible crosses	217
6.2.5	Investigating the function of the whole <i>Papaver S</i> ₁ locus in transgenic <i>A.thaliana</i>	221
6.3	DISCUSSION	226
7	GENERAL DISCUSSION	235
7.1	<i>Papaver S</i> -determinant interactions	237
7.2	Functional analysis of <i>Papaver rhoeas</i> self-incompatibility in transgenic <i>Arabidopsis thaliana</i>	240
8	LIST OF REFERENCES	244

APPENDIX I: Alignment of PrpS and Flower protein

APPENDIX II: Family trees of *A.thaliana* lines expressing *Papaver S*-determinants

APPENDIX III: Published papers

List of figures and tables

Chapter 1: Introduction

Figure 1.1. Schematic diagram of sexual reproduction in model plant <i>A.thaliana</i>	3
Figure 1.2. Reverse fountain cytoplasmic streaming	8
Figure 1.3. Schematic representation of death receptor-mediated apoptosis signalling	11
Figure 1.4. Subfamilies of plant RLKs	24
Figure 1.5. An illustration of the genetic basis of gametophytic and sporophytic SI	29
Figure 1.6. Schematic diagram of the <i>S</i> -locus	31
Figure 1.7. Schematic model of the SI response in <i>Brassica</i>	32
Figure 1.8. Schematic model of the <i>S</i> -RNase based SI response	36
Figure 1.9. Schematic model of the SI response in <i>Papaver</i>	41
Figure 1.10. The mechanism of ubiquitin-dependent proteasomal degradation	50
Figure 1.11. Structures of different types of E3 ligases	52
Figure 1.12. Organization and structure of 26S proteasome	53
Figure1.13. Involvement of UbP during SI	56
Table 1.1. Caspase-like activities that exists in plants	14
Table 1.2. Receptor-ligand pairs identified in plants	22

Chapter 2: Materials and Methods

Figure 2.1. Examples of aniline blue stained stigma squashes	61
--	----

Chapter 3: Investigation of the possible involvement of the ubiquitin-proteasomal pathway during SI in *Papaver* pollen

Figure 3.1. Mean length of <i>Papaver</i> pollen tubes treated with different concentrations of MG132 at two different time points	96
Figure 3.2. Mean length of pollen tubes pretreated with 40 μ M MG132 & induced SI.....	98
Figure 3.3. FDA viability of pollen tubes pretreated with 40 μ M MG132 & induced SI....	100
Figure 3.4. Caspase activity of pollen tubes pretreated with 40 μ M MG132 & induced SI.	101
Figure 3.5. Ubiquitination levels of poppy pollen pre-treated with 40 μ M MG132 and SI induced	103
Figure 3.6. Caspase activity of pollen tubes with induced SI and added 40 μ M MG132 in the pollen tube extract	104
Figure 3.7. Protein ubiquitination levels in poppy pollen tubes pre-treated with inhibitor of caspase activity and SI challenged at three different time points	106
Figure 3.8. Protein expression of poppy homologues of AtPUB17 and AtPOB1 E3 ligases during SI	108
Figure 3.9. Model of proteasomal degradation in SI-induced <i>Papaver</i> pollen tube.....	116
Figure 3.10. Alternative model of proteasomal degradation and caspase-3-like activation assumes that proteasome contains caspase-3-like activity.....	118
Figure 3.11. Model that assumes the existence of negative regulator of DEVDase activity, possibly POB1 homologue.....	121

Chapter 4: Investigation of the interaction between PrpS and PrsS

Figure 4.1. Structural prediction of PrpS ₁ as predicted by prediction programme TMHMM.....	128
--	-----

Figure 4.2. Amino acid sequence of four overlapping peptides	129
Figure 4.3. <i>In vitro</i> SI bioassay	129
Figure 4.4. Clustal W alignment of structural predictions of PrpS ₁ , PrpS ₃ and PrpS ₈ as predicted by TMHMM	130
Figure 4.5. Structural predictions of PrpS ₁ using different prediction programmes.....	131
Figure 4.6. Cartoon of possible structural topologies of PrpS ₁ as revealed by different prediction programmes	133
Figure 4.7. Binding assay with differential loading of peptides A1-A4	134
Figure 4.8. Binding assay with differential loading of peptide A3 detected with anti-PrsS ₁ and anti PrsS ₃ antibodies	135
Figure 4.9. Binding assay in S-specific manner with differential loading of A3	136
Figure 4.10. Clustal W alignment of amino acid sequence of predicted extracellular loop.	137
Figure 4.11. Alignment of peptides A1 for PrpS ₁ and PrpS ₈ and their scrambled controls.	137
Figure 4.12. Binding assay between A1 peptides of PrpS ₁ and PrpS ₈ and recombinant PrsS ₁ and PrsS ₈	138

Chapter 5: Functional analysis *in vitro* of the *Arabidopsis thaliana* expressing *Papaver rhoeas* PrpS₁ and PrpS₃

Figure 5.1. Schematic diagram presenting the outline of the <i>in vitro</i> functional analysis experiments	146
Figure 5.2. RT-PCR PrpS ₁ -GFP and PrpS ₃ -GFP expressing <i>A.thaliana</i> lines	154
Figure 5.3. Top 5 highest expressing PrpS-GFP lines	155
Figure 5.4. Western blot of PrpS ₁ expressing <i>A.thaliana</i> pollen, using two different extraction buffers.....	157

Figure 5.5. Schematic diagram of the SI experiment <i>in vitro</i>	159
Figure 5.6. <i>A.thaliana</i> pollen tube inhibition graph presenting pollen tube length	161
Figure 5.7. Rhodamine Phalloidin stained actin in <i>A.thaliana</i> pollen	165
Figure 5.8. Quantification of actin foci and filaments in PrpS ₁ -GFP expressing pollen	167
Figure 5.9. Viability of <i>A.thaliana</i> transgenic pollen expressing PrpS ₁ -GFP or PrpS ₃ -GFP	169
Figure 5.10. Viability of Ac-DEVD-CHO pretreated <i>A.thaliana</i> transgenic pollen expressing PrpS ₁ -GFP or PrpS ₃ -GFP	174
Figure 5.11. DEVDase activity of protein extract from PrpS ₁ -GFP or PrpS ₃ -GFP expressing <i>A.thaliana</i> pollen	177
Figure 5.12. DEVDase activity in <i>A.thaliana</i> pollen with induced SI or pre-treated with inhibitor Ac-DEVD-CHO prior to induction of SI	179
Figure 5.13. Effect of DEVDase inhibitor on the SI induced caspase-like activity	180
Figure 5.14. GFP expression in Col-0 protoplasts transformed with 35S:PrpS ₁ -GFP	182
Figure 5.15. Viability of <i>A.thaliana</i> wt protoplasts transfected with 35S:PrpS ₁ -GFP	183
Table 5.1. The cartoon illustrations of the constructs of the poppy PrpS determinants	144
Table 5.2. Segregation of Kan resistance and GFP expression in PrpS ₁ -GFP expressing transgenic <i>A.thaliana</i>	148
Table 5.3. Segregation of Kan resistance and GFP expression in PrpS ₃ -GFP expressing transgenic <i>A.thaliana</i>	152

**Chapter 6: Functional analysis *in vivo* of transgenic *A.thaliana* expressing *Papaver S-*
*determinants, PrsS and PrpS***

Figure 6.1. Scheme of combination of crosses in transgenic <i>A.thaliana</i> expressing different <i>Papaver S-</i> determinants	195
Figure 6.2. RT-PCR of PrsS ₁ and PrsS ₃ expressing <i>A.thaliana</i> lines	197
Figure 6.3. Top 5 highest expressing PrsS lines	198
Figure 6.4. RT-PCR of S ₁ -locus expressing <i>A.thaliana</i> lines	204
Figure 6.5. Images of <i>Papaver</i> pollen tubes incubated stigmatic protein extracts from transgenic <i>A.thaliana</i> flowers	206
Figure 6.6. Quantification of <i>Papaver</i> pollen tube length and tip diameter upon incubation with <i>A.thaliana</i> stigmatic protein extracts	207
Figure 6.7. Aniline blue staining of crosses with PrsS ₁ expressing <i>A.thaliana</i> stigmas	210
Figure 6.8. Aniline blue staining of crosses with PrsS ₃ expressing <i>A.thaliana</i> stigmas	212
Figure 6.9. Seed set of all the incompatible crosses and controls	216
Figure 6.10. Silique length and seed set of F ₁ seedlings	220
Figure 6.11. Analysis <i>in vivo</i> in S ₁ -locus expressing transgenic <i>A.thaliana</i> line BG6.....	222
Figure 6.12. Seed set analysis on the T ₃ generation of S ₁ -locus expressing <i>A.thaliana</i> BG6 plants	223
Figure 6.13. Aniline blue staining analysis of self pollination of BG6 flowers	225
Table 6.1. The cartoon illustrations of the constructs of the poppy PrsS determinants	193
Table 6.2. Segregation of Kan resistance and GFP expression in PrsS ₁ expressing transgenic <i>A.thaliana</i>	199

Table 6.3. Segregation of Kan resistance and GFP expression in PrsS ₃ expressing transgenic <i>A.thaliana</i>	199
Table 6.4. Segregation of Kan resistance and GFP expression in <i>S₁</i> -locus expressing transgenic <i>A.thaliana</i>	202

Chapter 7: General Discussion

Figure 7.1. Schematic model of the SI response in <i>Papaver</i>	195
--	-----

LIST OF ABBREVIATIONS

- ABA – abscisic acid
- ABP – actin binding protein
- ACE-H – apical cap extension-hydrodynamics
- ACR – Arabidopsis crinkly
- ACRE – Avr9/Cf9 rapidly elicited
- AGO7 – argonaute7
- AP – alkaline phosphatase
- ARC1 – Armadillo-repeat containing 1
- ARF – auxin response factor
- ARM – armadillo
- as-ODN – antisense oligonucleotide
- AtMC – *Arabidopsis thaliana* metacaspase
- Avr – avirulence
- BAK – BRI-associated receptor kinase
- BCIP – 5-bromo-4-chloro-3-indolyl phosphatase
- BR – brassinosteroid
- BRI – brassinosteroid insensitive
- BSA – bovine serum albumine
- BTB – bric-a-brac-tramtrac-broad
- CLE – clavata/ endosperm surrounding region
- CLV – clavata
- CP – 20S core protease
- CRP – cysteine-rich proteins
- DISC – death inducing signalling complex
- DMSO – dimethyl sulfoxide
- ECL – enhanced chemiluminiscence
- ECM – extracellular matrix
- EDTA – ethylenediamine tetraacetic acid
- EGF – epidermal growth factor
- ETI – effector-triggered immunity

ETS – effector-triggered susceptibility
FDA – fluorescein diacetate
Flg – flagellin
FLS – flagellin sensing
GABA – gamma-aminobutyric acid
GFP – green fluorescent protein
GM – germination medium
GPCR – G-protein coupled receptor
GSI – gametophytic self-incompatibility
HECT – homology to E6-associated protein C-terminus
HR – hypersensitive response
IDA – inflorescence deficient in abscission
IEF – isoelectric focusing
Kan – kanamycin
LRR – leucine rich repeats
MAMP – microbe associated molecular pattern
MAPK – mitogen activated protein kinase
MG132 – N-(benzyloxycarbonyl)-leucinyl-leucinyl-leucinal
MLPK – *M*-locus protein kinase
MOMP – mitochondrial outer membrane permeabilization
MS – Murashige and Skoog medium
MW – molecular weight
NBT – nitro blue tetrazolium
NO – nitric oxide
NS – not significant
PAGE – polyacrylamide gel electrophoresis
PAMP – pathogen-associated molecular pattern
PARP – poly-ADP-ribose polymerase
PBA – proteasome beta-subunit A
PBS – phosphate buffer saline
PCD – programmed cell death
PCR – polymerase chain reaction

PFA – paraformaldehyde
PiSBP – *Petunia inflata* S-RNase binding protein
PrpS – *Papaver rhoeas* pollen S
PRR – pathogen-recognition receptors
PrsS – *Papaver rhoeas* stigma S
PSK – phytosulphokine
PSKR – phytosulphokine receptor
PTI – PAMP triggered immunity
PUB – plant U-box
PVDF – polyvinyl difluoride
RAR – require for Mla12 resistance1
RBX – RING-box
RLK – receptor-like kinase
ROP – Rho-related GTPase from plants
RP – 19S regulatory particle
RT – room temperature
RT-PCR – reverse transcription PCR
s-ODN – sense oligonucleotide
SA – salicylic acid
SAM – shoot apical meristem
SAR – systemic acquired resistance
SBP – S-protein binding protein
SC – self-compatibility
SCR – small cysteine-rich
SDS – sodium dodecyl sulphonate
SDW – sterile distilled water
SGT1 – suppressor of the G2 allele of *skp1*
SI – self-incompatibility
SKP – S-phase kinase-associated protein
SLF/SFB – S-locus F-box/ S-haplotype-specific F-box
SLG – S-locus glycoprotein
SP11 – S-protein 11

sPPase – soluble inorganic pyrophosphatases
SSI – sporophytic self-incompatibility
SSK – SLF-interacting SKP1-like
SRK – *S*-locus receptor kinase
SUB – strubbelig
RING – really interesting new gene
ROS – reactive oxygene species
ta-siRNA – trans-acting short interfering RNA
TBS – Tris buffer saline
TBST – TBS-Tween
TM – transmembrane
TMM – too many mouths
TNF – tumor necrosis factor
TNFR – tumor necrosis factor receptor
TPD – tapetum determinant
TRAIL – TNF related apoptosis inducing ligand
TTS – transmitting tract specific
UbP – ubiquitin-26S proteasome
UT – untreated
VPE – vacuolar processing enzyme
Y2H – yeast 2 hybrid

CHAPTER 1

INTRODUCTION

1.1 PLANT SEXUAL REPRODUCTION

Plant reproduction is widely studied due to its immense importance for biotechnology and crop science, medicine, conservation biology and evolution. An important feature in the subject of plant reproduction is also the pollen tube, which is used as a model system for cell biology studies. The accessibility, easy *in vitro* germination and rapid growth makes it an excellent model to study mechanical, genetic and molecular principles of polarised tip growth, cytoskeleton organization, ion fluxes, periodic behaviour, endo- and exocytosis and cell-cell signalling (Cheung and Wu, 2008, Feijó et al., 2001, Hepler et al., 2001, Moscatelli and Idilli, 2009, Geitmann, 2010).

During plant sexual reproduction the parental male and female plant organs combine their genetic material. The resulting offspring forms from a diploid embryo created when two haploid gametes, generated by meiosis, fuse together to form a diploid zygote. Plant reproduction starts with pollination. When a compatible pollen grain, containing the male gamete, lands on the stigma, it adheres and hydrates. Following hydration, pollen germinates and produces a pollen tube, which, with its strictly apical cell growth, elongates through the tissue of pistil (see Figure 1.1) until it reaches the ovule. The pollen tube then releases its two sperm cells to the embryo sac where a double fertilization occurs (Boavida et al., 2005, Cheung et al., 2010, Lord and Russell, 2002).

After fertilization, embryogenesis takes place that ends with the production of seed. The seed then germinates and new plant starts growing and developing organs. When the plant is mature, flower development starts and within the flower, male and female gametophytes form in spatially distinct areas of this organ via the processes of microsporogenesis and

megasporogenesis respectively. When these spores are fully formed, a new cycle of pollination can occur.

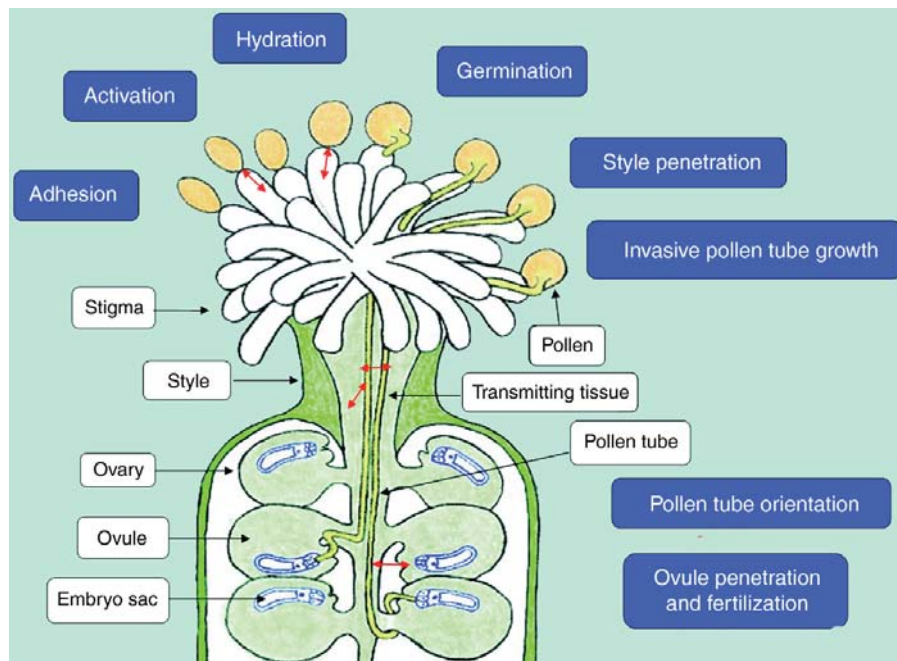


Figure 1.1: Schematic diagram of sexual reproduction in model plant *Arabidopsis thaliana*. Pollen adheres to stigma, germinates and produces a pollen tube, which grows through the stigmatic papillae towards the ovaries where double fertilization occurs. Main pistil organs are indicated in white boxes and biological processes are indicated in blue boxes, while red arrows indicate pollen-pistil interactions. Image adapted from Feijó, (2010).

The majority of flowering plants have, however, evolved mechanisms with which to cope when pollinated with genetically too similar pollen, i.e. incompatible pollen. This work focuses primarily on the pollination and prevention of self-fertilization aspect of plant reproduction, more specifically, on the phenomena of self-incompatibility, which will be described in greater detail in later section.

1.1.1 Pollen-pistil interactions: Pollination and fertilization

Pollen-pistil interaction involves an exchange of chemical signals between the male and female cells in a clear physical connection. Six major pollen-pistil interactions events have

been identified during pollination (Heslop-Harrison, 1975): pollen capture and adhesion, pollen hydration, germination of the pollen to produce a pollen tube, penetration of the stigma by the pollen tube, growth of the pollen tube through the stigma/style and entry of the pollen tube into ovule, resulting in discharge of sperm cells (Hiscock and Allen, 2008) (Figure 1.1).

The first step of pollination is the adhesion of pollen to the stigma. Pollen is released from the anthers in a dehydrated state and dispersed. After the initial capture of the pollen on the stigma, the pollen and stigma proteins combine and start the complex pollen-stigma interactions that are under tight genetic and cellular control (Swanson et al., 2004). Adhesion depends on the stigmatic surface (wet or dry stigmas, depending on the presence or absence of stigmatic secretion) and on the pollen adhesion components (Zinkl et al., 1999).

It was demonstrated that in the formation of the pollen-stigma interface, pollen coat and stigma lipids small cysteine-rich proteins (SCRs), reactive oxygen species (ROS), nitric oxide (NO) and gamma-aminobutyric acid (GABA) are engaged (reviewed in Hiscock and Allen, (2008), Higashiyama, (2010)).

In the compatible interaction, the pollen grain hydrates and germinates. Major factors implicated in this process in tobacco are lipids, present on stigma and pollen coat (Wolters-Arts et al., 2002), while in *Brassica* aquaporin-like protein MIP-MOD regulates the water supply to pollen (Dixit et al., 2001). Additional proteins identified in the hydration are pollen coat protein GRP17 in *A. thaliana* (Mayfield and Preuss, 2000), extracellular lipase EXL4 (Updegraff et al., 2009), water channel protein aquaporin in *Brassica* (Ikeda et al., 1997) and in tomato, pollen specific secreted protein LAT52, was demonstrated to interact with

stigmatic LeSTIG1, via receptor kinase LePRK2, to promote pollen tube growth (Tang et al., 2004). Pollen hydration step is important when we take into account SI mechanisms. It is usually the step, which is severely inhibited in case of incompatible pollen-pistil reactions in *Brassicaceae* (Takayama et al., 2000).

During pollen germination pollen tube penetrates from an aperture in the pollen cell wall through a process of secretion of digestive enzymes, and enters the stigmatic tissue (see Figure 1.1). Following germination, the pollen tube starts growing through the stigma, style and transmitting tract of the pistil towards the ovary (see Figure 1.1), where it is mediated mostly by the female guidance cues. Pistil influence on the pollen tube gene expression was recently demonstrated to be much higher than previously thought. The pollen tube transcriptome of pollen tubes growing *in vivo* involves ~700 genes more than pollen tubes grown *in vitro* (Qin et al., 2009). Pollen absorbs nutrients from the female tissue and interacts with the several components including pectins, stigma/stylar cysteine-rich adhesion protein, that function in adhesion mediated pollen tube guidance, GABA, that forms a gradient which controls pollen tube guidance to micropyle and arabinogalactan proteins among which are best characterised transmitting tissue specific (TTS) glycoproteins that form a glycosylation gradient that promotes pollen tube growth (Cheung and Wu, 1999, Park et al., 2000, Palanivelu et al., 2003). In the transmitting tract of *Nicotiana* a thioredoxin h was also identified and reported to interact with S-RNases and play a role in pollen-pistil interactions during the S-RNase based SI (Juárez-Díaz et al., 2006). During the penetration of pollen through the transmitting tract, extensin-like and expansin-like activities have been reported, as well as pectin methylesterases, that enhance pollen tube tip dynamics (Stratford et al., 2001, Grobe et al., 1999, Bosch et al., 2005).

In the final stages of pollen tube journey through the pistil, female guidance of the pollen tube to the embryo sac is important for successful fertilization, and synergid cells play crucial role in this step. Two synergid cells are flanking the entrance to the egg cell at the micropylar end of the female gametophyte and are the source of the chemoattractants for the pollen tubes. Their role was established in the past decade by studies in *Torenia fournieri* (Higashiyama, 2002, Okuda et al., 2009). Mathematical model describing the dynamics of pollen tube attraction towards the attractants released from the ovules is also established (Stewman et al., 2010). It was recently demonstrated that two synergid cells in *Torenia* secrete two cysteine-rich proteins (CRPs) LURE1 and LURE2 (Okuda et al., 2009). They were identified by expressed sequence tag analysis of the synergid cell of *Torenia*, 29 % of all the clones they have sequenced encode CRPs (Okuda et al., 2009). CRPs LUREs belong to subgroup of defensin-like proteins and are secreted toward the micropylar end of the synergid cell. Down-regulation of the LURE1 and LURE2 protein resulted in the decreased rates of pollen tube attraction and recombinant expression of LUREs exhibited strong attraction of pollen tubes *in vitro*, suggesting that LUREs are involved in synergid cell pollen tube attraction (Okuda et al., 2009). In *Zea mays* it was also reported that small predicted transmembrane protein ZmEA1 (*Zea mays* Egg Apparatus 1) plays a pivotal role in pollen tube attraction and guidance through the micropyle into the female gametophyte (Márton et al., 2005).

After pollen tube grows into the female gametophyte, it releases its two sperm cells: one fertilizes the haploid egg cell to form a diploid zygote and the other fuses with the diploid central cell nuclei giving rise to the triploid endosperm. RLK FERONIA/SIRENE and LORELEI were identified to be required for pollen tube arrest and burst in *A. thaliana*, and defensin-like protein ZmES4 in *Z.mays* (Amien et al., 2010, Escobar-Restrepo et al., 2007,

Capron et al., 2008). ZmES4 activates K⁺ channel KZM1, localised in the plasma membrane at the pollen tube tip. Interaction between ZmES4 ligand and KZM1 channel triggers rapid influx of potassium ions and osmotic stress resulting in pollen tube tip burst (Amien et al., 2010). During fertilization, each ovule is penetrated by a single pollen cell and it was demonstrated using two-photon microscopy that late arriving pollen tubes are repelled from the fertilized ovules or do not approach it at all (Cheung et al., 2010).

1.1.2 Pollen tube

Pollen is an organ that must survive in variety of different environments. To penetrate from the stigma towards ovule, pollen tubes have a rapid growth rate. They are one of the fastest growing plant cells known, reaching speeds of 200-300 nm.s⁻¹ (Cheung and Wu, 2008). This is an important characteristic, as the ovules are located at distances of several thousand times the diameter of the pollen grain away from the stigma (Cheung and Wu, 2008).

There are four distinct zones or domains in highly polarised growing pollen tubes:

- (1) the tip domain outlines an inverted cone and is rich in secretory vesicles
- (2) the sub-apical domain, that contains metabolically active organelles, like mitochondria and endoplasmic reticulum (ER)
- (3) the nuclear zone, that contains large organelles and male germ cells
- (4) vacuole domain, that contains large vacuoles and callose plugs (Aström, 1997, Boavida et al., 2005).

The apical and sub-apical domains are jointly referred to as clear region, while nuclear and vacuolisation zones are jointly referred to as the shank.

Growth is restricted to the apical area. As the tip advances a periodic callose deposition occurs in the zone far behind the tip, restricting the pollen protoplast to the most proximal region of the elongating tube. Pollen tube growth requires the presence of a tip-focused calcium gradient, an intact actin and microtubule cytoskeleton and is supported by active vesicle trafficking. Actin forms long filaments that help with the transport and create one of the hallmark features of the growing pollen tube, reverse fountain cytoplasmic streaming (Figure 1.2).

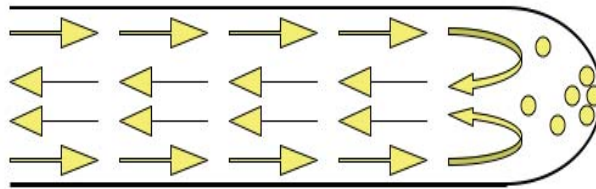


Figure 1.2.: Reverse fountain cytoplasmic streaming in pollen tube occurs opposite as the water in the fountain, hence name reverse fountain streaming. Reverse cytoplasmic streaming involves the movement of the cytoplasmic contents, with organelles and vesicles, toward the tip in the apical region of the tube where secretory vesicles will be discharged via exocytosis while excess membrane and recycled proteins will be retrieved via endocytosis (Zonia and Munnik, 2009).

Actin cytoskeleton, Ca^{2+} signalling and vesicle trafficking are regulated by ROP that are related to animal RAC (Rop/Rac), which have a role at the apex in regulating membrane trafficking and polar expansion (Fu et al., 2001, Yang, 2008, Fu, 2010). F-actin is present in the form of long filamentous cable-like structures in the shank of the pollen tube, that are responsible for the organelle and vesicle movement and reverse cytoplasmic streaming (Cai and Cresti, 2009). F-actin in the subapex is organised in a mesh-like structure, named actin collar, and in the tip, actin forms a dynamic network (Geitmann et al., 2000, Vidali et al., 2009). Actin binding proteins (ABPs) play a pivotal role in the dynamic actin signalling (Hussey et al., 2006).

In the recent years, ROS and phosphoinositides were demonstrated as additional pivotal signalling factors during the pollen tube growth, both of them tightly connected with Ca^{2+} signalling (Fu, 2010). It was demonstrated that ROS forms a gradient in the apical domain of the pollen tubes and by inhibiting ROS production, pollen tube growth was inhibited, while Ca^{2+} stimulates ROS production in pollen tubes (Potocký et al., 2007).

Cytosolic free calcium is an essential secondary messenger in many signal transduction processes in plants (reviewed in Dodd et al., 2010) and a tip-focused Ca^{2+} gradient is also required for growing pollen tubes. This apical gradient is maintained by Ca^{2+} influx at the tip via the opening of calcium channels. It has been shown to oscillate and it is thought that these oscillations are associated with the pollen tube growth *in vitro*, however, it was recently demonstrated in *A. thaliana* and *N.tabacum*, that such regular oscillations are not essential for pollen tube growth (Iwano et al., 2009, Holdaway-Clarke et al., 1997). $[\text{Ca}^{2+}]_{\text{cyt}}$ oscillations are controlling a wide range of intracellular processes, therefore the range of the $[\text{Ca}^{2+}]_{\text{cyt}}$ must be kept low ($\sim 2 \times 10^4$ lower than extracellular $[\text{Ca}^{2+}]$), for the stable equilibrium of Ca^{2+} in the pollen tube (Iwano et al., 2009). Malhó et al., (1994) and Malho and Trewavas, (1996) have shown, that calcium is involved in the reorientation of the growing pollen tube. They suggested that this element is part of a signal transduction system, which allows pollen tubes to respond to directional signals in the style that guide it towards the ovary. Mechanism of regulating Ca^{2+} is very complex and is interconnected also with other signalling pathways, such as ROP, ROS and phosphoinositidide signalling and influences many processes in the growing pollen tube; fusion of vesicles within the cell wall; regulation of cytoplasmic streaming; controlling the direction of growth, influencing actin cytoskeleton and mediating the SI response and programmed cell death (Malhó, 2006).

1.2 PROGRAMMED CELL DEATH (PCD)

PCD is an essential conserved cell death process used to remove the unwanted cells in plants during development and in response to external stimuli. It has been defined as a sequence of (potentially interruptible) events that lead to the controlled and organized destruction of the cell (Lockshin and Zakeri, 2004).

In animals there are three main types of cell death distinguished: apoptosis, autophagic cell death and necrosis (Kroemer et al., 2009). The major morphological features of animal apoptosis are reduction of cellular volume, chromatin condensation, nuclear fragmentation, plasma membrane blebbing, formation of apoptotic bodies, engulfment by phagocytes and clearance of dead cell contents by lysosomal degradation. Apoptosis in animals can be triggered by intrinsic stimuli, that can result from stress, radiation and others, and extrinsic stimuli, that is normally caused by binding of extracellular ligands, such as TNF- α (tumor necrosis factor), Fas ligand or TRAIL ligand (TNF related apoptosis-inducing ligand) to TNF receptors and activates caspase-dependent pathway (see Figure 1.3) (Spencer and Sorger, 2011). Death processes are triggered by initiator caspases-8 and -10 at DISCs (death inducing signalling complexes), that cleave the effector caspase's-3 and -7 pro-domain thus forming an activated protease and consequentially cell death occurs (Figure 1.3). However, in some cases mitochondrial outer membrane permeabilization (MOMP) leading to diffusion of the mitochondrial intramembrane space into the cytosol, is also required to activate effector caspases (type II apoptotic pathway). Mitochondrial permeabilization is a well studied mechanism and is controlled by Bcl-2 protein family (Figure 1.3): Bax and Bak (multidomain proteins causing mitochondrial pore formation); Bcl-2, Mcl-1 and Bcl-xL (inhibitors of Bax and

Bak); Bid and Bim (activators of Bax and Bak); and Bad, Bik and Noxa (sensitizers that act antagonistically to BCL-2-like proteins) (Spencer and Sorger, 2011, Oberst et al., 2008).

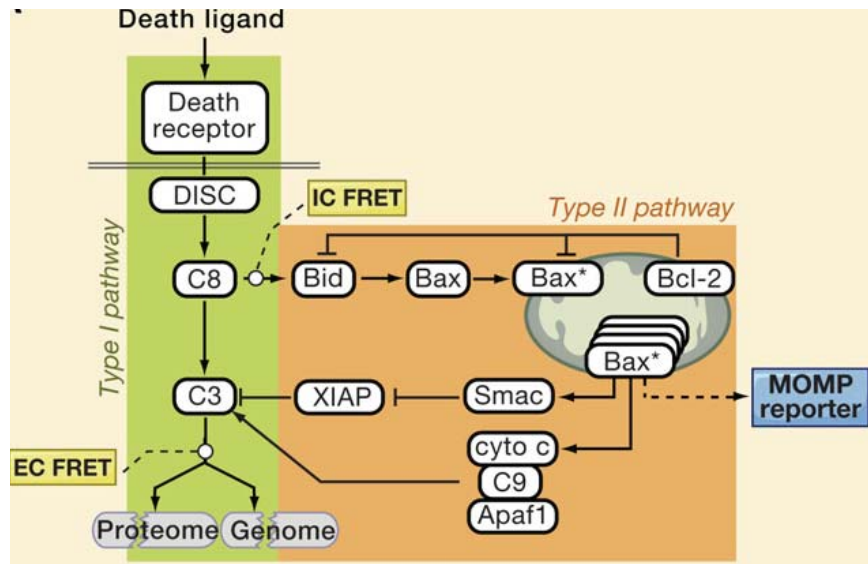


Figure 1.3.: Schematic representation of death receptor-mediated apoptosis signalling. Upon the receptor-ligand interaction, initiator caspase-8 (C8) is activated at DISC and cleaves Bid that will subsequently activate Bax and Bak to oligomerize. These oligomers will create a mitochondrial outer membrane pore (MOMP) and caused the release of apoptotic regulators (cytochrome c, Smac/Diablo). Cytochrome c binds with caspase-9 (C9) and Apaf-1 to form apoptosome. In type II pathway XIAP inhibits caspase-3 (C3) and -7 activity and promotes their UbP degradation. However, Smac, that is also released from mitochondria binds to XIAP and inhibits its action, therefore enabling C3 and C7 to confer cell death. Image adapted from Spencer and Sorger, (2011).

In contrast to animals, plants do not exhibit apoptotic bodies and also there are no phagocytes in plants. So, a recent classification emerged that set the ground for morphological classification and terminology of plant PCD (van Doorn et al., 2011). According to this new classification, two classes of PCD are distinguished: vacuolar cell death and necrosis. However, some examples of PCD in plants do not fit in either of these classes, so they are classified as separate categories. In contrast to necrosis, which is a form of cell-death that results from acute tissue injury and provokes an inflammatory response, PCD is carried out in a regulated fashion. PCD in plants is less well studied compared with animals, but at present there are vast array of plant cell culture models

and developmental systems are being researched by different research groups (Korthout et al., 2000, Sundström et al., 2009, Hatsugai et al., 2009, Thomas and Franklin-Tong, 2004, Coll et al., 2010, Bozhkov et al., 2004, Chichkova et al., 2010, Coffeen and Wolpert, 2004, Danon et al., 2004, Vercammen et al., 2004, Watanabe and Lam, 2011).

Plant vacuolar cell death is for example found during aerenchyma formation, xylem differentiation in vascular plants, leaf remodelling in *Monstera* or during the formation of embryo-suspensor (Gunawardena et al., 2004, Ohashi-Ito et al., 2010, Filonova et al., 2000). It is morphologically noticeable due to the increase of the vacuole volume, which contains hydrolytic enzymes that swallow up cell cytoplasm and degrade its contents. The disassembly of nuclear envelope was also observed as well as the formation of actin cables. Vacuolar cell death ends with the rupture of vacuole membrane or tonoplast and release of hydrolytic enzymes destroying the protoplast, however until rupture the organelles are intact (van Doorn et al., 2011). Biochemically, vacuolar cell death can be detected due to its autophagic activity, acidification of vacuoles, reorganisation of cytoskeletal elements and activation of vacuolar processing enzymes (VPEs).

The second type of plant PCD is necrotic PCD, which occurs in pathogen recognition during the hypersensitive response (HR) or in cells challenged by necrotrophic pathogens (van Doorn et al., 2011). It is distinguished from the vacuolar type by the absence of increasing size vacuole, mitochondrial swelling and shrinkage of protoplasts caused by the early rupture of plasma membrane with spilled and unprocessed corpses of necrotic cells. Biochemically, the necrosis can be detected by changes in mitochondria membrane potential, decreased respiration, accumulation of reactive oxygen species (ROS) and reactive nitrogen species (NO) as well as decline in ATP level (van Doorn et al., 2011, Christofferson and Yuan, 2010).

However, despite these two classifications, some unique types of plant PCD exist that cannot be attributed to either of those two groups. Such examples are HR cell death and PCD during self-incompatibility (SI) response (Thomas and Franklin-Tong, 2004, Hatsugai et al., 2009, Hofius et al., 2009).

1.2.1 Plant caspase-like proteases

Caspases play a critical role in animal apoptosis and are a family of cysteine proteases with specificity for aspartic acid, hence their name (Shi, 2002). There are no homologies to the caspases in plants, however, the caspase-like proteolytic activities have been identified in plants. Caspase-like activities have been detected using synthetic tetrapeptide substrates designed using the preferred cleavage site consensus of the members of the mammalian caspase family. Therefore the synthetic substrates are not caspase specific but they represent the optimal cleavage site of specific caspases (Stennicke and Salvesen, 2000). Caspase activities are often referred to using the amino acid sequence of the substrate cleaved (e.g. an activity against the substrate DEVD will be referred to as a DEVDase activity; see Table 1.1). Good biochemical evidence exists for the activation of plant proteases that cleave the substrates of caspases and therefore exhibit caspase-like activity in plants during PCD (for recent reviews see (Bonneau et al., 2008, van Doorn and Woltering, 2005, Piszczek and Wojciech, 2007, Woltering, 2010). Table 1.1 presents caspase-like activities that have been observed in plants to date.

Table 1.1: Plant caspase-like activities, plant species where they were identified and reference.

Activity	Species and tissue	Reference
YVADase (caspase-1-like)	Tobacco leaf tissue Barley embryonic suspension cells Tobacco BY2 cells White spruce seeds <i>Pisum sativum</i> seedlings <i>A. thaliana</i> seedlings <i>A. thaliana</i> fumonisin B-induced leaf lesion <i>Nicotiana</i> TMV infected leaves Seed integuments <i>P.rhoeas</i> pollen	(del Pozo and Lam, 1998) (Korthout et al., 2000) (Mlejnek and Prochazka, 2002) (He and Kermode, 2003) (Belenghi et al., 2004) (Danon et al., 2004) (Kuroyanagi et al., 2005) (Hatsugai et al., 2004) (Nakaune et al., 2005) (Bosch et al., 2010)
DEVDase (caspase-3-like)	Barley embryonic suspension cells Tobacco BY2 cells White spruce seeds <i>Pisum sativum</i> seedlings <i>Picea abies</i> embryogenic cell line <i>Avena sativa</i> leaves <i>A. thaliana</i> seedlings <i>P.rhoeas</i> pollen <i>A. thaliana</i> bact. inf. leaves	(Korthout et al., 2000) (Mlejnek and Prochazka, 2002) (He and Kermode, 2003) (Belenghi et al., 2004) (Bozhkov et al., 2004) (Coffeen and Wolpert, 2004) (Danon et al., 2004) (Thomas and Franklin-Tong, 2004) (Hatsugai et al., 2009)
IETDase (saspase)	<i>Avena sativa</i> leaves <i>P.rhoeas</i> pollen	(Coffeen and Wolpert, 2004) (Bosch and Franklin-Tong, 2007)
LEHDase	<i>Nicotiana benthamiana</i> leaves	(Kim et al., 2003)
LEVADase	<i>P.rhoeas</i> pollen	(Bosch and Franklin-Tong, 2007)
TATDase	Xanthi tobacco leaves	(Chichkova et al., 2004, Chichkova et al., 2008)
VEIDase	<i>P.rhoeas</i> pollen Barley seeds Norway spruce embryogenic cell line <i>A. thaliana</i> seedlings	(Bosch and Franklin-Tong, 2007) (Borén et al., 2006) (Bozhkov et al., 2004) Rotari & Gallois – unpublished
VEIDase (phytaspase)	Tobacco and rice	(Chichkova et al., 2010)
VKMDase (saspase)	<i>Avena sativa</i> leaves	(Coffeen and Wolpert, 2004)
metacaspases	<i>A. thaliana</i> seedlings <i>Picea abies</i> embryo	(Coll et al., 2010) (Sundström et al., 2009)

Metacaspases are a distant homologues of caspases that are found in plants, fungi and protozoa, and were demonstrated to play a role in plant PCD. They are arginine/lysine specific cysteine proteases. In *A. thaliana*, two types of metacaspases exist, type I and type II metacaspases (Watanabe and Lam, 2011, Sundström et al., 2009, Vercammen et al., 2004, Coll et al., 2010). Type II metacaspase, Tudor staphylococcal nuclease was identified in pine that is cleaved during PCD (Sundström et al., 2009). Recently, (Coll et al., 2010) demonstrated in *A. thaliana*, that type I metacaspases, AtMC1 and AtMC2 antagonistically control PCD. AtMC1 acts as a pro-death protein required for HR cell death, while AtMC2 antagonizes it.

Vacuolar processing enzyme (VPE) is a plant legumain and it exhibits YVADase activity. It was implicated to play its role during PCD in several different species in various pathways. It plays a vital role in the rupture of the vacuole membrane and HR cell death in response to plant virus infection (Hatsugai et al., 2004). VPE was also identified in *Papaver* pollen, by binding to DEVD-biotin probe (Bosch et al., 2010). It also exhibits DEVDase and IETDase activities in addition to predominant YVADase. Although it does not play a role in the SI response it is suggested to play a role in processing mitochondrial proteins (Bosch et al., 2010).

Another group of plant caspase-like proteins are saspases, subtilisin-like serine-dependent aspartate-specific proteases. They are involved in victorin-induced degradation of Rubisco during PCD in oats and exhibit VKMDase, VNLDase and VEHDase activities (Coffeen and Wolpert, 2004).

Chichkova et al., (2010) recently reported identification of phytaspase, a plant aspartate-specific protease, another subtilisin-like protease from tobacco and rice. It plays an

important role in regulation of PCD response to TMV infection and abiotic stresses, like oxidative and osmotic stresses. It possesses VEIDase activity and is localised in the apoplast, however during PCD it is partly re-localized inside the cell and so it might play a role in both positions (Chichkova et al., 2010).

There are many examples of PCD in plant development and in response to external stimuli (reviewed in Bonneau et al., 2008), and presented in Table 1.2 on page 22). An example of PCD in response to an external stimulus comes from the hypersensitive response (HR) after pathogen attack (reviewed in Coll et al., 2011), that can be compared to the SI-induced events in *Papaver*. So these two examples of PCD are described in more detail in the next two sections.

1.2.2 Hypersensitive response (HR-) induced PCD

Hypersensitive response (HR) is a mechanism of cell death that exhibits features of necrotic cell death but in addition also growth of the vacuole and rupture of the vacuole membrane followed by the release of lytic vacuolar contents and also VPEs. HR is a genetically controlled mechanism, based on the specific interactions between the products of the complementary genes of plant and pathogen, resulting in shrinkage of the cytoplasm, chromatin condensation, vacuolization and disruption of chloroplasts, all of that leading to rapid and localized cell death at the site of infection. In this way plants protect themselves and prevent spread of pathogens into healthy tissues (Dangl and Jones, 2001, Coll et al., 2011). When a microbial pathogen invades the plant tissue, a defence mechanism is initiated. Pathogens are inhibited by a combination of a layer of

dead cells, the local production of antimicrobial compounds, and the induction of systemic acquired resistance in the host (Dickman et al., 2001, Lincoln et al., 2002).

In the recognition of 'non-self', plant immune responses are of two types: one against general microorganisms and one against specific pathogen races (Chisholm et al., 2006, Jones and Dangl, 2006). The general defense mechanism is known as a pathogen- or microbe- associated molecular pattern (PAMP/MAMP) triggered immunity (Schwessinger and Zipfel, 2008, He et al., 2007a) and is triggered by extracellular surface receptors, called pattern-recognition receptors (PRRs). PRR recognition PAMP/MAMP results in the activation of defense responses against the pathogenic and non-pathogenic microbes (He et al., 2007a). In plants there are numerous PRRs, majority belonging to the receptor-like kinase (RLK) transmembrane proteins (Shiu and Bleecker, 2001). They are very specific and can recognize general features of microorganisms, such as bacterial flagellin (Zipfel et al., 2004, Gómez-Gómez and Boller, 2000). As a result of the co-evolution, plant pathogens have developed various strategies to overcome PAMP triggered immunity (PTI). One of them is effector-triggered susceptibility (ETS), which deploys PTI-suppressing pathogen effectors. The second and more specific defense mechanism against pathogen ETS is known as effector-triggered immunity (ETI), which is stimulated by plant resistance proteins (R-proteins) recognizing pathogens effector proteins, avirulence (Avr) proteins. ETI is very rapid and overblown defense response compared to PTI (Jones and Dangl, 2006, Boller and Felix, 2009).

One of the early actions in ETI is the oxidative burst; a generation of reactive oxygen species (ROS), such as hydrogen peroxide (H_2O_2), hydroxyl radicals ($\bullet OH$), superoxide anions ($O_2\bullet^-$) and nitric oxide (NO) and development of localized PCD of infected cells and this is

known as HR, the final defense mechanism in plants (Nimchuk et al., 2003). As a result of the ETI activation, an increased accumulation of salicylic acid (SA) is also observed. SA induces the induction of various pathogenesis-related (PR) genes and the activation of systemic acquired resistance (SAR) (Nimchuk et al., 2003).

Few components regulating R-protein interaction and responses have been characterized. ACRE (Avr9/Cf9 rapidly elicited) genes are such example and several of them encode Ubiquitin E3 ligases (Craig et al., 2009). Among them is ACIF1 (Avr9/Cf-0-induced F-box1), a positive regulator of HR against fungal, bacterial and viral pathogens (van den Burg et al., 2008). Plant U-box proteins (PUB) have also been reported to act as a positive or negative regulators of plant immunity. PUB17, for example, an *A. thaliana* homolog of tobacco ACRE276 (also closely related to *Brassica* ARC1) acts as a positive regulator of HR in a response to the infection of Cf9 expressing tobacco with Avr9 peptide (Yang et al., 2006). The functional involvement of ACRE276 for a resistance against *Cladosporium fulvum* was demonstrated by silencing experiments where the ACRE276 silencing caused a reduced HR and breakdown of the Cf9-mediated resistance against *C. fulvum*, which could complete a whole lifecycle in RNAi silenced tobacco expressing Cf9 and in VIGS silenced tomato plants. The expression of *AtPUB17* in *ACRE276* RNAi plants lead to the restoration of Cf9/Avr9 induced cell death, thus demonstrating the role of the E3 ubiquitin ligases (Yang et al., 2006). On the other hand, PUB22, PUB23 and PUB24 act cumulatively as negative regulators of resistance, as triple mutant *pub22/pub23/pub24* displayed increased oxidative burst and cell death (Trujillo et al., 2008).

Hatsugai et al., (2009) recently demonstrated the role of the proteasome in HR induced cell death as a response to bacteria attack. They identified a novel plant defense strategy to bacteria attack by membrane fusion of vacuole membrane and plasma membrane. Such a

fusion forms a tunnel from the inside of cell to the outside and enables the discharge of vacuolar content and defense proteins, as they demonstrated by the use of fluorescent proteins (Hatsugai et al., 2009). Outside the cell, plant defense proteins attack the bacterial cells, while hydrolytic enzymes in plant cell cause HR cell death (Hatsugai et al., 2009). Moreover, with the use of inhibitors of caspase-3 activity and proteasome inhibitors, Hatsugai et al., (2009) also demonstrated, that such a cell death and membrane fusion are proteasome-dependent and shown that proteasome subunit PBA1 acts as a caspase-3-like enzyme.

1.2.3 Self-incompatibility (SI) induced PCD in incompatible *Papaver*, *Pyrus* and *Olea* pollen

SI is a genetic mechanism that prevents self-fertilization by recognition and rejection of self-pollen, thus promoting outbreeding (described in details in Section 1.4.). There are several different mechanisms of SI in different species, like gametophytic SI in *Papaver*, gametophytic S-RNase-based SI in *Nicotiana*, *Petunia*, and *Pyrus*, sporophytic SI in *Brassica*, and some other less studied SI types, for example SI in *Olea*.

PCD was initially identified as a final and key downstream mechanism during SI in *Papaver rhoeas* pollen tube (Thomas and Franklin-Tong, 2004). PCD in the incompatible *Papaver* pollen is characterized by loss of pollen viability, depolymerization of actin cytoskeleton, activation of ROS and NO, SI-mediated DNA fragmentation and increased caspase-3-like activity (Bosch and Franklin-Tong, 2007, Wilkins et al., 2011). Recently, PCD was also implicated in response to SI in *Pyrus pyrifolia* (pear) pollen and *Olea europea* (olive) stigmatic cells (Serrano et al., 2010, Wang et al., 2009a, Wang et al., 2010). *P. pyrifolia*

from family Rosaceae is the first example of gametophytic S-RNase based SI where nuclear DNA degradation was demonstrated in incompatible pollen tube *in vivo* and *in vitro*, prior to the inhibition of incompatible pollen tube (Wang et al., 2009a, Wang et al., 2010). In addition to DNA degradation, collapse of membrane potential and cytochrome c leakage in the cytosol were also demonstrated, indicating that SI in pear pollen could result in PCD of incompatible pollen (Wang et al., 2009a, Wang et al., 2010).

The *O. europea* SI system is less well understood and studied, however it is implicated with the stylar gametophytic SI (Serrano et al., 2010). Morphological changes with vacuolization of the cells, chromatin condensation, plasma membrane blebbing and loss of cell integrity were observed in the *Olea* stigmas. Trypan blue staining confirmed loss of papillar and pollen cell viability in incompatible conditions, DNA degradation was demonstrated by TUNEL and DEVDase activity were observed in both pollen and pistils of *Olea* under free pollination (Serrano et al., 2010).

1.3 RECEPTORS & CELL SIGNALLING

Cells coordinate their intracellular status with the external environment by means of a large number of clearly defined signalling pathways. The interaction of a typical cell with the extracellular matrix and with neighbouring cells influences a variety of signalling events. Signalling pathways can be extracellular, activated by an external stimuli or generated within the cell. There are various signals received by the cells: chemical signals (i.e. specific ligands, such as PrsS in case of *Papaver rhoeas* SI signalling, or hormones), electromagnetic radiation (such as light) or mechanical inputs (such as touch). The purpose of signalling is to

encode information and convey a message about the internal or external environment into chemical signals, to which the cell can respond. This is done through the reception of the signal, which is then transduced intracellularly until a cellular response is activated. Information is communicated either through direct protein-protein interactions or by diffusible elements, usually referred to as second messengers.

Plant signalling is mediated, as in many animal systems, by hormones, steroids, sterols and lipids, reactive oxygen species (ROS) and nitric oxide (NO), signalling peptides, and various small proteins (Matsubayashi, 2003, Mittler et al., 2004, Wang, 2004, Vert et al., 2005). Only some of these signalling molecules have their receptor components identified and the next section 1.3.1 gives an overview.

1.3.1 Plant receptors

Plant receptors have been classified according to their structural characteristics. The largest group are receptor-like kinases (RLKs), comprising a family of over 600 genes in *A. thaliana* (Shiu et al., 2004). Other plant receptors include G-protein coupled receptors (GPCRs) and other receptors for hormone signalling, some of which are components of the ubiquitin-26s proteasome (UbP) pathway (Chow and McCourt, 2006, Spartz and Gray, 2008). Wheeler et al., (2009) reported identification of a pollen transmembrane receptor PrpS, which was identified as the male determinant of SI in *Papaver*. This type of receptor has no homology to any other known transmembrane protein and it represents a completely new group of plant receptors. Table 1.2. summarizes the plant receptors and their corresponding ligands in cases where they have been identified.

Table 1.2.: Receptor-ligand pairs identified in plants

Different types of receptors are highlighted by different colours for easier overview: RLKs are in blue, GPCR is in brown, PrpS is in red and hormone receptors are in green.

Ligand	Receptor	Type of receptor	System	References
Brassinosteroids (BR)	BRI1/BAK1	LRR-RLK	Plant Growth control: cell expansion and division, senescence, male fertility, pollen development fruit ripening, response to environmental factors	(Ye et al., 2011, Clouse, 2011, Kinoshita et al., 2005)
CLAVATA3 (CLV3)	CLV1/CLV2	LRR-RLK	Growth regulation of apical shoot meristem	(Clark et al., 1997, Brand et al., 2000, Ogawa et al., 2008)
TRACHEARY ELEMENT DIFFERENTIATION INHIBITORY FACTOR (TDIF)/CLE41 & CLE44	PHLOEM INTERCALATED WITH XYLEM/TDIF RECEPTOR (PXY/TDR)	LRR-RLK	Vascular cell division	(Fisher and Turner, 2007, Etchells and Turner, 2010, Ito et al., 2006, Hirakawa et al., 2008)
IINFORESCENCE DEFFICIENT IN ABSCISSION (IDA)	HAESA/HAESA-LIKE2 (HAE/HSL2)	LRR-RLK	Control of floral abscission in Arabidopsis	(Cho et al., 2008, Stenvik et al., 2008)
systemin	SR160	LRR-RLK	Defense signalling	(Scheer and Ryan, 2002)
Phytosulphokine (PSK)	PSK receptor (PSKR)	LRR-RLK	Cellular de-differentiation and re-differentiation	(Matsubayashi and Sakagami, 2006)
Bacterial flagellin (flg22)	FLAGELLIN SENSING2 (FLS2)	LRR-RLK	Plant innate immunity; bacterial disease resistance; mediating stomatal response	(Gómez-Gómez and Boller, 2000, Zeng and He, 2010, Zipfel et al., 2004)
EPIDERMAL PATTERNING FACTOR1 (EPF1) & EPF2	ERECTA (ER) & TOO MANY MOUTHS (TMM)	LRR-RLK	Stomatal initiation and development	(Hara et al., 2007, Hara et al., 2009); (Hara et al., 2009, Hunt and Gray, 2009, Shpak et al., 2005)
Not identified	STRUBBELIG (SUB)	LRR-RLK	Epidermal maintenance and cell specification	(Chevalier et al., 2005, Yadav et al., 2008)

TAPETUM DETERMINANT1 (TPD1)	EXCESS MICROSPOROXYTES1/ EXTRASPOROGENOUS CELLS (EMS1/EXS)	LRR-RLK	Anther tissue development and microsporocyte numbers	(Canales et al., 2002, Zhao et al., 2002, Yang et al., 2005, Jia et al., 2008)
CLAVATA3/ ENDOSPERM SURROUNDING REGION (CLE40)	ARABIDOPSIS CRINKLY 4 (ACR4)	TNFR-RLK	Root meristem development	(Becraft et al., 1996, De Smet et al., 2008, Gifford et al., 2005, Stahl et al., 2009)
S-locus cysteine rich (SCR) also known as S-protein11 (SP11)	S-locus –RLK (SRK)	SRK-RLK	Self-Incompatibility in <i>Brassica</i>	(Kachroo et al., 2001, Takayama et al., 2001)
Abscisic acid (ABA)	G-PROTEIN COUPLED RECEPTOR (GPCR)	GPCR	ABA signalling in guard cells	(Liu et al., 2007b)
<i>Papaver rhoeas</i> stigma S (PrsS)	<i>Papaver rhoeas</i> pollen S (PrpS)	PrpS	Self-Incompatibility in <i>Papaver</i>	(Wheeler et al., 2009)
Ethylene & Cytokinins	ETR1, ERS1, ETR2, EIN4 & ERS2 for ethylene CRE1, AHR2 & AHR3 for cytokin	Two component Histidine kinase sensors	Regulation of cell division and differentiation, promotion of fruit ripening.	(Chow and McCourt, 2006)
Auxin, Jasmonic acid (JA)	Ubiquitin protein ligase SCF ^{TIR1} , SCF ^{COI1} ,	F-box proteins	Plant growth and development	(Katsir et al., 2008, Kepinski and Leyser, 2005, Dharmasiri et al., 2005)
Gibberellins (GA)	GID1	Hormone-sensitive lipases	Seed germination, stem elongation, leaf expansion, pollen maturation and induction of flowering	(Ueguchi-Tanaka et al., 2005)

1.3.1.1 Plant receptor-like kinases

RLKs represent nearly 2.5 % of the total number of proteins encoded in the genome of *A. thaliana* and have diverged to perform different roles (Shiu et al., 2004). The first plant RLK was identified in *Zea mays* (Walker and Zhang, 1990). Its role was determined because of

similarity to the *Brassica* *S*-locus glycoprotein, implicating RLKs in mediating self-incompatibility (Walker and Zhang, 1990).

RLKs encode a typical single-pass, transmembrane-spanning domain, with an extracellular N-terminal domain and an intracellular C-terminal serine/threonine (Ser/Thr) kinase domain. Recently it was reported that LRR RLKs, such as brassinosteroid insensitive 1 (BRI1) receptor and BRI1-associated receptor kinase (BAK1), can autophosphorylate on tyrosine residues in addition to Ser/Thr and are thus dual specificity kinases (Oh et al., 2009, Oh et al., 2010, Jaillais et al., 2011).

Plant RLKs consist of several subfamilies, recognised because of their distinct extracellular domains that display variable structural features that bind different types of ligands, like *S*-domain, leucine-rich repeats (LRR), epidermal growth factor repeats (EGF) and lectins (Figure 1.4.). These will be briefly explained in the next section.

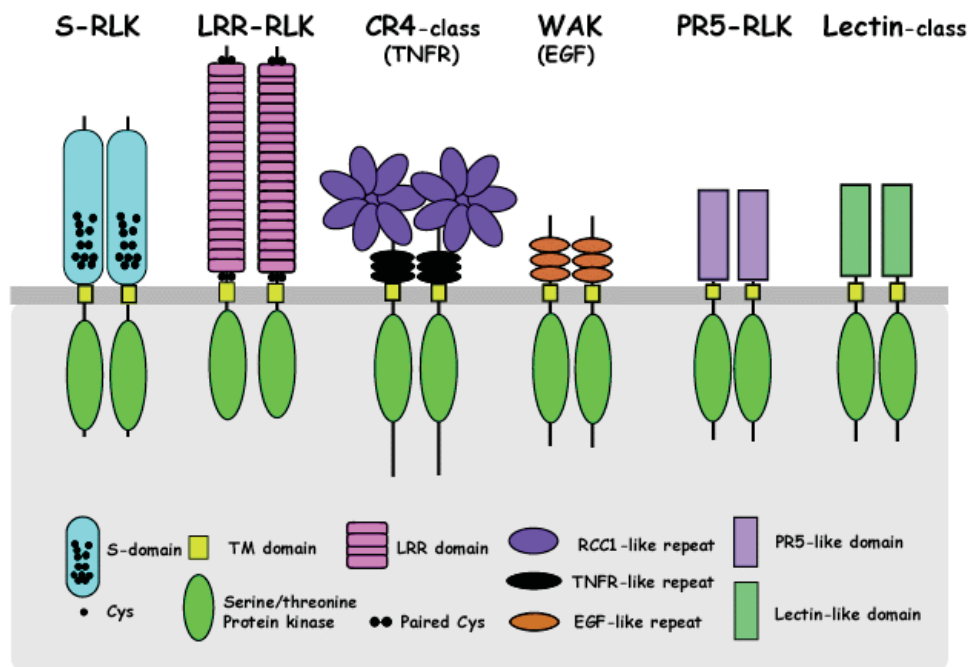


Figure 1.4.: Subfamilies of plant RLKs, based on the structure of the extracellular domain: *S*-domain class RLKs based on *S*-receptor kinase (SRK) RLKs; leucine rich repeats (LRR) RLKs are the largest subfamily of RLKs; tumor-necrosis factor receptor (TNFR)-like class RLKs; epidermal growth factor (EGF) class RLKs; PR5 like receptor kinase (PR) class RLKs; lectin class RLKs (Adapted from the website of Torii Laboratory)

1.3.1.1.1 LRR-RLKs

The largest subfamily of RLKs are the leucine rich repeats (LRR-RLKs) with over 200 members in *A. thaliana*, all containing tandem domains of approximately 24 amino acids featuring conserved leucines (Figure 1.4). Despite the similarity of the extracellular domain of the LRR-RLKs they bind a very diverse set of ligands, including: brassinosteroids, peptides, such as phytosulfokine and systemin and even secreted proteins (e.g. CLV3). Accordingly, LRR RLKs play critical roles in various stages of plant growth and development (see Table 1.2). For example, LRR RLKs are involved in the maintenance of the shoot apical meristem (SAM) where the CLAVATA (CLV) signalling pathway plays a central role in the regulation of SAM by controlling the size of the stem cell population (Fletcher and Meyerowitz, 2000, Clark et al., 1997). LRR RLKs are also involved in the brassinosteroid signal transduction pathway, which is regulated by the BRs. BRs are growth promoting steroid hormones (Grove et al., 1979). BR signal transduction and its mechanism is one of the best understood among the plant RLK family. Their role is associated with wide range of processes, such as light signalling, PCD, innate immunity response, male fertility, pollen development, fruit ripening, regulated senescence, cell expansion and division (for recent review see Clouse, 2011).

1.3.1.1.2 SRK RLKs

The *S*-locus receptor-like kinases (SRK) are described in greater detail in the section 1.4. Highly polymorphic SRK has been identified as a female determinant of *Brassica* SI and is specifically expressed in the plasma membrane of the stigmatic surface (Stein et al., 1996). It consists of an SLG-like extracellular domain, a single transmembrane domain and a

cytoplasmic Ser/Thr kinase domain (Figure 1.4) (Stein et al., 1991). The ligand for SRK is a pollen coat protein SCR/SP-11. The receptor-ligand interaction, activated in an allele-specific manner, triggers intracellular signalling cascade resulting in the pollen tube inhibition (Kachroo et al., 2001, Takayama et al., 2001) also reviewed in (Nasrallah, 2005, Takayama and Isogai, 2005). SRK RLKs also have another function. It was demonstrated that some RLKs could interact with Calmodulin (CaM), a small protein containing two globular domains with EF hands domain that bind Ca^{2+} (Vanoosthuysse et al., 2003, Charpentreau et al., 2004, Gifford et al., 2007). Recently, a protein from the SRK family, a calmodulin-binding RLK (CBRLK1) was identified in *A. thaliana* and *Glycine soya* (Kim et al., 2009, Yang et al., 2010). CBRLK binds specifically to a Ca^{2+} -dependent calmodulin binding domain (CaMBD) in the C-terminus (kinase domain), and there is a possibility that the interaction of CaM with SRK CBRLK1 plays a role in recycling of RLKs in plants (Kim et al., 2009).

1.3.1.1.3 Other RLKs

Among other classes of plant RLKs, illustrated in Figure 1.4. are TNFR, EGF, PR and lecitin class of RLKs. TNFR class is best represented by the ACR4 (ARABIDOPSIS CRINKLY4). ACR4 is involved in the maintenance of the root meristem and is expressed in differentiating root cells. ACR4 acts together with CLE40 peptide, a CLV3 homologue, which is expressed in fully differentiated columella cells (cell layer at the root tip, which forms the root cap together with the lateral root cap cells), to control the expression of transcription factor WOX5 (WUSCHEL-RELATED HOMEODOMAIN5) in the quiescent centre in order to maintain distal root stem cells (De Smet et al., 2008, Stahl et al., 2009). The root meristem

signalling works in opposite direction to the shoot signalling. In root signalling, signals originate from differentiated cells and determine the size and position of the root stem cell niche. Another role implicated for ACR4 is promoting initiation of lateral roots (De Smet et al., 2008).

1.3.1.2 G-protein coupled receptor

The GPCR family of receptors is also known as a seven transmembrane domain (7TM) receptor and it acts as a guanine nucleotide exchange factor. G-protein signalling cascade is composed of heterotrimeric protein complexes, which are composed of α -, β - and γ -subunits and GPCR. These complexes link perception by GPCRs with downstream signalling cascade (Jones and Assmann, 2004). A change in GPCR conformation upon the perception of the signal leads to the conformational change in the α - subunit and an exchange of GDP for GTP. This reorientation disrupts the interaction between α and β subunits and promotes dissociation of the complex into $G\alpha$ and $G\beta\gamma$ dimers, which can interact with an array of downstream signalling molecules (Jones and Assmann, 2004).

The genome of *A. thaliana* encodes around 25 GPCR candidate proteins (Grill and Christmann, 2007). In plants this family of receptors mediates various responses to adjust cell growth and differentiation, metabolism, embryogenesis, abscisic acid (ABA) and pathogen-associated molecular pattern (PAMP) regulation of guard cell ion channels and stomatal apertures and ROS signalling (Zhang et al., 2011).

1.3.1.3 PrpS receptor in *Papaver rhoeas*

Papaver pollen *S*-determinant (PrpS) will be described in greater detail in the next section

1.4. PrpS is a novel transmembrane protein, localized in pollen plasma membrane. Its structure has not yet been resolved, but it most likely contains four transmembrane domains with an extracellular loop of 35 amino acids, which is the binding side for its cognate ligand (Wheeler et al., 2009). The ligand for PrpS is globular stigmatic protein PrsS. The *S*-specific interaction between PrpS and PrsS triggers downstream signalling cascade resulting in the PCD of pollen tube and thus prevention of self-fertilization (Thomas and Franklin-Tong, 2004). The identification of PrpS, a predicted novel transmembrane protein is of considerable interest, since very few plant ligand-receptor partners have been identified to date. Given that most of the transmembrane plant receptors identified to date are plant receptor kinases, the discovery of the PrpS could represent a novel class of receptor.

1.4 SELF-INCOMPATIBILITY

The majority of plants develop both male and the female organs on the same plant in close proximity. For most plants, like for mammals, the problem of self-fertilization is a serious one. In mammals inbreeding can result in genetic disease and poor health, and inbred plants also experience decreased fitness as the benefits of out-crossing are lost and inbreeding is encouraged with a resulting loss of genetic variability. In order to avoid self-pollination and ensure that their offspring benefits from hybrid vigour, plants have developed a number of different mechanisms. The most widespread mechanism for prevention of inbreeding is SI; a

system where self-pollen is “rejected” at the molecular level. It is estimated that some form of SI is present in ~60 % of all flowering plants (Hiscock and Kües, 1999).

SI is genetically controlled cell-cell recognition system where self-pollen is recognised by pistil and inhibited in an *S*-specific manner. There are two major mechanisms of SI: sporophytic (SSI) and gametophytic (GSI) (see Figure 1.5.).

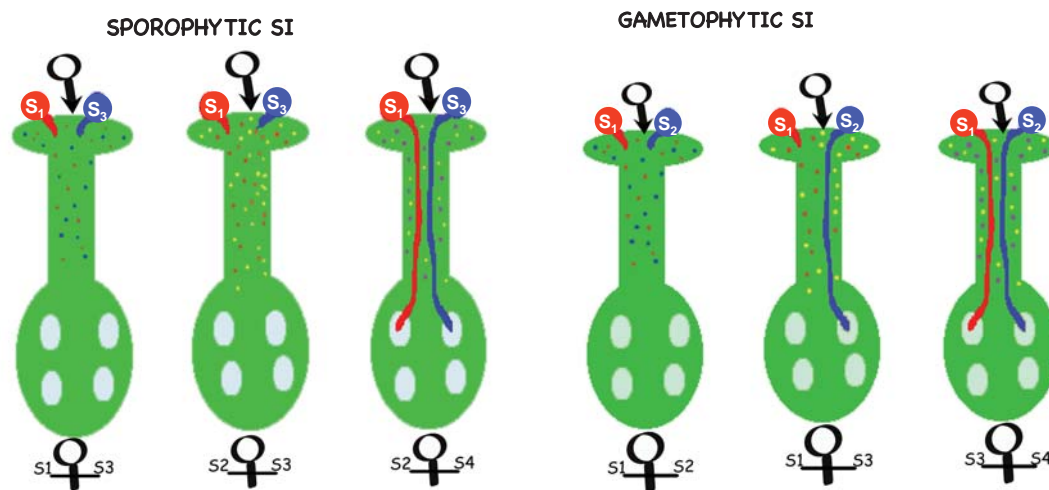


Figure 1.5.: An illustration of the genetic basis of gametophytic and sporophytic SI. For the sporophytic type, the SI phenotype of pollen is determined by the *S*-genotype of its diploid parent, thus each pollen grain carries the products of two *S*-genotypes. If an S_1S_3 pollen pollinates S_1S_3 or S_2S_3 stigma the outcome is incompatible interaction, while pollination of S_2S_4 stigma results in compatible pollination and fertilization. For the gametophytic type, the SI phenotype of pollen is determined by the *S*-genotype of its haploid genome, thus each pollen grain carries the product of one *S*-genotype. If S_1 and S_2 pollen lands on S_1S_2 stigma it results in self-incompatible reaction, while pollination of S_1S_3 stigma results in half-compatible situation where S_1 pollen is inhibited and S_2 allowed to grow and fertilize, and pollination of S_3S_4 stigma results in completely compatible situation. The spots in the pistils represent *S*-allelic component of the female *S*-determinants (i.e. in the sporophytic SI model, *Brassica* SRK₁ is represented by blue spots, SRK₃ by red spots, SRK₂ by yellow spots and SRK₄ by purple spots, while in gametophytic SI model spots represent *S*-RNases or PrsS proteins).

The pollen SI phenotype in SSI is determined by diploid genome of its parents (sporophyte), whereas in GSI the pollen SI phenotype is determined by its own haploid (gametophytic) genome. GSI is the most widespread SI system and has been extensively studied in the Solanaceae (*Lycopersicon* (tomato), *Nicotiana* (tobacco), *Petunia* (Petunia) and *Solanum* (potato)), Rosaceae (*Malus* (apples), *Prunus* (apricots, almonds, cherries) and *Pyrus* (pears)),

Plantaginaceae (*Antirrhinum* (snapdragons)), Poaceae (*Lolium*) and Papaveraceae (*Papaver* (poppy)). The SSI system has been extensively studied in Brassicaceae but also occurs and is studied in Asteraceae (Oxford ragwort), Convolvulaceae (sweet potato relative *Ipomea*) and Betulaceae (hazelnut). Interestingly, not only SSI and GSI have different mechanisms, but also there are also differences in GSI within different plant families, almost certainly as the result of SI evolving independently many times (Takayama and Isogai, 2005, McClure and Franklin-Tong, 2006, Allen and Hiscock, 2008, Klaas et al., 2011).

SI is usually controlled by a single, polymorphic *S*-locus with multiple alleles and can be compared with major histocompatibility complex (MHC) loci in mammals and mating type loci in fungi and algae. The exception is GSI in grasses, where SI is controlled by two loci, *S* and *Z* (Klaas et al., 2011). The *S*-locus in Brassicaceae, Solanaceae and Papaveraceae consists of at least two polymorphic genes, one encoding the male component and the second encoding the female component (Figure 1.6.) (Takayama and Isogai, 2005). This multi-gene complex is known to be inherited as one segregating unit. The variants of this gene complex are known as *S*-haplotypes rather than alleles. The recognition of self or non-self operates at the level of protein-protein interactions between male and female components. Incompatible interactions occur when both *S*-determinants are derived from the same *S*-haplotype.

a

Family	SI type	Male determinant	Female determinant
Brassicaceae	SSI	SP11/SCR	SRK
Solanaceae, Rosaceae, Plantaginaceae	GSI	SLF/SFB	S-RNase
Papaveraceae	GSI	PrpS	PrsS

b

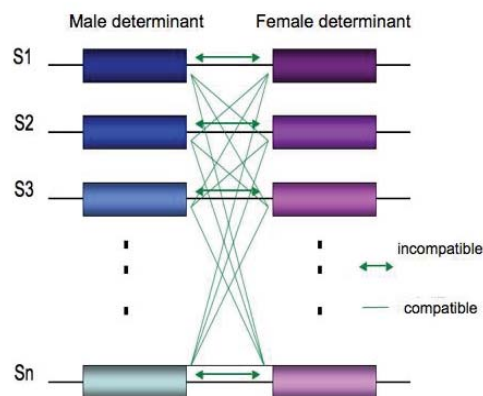


Figure 1.6.: (a) Male and female determinants of SI: in Brassicaceae the SSI type female component is an *S*-receptor kinase (SRK) and the male component is an *S*-cysteine rich (SCR)/*S*-locus protein 11 (SP11); in the GSI type found in Solanaceae, Rosaceae and Plantaginaceae the female determinants are *S*-RNases and male determinant are *S*-locus F-box (SLF)/*S*-haplotype-specific F-box (SFB); in GSI in Papaveraceae the female component are PrsS proteins while the male determinant was recently identified as PrpS protein (Takayama and Isogai, 2005, Wheeler et al., 2009). (b) A schematic diagram of the *S*-locus, which containing pollen (blue bars) and pistil (pink bars) determinants and basis of SI. The interaction of pollen and pistil determinant with the same *S*-haplotype (i.e. encoded by the same allele) results in incompatible response (green line with arrow ends), while in case of different *S*-haplotype interaction a compatible response is observed (green line without ends).

1.4.1 Sporophytic SI in the Brassicaceae

The *S*-locus encoded highly polymorphic receptor-ligand pair that determines SI specificity in *Brassica*, are the *S*-receptor kinase (SRK), that is expressed in the epidermal cells of stigma, and *S*-cysteine rich (SCR) protein, also identified as *S*-protein 11 (SP11), expressed in the pollen coat (Stein et al., 1991, Suzuki et al., 1999, Schopfer et al., 1999, Takayama et

al., 2001, Takayama et al., 2000). The proposed mechanism of SI is presented in Figure 1.7. Incompatible pollen tube growth is inhibited very rapidly at the stigma surface.

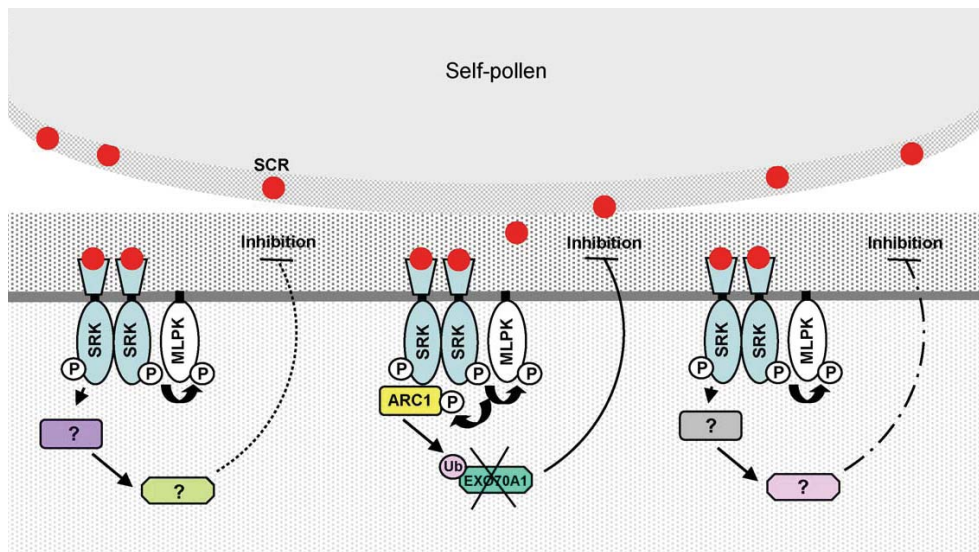


Figure 1.7.: Schematic model for recognition of self pollen and mechanism of sporophytic SI in *Brassica*. Male determinant of SI are SCR molecules expressed in pollen coat and female determinant are SRKs, expressed in stigmatic epidermal cells. Upon landing of self pollen on the stigma, SCR peptide is delivered to the stigma epidermal surface where it binds to the extracellular domain of cognate SRK. This causes autophosphorylation of the receptor and triggers signalling cascade, the cartoon proposes three different SI cascades. MLPK acts as a signalling intermediate. The cartoon in the middle illustrates SI model that involves ubiquitination of EXO70A1 by ARC1, while the cartoons on the side illustrate the existence of unknown compounds in the ARC1/Exo70A1-independent signalling pathways (Image adopted from Tantikanjana et al., 2010).

SRK, encodes a single pass transmembrane Ser/Thr kinase that is anchored to the stigma epidermis, presenting its highly polymorphic extracellular *S* domain to the ligand molecules on the pollen surface (Nasrallah, 2002). The extracellular, *S*-locus glycoprotein (SLG)-like extracellular domain is the site of interaction with pollen SCR ligand (Stein et al., 1991). There are several splice variants of SRK, such as eSRK (glycosylated extracellular SRK) and tSRK (membrane bound form of eSRK) (Shimosato et al., 2007). SRK has a plasma membrane localization, however, it is distributed in the smaller patches or SI domains, where it is kept in the ready-to-be-activated state (Ivanov and Gaude, 2009). SRK is also localised in the endosomes, below the plasma membrane surface, where the thioredoxin THL1 keeps it in the unactivated state (Ivanov and Gaude, 2009).

The *S*-specific interaction of SP11/SCR with SRK is localised on the interacting area of the stigmatic papillae, while the rest are ready to react on their own independent interactions. The *S*-specific interaction induces the autophosphorylation of SRK, triggering a signalling cascade that results in the rejection of self-pollen (Kachroo et al., 2001, Takayama et al., 2001, Ivanov et al., 2010). Inhibition occurs within minutes of pollination and the papillae cell wall may not even be penetrated. Downstream of SRK signalling were found proteins ARC1 (Armadillo-repeat containing 1) and MLPK (*M*-locus protein kinase) (see Figure 1.7) (Murase et al., 2004, Stone et al., 1999).

Membrane anchored cytoplasmic serine/threonine kinase was identified by positional cloning of the *M* (modifier) locus (Murase et al., 2004) and is thought to act with phosphorylated SRK to phosphorylate ARC1. ARC1 was identified with Y2H screening for interactors of SRK kinase domain and it encodes a U-box E3 ligase with an arm repeat region (Stone et al., 2003, Stone et al., 1999). ARC1 is a positive regulator of the SI because the downregulation of ARC1 results in the partial breakdown of the SI (Stone et al., 1999). As an ARC1 binding protein, EXO70A1, component of an exocyst complex, was recently identified (Samuel et al., 2009). It normally promotes compatible pollinations as its reduced expression disturbed non-self pollen tube growth, therefore ARC1 mediated ubiquitination and proteasomal degradation of EXO70A1 is required for normal SI to occur (Samuel et al., 2009).

However, recent re-analysis of the *Brassica* SI signalling network revealed that it is much more complex than previously thought and that downstream signalling components identified so far (MLPK, ARC1, EXO70A1) are not required for SI, at least not for a *Brassica* SI in *A. thaliana* (see Figure 1.7) (Tantikanjana et al., 2010).

Tantikanjana et al., (2009) reported, that SRK also plays a role in pistil elongation. This additional role of SRK, whose expression was detected throughout the pistil, was identified in *rdr6* mutants of transgenic *Arabidopsis thaliana*, expressing *Arabidopsis lyrata* SI genes. RDR6 functions in production of trans-acting short interfering RNA (ta-siRNA), and was found to enhance SI and causes stigma exertion. In this mutant background they demonstrated that *SRK* gene further enhances pistil elongation and stigma exertion, which indicates that positive regulators of SI are regulated by ta-siRNAs and that SI trait and physiological distance between stigma and anthers have coevolved (Tantikanjana et al., 2009). They also identified targets of ta-siRNA as AGO7 (ARGONAUTE 7), that is an ARF (auxin response factor) and ARF3 and ARF4 are already demonstrated regulators of pistil development (Tantikanjana et al., 2009, Tantikanjana et al., 2010).

1.4.2 S-RNase based gametophytic SI

GSI in the Solanaceae (petunia, potato, tobacco, tomato, etc.), Rosaceae (apple, cherry, almond, pear, etc) and Plantaginaceae (*Antirrhinum*) share a common pistil S-determinant, an S-RNase. In these families inhibition of pollen tubes occurs in the transmitting tract of the style. Incompatible pollen grains lands on the stigma, hydrates and germinates as normal. The pollen tube grows through the stigmatic papillae and the transmitting tract of the style. It is only once pollen tubes reach about one-third of the way through the style that growth is arrested (Kao and Tsukamoto, 2004).

The S-RNases were identified by searching for pistil specific proteins that exhibited S-allele-specific differences in molecular weight and isoelectric point, as the allelic variants of protein involved in SI must be divergent in sequence in order to serve as a recognition

molecule. Using gain of function and loss of function experiments the S-RNase was demonstrated as the *S*-determinant in *Petunia* (Lee et al., 1994). S-RNases are produced in the transmitting cells and secreted in the transmitting tract where the pollen is growing and they contain five conserved domains and two hypervariable regions (HVa and HVb) (Matton et al., 1997). The second gene at the highly polymorphic *S*-locus that controls SI is the *SLF* (*S*-Locus F-Box)/*SFB* (*S*-haplotype-specific F-box) gene, which encodes the pollen *S*-determinant (Sijacic et al., 2004, Qiao et al., 2004a). *SLF/SFB* are members of F-box family of proteins, which generally function as a component of an E3-ubiquitin ligase complex and are involved in ubiquitin mediated protein degradation of non-self S-RNases. Recently new discoveries were made in *Petunia* where it was demonstrated that several related *SLF* factors encode pollen *S*-determinant and each *SLF*-type recognizes a range of S-RNases (Kubo et al., 2010).

Two proposed models, degradation and compartmentalization, can explain the self-compatibility and SI, and are presented in Figure 1.8. Degradation model of S-RNase-based SI (Figure 1.7.a) is based on the destruction of S-RNases upon the interaction of *SLF* and S-RNase (Hua et al., 2008). It proposes that *SLF* determinants act collaboratively to prevent RNA degradation by non-self S-RNases and it also enables a wider variety of mating partners (Kubo et al., 2010). *SLF* determinants collaboratively mediate ubiquitination and degradation of the non-self S-RNases through the F-box domain, so that only self S-RNases function inside incompatible pollen tube (Meng et al., 2011). For example, during incompatible pollination of S_1S_2 style by S_2 pollen, the S_1 - and S_2 -RNases are taken up by S_2 pollen tube. The strong interaction between SLF_2 and S_1 -RNase would result in degradation of S_1 -RNase as a consequence of ubiquitin-mediated proteasomal degradation, while the self S_2 -RNase would remain intact. However, in the case of pollination of the S_1S_2 style by

heteroallelic S_1S_2 pollen, SLF₁ would preferentially interact with non-self S_2 -RNases and SLF₂ with S_1 -RNase, thus resulting in heteroallelic pollen compatible with S_1S_2 pistil (Meng et al., 2011). Using both allelic products of SLF, produced in heteroallelic pollen together mean that heteroallelic pollen is accepted by pistils, regardless of the S -genotype (Meng et al., 2011). However during incompatible pollination none of the SLF varieties bind and degrade self- S -RNases, which are therefore free to degrade the RNA of pollen tube (Kubo et al., 2010).

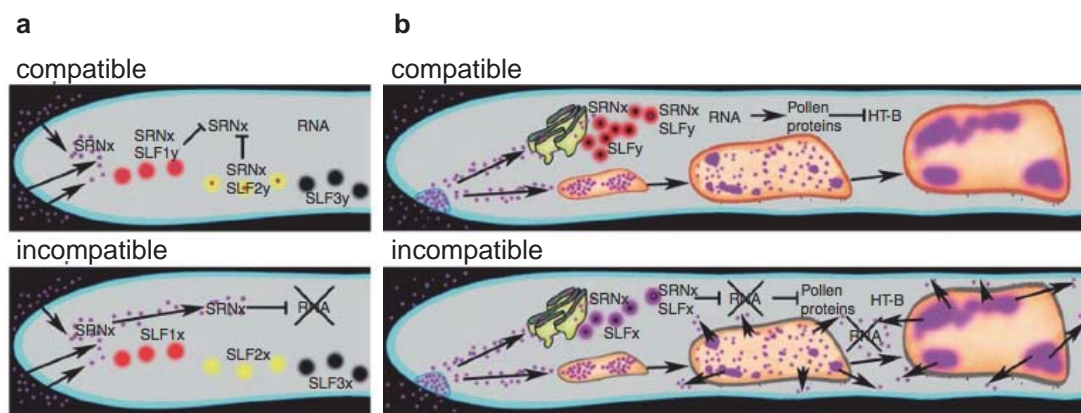


Figure 1.8.: Two models for S -RNase based SI. (a) Degradation model: multiple SLF proteins are linked to certain S -RNase and act collaboratively. In the compatible situation (top) the array of SLF proteins (for example SLF_{1y} and SLF_{1x}) bind to S_x -RNase thus preventing degradation of pollen RNA. During incompatible interaction (bottom) pollen SLF proteins, for example SLF_{1x}, SLF_{2x} and SLF_{3x} do not bind self- S -RNase, which degrades the pollen RNA and thus inhibits pollen tube growth. (b) Compartmentalization model: during compatible pollination (top), the non-self RNase enters the pollen tube and are most likely compartmentalized into vacuoles and HT-B proteins are degraded. It is proposed that SLF promotes degradation of the non-self RNases that are not compartmentalized by 26S proteasome. The RNA of the pollen remains intact. In incompatible pollination (bottom), the S -RNase and HT-B enter the endomembrane system by endocytosis. HT-B is required for S -RNase to exert its cytotoxic activity. When self S -RNase enters pollen tube, the conformational change occurs in SCF^{SLF}. The self- S -RNase-SLF interaction inhibits the pollen protein responsible for HT-B degradation. Self-interaction therefore suppresses HT-B degradation. S -RNase is not degraded and its cytotoxicity results in RNA degradation and consequent pollen tube growth inhibition (Goldraij et al., 2006, Kubo et al., 2010, McClure, 2006). Image from McClure et al., (2011).

The S -RNase compartmentalisation model involves S -RNase compartmentalisation by the pollen tube endomembrane system (Figure 1.8.b) (McClure et al., 2011, McClure, 2009, Goldraij et al., 2006). Compartmentalisation is a common mechanism for controlling potential cytotoxins and probably protects both transmitting tract cells and pollen tubes

(McClure, 2006). S-RNases form complexes with other proteins: 120K, which is a 120 kDa glycoprotein abundant in the stylar ECM, and HT-B, a small asparagine-rich protein (McClure et al., 1999, Cruz-Garcia et al., 2005). S-RNase, 120K and HT-B are taken up by endocytosis and sorted to the vacuole (Goldraij et al., 2006). In a compatible reaction, S-RNase remains compartmentalised and HT-B levels are downregulated, so although S-RNase is present, it is not cytotoxic because it is sequestered. In an incompatible reaction, HT-B facilitates the S-RNase transport from endomembrane compartment to the cytoplasm where S-RNases, bound by 120K acts cytotoxicaly and degrade self-RNA thus leading to the inhibition of pollen tube growth (Goldraij et al., 2006, McClure, 2006).

1.4.3 Gametophytic SI in Papaveraceae

In *Papaver rhoeas*, the SI system is also under the control of a single, highly polymorphic, multiallelic, *S*-locus with gametophytic control of pollen *S*-gene expression (McClure et al., 1989). It is distinctly different to the S-RNase based SI system. In *Papaver*, the inhibition of the pollen tube is extremely quick and occurs soon after polarity is established during germination on the surface of the stigma. It has been estimated that around 66 *S*-alleles exist in poppy, several of which have been cloned (Foote et al., 1994, Walker et al., 1996, Kurup et al., 1998). The female component are small and secreted, ~15 kDa proteins, named PrsS (*Papaver rhoeas* stigma *S*) that act as a signalling ligand (Foote et al., 1994, Wheeler et al., 2009). *S*-stigma extracts and also recombinant PrsS have been shown to have *S*-specific pollen inhibitory activity when tested in an *in vitro* SI bioassay (Kakeda et al., 1998, Jordan et al., 1999).

1.4.3.1 Pistil S-determinant

The stigmatic *S*-alleles *PrsS₁*, *PrsS₃*, *PrsS₈* and *PrsS₇* from *Papaver rhoeas* and one from *Papaver nudicaule* have been cloned and sequenced nearly 2 decades ago (Foote et al., 1994, Walker et al., 1996, Kurup et al., 1998). The first one analysed was *PrsS₁* and the protein was scraped directly from the stigmatic papillae of the flowers onto the isoelectric focusing (IEF) gel surface and separated by polyacrylamide gel electrophoresis (PAGE)-IEF (Foote et al., 1994). Silver staining revealed two proteins *PrsS_{1a}* and *PrsS_{1b}* with isoelectric points 7.55 and 6.90, while the sodium dodecyl sulphonate (SDS)-PAGE analysis showed that both separated into two proteins with size ~16.7 and ~14.7 kDa (Foote et al., 1994). Northern analysis showed that the gene was expressed specifically in stigmas with the expected temporal expression, while Southern analysis indicated that it was a single copy gene (Foote et al., 1994). *PrsS₁* was produced as recombinant protein in *E.coli* (Foote et al., 1994).

PrsS proteins are easily extracted from *Papaver* stigmatic surface and have predicted signal peptide, suggesting they are secreted proteins. Secondary structure predictions suggest that they are comprised of 6 β -strands and 2 α -helixes, joined by 7 hydrophilic loops. They are cysteine-rich proteins with 4 identically positioned cysteine residues involved in disulphide bridge formation (Kakeda et al., 1998). It was demonstrated using a mutagenesis approach that residues in the hydrophilic loop number 6 are most likely to interact with the pollen *S*-determinant as the mutation of Asp79 of this loop resulting in complete loss of biological function (Kakeda et al., 1998).

1.4.3.2 Pollen *S*-determinant

Identification of pollen *S*-determinant has been long and difficult. A potential candidate was identified as integral membrane glycoprotein, *S*-protein binding protein (SBP) (Hearn et al., 1996). The problem was that SBP did not bind to PrsS in an *S*-haplotype specific manner. The exact role and identity of SBP is yet to be found although it is thought to play an important role in SI.

So what are exactly criteria that a putative pollen *S*-determinant must meet? Firstly it must be linked to the pistil gene at the *S*-locus and it must have had co-evolved together with the pistil *S*-alleles. It must also be sufficiently polymorphic, exhibit correct temporal and spatial expression and it must play a functional role in the SI response.

Pollen *S*-determinant, PrpS, meets all of the above criteria (Wheeler et al., 2009). ORF of PrpS₁ was identified very close (475 bp) to the pistil *S* gene when genomic DNA library, from the *S*₁ containing *Papaver* plants, was screened using the *S*₁ pistil gene as a probe. With two more alleles identified (PrpS₈ and PrpS₃), high level of polymorphism was confirmed. PrpS₁ and PrpS₈ sequences are only 59 % identical at the amino acid level (for comparison, PrsS₁ and PrsS₈ have 64 % sequence identity) (Wheeler et al., 2009, Kurup et al., 1998). PrpS₁ and PrpS₃ are 50 % identical and PrpS₃ and PrpS₈ 53 % identical on amino acid level. PrpS is a 20.5 kDa hydrophobic protein that is predicted to contain three to five membrane spanning domains. It was determined by expression analysis using RT-PCR that it is specifically transcribed in pollen with the highest levels of expression at the anthesis and the western analysis showed that it was only detected in the pollen membrane-enriched fraction. Immunolocalization analysis, using a specific PrpS₁ antisera, visualized PrpS at the plasma membrane of *S*₁ pollen tube (Wheeler et al., 2009).

Functionality of PrpS involvement in SI was demonstrated by the *in vitro* SI bioassays where PrpS peptide representing extracellular domain alleviated SI response, while randomised peptide did not. Antisense oligonucleotides (as-ODNs) and sense oligonucleotides (s-ODNs) were used in the *in vitro* assays to check that PrpS could function in an *S*-specific manner. Plants with the S_1S_3 alleles were used and maximum inhibition was observed with S_1 and S_3 s-ODNs. S_1 and S_3 as-ODNs did not stop pollen tubes from growing while as-ODNs from *PrPS₈* had no effect on pollen inhibition (Wheeler et al., 2009). *S*-specific binding between PrpS and PrsS was detected with slot-blot peptide binding assay (Wheeler et al., 2009). PrpS has no homology to any protein in the existing databases and it is predicted to be a novel transmembrane protein (Wheeler et al., 2009). Due to the nature of the early poppy SI response, which includes an instantaneous influx of external Ca^{2+} via channels and rise in cytosolic Ca^{2+} , the finding of pollen specific gene adjacent to stigma *S* that encodes a putative transmembrane protein could be of great potential significance.

1.4.3.3 Mechanism of SI in *Papaver*

When incompatible pollen lands on a receptive stigma, secreted PrsS proteins interact with pollen transmembrane PrpS and thus trigger a Ca^{2+} -dependent signalling cascade, affecting many downstream cellular components, such as pyrophosphatase activity, MAPK, actin and tubulin cytoskeleton, ROS and NO, caspase-like activities, and ultimately leading to the PCD of the pollen tube (for recent review see Poulter et al., 2010b). Next sections discuss these events, which are also schematically presented in Figure 1.9.

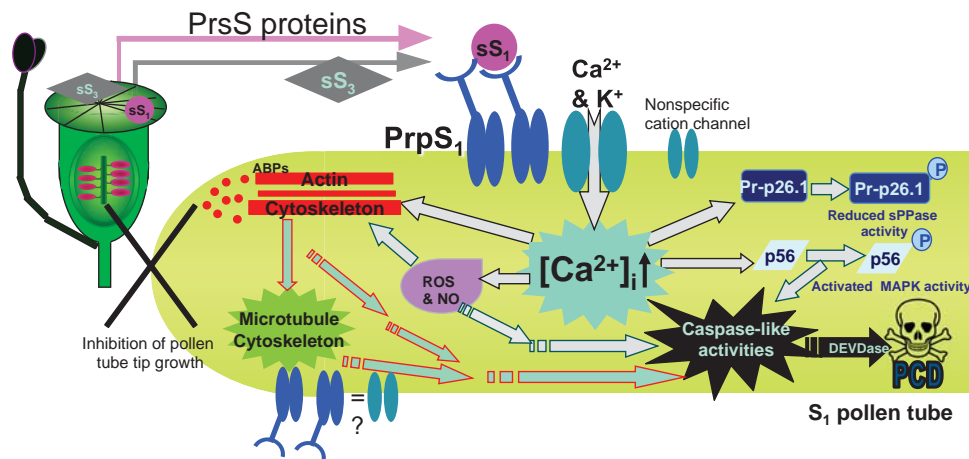


Figure 1.9.: Schematic model of the SI response in *Papaver*. Upon interaction of secreted stigmatic PrsS proteins and pollen transmembrane protein PrpS, a downstream signalling network is triggered, starting with an increase in K^+ and $[Ca^{2+}]_i$ who is signalling to the inhibition of pyrophosphatase activity and pollen tube tip growth, activation of MAPK, depolymerization of actin and microtubule cytoskeleton and appearance of punctate actin foci, activation of ROS and NO and activation of caspase-like activities, leading to the PCD of the pollen tube.

1.4.3.3.1 Role of Ca^{2+} in the SI response

Calcium plays an important role in the SI-specific response in *P. rhoeas* pollen tubes. Ca^{2+} imaging studies revealed a rapid, transient increase in pollen $[Ca^{2+}]_i$, when pollen tubes were treated with incompatible but not compatible PrsS (Franklin-Tong et al., 1993, Franklin-Tong et al., 1995, Franklin-Tong et al., 1997). In the growing pollen tubes, a tip-focused gradient of the intracellular Ca^{2+} concentration $[Ca^{2+}]_i$ can reach 1-2 μM , while in the shank region basal levels of $[Ca^{2+}]_i$ are low, with a mean value of ~ 200 nM. The SI challenge resulted in instantaneous and dramatic increase of $[Ca^{2+}]_i$ in the shank and sub-apical region of pollen tubes, while tip-focused oscillating $[Ca^{2+}]_i$ gradient rapidly disappeared (Franklin-Tong et al., 1995, Franklin-Tong et al., 2002). The SI induced increase in $[Ca^{2+}]_i$ was blocked with calcium blocker La^{3+} and Gd^{3+} , providing confirmation that Ca^{2+} influx is required for the increase in $[Ca^{2+}]_i$ during the incompatible reaction (Franklin-Tong et al.,

2002). Influx of extracellular Ca^{2+} in the shank of pollen tube acts as a secondary messenger that triggers signalling cascades which results in irreversible inhibition of incompatible pollen tubes (Figure 1.9). Recently, a nonspecific cation channel activities were identified as being activated in incompatible *Papaver* pollen by using whole-cell patch clamping that are permeable for monovalent (K^+ and NH_4^+) and divalent ($\text{Ba}^{2+} \geq \text{Ca}^{2+} \geq \text{Mg}^{2+}$) ions upon the S-specific incubation with PrsS proteins (Wu et al., 2011). While Ca^{2+} ions are well demonstrated to play an important role in pollen tube germination and growth, the role of K^+ is less well documented. So far in growing pollen tubes hyperpolarization-activated Ca^{2+} channels, stretch activated Ca^{2+} -permeable cation channel and Ca^{2+} pump ACA9 have been identified (reviewed in Michard et al., 2009). Role of K^+ was demonstrated recently in maize pollen, where small CRP ZmES4 protein was identified to activate the potassium channel KZM1 in the final step of fertilization and causes the K^+ influx and subsequent burst of the pollen tube that enables sperm cells to be released (Amien et al., 2010). There is a parallel with the PrsS-activated channel activity in *Papaver* pollen; both pollen systems respond to a clearly defined biological stimuli in a form of small CRP protein, that stimulates channel activity, leading to influx of K^+ ions, and in case of poppy pollen also to Ca^{2+} ions (Amien et al., 2010, Wu et al., 2011).

1.4.3.3.2 Role of soluble inorganic pyrophosphatases in poppy SI

Soluble inorganic pyrophosphatases (sPPases) are enzymes that catalyse the hydrolysis of inorganic pyrophosphate to inorganic phosphate and are Mg^{2+} dependent. sPPases are regulating biosynthesis and biochemical pathways in prokaryotes and eukaryotes. They have essential role in plant cells, driving biosynthetic reactions and generating ATP and

biopolymers such as pectin, hemicellulose and cellulose (Cooperman et al., 1992). Examples of cytosolic sPPases in plants are rare because plant sPPases are localized primarily to plastids rather than the cytosol (Gross and Ap Rees, 1986). Possible explanations for this could be that sPPases are abundant in metabolically active cells and thus, pollen tubes may express cytosolic sPPases because they require high metabolic activity to generate new membrane and cell wall for pollen tube extension (de Graaf et al., 2006).

In *Papaver* pollen the sPPases play a crucial role, as they provide the driving force for biosynthesis of pollen tube germination and growth. Ca^{2+} -dependent hyperphosphorylation of Pr-p26.1a/b (two soluble inorganic pyrophosphatases) leads to the reduced sPPase activity and occurs at around 90 s after SI (de Graaf et al., 2006, Rudd et al., 1996). sPPases can be inhibited by Ca^{2+} and by phosphorylation and this causes arrest of pollen tube growth, highlighting the importance of this regulatory mechanism during the SI response in *Papaver* pollen (Figure 1.9) (de Graaf et al., 2006).

1.4.3.3.3 Role of MAPK in poppy SI

Another target downstream of the Ca^{2+} signals, triggered by the SI response in poppy, is protein p56, named after its 56 kDa size, and is identified as MAPK (Li et al., 2007, Rudd et al., 2003). Its activation is peaking 10 min post SI implicated its role in signaling in incompatible pollen tube and regulation of PCD (Figure 1.8) (Li et al., 2007, Rudd et al., 2003).

MAPKs are the key elements of a of protein kinase cascade that can trigger responses to a wide variety of signals and stimuli. Collectively, different MAPK cascades regulate important cellular processes including gene expression, cell proliferation, cell survival and

death in eukaryotic cells (Chang and Karin, 2001). MAPKs were known to be functionally involved in regulating PCD in plants (Ligterink et al., 1997, Kroj et al., 2003) and the same was demonstrated for p56 in incompatible *Papaver* pollen (Li et al., 2007). The crucial role for p56 during SI in *Papaver* was demonstrated using specific MAPK inhibitor U0126, by whom the DNA fragmentation, PARP cleavage and SI-induced DEVDase activity were inhibited and loss of pollen viability rescued. Therefore, this represented the first evidence for MAPK signalling in pollen tubes during SI (Li et al., 2007).

1.4.3.3.4 Role of actin in poppy SI

One of the most rapid and dramatic physiological changes observed during *Papaver* SI response is a dynamic rearrangement of the actin cytoskeleton in the pollen tube, within 1-2 min after a challenge with incompatible PrsS proteins (Figure 1.9) (Geitmann et al., 2000, Snowman et al., 2002). F-actin filaments depolymerize and stable punctate actin foci are formed, whose size increases with time and are most characteristic 3 h post SI (Poulter et al., 2010a). Those punctate actin foci are the large aggregates of the F-actin that can reach up to 1 μm in diameter and are very resistant to high concentrations of latrunculin B, actin depolymerising drug that prevents polymerization of F-actin (Poulter et al., 2010a). Associated with the punctate actin foci are several ABPs, such as CAP and ADF (Poulter et al., 2010a).

Isolation of F-actin from untreated and SI pollen protein extracts and subsequent analysis by mass spectrometry FT-ICR-MS revealed a large amount of proteins implicated in binding the F-actin, however, the peptides were screened against Arabidopsis database. Among most prominent candidates that were more abundant in SI sample compared to the untreated

sample were: 14-3-3 proteins, Rab-like proteins, heat-shock proteins and chaperonins, and further investigations of them would provide important information about the complex actin signalling network in incompatible poppy pollen tube (Poulter et al., 2011, Poulter et al., 2010a).

An additional target of SI in incompatible pollen tube is also the microtubule cytoskeleton (Figure 1.9); cortical microtubules rapidly depolymerize upon the addition of PrsS, while the microtubules around the generative cell are more stable, still evident 1 h post-SI, as identified by immunolocalization studies (Poulter et al., 2008). Microtubule and actin cytoskeleton show different and distinct temporal alterations upon SI. There is one-way cross-talk between the two cytoskeletal elements since the actin depolymerization induced by latrunculin B can trigger depolymerization of microtubules but not *vice versa*, demonstrating that actin alterations act upstream of microtubule alterations (Poulter et al., 2008).

F-actin depolymerization or stabilization can push the cell into PCD and a first indication of this in *Papaver* pollen tubes was provided when DNA fragmentation was observed by using latrunculin B, and by jasplakinolide that stabilizes actin filaments, but was reduced when pollen was pretreated with the inhibitor of DEVDase activity, Ac-DEVD-CHO (Thomas et al., 2006). It was also established that stabilization of actin filaments by jasplakinolide prior to depolymerization of actin cytoskeleton by SI induction or latrunculin challenge could rescue pollen DNA degradation, thus preventing PCD (Thomas et al., 2006). Despite the evidence for the crosstalk between actin and microtubule cytoskeleton and the crucial role of actin cytoskeleton during the PCD, microtubule depolymerization or stabilization does not trigger PCD (Poulter et al., 2008).

1.4.3.3.5 Programmed cell death triggered by poppy SI

PCD was first indicated in incompatible *Papaver* pollen by Jordan et al., (2000) with the identification of nuclear DNA fragmentation and inhibition of pollen viability, which was observed in an *S*-specific manner. PCD was demonstrated with the rapid increase in cytochrome *c* release, detected upon pollen challenge with incompatible PrsS proteins, cleavage of bovine Poly-ADP-Ribose Polymerase (PARP), classic substrate for caspases, that generated a 24 kDa PARP cleavage product and activation of caspase-3-like activity (Franklin-Tong et al., 1996, Thomas and Franklin-Tong, 2004). Pretreatment of pollen tubes with the inhibitor of caspase-3-like (or DEVDase) activity, Ac-DEVD-CHO, prior to the SI induction resulted in a significant reduction in the amount of DNA fragmentation measured by TUNEL, thus demonstrating DEVDase activity in the SI-mediated DNA fragmentation (Thomas and Franklin-Tong, 2004). DEVDase activity and several other caspase-like activities were demonstrated by caspase-like cleavage assay using tetrapeptide substrates with fluorescent probe attached (e.g. Ac-DEVD-AMC). Live cell imaging revealed DEVDase activity between 1-2 h post SI in the cytosol of incompatible pollen tube, which moved to the nucleus with the progression of SI, peaking at 5 h post SI (Bosch and Franklin-Tong, 2007). Major caspase-like activity identified was DEVDase, however, a significant increase in VEIDase (caspase-6-like) activity was also detected and significantly lower YVADase (caspase-1-like) and LEVDase (caspase-4-like) activities (Bosch and Franklin-Tong, 2007).

1.4.3.3.6 Role of ROS in *Papaver* SI

ROS and NO are well established to regulate rate and orientation of pollen tube growth and are involved in the polarized growth of pollen tubes (Prado et al., 2008, Potocký et al., 2007). They were recently demonstrated to play an important role during S-RNase based GSI in incompatible pear pollen, where S-RNases disrupt tip-localized ROS and arrest ROS production in mitochondria, which subsequently decreased Ca^{2+} currents and induced depolymerization of actin cytoskeleton and DNA degradation (Wang et al., 2010).

The role of ROS and NO signaling was also demonstrated *in vitro* in the incompatible *Papaver* pollen (Wilkins et al., 2011). Upon the S-specific PrsS challenge of pollen tubes, the increases in ROS were visualised using specific probes at around 5 min post SI, followed by an increase in NO at around 10-20 min (Wilkins et al., 2011). The crosstalk between the two signalling molecules was also established, using H_2O_2 that stimulates ROS production and DPI, that inhibit ROS, and examined the NO production using fluorescence probes (Wilkins et al., 2011). In incompatible poppy pollen tubes, the increases in $[\text{Ca}^{2+}]_{\text{cyt}}$ stimulated increase in ROS and NO. The connection with depolymerization of the actin cytoskeleton and subsequent appearance of punctate actin foci and an increase in DEVDase activity was also made, using ROS scavengers DPI (diphenyliodonium chloride) or TEMPOL and NO scavenger cPTIO, placing ROS and NO, demonstrating that alleviated ROS and NO production reduced the formation of punctate actin foci and DEVDase activity. Thus, ROS and NO production is placed to act downstream of Ca^{2+} signalling, but upstream of the actin cytoskeleton alterations and DEVDase activity (Wilkins et al., 2011).

1.5 *Arabidopsis thaliana* AS A MODEL FOR SELF-INCOMPATIBILITY

Arabidopsis thaliana, also known as thale cress or mouse-ear cress is a small flowering plant from family Brassicaceae. Its importance in plant science is not due to agronomic significance but due to its use as a model plant organism. It has a small genome of 125 Mb that was sequenced, which makes it extremely useful for genetic manipulations. *A. thaliana* is amenable and susceptible for genetic transformation by *Agrobacterium tumefaciens* and large collections of mutants exist in various ecotypes. *A. thaliana*'s lifecycle is very rapid, lasting only 6 weeks and it produces large amount of self-progeny due to its self-compatible state. That has made it an ideal plant for research as it can give results to test hypotheses quickly and there is a large worldwide research community working with it.

A. thaliana is already well-established model for expression of *Brassica*-type of SI (Rea et al., 2010, Nasrallah et al., 2002, Nasrallah et al., 2004). *A. thaliana* lost SI and became self-compatible ~1 million years ago by a mutation in the *SCR* gene, a 213 bp inversion (Tang et al., 2007, Tsuchimatsu et al., 2010). Studies on transgenic *A. thaliana* expressing *A.lyrata* and *C.grandiflora* *S*-determinants revealed that transition from SI to self-fertility occurred multiple times by independent mutations in different accessions of *A. thaliana* as they identified polymorphisms at the *S*-locus and at the SI modifier loci (Sherman-Broyles et al., 2007, Boggs et al., 2009c). These polymorphisms were explained by different strength of SI, from developmentally stable SI to very transient, weak SI or no SI, in different accessions of *A. thaliana*, when it was transformed with a functional SRK/SCR gene pair from *A.lyrata* (Boggs et al., 2009c). The approach of transgenic *A. thaliana* expressing *A.lyrata* and *C.grandiflora* SRK/SCR not only provided information on evolution of selfing but also

enabled new detailed studies of the basis of the SI *S*-specificity. Over 100 residues were tested by mutagenesis in different regions of extracellular domain of SRK, but only six amino acid residues clustered at the same positions within two variants tested were identified to be responsible for SCR-specific activation of SI (Boggs et al., 2009a). The Colombia ecotype of *A. thaliana* was expressing the transient SI and when it was used in mutational analysis a mutation was revealed in RNA-dependent RNA polymerase (RDR6) functioning as a negative regulator of SI in trans-acting siRNA (ta-siRNA) production. This mutation caused an enhancement of SI, pistil elongation and stigma exertion, indicating dual role for SRK in SI and pistil development (Tantikanjana et al., 2009).

New information and questions appeared regarding the role of ARC1 and MLPK1 proteins as well as links between SI and pathogen resistance pathway (Rea et al., 2010). They crossed SRK/SCR expressing *A. thaliana* plants with plants carrying the mutations in various plant-defense implicated loci. If either of numerous plant resistance pathways examined (such as *etr1-1*, *ein2-1*, *npr1-1*, *pad4-1*, *rar1-21*, *sgt1b* or *eds1-1*) would be important for SI pathway then the breakdown of the SI was expected, however, in neither of the analysed crosses or its progeny the breakdown of SI was observed, indicating that these pathways are not required for SI and also illustrating the importance of such a transgenic *A. thaliana* model.

1.6 THE UBIQUITIN-26S PROTEASOME SYSTEM

So far I have given the background on the plant reproduction, signaling, PCD and SI, and I have also made comparisons between SI and HR. Ubiquitin-dependent proteasomal degradation (UbP) plays an important part of HR as well as some SI models. Part of my

studies, presented later in this thesis were involved with investigation of involvement of UbP during SI in *Papaver*, this section gives background on UbP pathway.

All aspects of plant physiology and development are controlled by regulated synthesis of new polypeptides and degradation of existing proteins. Posttranslational addition of the ubiquitin (Ub) to the proteins serves as a tag for the proteasomal degradation by the 26S proteasome, using ATP as an energy source (see Figure 1.10). Substrates for UbP degradation are long-lived proteins or damaged, misfolded or mutated proteins which can cause damage in the cell if they accumulate and so UbP degradation plays a vital role in regulation of various cell signaling processes in plant physiology and development (Vierstra, 2009, Dreher and Callis, 2007). The UbP complex is extremely important for plants since ~ 6 % of proteome (> 1300 genes) in *Arabidopsis* genome is involved in the UbP pathway (Vierstra, 2009). Molecular genetic analyses have also connected individual components of the proteasome to almost all aspects of plant biology, including the cell-cycle, embryogenesis, photomorphogenesis, circadian rhythms, hormone signaling, disease resistance, senescence and self incompatibility (Vierstra, 2003, Vierstra, 2009).

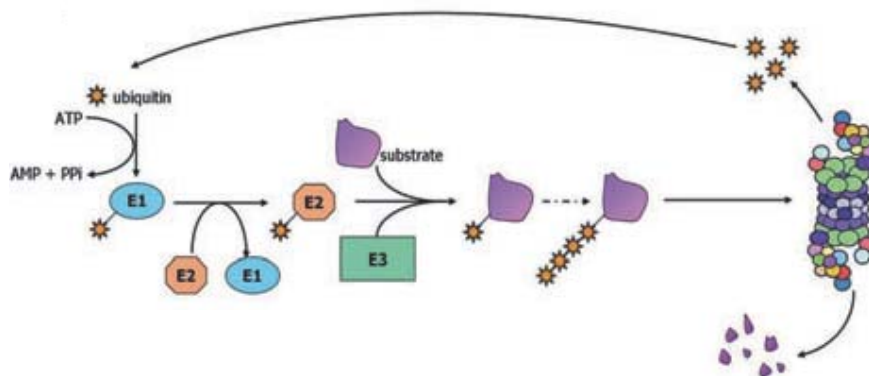


Figure 1.10.: The mechanism of UbP system. Ub activating enzyme E1 activates Ub, which is then transferred to an Ub conjugating enzyme E2 and attached to the target protein by Ub ligase E3. Once the polyUb tail is long enough, protein is targeted to the 26S proteasome and degraded, while Ub is recycled. Image adapted from Dielen et al., 2010.

Ubiquitin (Ub) is a 76 amino acid globular protein that is highly conserved in all eukaryotes (yeasts, animals, and plants). Proteins are marked for degradation when a covalent inter-Ub linkages are made from C-terminal glycine to lysine of the previous Ub to form a poly-Ub chain (polyubiquitination), although some proteins could also be ubiquitinated with a single molecule (monoubiquitination) or on multiple lysine residues by single Ub molecules (multi-monoubiquitination) (Vierstra, 2009, Komander, 2009).

Ubiquitination is a multi-step process. Ub becomes activated by attachment to the Ub-activating enzyme, E1, in an ATP-dependent step. The Ub is then transferred to the second enzyme, called Ub-conjugating enzyme, E2. The final transfer of Ub to the target protein is mediated by a third enzyme, called ubiquitin-ligase, or E3, which is responsible for the selective recognition of appropriate substrate proteins. In some cases, the Ub is first transferred from E2 to E3 and then to the target protein. In other cases, the Ub may be transferred directly from E2 to the target protein in a complex with E3. Most cells contain a single E1, but have many E2s and multiple families of E3 enzymes. Different members of the E2 and E3 families recognize different substrate proteins, and the specificity of these enzymes is what selectively targets cellular proteins for degradation by the UbP pathway (Vierstra, 2009).

In *A.thailana* genes coding for different E3 components fall into different families, based on their domains. HECT (homology to E6-associated protein C-terminus), U-box and RING (really interesting new gene) (Figure 1.11.a,b) are composed from a single polypeptide which has characteristic recognition site for binding of E2 with Ub and different protein binding sites with motifs such as Armadillo (ARM), LRR, Serine/Threonine kinases and others (Jackson et al., 2000).

The largest group of E3 ligases are cullin-RING ligases (CRL), which contain subunits cullin, RBX1 (RING-box1) and other variable target and are further divided into subtypes (Figure 1.11.c).

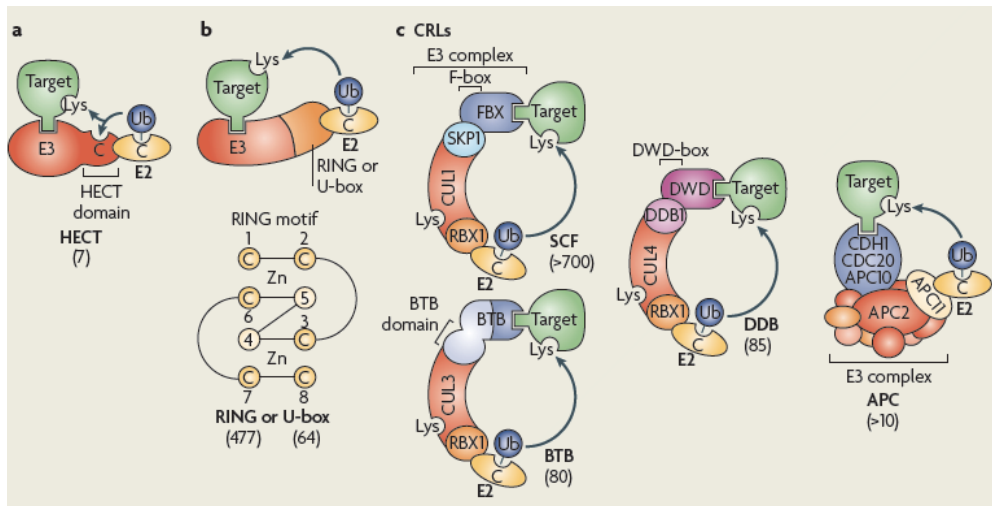


Figure 1.11.: Structures of different types of E3 ligases: (a) HECT; (b) U-box/RING; (c) CRLs are divided in subtypes: SCF (SKP1 (S-phase kinase-associated protein1)-CUL1 (cullin1)-F-box) use F-box proteins for their target specificity, BTBs (bric-a-brac-tramtrac-broad complex) proteins and the third are DDB (DNA damage-binding) using WD40 domain for target recognition; (d) APC (anaphase promoting complex) E3 ligase. Image from Vierstra, 2009.

SCF ligases consist of 4 different polypeptides (SKP1 (S-phase kinase-associated protein1)-CUL1 (cullin1)-F-box (SCF) and RBX1). Specificity of the SCF complex is conferred by the F-Box domain, which contain on its C-terminus one of many protein interaction motifs (ARM, LRR, WD-40, Kelch, DEAD-Box,...) and signature F-Box motif on N-terminus for binding the SKP1, which bind CUL1 through SKP1 bridging protein (ASK1 in *A. thaliana*). Fourth component is RBX1 and it contains RING domain where E2-Ub binds. This unique organization of SCF E3s provides an effective mechanism for recognizing many substrates simply by exchanging F-Box subunits.

Second subtypes are E3s that use BTB (bric-a-brac-tramtrac-broad) complex proteins for target recognition and the third are DNA damage-binding E3s who use WD40 domain for target recognition (Craig et al., 2009, Dielen et al., 2010, Vierstra, 2009).

1.6.1 The 26S Proteasome

The 26S proteasome is a 2 MDa complex that degrades Ub-tagged substrates (see Figure 1.12). It is divided into two particles, the 20S core protease (CP) and the 19S regulatory particle (RP). The CP is created by the assembly of stacked heptameric rings of related α and β subunits (see Figure 1.12). Three of the seven β subunits are responsible for the proteolytic activity: β 1 (PBA1), that has caspase-like activity, β 2 (PBB1/2) that has trypsin-like activity and β 5 (PBE1/2), that has chymotrypsin-like activity (Gu et al., 2010).

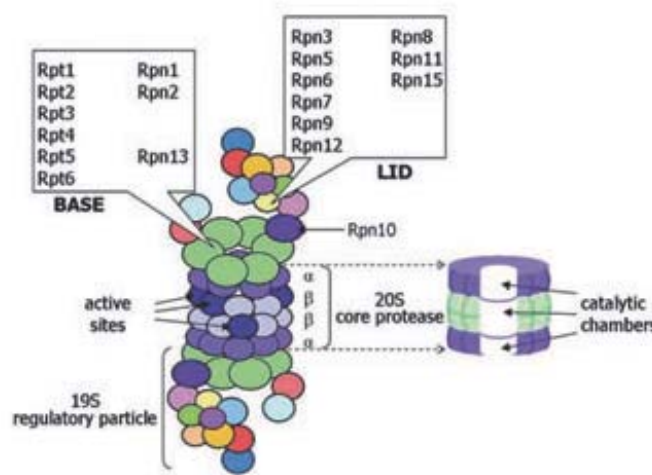


Figure 1.12.: Organization and structure of 26S proteasome. It is comprised of 31 sub-units that are divided into two particles, the 20S core protease (CP) and the 19S regulatory particle (RP) (Vierstra, 2009). The CP is a broad-spectrum ATP- and Ub-independent peptidase created by the assembly of four, stacked heptameric rings of related α (outer rings) and β subunits (inner rings). The central catalytic chamber is housed by β -rings that carry proteolytic activity. Access to this proteolytic chamber is restricted by a narrow gated channel, created by the α -subunit rings that allows only unfolded proteins to enter (Glickman, 2000, Dielen et al., 2010). Each end of the CP is capped by a 19S RP, that is formed by the lid and the base complexes (Kurepa and Smalle, 2008). The RP presumably helps to identify appropriate substrates for breakdown, releases the attached Ubs, opens the α -subunit ring gate, and directs entry of unfolded proteins into the CP lumen for degradation (Vierstra, 2003). Image from Dielen et al., 2010.

Recently, a direct connection between proteasome activation and plant PCD was established by Hatsugai et al., (2009), where they demonstrated, using genetical, biochemical and biological approaches, that proteasome subunit PBA1 had a DEVDase activity. It acts as a

long sought plant caspase-3-like enzyme and is responsible for the vacuolar membrane and plasma membrane fusion-induced HR cell death in response to bacteria attack. By using a proteasome inhibitors β -lactone and more specific Ac-APnLD-CHO, inhibitor of the β 1 subunit, and caspase-3 inhibitor they demonstrated that the DEVDase activity and the PBA1 activity were abolished, and the HR was prevented (Hatsugai et al., 2009). In animals and yeast, β 1 subunits of the proteasomes are long known to have caspase-like sites (Kisselev et al., 2003).

Identification of selective proteasome inhibitors has allowed a definition of the roles of the UbP pathway in various cellular processes (Lee and Goldberg, 1998, Kisselev and Goldberg, 2001). Proteasome inhibitors represent valuable tool to enhance cell content in the protein studies since proteins destined for rapid degradation are often hard to isolate or express. The most widely used are the peptide aldehydes, such as Cbz-leu-leu-leucinal (MG132), acting on a chymotrypsin-like activity, or lactacystin and β -lactone.

Recently a development of small membrane permeable fluorescent probe was presented that interact with the plant proteasome catalytic subunit and can allow the quantification of proteasome activities for *in vitro* and *in vivo* studies (Gu et al., 2010, Kolodziejek et al., 2011). It was also demonstrated that plant proteasome activity was inhibited using caspase-3 inhibitor. This activity-based probe will certainly expand studies on plant proteasomes in the future.

1.6.2 Ubiquitination and self-incompatibility

SI mechanisms are described in details in the section 1.4. The link between the S-RNase-based GSI system and ubiquitination is the male *S*-determinant, an F-box protein (SLF/SFB) which is part of an SCF ubiquitin ligase complex (SCF^{SLF/SFB}) (Meng et al., 2011, McClure et al., 2011). The compartmentalization models of SI presumes, that following pollination, self and non-self S-RNases are localized in the pollen tube. In the compatible interaction S-RNases are ubiquitinated by SCF^{SLF/SFB} and afterwards degraded by the 26S proteasome, while S-RNases in the incompatible interaction are left intact and due to their cytotoxic activity they degrade RNA of the pollen tube and inhibit the pollen growth (Figure 1.13.b) (Goldraij et al., 2006, Meng et al., 2011). However, the issue emerging is, that SCF E3 ligases interact with the F-box protein with Skp1 and also with the specific substrate for degradation through the specific protein-protein interaction domain (ARM, WD40, leucine-rich repeats, etc) and none of that domains have been identified in SLF. Additionally, in the *Antirrhinum*, the SCF complex was termed a conventional SCF complex that contains novel SSK1 protein (SLF-interacting SKP1-like1), but is not encoded by polymorphic gene, but monomorphic and might be important for the interaction with AhSLF2 (Zhao et al., 2010). In *Petunia inflata*, the SLF complex is also not as simple as initially thought but might be a component of new E3 ligase complex, containing PiCUL1-g and PiSBP1 (*P. inflata* S-RNase Binding Protein1, a RING-HC protein), and it does not contain SKP1 or RBX1 (Hua and Kao, 2006). So in order to organise the complex, instead of Skp1, the PiSBP1 forms complex with PiCUL1-G and PiSLF, and also interacts with E2, like RBX1 (it plays a dual role) (Hua and Kao, 2006). It is believed they might have more general role as they are expressed in all the tissues (Hua and Kao, 2006).

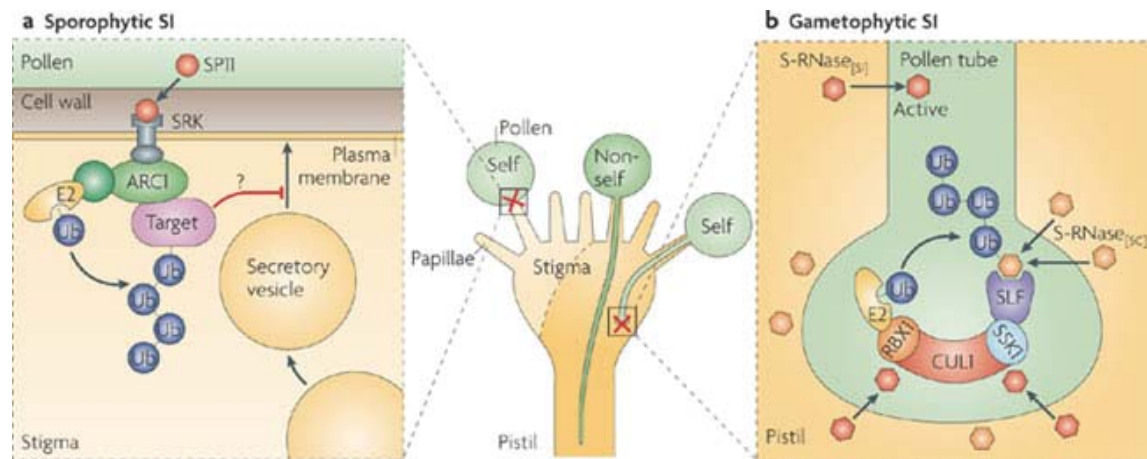


Figure 1.13. Involvement of UbP during SI. (a) Sporophytic SI is controlled by ARC1 U-box E3 ligase. Phosphorylation and presumably activation of ARC1 is triggered upon recognition of SP11 from pollen and SRK on papillae surface of stigma. Self-fertilization is prevented as ubiquitylation by ARC1 block water and nutrients needed for pollen germination. (b) Gametophytic SI is controlled by a SCF E3 ligase assembled with polymorphic SLF. Growth of self pollen is inhibited by the entrance of cognate S-RNase in transmitting tract. Non-self S-RNases are disabled with an ubiquitylation, and consequently degradation, by the SCF^{SLF} E3 with help of SSK1. Image from Vierstra, 2009.

Ubiquitination was also reported from the sporophytic SI (see Figure 1.13.a). In *Brassica napus* SI an U-box protein ARC1 (Armadillo repeat containing protein 1) was identified, which is a close homologue to the *A. thaliana* PUB17 and *Nicotiana* ACRE276, both playing an important role in hypersensitive response (Stone et al., 2003, Yang et al., 2006). The positive role of ARC1 was identified by the antisense suppression of *ARC1* in the stigma that lead to pollen tube growth of incompatible *Brassica* pollen (Stone et al., 1999). During the SI in Brassicaceae, ARC1 binds to the SRK (*S*-locus receptor kinase), a female determinant of *Brassica* SI, and functions downstream of activated SRK by interacting with Exo70A1 (see Figure 1.4.5.a) (Stone et al., 2003, Samuel et al., 2009). ARC1 was also demonstrated to colocalize with the subunits of the proteasome and the increase in ubiquitinated proteins was observed in the SI pistils (Stone et al., 2003). Exo70A1 is thus negatively regulated by SI through ARC1-mediated ubiquitination (Samuel et al., 2009).

1.7 SUMMARY AND OBJECTIVE

To summarize, in the introduction I have presented in details the SI system, which represents my main research. I also gave the background on plant reproduction, the role of pollen tube, PCD, HR, plant cell-cell signalling, plant receptors, use of *A. thaliana* as a model system and UbP degradation. The reason for such a broad range of topics is that this thesis presents research on three inter-related projects, studying the mechanism of self-incompatibility (SI) in *Papaver rhoeas* and *Arabidopsis thaliana*. My objectives were:

- Elucidating the possible involvement of ubiquitin proteasome (UbP) signalling pathway during SI in *Papaver* pollen

The aim was to investigate the link between the two different mechanisms and to establish the role of UbP degradation during *Papaver* SI-induced PCD. Functional involvement of UbP pathway was investigated using inhibitors of proteasomal degradation, MG132, measuring levels of ubiquitination, inhibition of pollen tube growth, pollen viability and signalling to the caspase-like activity.

- Analysis of *Papaver* pollen *S*-determinant, PrpS and interaction between PrpS and PrsS

The aim was to establish the nature of the *Papaver* pollen determinant and to characterize the PrpS binding to PrsS.

- Characterization and functional analysis of *Papaver S*-determinants in *A. thaliana*.

This project was initiated in order to test whether the *Papaver* SI system might work when the *S*-determinants were moved to another species. Several lines of investigation were followed in order to achieve that. Initially, the segregation analysis and the expression analysis of PrpS and PrsS was carried out. Functional

analysis studies were then conducted *in vitro* on transgenic *A. thaliana* pollen expressing PrpS-GFP fusion proteins and *in vivo*. *In vitro* analysis investigated the major characteristics of the poppy SI response, such as *S*-specific inhibition of pollen tube growth, formation of punctate actin foci and *S*-specific loss of viability. Following successful *in vitro* analysis, *in vivo* analysis was attempted by performing crosses between *A. thaliana* expressing PrsS protein and PrpS-GFP, respectively.

CHAPTER 2.

Materials and Methods

2.1. Plant material: *Papaver rhoeas*

2.1.1. *Papaver* plant cultivation

Seeds of *Papaver rhoeas* L. (Shirley) of both known and unknown pedigree were first allowed to germinate in humidified Petri dishes for ~2 days. Germinated seeds were potted in John Innes No. 1 potting compost and kept in a greenhouse at 15 °C. Resultant plants were thinned to one per pot after growing to a height of between 5 and 10 cm. Around 8 weeks later, plants were allowed to harden outside for around 4 weeks and were then transplanted to a field in rows with approximately 50 cm between plants and 90 cm between rows (Wheeler, 2001)

2.1.2. Determination of *Papaver* S-genotype

The S-haplotype was determined by pollinating each plant with pollen of known S-genotype. Once plants were in flower, two flowers, 1-2 days prior to anthesis, were emasculated using forceps and covered with a cellophane bag, to prevent entrance of insect pollinators. Emasculated flowers were pollinated the next day by application of pollen with a fine paintbrush directly onto the stigmatic rays. After pollination, cellophane bags were replaced over the flower and stigmas were harvested one day after pollination. The pollinated portion of the stigma was removed with a scalpel, placed in aniline blue, and left overnight to allow the stigmas to soften. A sample of the stigma was then placed on a microscope slide and observed under a microscope using UV illumination (see Figure 2.1.a,b). All families grown were two-class families and thus were pollinated with two classes of pollen, one to provide a fully incompatible pollination and one to provide a half-compatible pollination. Those

stigmas exhibiting fully incompatible pollination had easily identifiable callose in the pollen grains and few, if any, pollen tubes. Those exhibiting half-compatible pollinations had 50 % reacting as above whilst the remainder had no callose in the grain and long pollen tubes with callose plugs at intervals along the length of the tube.

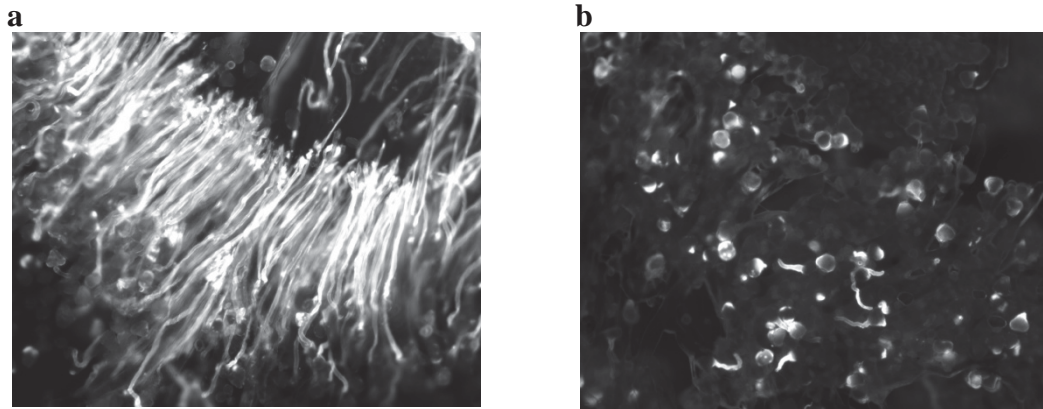


Figure 2.1: Examples of aniline blue stained stigma squashes (a) compatible pollination and (b) incompatible pollination in poppy as visualised using UV-illumination.

2.1.3. Collection of *Papaver* pollen

Flowers with a long stem at 1 day prior to anthesis were harvested approximately 15 cm below the bud. Petals and sepals were removed while buds were placed in a cellophane bag and hung upside-down on the bench in the aerated glasshouse overnight, leaving anthers to shed pollen. Pollen was released by vigorous shaking, and collected by tipping into gelatin capsules. Capsules were then dried over silica gel at room temperature (RT) for about 1 h before freezing at -20 °C.

2.1.4. *Papaver* pollen tube growth *in vitro*

Pollen was hydrated for at least 30 min in a moist chamber at 25 °C. The shape of pollen grains was used to assess the state of hydration. When desiccated, pollen grains take an elliptical form, when hydrated pollen grains appear spherical. Following hydration, pollen was re-suspended in liquid germination medium (GM). Then pollen grains were plated on solid GM (GM plus 1.2 % agarose) in 9 cm Petri dishes. Normally, for 10 mg of pollen, 1.0 – 1.2 mL of GM was required. Pollen was grown for at least 45 min and assessed for percentage germination prior to experimentation. Following growth, pollen was treated as required for the experiment.

Liquid Growth Medium (GM):

13.5 % (w/v) sucrose
0.01 % H₃BO₃
0.01 % KNO₃
0.01 % Mg(NO₃)₂·6H₂O
0.036 % CaCl₂·H₂O

The solution was made as 13.5 % sucrose and then 0.5 % of GM salts stock was added to make up liquid GM.

Growth Medium Salt Stock:

2 % (w/v) H₃BO₃
2 % (w/v) KNO₃
2 % (w/v) Mg(NO₃)₂·6H₂O
7.2 % (w/v) CaCl₂·H₂O

Solid GM:

liquid GM with addition of 1.2 % agarose

2.1.5. Production of *Papaver* seeds

Emasculated *Papaver* flowers were pollinated with pollen of known *S*-genotype, covered with cellophane bag and left for approximately 6 weeks. After approximately 6 weeks seeds were collected from seed pods and stored in paper bags at 4 °C.

2.2. Plant material: *Arabidopsis thaliana*

2.2.1. *A. thaliana* cultivation

Equivalent of 50 μL of seeds of transgenic *A. thaliana* and untransformed Col-0 were sterilised with 500 μl of 20 % commercial bleach and continuously mixed with gentle shaking for 20 min. Seeds were then washed 4 times with 500 μL of sterile distilled water (SDW) and mixed by shaking for 15 min each time, then, centrifuged quickly to decant. Finally, seeds were resuspended in 200 μL of fresh SDW. Meanwhile, plates with Murashige and Skoog (MS) media were prepared by pouring autoclaved media with selection marker (50 $\mu\text{g } \mu\text{L}^{-1}$ Kanamycin, 25 $\mu\text{g } \mu\text{L}^{-1}$ Basta) for transgenic seeds or without for untransformed Col-0 seeds. Using a cut end sterile pipette tip seeds were plated in sterile conditions. The plated seeds were kept at 4 °C for two days in order to break dormancy and to synchronise seed germination before moving them to constant temperature room at 22 °C for two weeks. The amount of grown seedlings on the plates was determined for segregation analysis.

Transgenic *A. thaliana* lines with poppy *S*-determinants and untransformed Col-0 seeds were planted in pots labelled individually with yellow stick for genetically modified plants and white stick for untransformed plants. Immediately after transferring seedlings to pots, the tray was covered with cling-film for 2 days. *A. thaliana* plants were grown in pots, containing Levington M2 compost with Silvapearl in the greenhouse at 20 – 22 °C and under 16/8 h photoperiod conditions. Seeds were sown every two weeks. Plants were usually potted every two weeks and it normally took two to four weeks for the plants to flower. When plants flowered, each pot was placed in plant sleeve to contain the pollen spreading.

The plants were numbered from the first generation, with the number indicating original line, and the subsequent number of each generation after the dot. Generation numbers were separated by dot (.) or by the hyphen (-) for easier indication.

Murashige-Skoog (MS) media:

2.2 g L⁻¹ of MS powder

pH adjusted to 5.6-5.8

1 % of agar

Media was autoclaved before use.

2.2.2. *A. thaliana* plant conditions

A. thaliana pollen is notorious for its difficulties in germination and only recently some detailed studies on *A. thaliana* pollen tube germination emerged (Fan et al., 2001, Boavida and McCormick, 2007, Bou Daher et al., 2009, Johnson-Brousseau and McCormick, 2004). The difficulties regarding *A. thaliana in vitro* pollen germination were connected with its tricellularity (Boavida and McCormick, 2007, Bou Daher et al., 2009), and so far, majority of pollen being studied was from bicellular species (poppy, tobacco).

However, despite the studies performed on *A. thaliana* pollen germination, the work on *A. thaliana* was more demanding than *Papaver* pollen. There were numerous differences in the research procedures of pollen assays in *A. thaliana* and *Papaver*, the most obvious one was pollen collection. While poppy pollen collection occurred once a year in a bulk batches with pollen being stored at -20 °C, fresh *A. thaliana* pollen was collected on a day of the experiment, as it was difficult to obtain a bulk batch. *A. thaliana* was producing new flowers every day and pollen was collected from day 0 flowers - stage 13 (Smyth et al., 1990). It was observed and reported that with the older flowers and older plants pollen germination rates

were decreasing (Boavida and McCormick, 2007), so in order to ensure reproducibility of results, only newly opened flowers were harvested for pollen collection.

2.2.3. Collection and germination of *A. thaliana* pollen

In the morning, 40 *A. thaliana* flowers (stage 13) were collected in a 500 µL microfuge tube containing liquid *A. thaliana* pollen GM (AtGM). Pollen was harvested by vigorous shaking and then the flowers were transferred into a second tube containing AtGM in order to obtain maximal amount of pollen. The process was repeated once more before the flowers were discarded. The AtGM with the pollen grains was centrifuged for 2 min at 3500 rpm and the excess liquid medium was removed. The pollen was pooled together, and resuspended in fresh AtGM and centrifuged again (2 min, 3500 rpm). Following centrifugation, the excess liquid was removed so that the final volume left in the tube for pollen germination was 100 µL. Pollen was pre-germinated for at least 45 min and assessed for percentage germination prior to experimentation. Following growth, pollen was treated as required for the experiment.

Arabidopsis thaliana liquid germination medium (AtGM):

18 % sucrose

0.01 % H₃BO₃

1.0 mM CaCl₂

1.0 mM Ca(NO₃)₂

1.0 mM MgSO₄

Sucrose was dissolved prior to the addition of the other salt components. pH adjusted to 7.0 and sterilised by filtration before use.

2.2.4. Collection of *A. thaliana* seeds

Trays with *A. thaliana* plants, which had fully formed siliques and no more flowering buds were lifted from the table so their water supply was disabled and plants were allowed to dry for about two weeks. Seeds were collected by gently shaking *A. thaliana* plants on the paper surface. Before placing them in a microfuge tube, seeds were sieved so as to remove remaining plant debris. Seeds from each plant were collected in separate clearly labelled tubes.

2.3 Experiments

2.3.1. Production of recombinant PrsS proteins

Transformant *E. coli* cells expressing PrsS₁, PrsS₃ and PrsS₈, separately, were plated from a glycerol stock, onto plates containing LB-agar medium with 50 µg mL⁻¹ ampicilin (LB-Amp) and incubated at 37 °C for about 16 h. The next day the colony was grown for 16 h in a 2 L flask containing 200 mL of LB-Amp at 37 °C on a shaker (200 rpm). Half of the culture (100 mL) was transferred into another 2 L flask with fresh 100 mL of LB-Amp. Protein over-expression was induced with 0.5 mM IPTG and incubated for 6 h at 37 °C with shaking at 200 rpm. A sample of the culture can be used for analysis of induction by SDS-PAGE. Culture was centrifuged at 5000 rpm at 4 °C for 10 min in Beckman centrifuge and pellets were stored at -20 °C until needed.

For the analysis, the pellet was resuspended in 200 mL of cold lysis buffer and centrifuged for 10 min at 5000 rpm at 4 °C. The pellet was resuspended in 20 mL of ice-cold lysis buffer, transferred in smaller tubes and then, lysozyme was added at a final concentration of

0.2 mg mL⁻¹ and 0.25 mM PMSF. Reaction mix was incubated at 4 °C for 1.5 h before 3 mM sodium deoxycholate was added with 0.125 mM PMSF and incubated at 37 °C for 30 min, during which time the solution became very viscous. After that, samples were sonicated on ice for at least 5 times for 30 s pulses at 10 amplitude microns with at least 30 s break in between to allow cooling between each pulse. Following the sonication step, the solution was centrifuged at 5000 rpm for 20 min at 4 °C. The pellet was washed with 20 mL of cold lysozyme buffer. The whole cycle of pellet washing, sonications and centrifugation was repeated for 5-7 times, the pellet being frozen over night at -20 °C where necessary.

Proteins in inclusion bodies in the pellet were then solubilised in 6 M guanidine hydrochloride and 500 mM 2-mercaptoethylamine by shaking in orbital shaker for 4 h at 22 °C. In contrast with the previous protocol, which instructed to solubilize for 2 h, it was found that protein yield was increased by solubilising for 4 h. Following solubilisation, the suspension was centrifuged (15 min, 5000 rpm) at 20 °C and the supernatant was kept for protein refolding in a cold refolding buffer. Refolding took place at 4 °C by adding protein aliquots very slowly into the buffer while being stirred. The solution was incubated at 4 °C for 16 h with constant agitation. Refolded proteins were dialysed in three exchanges of at least 5 L of the cold dialysis buffer: in the morning, afternoon and overnight. The next day, the last set of the dialysis buffer was discarded (except for ~100 mL). Pressure was removed from the dialysis tubes by removing the clips. The tubes were then placed in the beaker with ~2 cm of dialysis buffer. Over that, the solid PEG6000 was generously sprinkled while the beaker was gently shaken. More PEG6000 was regularly added during the day until protein had concentrated to ~10 % of its original volume. When the desired volume was reached, PEG was washed from the tubes with distilled water, and proteins were aliquoted 1 mL to microtubes and snap-frozen in liquid nitrogen. Proteins were stored at -80 °C until required.

At every stage of the protocol, small samples were taken to check protein concentrations either on a protein gel (by SDS-PAGE) or with Bradford assay (Bradford, 1976).

Lysis Buffer:

50 mM Tris·HCl; pH 8
100 mM NaCl
1 mM EDTA

Refolding Buffer:

100 mM Tris
2 mM EDTA
500 mM L-arginine hydrochloride
10 mM cystamine dihydrochloride
5 % glycerol
pH 8

Dialysis Buffer:

50 mM Tris·HCl, pH 8
100 mM NaCl
2 mM EDTA

2.3.2. Treatments of pollen tubes

Following successful pollen germination, pollen tubes were treated with PrsS proteins for SI response, incubated with various drugs or pretreated with drugs and then with PrsS proteins.

PrsS proteins:

Recombinant PrsS proteins (Kakeda et al., 1998) were dialysed over night at 4 °C from Tris buffer into GM (for experiments with poppy pollen) or AtGM (for experiments with Arabidopsis pollen) using dialysis tubing with 12000 – 14000 Mw cutoff. In 1 L of GM or AtGM, 1 mL of PrsS proteins could be dialysed. After dialysis, the protein concentration was determined by Bradford assay (Bradford, 1976) using bovine serum albumin as standard. For an induction of the SI response, PrsS proteins were added to pollen growing *in vitro* at a final concentration of 10 µg mL⁻¹ unless stated differently.

Treatment with N-(benzyloxycarbonyl)-leucinyll-leucinyll-leucinal (MG132):

Pollen tubes growing *in vitro* were pretreated with 40 μ M MG132 for 30 min prior to the addition of recombinant PrsS proteins and left for 5 h. Controls comprised of 40 μ M MG132 treatment and were left for the same time. DMSO was used as a solvent control.

Treatment with Ac-DEVD-CHO:

Tubes were pretreated with 100 μ M Ac-DEVD-CHO for 60 min prior to addition of S-proteins and left for 5 h. Controls comprised of 100 μ M Ac-DEVD-CHO and were left for the same time.

2.3.3. Pollen protein extraction

Pollen tubes grown under specified conditions were collected from the Petri dish using a pipette with a cut tip, placed into a 1.5 mL microtubes (poppy pollen) and centrifuged (1 min, 13200 rpm) in a tabletop microcentrifuge. In the case of the Arabidopsis pollen experiments, centrifuging was for 2 min at 4000 rpm. Then the supernatant was discarded and an equal volume of 2X Tris extraction buffer with protease inhibitor or TM extraction buffer was added to the volume left in the microtube to make a final 1X concentration. Samples were roughly grounded using plastic grinders in the microtube before being snap-frozen in liquid N₂ and stored at -20 °C until required.

Sample protein extracts were prepared by sonication 5 x 5 s at 10 amplitude microns (poppy pollen) or 5 x 2 s (Arabidopsis pollen) and kept on ice during sonication to prevent overheating. After sonication, samples were kept on ice for 15 min and then centrifuged (30 min at 13200 rpm at 4 °C). The supernatant was recovered into a microtube and then

centrifuged again (10 min, 13 200 rpm at 4 °C). The pellet was frozen at -20 °C. Clear supernatant was carefully recovered into a microtube. Samples were kept on ice during all the steps.

The protein concentration was determined by Bradford assay (Bradford, 1976) and then samples were used for SDS-PAGE or caspase-like activity assays.

2X Tris extraction buffer:

100 mM Tris-HCL pH 8
200 mM NaCl
2.0 mM EDTA
1.0 M sucrose
2 X final protease inhibitor cocktail

Extraction buffer for caspase assay:

50 mM NaOAc
10 mM L-cysteine
10 % glycerol
0.1 % Chaps
pH 5 and pH 6

2x Tris Extraction buffer for TM proteins:

2x Tris extraction buffer
0.2 % Triton X-100

Extraction buffer for TM proteins:

30 mM Hepes
2 % Triton X-100
300 mM NaCl
30 % Glycerol
5 mM MgCl₂
2 mM β-mercaptoethanol
pH 7.5

2.3.4. Bradford Assay

Protein concentration was estimated through the Bradford assay (Bradford, 1976) using BSA as standard. Protein assay reagent (BioRad, UK) (which contains Coomassie® Brilliant Blue G-250) was added to diluted protein samples, and its absorbance measured at 595 nm with a spectrophotometer.

For most of the experiments, protein concentration needed to be calculated as accurately as possible, so two replicates were measured for each sample and also compared with a BSA.

2.3.5. SDS-Polyacrylamide gel electrophoresis (SDS-PAGE)

2.3.5.1. Preparation of SDS-PAGE

Gels were cast using the BioRad self-assembly kits using standard procedures.

2.3.5.2. Protein staining on the polyacrylamide gel

After electrophoresis, gels were soaked for 1–2 h at room temperature in a Coomassie staining solution and then, destained by incubating the gel in a destaining solution for 2 h or until the bands were clearly apparent. Finally, gels were dried using vacuum drier for 1.5 h at 70 °C.

Coomassie staining solution:
0.1 % Coomassie Blue R-250
45 % (v/v) methanol
10 % glacial acetic acid

Destaining solution:
30 % (v/v) methanol
10 % (v/v) glacial acetic acid

2.3.6. Western blot

2.3.6.1. Protein transfer

After protein separation by SDS-PAGE the resolving gel was then transferred onto a sponge and two sheets of filter paper (Whatman) soaked in the protein transfer buffer. A nitrocellulose membrane (Hybond-C extra, Amersham) was cut to size and laid over the gel. A glass rod was used to remove any air bubbles. Two more sheets of filter paper (Whatman) were laid on top of the membrane and finally a sponge was laid on it. The layered arrangement was sandwiched between two electroblotting pads (BioRad). This was then inserted into the electroblotting tank (BioRad), which was filled with protein transfer buffer.

An ice block was also placed in the tank to prevent a overheating due to the high voltage used for blotting. BioRad power packs were used to blot the gel at 350 mA for 2 h. Following transfer, the nylon membrane was removed and placed in blocking solution at 4 °C for 16 h.

Protein transfer buffer:

20 % (v/v) methanol
0.2 M glycine
25 mM Tris

Blocking solution:

10 % (v/v) 10x TBS
0.01 % Tween
5 % (w/v) milk powder

10 x Tris Buffered Saline (TBS):

24.22 gL⁻¹ Tris
80 gL⁻¹ NaCl
pH 7.6

2.3.6.2. Protein immunodetection

After blocking the membrane, it was incubated with primary antibodies (diluted at varying concentrations depending on the antibody being used), in a blocking solution for 2 h at room temperature. Then, three washes of 10 min each blocking solution were carried out and then, incubated with the secondary antibody. If the primary antibody was raised in mouse, an alkaline phosphatase-conjugated anti-mouse immunoglobulin was used as the secondary antibody (alkaline phosphatase detection), while if the primary one was raised in goat, a horse radish peroxidase-conjugated anti-goat immunoglobulin was used (enhanced chemiluminescence detection) diluted 1:5000 in blocking solution for 1 h. The blot was then washed 1x 10 min in blocking solution and 3x 10 min in 1X TBS-Tween.

Primary antibodies:

Monoclonal anti-ubiquitin (Sigma); titre 1:5000

Monoclonal anti-ubiquitin (Santa Cruz); titre 1:5000

Monoclonal anti-ubiquitin (donated by Dr Ari Sadanandom); titre 1:2500

Poly-clonal anti PrpS₁ C terminus (60C); titre 1:500 or 1 :1000

Secondary antibodies:

Anti-mouse HRP; titre 1:5000

Anti-mouse AP; titre 1:5000

Anti-rat AP; titre 1:5000

Anti-goat HRP; titre 1:5000

2.3.6.2.1. Enhanced chemiluminescence detection

ECL western blotting reagents were used to detect the HRP conjugated secondary antibody. Solutions A and B (Yakunin and Hallenbeck, 1998) were mixed 1:1 and poured over the blot for 1 min. Excess reagents were removed. Blots were analysed using FluorS Multi-imager and Quantity One software (Biorad).

Solution A

100 mM glycine, pH 10 (with NaOH)

0.4 mM luminol

8 mM 4-iodophenol

Solution B

0.12 % (w/w) H₂O₂ in SDW

2.3.6.2.2. Light intensity evaluation of western blots (ECL detection)

Light intensity was evaluated on images taken with the Fluor-S Multiimager system using Quantity One software. First, a rectangular volume was created around the area of interest and then a volume analysis report was requested for this area. Results came out as Volume in units counts per square millimeter ($\text{CNT} \cdot \text{mm}^2$) or Adjusted Volume ($\text{CNT} \cdot \text{mm}^2$). Adjusted volume refers to volume minus background volume.

2.3.6.2.3. Alkaline Phosphatase detection

66 μl NBT (nitro blue tetrazolium) and 33 μl BCIP (5-bromo-4-chloro-3-indolyl-phosphate) was added to 9.9 ml alkaline phosphatase detection buffer. The solution was poured over the blot and left in darkness until a colour change was observed where the Alkaline phosphatase-conjugated secondary antibody was present.

Alkaline phosphatase detection buffer:

100 mM NaCl
5 mM MgCl_2
100 mM Tris
pH 9.5

2.3.6.3. Modified western blot for detection of membrane proteins

Since the proteins are likely to aggregate during boiling, the protocol for protein loading on the SDS-PAGE gel was modified so the sample was not boiled prior to loading on the gel. Omitting the boiling step, SDS-PAGE was undertaken as described in section 2.3.5.1. Protein transfer in western blot was done as described in section 2.3.6.1. The modification

was at the end of the transfer when the blot was incubated in a stripping buffer for 15 min at 55 °C with mild agitation (Kaur and Bachhawat, 2009). The stripping buffer was washed from the blot with several washes with 1x TBST at RT until the β -mercaptoethanol smell was no longer detected. Then, the membrane was placed in a blocking solution at 4 °C overnight and immunodetection was undertaken as described in section 2.3.6.2.

Stripping buffer:

100 mM β -mercaptoethanol

2 % SDS

62.5 mM Tris-HCl pH 6.7

2.3.7. Slot-blot binding assay

Four overlapping 15-mer peptides, spanning the predicted 35 amino acid extracellular domain of PrpS₁ and a scrambled peptide were synthesized by Alta Bioscience (University of Birmingham, UK). These peptides were bound to a polyvinyl difluoride (PVDF) membrane using a slot-blotter. The membrane was properly labelled and pre-wetted with methanol for 10 s. Then, it was incubated with MilliQ water for 10 min on a shaker and finally incubated in PBS for 10 min with constant gentle shaking. The slot-blot filtration manifold was attached to a vacuum pump and after the insertion of the membrane, the slot-blot system was assembled and the vacuum pump was turned on. Different amounts of peptides (10 μ g, 1.0 μ g and 0.1 μ g) in the final volume of 50 μ L were bound to the membrane. The scrambled peptide control was used at the same concentrations, while the recombinant PrpS at concentration 0.1 μ g. The membrane carrying the PrpS peptides was immediately rinsed with PBS and then incubated with 5 % skimmed milk in PBS for 1 h at room temperature. The membrane was then incubated with 20 μ g mL⁻¹ recombinant PrpS₁

protein previously dialysed, as described above, against PBS at room temperature for 16 h to allow binding. Then, membrane was washed with PBS and blocked with 5 % milk in TBST for 1 h at room temperature. The membrane was then incubated for 2 h with the primary antibody raised against PrpS₁ to detect S protein binding to PrpS. Following incubation, the membrane was washed with 5 % skimmed milk in TBST and then incubated with anti-rabbit antibody conjugated with alkaline phosphatase. Detection was done with NBT/BCIP in alkaline phosphatase detection buffer as described above.

Peptides:

PrpS₁ A1 - VKLLGLVLHRLSFSE

PrpS₁ A2 - LHRLSFSEDQKWVVA

PrpS₁ A3 - DQKWVVAFGTAAICD

PrpS₁ A4 - TAAICDVLLVPKNML

PrpS₁ A1 scrambled 1 - ELGVKLHSLSVLRFL

PrpS₁ A3 scrambled 1 - FTVDVKDCAAAGQI

PrpS₈ A1 - LKLLGWVLQHLTVTE

PrpS₈ A1 scrambled 1 - GLTWLQLKEVHLTVL

Phosphate Buffer Saline (PBS):

137 mM NaCl

2.7 mM KCl

10 mM Na₂HPO₄

2 mM KH₂PO₄

Primary antibodies:

Polyclonal anti-PrsS₁; titre 1:6000

Polyclonal anti-PrsS₃; titre 1:5000

Polyclonal anti-PrsS₈; titre 1:4000

Secondary antibody:

Anti-rabbit AP; titre 1:5000

Prior to use, both antibodies were cleaned up using an Immobilised *E. coli* lysate kit, Pierce, Rockford (see next chapter 2.3.8).

2.3.8. Purification of antibodies using Immobilised *E.coli* lysate kit

Possible non-specific antibodies contained in the primary antibody preparations were eliminated by chromatography using a column with immobilised *E. coli* total proteins. The antibody solution was passed through an *E. coli* protein column, previously equilibrated with 10 mL TBS buffer (BupHTM Tris buffered saline dissolved in 500 mL of SDW). After adding a 1 mL crude antibody solution to the column, an extra 100 µL TBS was added and fractions were collected in a 1.5 mL microtube. Protein concentration of all fractions was determined through Bradford assay (Bradford, 1976). Fractions with the highest protein concentration were pooled. Finally, the column was washed with at least 10 mL regeneration buffer, followed by 10 mL TBS plus 0.02 % sodium azide for storage.

2.3.9. Pollen tube length measurement

Pollen tubes were grown and given the appropriate treatment and mounted on glass slides. Pollen was observed using a Nikon Eclipse Te300 microscope attached to a cooled coupled device (CCD) camera supplied by Applied Imaging, UK. Capture and analysis of images was achieved with a Nikon NIS elements 3.2 image analysis system. Images were saved as jp2 files. Tube lengths were measured (50 tubes per treatment; $N = 3$) with the NIS elements 3.2 software. Measurements were exported into a Microsoft Excel file where statistical analysis was performed.

2.3.10. Programmed cell death – caspase-like activity assay

To determine the presence of caspase-like activity, we used the fluorogenic caspase-3 substrate Ac-DEVD-AMC (Calbiochem). Pollen (*Papaver* or *Arabidopsis*) was hydrated and grown as described in sections 2.1.4 and 2.2.3, respectively. After ~1 h of growth, pollen tubes were treated as indicated in each experiment. Pollen was left in GM containing the indicated treatment for 5 h at room temperature as this period gives the highest caspase activity if PCD was occurring (Bosch and Franklin-Tong, 2007). The pollen was then collected into 1.5 ml microtubes and the protein extracted as described in section 2.3.3 and the protein concentration was determined as described in section 2.3.4. The protein concentration was adjusted to $1 \mu\text{g } \mu\text{L}^{-1}$ by diluting the extract in the sodium acetate extraction buffer (pH 6) and protein concentration was measured again.

Samples with $10 \mu\text{g}$ were extracted with pH 6 caspase extraction buffer and were loaded into 96 well plate in duplicates, incubated with $50 \mu\text{M}$ Ac-DEVD-AMC (Calbiochem),

fluorogenic caspase-3 substrate in caspase buffer and adjusted to pH 5, since this is the optimum pH for caspase action in poppy pollen (Bosch and Franklin-Tong, 2007). If protein extracts were less than $1 \mu\text{g } \mu\text{L}^{-1}$, the appropriate volume of protein extract was added into the well of the 96 well plate to make $10 \mu\text{g}$ of protein. The other samples in that experiment were made up to the greatest volume by adding the appropriate amount of pH 6.0 sodium acetate buffer so that all wells had the same volume of pH 6 buffer and protein. Fluorescence was monitored at 460 nm using a time-resolved fluorescence plate reader (FLUOstar OPTIMA; BMG LABTECH) every 15 min over a time period of 5 h. The caspase activity for each sample was calculated by subtracting the fluorescence reading of the first cycle from the final (21st) cycle reading. Results are presented as percentage caspase activity relative to the DMSO or GM control.

2.3.11 Cell Death

2.3.11.1. Cell Death – Viability test

Poppy pollen tubes were grown and treated with appropriate drugs, then incubated with $10 \mu\text{g}$ fluorescein diacetate (FDA) per mL of liquid GM for 5 min at room temperature and mounted on glass slides. Pollen was visualized under a Nikon Eclipse Te300 microscope attached to a cooled coupled device (CCD) camera supplied by Applied Imaging, UK. Capture and analysis of images was achieved with a Nikon NIS elements 3.2 image analysis system. Images were saved as jp2 and tif files. Pollen tubes were counted (30 tubes per treatment; N=3) in the following categories: (1) total, (2) green (alive) and (3) unstained (dead).

Arabidopsis pollen viability assay was based on using Evans blue dye. FDA was not an appropriate stain as the pollen was expressing GFP and the wavelengths overlapped. Pollen was stained with 0.05 % Evans blue for 15 minutes. After incubation, the sample was washed four times with SDW in order to remove excess dye. Aliquots of 20 μ L were mounted on microscope slides and pollen was visualised using brightfield microscopy (Nikon Eclipse Te300). Scoring categories were: (1) total, (2) unstained (alive) and (3) dark stained (dead). Each experiment was done in triplicate with 180 pollen counted each time. Statistical analysis by Chi square was performed in Microsoft Excel.

2.3.11.2. Pretreatment with tetrapeptide inhibitor Ac-DEVD-CHO

A. thaliana pollen was pretreated with 100 μ M Ac-DEVD-CHO for 1 h before SI was induced by adding stigmatic PrsS₁ or PrsS₃ recombinant proteins to PrpS₁-GFP and PrpS₃-GFP expressing pollen growing *in vitro*, respectively, at final concentration 20 μ g/mL. Negative control was comprised of pollen, incubated in Ac-DEVD-CHO only, untreated pollen, grown in AtGM only or pollen with induced SI reaction without DEVDase inhibitor. Pollen was incubated for 8 h and then stained as described in previous section 2.3.11.1.

2.3.12. Actin labelling

Arabidopsis pollen was collected and germinated as described in section 2.2.3. Samples were fixed in a 1.5 microtube with 124 μ g mL⁻¹ m-Maleimidobenzoyl-N-hydroxysuccinimide ester (MBS) for 6 min and then paraformaldehyde (PFA) was added to a final concentration of 2 % and the samples were incubated for 1.5 h at 4 °C. After fixation, PFA was eliminated

with 3 washes of 1 mL TBS, removing the supernatant after each wash by centrifuging at 3 600 rpm for 2 min. After the last wash, samples were incubated with TBS plus 0.1 % Triton for 40 min to permeabilise the pollen tubes. Tubes were stained with 66 nM Rhodamine-Phalloidin and samples were left for 16 h at 4 °C or 2 h at room temperature. Then, 10 µL of sample was pipetted onto a microscope slide and 5 µL of Vectashield with DAPI was added before slides were covered with a cover slip and sealed with transparent nail polish. Samples were visualised using epifluorescence or confocal microscopy. Epifluorescence was performed on a Nikon Tε300 fluorescence microscope. The slides were searched for intact pollen tubes. The nuclei were then visualised using the DAPI filter before switching to a TRITC filter to see if there was any Rhodamine-Phalloidin labelling of F-actin. Capture and analysis of images was achieved with a Nikon NIS elements 3.2 image analysis system. Images were saved as jp2 and TIF files and then manipulated using Image J and Adobe Photoshop.

Confocal laser scanning microscopy was performed by Katie Wilkins on Leica SP2 Inverted Confocal system. Full z-series sections of the pollen tubes were taken, 0.5 µm thick.

GFP images were taken using Argon 488 nm laser, using 5 % of the power, emission bandwidth was 500 – 530 nm using 550.1 gain. Rh-Ph images were taken using 543 nm laser, using 100 % power, emission bandwidth was 565 – 600 nm, using 550.1 gain.

Images from the confocal were saved as tiff files then viewed and manipulated using ImageJ software.

Scanning settings:

4x average scan

400 hz scan

512 x 512 pixel frame

63x oil immersion lens

2.3.13. Leaf mesophyll protoplast production

Leaves from 3-4 weeks old *Arabidopsis* plants were cut with a surgical knife into very thin strips on a clean paper surface and transferred to the Petri dishes containing 15-20 mL of enzyme solution. Leaves were incubated in a Petri dish sealed with Parafilm and wrapped in aluminium foil at 22 °C for 16 h. Care was taken to keep the Petri dish as still as possible not moving or shaking it at any point. Then, the enzyme solution was pipetted with a sterile Pasteur pipette very carefully to avoid disturbing the leaves, otherwise the protoplasts would be released too early. Protoplasts were released by adding 10 mL K3 media on the plate, which was then gently swirled. Protoplast containing medium was passed through a nylon filter in a sterile 20 mL plastic tube with a round bottom. The tube was left to stand still for 40 – 60 min and during this time the protoplasts floated to the top of the solution. The upper layer with protoplasts was transferred into a new round bottom tube using sterile Pasteur pipette. Then, protoplasts were washed with 5 mL K3 medium, which was carefully pipetted into the tube. The tube was left to stand again for ~1 h to allow protoplasts to float again. At this stage, small aliquot was taken to assess protoplasts viability using FDA, while the main part of protoplasts were transfected using 5 – 20 µg of plasmid pEarleyGate purified by Midiprep kit (Qiagen). 250 µL of suspended protoplast solution was added per tube with DNA and an equal volume of PEG solution was added to the mixture of DNA and protoplasts and incubated for 30 min at RT. The PEG solution was diluted by adding 2 mL K3, and tubes allowed to stand for 1 – 2 h to let the protoplasts float to the top. The solution underneath the protoplasts was carefully withdrawn and a new aliquot of 2 mL K3 medium was added to the protoplasts and left to incubate for 16 h in the dark at RT. The following day transient expression of the gene of interest was verified.

K3 medium:

Prepared from following stock solutions
10x B5 medium with vitamins
200x MES (0.1 g/mL)
500 x myo-inositol (0.05 g/mL)
100x NH₄NO₃ (25 mg/mL)
100x CaCl₂*2H₂O (75 mg/mL)
100x D-xylose (25 mg/mL)
0.4 M sucrose
pH adjusted to 5.6 – 5.7 using 1.0 M KOH
Solution was filter sterilized and stored at 4 °C.

Protoplasts suspension solution medium

0.4 M Mannitol
20 mM CaCl₂*2H₂O
5 mM MES pH 5.7
filter sterilized and stored at 4 °C.

“Enzyme solution”:

0.5 % cellulase (R-10)
0.2 % macerozyme (R-10)
prepared in K3 medium, filter sterilized and stored at -20 °C.

PEG solution

40 % PEG 4000 (Fluka)
0.4 M mannitol
100 mM Ca(NO₃)₂
warmed in the 60 °C water bath
pH 7.0 adjusted with 1.0 M KOH
Filter sterilized and aliquoted, stored at -20 °C

2.3.14. PCR screening for the presence of inserts in transgenic plants

Leaf disks were obtained from *Arabidopsis* transgenic plants and untransformed Col-0 as a control in small PCR microtubes. To extract DNA, 50 µL of an extraction buffer was added and the leaf disk was grinded using a sterile filter tip, incubated at 95 °C for 10 min and cooled on ice for 2 min. After that, 50 µL of a dilution buffer was added, and the mixture was vortexed and centrifuged (1 min, 13200 rpm). For each PCR reaction 1 µL of DNA was used. The presence of inserts was analysed by electrophoresis on a 0.8 % agarose gel.

Oligonucleotide primers were supplied by MWG-Biotech.

Extraction Buffer

0.1M Tris-HCl, pH 9.5
0.25 M KCl
0.01 M EDTA

Solutions were prepared by aseptic work and filter sterilized before use.

Dilution Buffer

3 % BSA

PCR mix:

12.5 μL ReddyMixTM PCR Master Mix (Thermo Scientific)
1 μL forward primer
1 μL reverse primer
1 μL DNA
9.5 μL dH₂O

PCR conditions:

93 °C – 3 min 1x

93 °C – 1 min
57 °C – 1 min
72 °C – 1 min } 35x

72 °C – 10 min 1x

Used primers:

Forward PrsS₁: 5'-GGAGCATTGGCATCCATTGCCG-3' T_m = 64 °C

Reverse PrsS₁: 5'-CCATTATCTTCCAGAGGCACTGGG-3' T_m = 64.4 °C

Forward PrsS₃: 5'-CGATCCACTGCCAATCAGAAGACG-3' T_m = 64.4 °C

Reverse PrsS₃: 5'-GTGGAGCACCTTCCGCCGTCG-3' T_m = 67.6 °C

Forward PrsS₈: 5'-GGTAATGGCCATAGCATCGGG-3' T_m = 61.8 °C

Reverse PrsS₈: 5'-CATCCGTTGTCTTCCACAGGC-3' T_m = 61.8 °C

Forward clon. PrpS₁: 5'-CCATGCCCCGAAGTGGAAGTGTTG-3' T_m = 66.1 °C

Reverse clon. PrpS₁: 5'-CCTTAAGCTTGAGTTATAAGATGAGGGGAATCC-3' T_m =
67.0 °C

Forward PrpS₃: 5'-CCATGCTCTTACGTGGAAAGACC-3' T_m = 62.4 °C

Reverse PrpS₃: 5'-GGCTGCAGAAGTGGCTTCATC-3' T_m = 61.8 °C

Forward PrpS₈: 5'-CCCTATTTGGATCCGCACTTGCC-3' T_m = 64.2 °C

Reverse PrpS₈: 5'-GAGGATTCAGAGGAGTTGCCC-3' T_m = 64.0 °C

2.3.15 DNA analysis by agarose gel electrophoresis

For the gel, agarose was fused in 0.5X TBE by heating the solution until it was completely clear. Then, $0.5 \mu\text{g mL}^{-1}$ ethidium bromide was added to the molten agarose. Gels were poured and electrophoresed using Hybaid or Biorad electrophoresis kits. Images of gels were captured using a FluorS Multi-imager and analysed using Quantity One software if necessary. An estimation of size was achieved by parallel electrophoresis of an aliquot of 1 kb ladder (Invitrogen).

10 x TBE:

0.9 M Tris
0.9 M Orthoboric acid
25 mM EDTA

DNA loading buffer:

40 % (v/v) glycerol
0.25 % (w/v) bromophenol blue

2.3.16. Semi-quantitative RT-PCR

2.3.16.1 RNA extraction

Total RNA was extracted using RNeasy Mini Kit (Qiagen). All materials and water was pretreated with 0.05 % or 0.1 % diethylpyrocarbonate (DEPC), respectively. DEPC reacts with histidine residues on the proteins and thus it inactivates RNases. However, it can react with RNA as well. Therefore, it was necessary to autoclave DEPC incubated solutions before the experiment. DEPC is heat-sensitive and is degraded by autoclaving.

For each extraction, 20 *A. thaliana* (transgenic or untransformed) flowers were collected. Flowers were frozen in liquid nitrogen and grinded thoroughly in microtubes using a plastic rod. β -mercaptoethanol was diluted 1:100 in RLT buffer and 450 μl of the solution added to the grounded flowers and mixed by vortexing. The sample was then added to a lilac QIAshredder column spin column and centrifuged (2 min, 13200 rpm). The flow-through

was transferred to a new microtube, 0.5 V of 100 % ethanol was added, the solution mixed by pipetting, then immediately transferred to a pink RNeasy column and centrifuged (15 s, 13200 rpm). The flow-through was discarded and 700 μ L RWI buffer added to the new column before centrifugation (15 s, 13,200 rpm). The flow-through was discarded and the column transferred to a new collection tube. 500 μ L RPE buffer was added to the column, centrifuged (15 s, 13200 rpm) and the flow-through discarded. Another 500 μ L of RPE buffer was added to the column again and centrifuged (2 min, 10000 rpm) to ensure the membrane was dry. The column was transferred into a new microtube and centrifuged (1 min, 13200 rpm). Finally, the column was transferred to a final microtube, 30 μ L of RNase free water added and centrifuged (1 min, 13200 rpm). Then, another 10 μ L of RNase free water was added to completely elute everything and centrifuged (1 min, 13200 rpm). 5 μ L of RNA was used to analyse by electrophoresis and the rest stored at -80 °C until required.

2.3.16.2. RNA analysis by agarose gel electrophoresis

Analysis of RNA samples was accomplished by electrophoresis on agarose gels using 5 μ L of RNA loading dye. No ladder was used due to the possible contamination with RNases. 1 % agarose gel was made up in 0.5x TBE using RNase free SDW and poured in RNase free gel tank. Electrophoresis settings and gel visualisation are described in chapter 2.3.15.1. RNA was stained with ethidium bromide, which was previously added to the agarose solution at a final concentration of 0.5 μ g mL⁻¹.

2.3.16.3. DNase treatment of RNA

In order to remove contaminating DNA, 10 μ L of RNA was mixed with 10 μ L of DNase solution and incubated at RT for 15 min. 2 mM EDTA was added and the mixture was incubated at 65 °C for 10 min. Then, 80 μ L of RNase free water was added and phenol extraction proceeded by addition of equal volume of phenol. The solution was mixed and centrifuged (5 min, 13200 rpm). The upper aqueous layer was removed and transferred to a clean tube and an equal volume of chloroform was added. Again, the sample was vortexed and centrifuged (5 min, 13200 rpm). The top layer with aqueous phase was removed, transferred to the fresh tube and 1 μ L of glycogen (Roche) was added, which serves as a carrier to promote nucleic acids precipitation. RNA was precipitated by adding 2.5 V of 70 % ethanol, vortexed well, incubated at 70 °C for 30 min and centrifuged (10 min, 13200 rpm). Supernatant was carefully removed. RNA pellet was washed with 70 % ethanol. The pellet was dried in a vacuum chamber for 15 min and resuspended in 20 μ L of RNase free water.

DNase solution:

2 μ L 10x DNase I buffer
1 μ L recombinant RNasin (Promega)
1 μ L DNase (Invitrogen)
6 μ L RNase free SDW

2.3.16.4. cDNA synthesis by RT-PCR

Isolated total RNA was used in RT-PCR reaction One-step RT-PCR kit (Qiagen). cDNA was analysed by electrophoresis as described in section 2.3.15.1. Sample loading was

compared to glyceraldehyde-3-phosphate dehydrogenase C (GAPC), whose cDNA was also amplified and used as RT-PCR standard and loaded in parallel on the same gel.

RT-PCR mix:

2 μ L RNA
10 μ L 5x buffer
2 μ L dNTP
1 μ L forward primer
1 μ L reverse primer
1 μ L recombinant RNasein
2 μ L enzyme mix
31 μ L RNase free dH₂O

RT-PCR conditions:

50 °C – 30 min	1x
95 °C – 15 min	1x
94 °C – 1 min	} 30x
57 °C – 1 min	
72 °C – 1.5 min	
72 °C – 10 min	1x

Primers:

GAPC forw: 5'-CACTGACAAAGACAAGGCTGCAGC-3' T_m = 64.4 °C

GAPC rev: 5'-CCTGTTGTCGCCAACGAAGTCAG-3' T_m = 64.2 °C

CHAPTER 3

**Investigation of the possible involvement of the
ubiquitin-proteasomal pathway during SI in
Papaver pollen**

3.1. INTRODUCTION

As mentioned in the introduction (section 1.6), the Ubiquitin-mediated 26S proteasomal (UbP) degradation of proteins is required to maintain the cellular homeostasis and regulation of various cellular functions. Protein substrates are covalently attached to a small protein, ubiquitin, by the sequential action of three enzymes. Ubiquitin is first activated by an ubiquitin-activating enzyme E1 and transferred to the ubiquitin-conjugating enzyme E2. E2 binds to the ubiquitin-protein ligase E3 that catalyzes the formation of a covalent bond of ubiquitin molecules sequentially attached through Lys-48 of the previous ubiquitin (Hershko and Ciechanover, 1998). A chain of at least four ubiquitins is required for degradation by the 26S proteasome. Monoubiquitinated proteins or proteins tagged with the ubiquitin chain through the Lys-63 are not targeted for degradation but they are involved in various events such as subcellular localization or protein activation or protein-protein interaction (Dielen et al., 2010).

The specificity of the UbP pathway is mainly determined by the wide range of diverse E3 ligases that recognise substrates through the specific protein recognition domains (see introduction for details). In *A. thaliana* there are more than 1400 genes that encode different components of the UbP pathway and among them around 1300 encode different predicted E3 ligases (Smalle and Vierstra, 2004). There are four major groups of E3 ligases: monomeric HECT-domain E3 ligases and three groups that contain RING domain; monomeric RING/U-box E3 ligases and complex Cullin RING E3 ligases and APC E3 ligases. The Cullin RING ligases are further divided based on the different subunits of Cullin that they contain: the SCF complex contains SKP1, Cullin-1 protein F-box for protein specificity and RBX1; the complex with Cullin-3 subunit contains RBX1 and BTB1/POZ

domain, and Cullin-4 based complex contains RBX1, DDB1 and WD (Vierstra, 2003, Vierstra, 2009).

The 26S proteasome is a large cylindrical multisubunit complex, consisting of the 20S central core domain, that is comprised of four stacked rings of α and β subunits (each ring is composed of seven proteins), and the 19S regulatory “cap” structure, that can be divided into lid and base components. The 19S regulatory particle recognizes polyubiquitin tags attached to the target protein substrates, initiates the degradation process in the core and also removes the Ub chains (Voges et al., 1999, Kurepa and Smalle, 2008).

UbP degradation was demonstrated as playing a role in plant-pathogen interactions and some aspects of plant reproduction. The UbP pathway is involved in plant-pathogen interaction at several different levels. Plant-pathogen interactions start with the perception of the PAMPs, which are mediated by plasma membrane located pattern recognition receptors. This is the first step towards PAMP-triggered immunity, achieved through the cascade of downstream events (reviewed in Trujillo and Shirasu, 2010). The ubiquitination pathway, but not the 26S proteasome, is involved in the basal host resistance of barley epidermis that is attacked by powdery mildew (Dong et al., 2006). Plant pathogens developed several strategies by which they interfered with the plant UbP pathway. They can recruit E3 ligases and target crucial defense plant proteins for degradation by the 26S proteasome. For example *P.syringae* AvrPtoB acquired E3 ligase activity through which it conjugates the Ub chain on plant Fen or FLS2 proteins that stand guard against pathogen invasion, targets them for proteasomal degradation, and thus creates the way to infect the plant (Göhre et al., 2008, Rosebrock et al., 2007). Pathogens also developed a way to inhibit plant 26S proteasomal degradation, for example the *P. syringae* protein SylA inhibits the β 1/2/5 subunits of the core particle of 26S proteasome (Groll et al., 2008).

Yang et al., (2006) reported that the E3 ligase, PUB17 from *A. thaliana* and its functional tobacco homologue ACRE276 act as positive regulators of cell death and defense responses in Solanaceae and Brassicaceae. In addition, (Sadanandom et al., 2008) reported the identification of the BTB/POZ domain transcriptional repressor, AtPOB1, that interacts with the ARM repeat of PUB17 to control disease resistance in plants. Plants that were deficient in POB1 produced spontaneous cell death, demonstrating its critical role in plant cell death.

Another important involvement of the 26S proteasome in hypersensitive response was demonstrated by (Hatsugai et al., 2009). They demonstrated a direct link between proteasome activity and plant PCD by identifying that the proteasomal subunit PBA1 acts as a long sought plant caspase-3-like enzyme. Proteasome and its caspase-3-like activity are required during bacterial infection to degrade a yet unknown negative regulator of membrane fusion, thus enabling the fusion of the plant plasma membrane and the vacuole membrane. In this way pores are created that enable the discharge of vacuole content and defence proteins outside the cell, inhibiting bacteria infection and causing HR cell death.

Ubiquitination and proteasomal degradation were also demonstrated as playing a role in some aspects of plant reproduction: free ubiquitin is required for pollen tube adhesion and guidance in lily (Kim et al., 2006) and proteasomal degradation is necessary for normal pollen tube development in *Picea* (Sheng et al., 2006) and kiwi (Speranza et al., 2001). Moreover, ubiquitination and proteasomal degradation are essential during S-RNase based gametophytic SI in Solanaceae, Rosaceae and Plantaginaceae, and in sporophytic SI in Brassicaceae (for recent reviews see Meng et al., (2011), Tantikanjana et al., (2010), Yee and Goring, (2009)). During an S-RNase-based incompatible response, self and non-self S-RNases enter pollen tube. The hypothesis whose S-specificity was not yet demonstrated in all GSI species is that pollen determinants recognize the non-self S-RNases and target them

for the proteasomal degradation while self S-RNases are not recognized and are allowed to degrade the RNA of an incompatible pollen, therefore preventing self-fertilization (Kao and Tsukamoto, 2004, Meng et al., 2011, Liu et al., 2009, Qiao et al., 2004b, Hua and Kao, 2006). In the S-RNase based SI system the pollen S-determinant is an S-locus F-box protein (SLF or SFB), a component of a SKP1-Cullin1-F-box (SCF) complex (Sijacic et al., 2004, Lai et al., 2002, Entani et al., 2003, Ushijima et al., 2003). In *Antirrhinum*, the SLF is conventional SCF complex with a novel SKP1-like protein SSK1 (Huang et al., 2006), while in *Petunia* the SLF is part of a novel E3 ligase complex. The other components of the PiSLF complex in *Petunia* are PiCUL1-G and PiSBP1 (*P. inflata* S-RNase Binding Protein1), a RING-HC protein in addition to PiSLF (Hua and Kao, 2006). However, the novel E3 ligase identified does not contain SKP1 or RBX1.

The sporophytic SI mechanism found in Brassicaceae also involves components of UbP pathway. The ARC1 protein, an E3 ligase that is a member of PUB family of proteins, acts as a regulator of the *Brassica* SI response in the stigmatic papillae (Stone et al., 2003). ARC1 mediates the ubiquitination of EXO70A1, a putative component of an exocyst system, which regulates secretion (Samuel et al., 2009). In addition, an ubiquitin specific protease, a homologue of AtUBP22, was identified in rye pistils and its role was implicated in the SI in grasses (Hackauf and Wehling, 2005).

The self-incompatibility (SI) and hypersensitive response (HR) are important examples of signaling pathways triggered in response to incompatible interaction between two cognate proteins, resulting in PCD in plants. The mechanisms of HR and SI in *Papaver* share many similarities, such as: increased levels of $[Ca^{2+}]_i$, Ca^{2+} -dependent phosphorylation of proteins, generation of reactive oxygen species and cessation of cytoplasmic streaming and caspase-3-like induced PCD (Geitmann et al., 2004). Ubiquitin-dependent proteasomal (UbP)

degradation is an important component of PCD during HR and has also been reported to play an important role in other SI systems, like GSI in *Petunia* and *Pyrus*, and SSI in *Brassica*, but has not yet been reported during SI in *Papaver*.

The majority of studies on the UbP pathway use the inhibitors of the proteasome activity due to their quick entering of cells and rapid reversibility of their action (Kisselev and Goldberg, 2001). The most desirable proteasome inhibitors are those specifically targeting the proteasome without affecting activities of other serine or cysteine proteases. Among the proteasome inhibitors, MG132 represents a potent cell-permeable proteasome inhibitor and is widely used. MG132 is a peptide aldehyde Z-Leu-Leu-Leu-CHO that inhibits the proteasome activity by covalently binding to the active site of the β -subunits in the core particle (Zhang et al., 2009). The specificity of MG132 was demonstrated in numerous studies on different systems, for example using a biochemical approach by tracking degradation of several proteins known to be substrates for proteasome degradation in yeast cells (Liu et al., 2007a). In plants, the use of the proteasome inhibitor MG132 was found to inhibit length of tracheary elements in *Zinnia* cell cultures and also in *A. thaliana* (Zhao et al., 2008). (Vacca et al., 2007) reported that MG132 prevented cells from PCD induced with HS in tobacco BY2 cells. In growing pollen tubes, MG132 affects pollen tube morphology (Sheng et al., 2006, Speranza et al., 2001), and mitochondrial dynamics and causes vacuolization in the pollen tube (Sheng et al., 2010).

AIMS

The aim of this study was to investigate whether there is a link between *Papaver* SI and UbP pathway and if so what role does the UbP degradation play during the pollen SI reaction in

Papaver. This work was carried out in collaboration with Dr. Ari Sadanandom from University of Durham, whose research is focused on the role of ubiquitin-mediated proteolysis during disease resistance in plants (Yang et al., 2006, Sadanandom et al., 2008). We aimed to establish a link between ubiquitination and other PCD events that occur in the pollen tube during SI reaction. This could provide an important information about cell death signalling and might also provide further insights into two mechanistically similar cell responses, SI and HR. In order to investigate the involvement of the UbP pathway during SI-induced PCD pathway in *Papaver* pollen, the SI response was characterized in the presence of the proteasomal degradation inhibitor MG132. Pollen viability, pollen tube growth inhibition, and the level of protein ubiquitination during the SI reaction were determined.

3.2. RESULTS

3.2.1. The proteasome inhibitor MG132 affects pollen germination and tube growth

In order to investigate whether the UbP pathway has any role in poppy pollen germination and growth, a pharmacological approach using the reversible proteasome inhibitor MG132 was used. Initially we wished to determine the concentration of the MG132 that would be effective without inhibiting pollen tube growth or causing the alterations to pollen tube morphology. The effect on normal pollen tube growth of different concentrations of MG132, in range of 10 to 100 μ M (see Figure 3.1), was determined. Different concentrations of MG132 were applied to pre-germinated poppy pollen tubes *in vitro*. Pollen was left to incubate for 30 min or 3.5 h when the pollen tube lengths of 39 tubes were measured (See

Figure 3.1). Figure 3.1 presents the effect of different concentrations of MG132 on the length of pollen tubes.

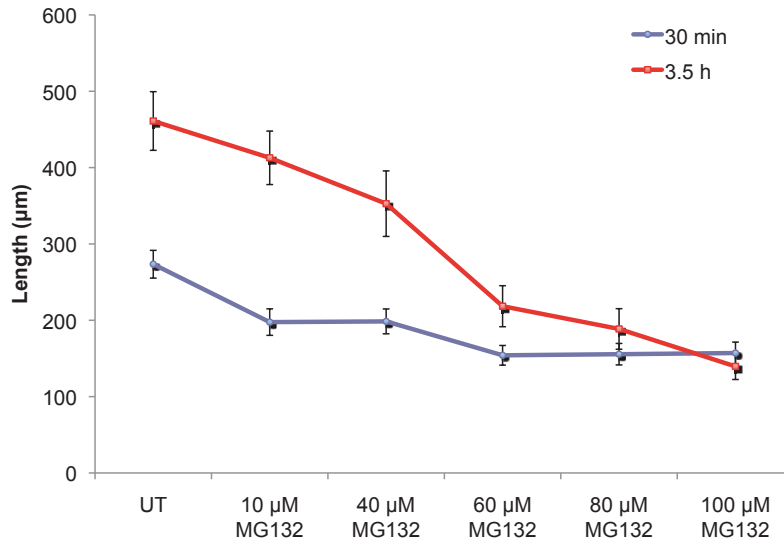


Figure 3.1. Mean length of *Papaver* pollen tubes treated with different concentrations of MG132 at two different time points 30 min (blue line) and 3.5 h (red line). UT-untreated pollen tubes. N=3 repeats, n=39 tubes measured. Error bars represent \pm Standard Error of means.

The average pollen tube length of the untreated control after 3.5 h incubation was 461 μm and it decreased when pollen was pretreated with MG132 (see Figure 3.1). The difference in pollen tube length between untreated and 10 μM was not significant ($P=0.085$; nonsignificant), nor was the difference in length significant between pollen that was pretreated with 10 or 40 μM MG132 ($P=0.122$; nonsignificant). When comparing the pollen tube length of pollen that was pretreated with 40 or 60 μM MG132, the difference was highly significant ($P=7.8 \times 10^{-06}$; ***). When pollen was pretreated with 80 or 100 μM MG132 the pollen tube growth was inhibited significantly ($P=1.4 \times 10^{-14}$ and $P=5.3 \times 10^{-19}$, ***, respectively), see Figure 3.1. Higher concentrations of MG132 (80 and 100 μM), caused severe pollen tube swelling and balloon-like pollen tube tips. So they were not considered further. Some signs of pollen tube tip swelling were also observed at 60 μM

MG132 but not at 40 μ M MG132. Therefore 40 μ M MG132 was chosen as the most effective concentration to inhibit proteasomal degradation without causing major morphological changes in further experiments. This concentration is also consistent with the reports from the literature (Wang et al., 2009b, Sheng et al., 2006, Sheng et al., 2010, Speranza et al., 2001, Liu et al., 2007a). Reports from the other pollen tube systems like *Picea* (Sheng et al., 2006) and kiwi (Speranza et al., 2001) show that MG132 alters pollen tube morphology, causes tube tip swelling, tube branching and germination of more than one tube per grain but the removal of inhibitor restored growth. These effects were not so dramatic in case of poppy pollen germination, however tube swelling and branching was detectable when pollen was pretreated with 80 or 100 μ M MG132 concentrations of MG132.

3.2.2. Effect of inhibition of proteasomal activity on pollen tube growth

After establishing the optimal concentration of MG132 for these studies and the effect it had on pollen tube growth, we examined whether the proteasomal activity was involved in poppy SI. Pollen was pretreated with 40 μ M MG132 for 30 min and then SI was induced by incubating pollen with recombinant PrsS proteins for 3 h. The length of the pollen tubes was measured to examine whether the inhibition of proteasomal activity by MG132 would affect the inhibition of pollen tube growth caused by the SI response and rescue pollen from SI (see Figure 3.2).

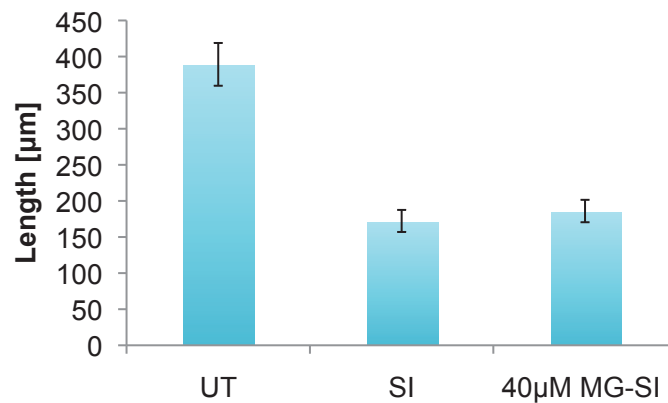


Figure 3.2.: Mean length of pollen tubes pretreated with 40 µM MG132 and induced SI (MG-SI). UT - untreated control of pollen tubes grown in GM only, SI - pollen tubes incubated with recombinant stigmatic PrsS proteins; N=3 repeats; n=50 pollen counted. Error bars represent ± Standard error of means.

Mean length of *Papaver* pollen tubes pretreated with 40 µM MG132 and then SI induced (MG-SI) was 186 ± 15 µm (n=50 pollen tubes, N=3 repeats), which was not significantly different compared to the *Paper* pollen with induced SI (172 ± 15 µm; P=0.314; nonsignificant). The required additional control would be length of pollen incubated only with 40 µM MG132 but as it can be seen in Figure 3.1., that 40 µM does not significantly affect length when compared to non-treated. These results suggest that MG132 has no effect on the SI induced inhibition of pollen tube growth (see Figure 3.2). When compared to the mean length 389 ± 30 µm for the untreated (UT) control (n=50 pollen tubes, N=3 repeats), both values were highly significantly different (P= 3.13×10^{-22} compared to MG-SI treated pollen tubes and P= 8.67×10^{-25} compared to SI treated pollen tubes; ***), see Figure 3.2. Taken together, these data demonstrate that inhibition of proteasomal activity cannot rescue the pollen tube growth after the induction of SI.

3.2.3. Effect of inhibition of proteasomal activity on pollen tube viability

Since pollen tube length measurements did not give any indication of a link between SI and proteasome inhibition, we decided to test whether MG132 treatment can rescue the viability of pollen tubes after SI challenge. SI results in cell death, so if ubiquitination and proteasomal degradation were involved in SI, then the inhibition of proteasomal activity by MG132 might prevent pollen cell death and would therefore increase pollen viability compared to SI induced pollen.

Pollen tube viability was assessed using fluorescein diacetate (FDA). FDA penetrates through the cell membrane and inside the cell intracellular esterases cleave off the diacetate group producing the highly fluorescent product fluorescein (Breeuwer et al., 1995). The fluorescein will accumulate in cells which possess an intact membrane, so green fluorescence can be used as a marker of cell viability, whereas cells that do not possess an intact membrane or an active metabolism do not exhibit green fluorescence. Pollen tubes were grown and treated with MG132 and incompatible PrsS-proteins as described in the previous section. Pollen tubes were incubated with 10 µg/mL FDA in liquid GM for 5 min and examined, as described in the materials and methods section (see Figure 3.3).

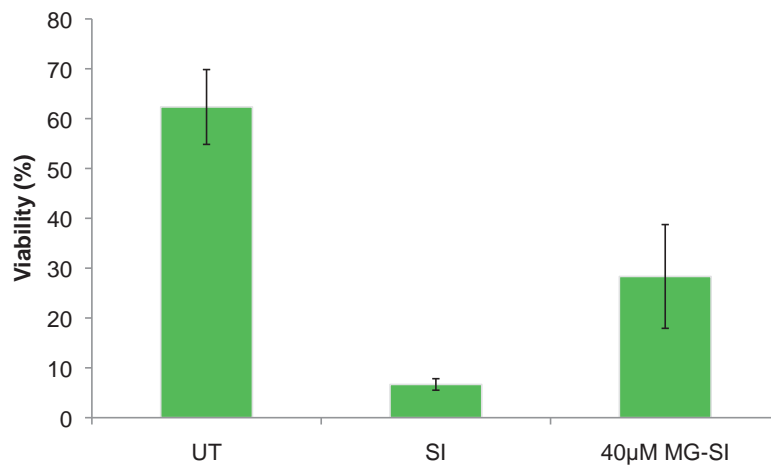


Figure 3.3.: FDA viability of pollen tubes pretreated with 40 µM MG132 and induced SI (MG-SI). UT - untreated control of pollen tubes grown in GM only; SI - the viability of pollen tubes incubated with the recombinant stigmatic PrsS proteins. N=3 repeats; n=100 pollen counted. Values correspond to mean number of viable pollen ± Standard Deviation of means.

Untreated pollen tubes had a mean viability of 62 %, which was highly significantly different to the 6.7 % viability of SI treated pollen ($P=1.23 \times 10^{-16}$; ***). MG132 partly rescues pollen from SI induced cell death. When pollen tubes were pretreated with 40 µM MG132 prior to SI induction, we observed 325 % increase in pollen viability. The difference between SI and MG-SI treated pollen tubes was significantly different ($P=5.53 \times 10^{-05}$; ***) and so was the difference between the UT control and the MG-SI treated pollen tubes ($P=1.37 \times 10^{-06}$; ***). The data presented in this section demonstrate that MG132 can partly rescue the SI-induced cell death of *Papaver* pollen tubes. Because MG132 inhibits proteasomal activity, this suggests that ubiquitination-dependent proteasomal degradation is a component of *Papaver* SI.

3.2.4. Proteasomal degradation and PCD in incompatible poppy pollen

In order to investigate further whether proteasomal degradation might be functionally involved in SI induced PCD we measured caspase-like activity in incompatible pollen tubes

that were pretreated with the inhibitor of proteasomal activity MG132. SI triggers PCD involving DNA fragmentation and DEVDase activity in incompatible *Papaver* pollen (Thomas and Franklin-Tong, 2004). Caspase-like activities stimulated by SI have been characterised more directly, and in more detail, using AMC-based peptide caspase substrates that act as fluorogenic indicators for caspase activities, by exhibiting fluorescence upon specific protease cleavage (Bosch and Franklin-Tong, 2007). The prediction was that if ubiquitination and proteasomal degradation were involved in SI-induced PCD then the proteasome inhibitor would prevent PCD in incompatible pollen tubes and caspase-like activity would be lower compared to non-treated, SI-induced pollen tubes. We measured the caspase-3-like/DEVDase activity of protein extracts from SI challenged pollen tubes treated in the presence and absence of MG132 using Ac-DEVD-AMC tetrapeptide (see Figure 3.4).

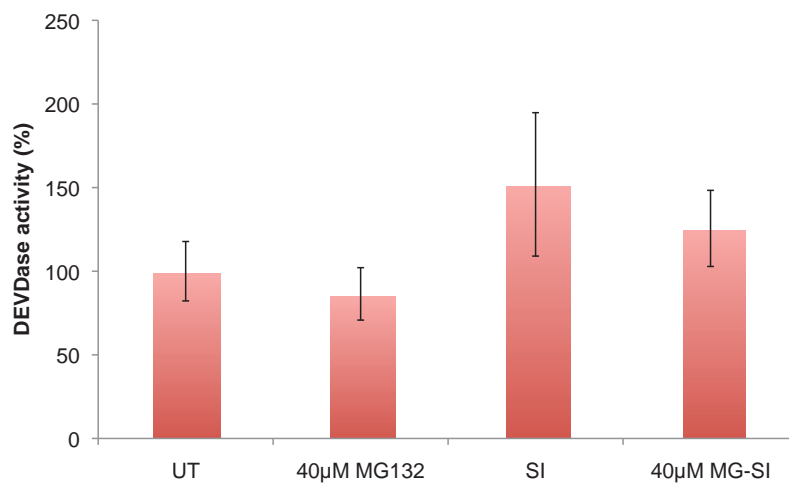


Figure 3.4.: DEVDase activity of pollen tubes pretreated with 40 µM MG132 and induced SI (MG-SI). UT – activity of untreated control of pollen tubes grown in GM only, 40 µM MG – activity of pollen that was incubated with MG132, SI - DEVDase activity of pollen tubes incubated with recombinant stigmatic PrsS proteins. N=3 repeats. Error bars represent ± Standard Deviation of means.

Pollen tubes grown in GM only (UT) or in GM with 40 µM MG132 exhibited very low DEVDase activity (see Figure 3.4). DEVDase activity of the pollen tubes incubated with 40 µM MG132 only was 14 % lower compared to UT control and was not significantly

different ($P=0.143$; nonsignificant). DEVDase activity increased by 52 % in pollen tubes where the SI response was induced by recombinant stigmatic PrsS proteins, and this increase was significant compared to the UT control ($P=0.021$, *). Pollen tubes that were pretreated with 40 μM MG132 before the SI was induced exhibited 26 % lower DEVDase activity compared to the SI samples. The inhibition of proteasomal activity affected DEVDase activity ($P=0.046$; *). Pollen tubes that were pretreated with 40 μM MG132 before the incompatible response was triggered were also significantly different compared to pollen tubes that were incubated with 40 μM MG132 only or with UT control ($P=0.034$ and $P=0.014$, respectively; *). These data, presented in Figure 3.4., demonstrate that the inhibition of proteasomal activity by MG132 had a small but significant effect on pollen tubes as it partly inhibited the DEVDase activity. It suggests a potential link between DEVDase activity and proteasomal activity in incompatible *Papaver* pollen tubes, even though the DEVDase activity stimulated by SI was not very high and MG132 did not reduce activity very much.

3.2.5. Effect of proteasomal inhibition by MG132 on the ubiquitination levels in incompatible pollen tubes

In the previous sections we provided preliminary evidence that proteasomal degradation might play a role during the SI reaction in poppy pollen tubes. As ubiquitination via Lys48 is tightly connected with the proteasomal degradation we wished to determine whether the levels of ubiquitination might change upon SI in *Papaver* pollen. Proteins were extracted from poppy pollen tubes pretreated with 40 μM MG132 before the induction of SI by

recombinant stigmatic PrsS and controls, and run on a SDS-PAGE, blotted and then probed with α -ubiquitin antibody. Figure 3.5.a shows the pattern of ubiquitination of total protein extracts. Figure 3.5.b shows corresponding relative light intensity evaluation of the blot.

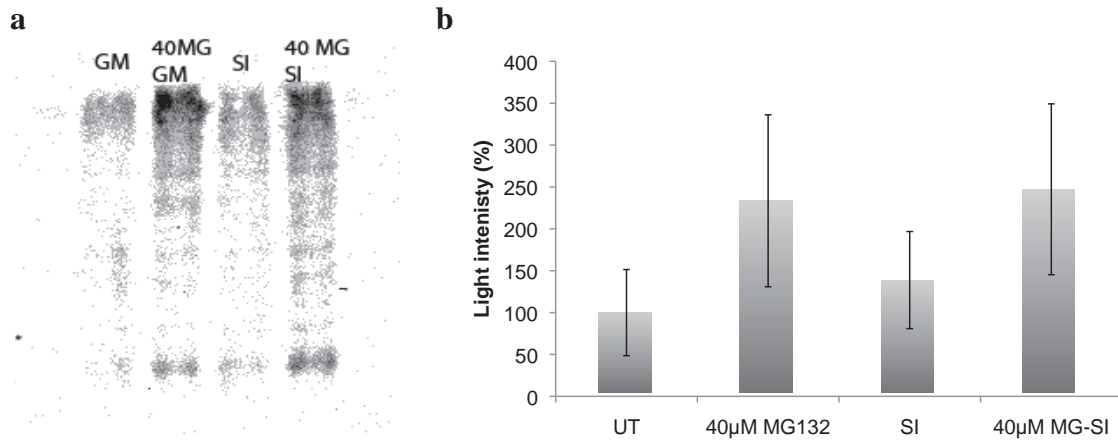


Figure 3.5.: Ubiquitination levels of poppy pollen pretreated with 40 μ M MG132 and SI induced (a) Representative image of western blot of MG-SI protein extracts probed with ubiquitin antibody; (b) percentage of average relative light intensity of ubiquitinated protein extracts; N=4, Error bars represent \pm St. Error. GM – extract from untreated pollen; 40MG GM – extract from pollen incubated in 40 μ M MG132; SI – extract from pollen that had induced SI reaction; 40 MG SI – extract from pollen that was pretreated with 40 μ M MG13 before the induction of SI by PrsS proteins.

The ubiquitination signal was measured on the whole band of the western blot. The untreated pollen sample was given value 100 %. When tubes were grown in GM with the proteasome inhibitor MG132 the level of ubiquitination increased by 133 % due to the probable inhibition of proteasomal degradation, so more ubiquitinated proteins appeared to be accumulated in the pollen tubes. When SI was induced, the level of ubiquitination was more intense by 39 % compared to the control UT sample, suggesting that ubiquitination was increased by the SI response. The strongest signal was obtained when samples were pretreated with proteasome inhibitor before inducing SI and despite the increase in ubiquitination by MG132 on its own, this could implicate a possible role for ubiquitin-dependent proteasomal degradation during SI responses.

3.2.6. Proteasomal degradation acts upstream or in parallel with caspase-3-like activity

In order to determine whether proteasomal degradation of proteins acts upstream, downstream or together with caspase-like activity, MG132 was added to the protein extracts and DEVDase activity was measured. If proteasomal degradation acts downstream of DEVDases, then it would be expected that there would be no changes in the level of DEVDase activity, but if it acts upstream or in cooperation with caspase-3 like enzymes, then we would expect to see an increase or decrease in DEVDase activity.

Proteins of pollen tubes treated with incompatible PrsS-proteins and control pollen tubes were extracted as described in the materials and methods section. In these extracts, DEVDase activity was already stimulated by SI before the extracts were mixed with 40 μ M MG132 and the control sample was mixed with DMSO, which was the solvent for MG132 (see Figure 3.6).

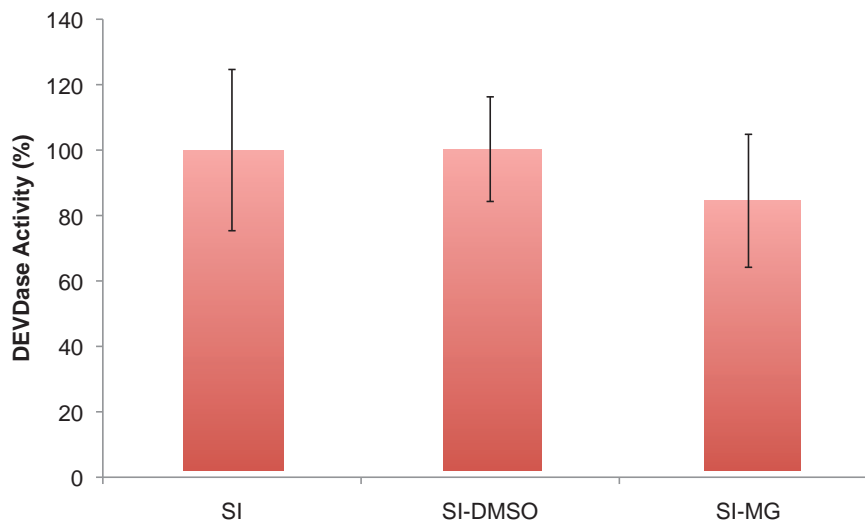


Figure 3.6.: Caspase activity of pollen tubes with induced SI and added 40 μ M MG132 in the pollen tube extract (MG-SI). SI presents the DEVDase activity of pollen incubated with the recombinant stigmatic PrsS proteins; SI-DMSO presents activity of pollen that had added DMSO in the SI pollen tube extract; N=3 repeats. Error bars represent \pm Standard Deviation of means.

As can be seen from Figure 3.6, the DEVDase activity of SI extracts with added inhibitor of proteasomal activity MG132 was significantly decreased by 15 % compared to SI induced DEVDase activity (P=0.026; *). The DMSO solvent had no effect on the DEVDase activity when added to the SI challenged pollen protein extract (P=0.963, NS), indicating that the proteasome inhibitor MG132 reduces the DEVDase activity.

These data suggest that inhibition of proteasomal activity by MG132 in incompatible *Papaver* pollen tubes has a small but significant effect on activated caspases and that it acts upstream or alongside of caspase-3 like activation.

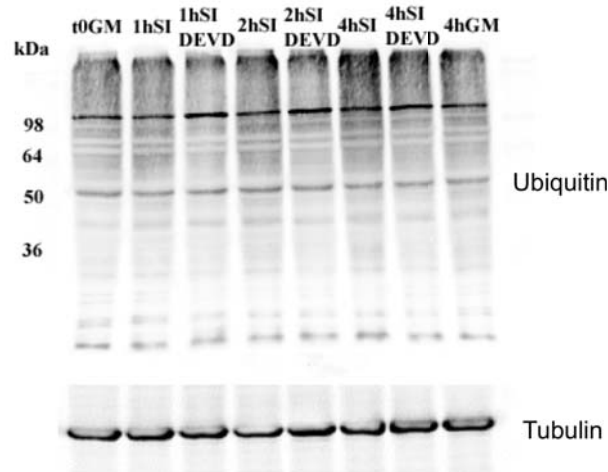
3.2.7. Caspase-3 inhibitor decreases ubiquitination

In order to make a firmer connection between PCD in poppy SI and ubiquitination, an experiment using the caspase-3 inhibitor, Ac-DEVD-CHO, was performed. Pollen tubes were pretreated for 1 h with Ac-DEVD-CHO and then challenged with incompatible stigmatic recombinant PrsS-proteins for 3 different time points: 1 h, 2 h and 4 h. Total protein extracts were separated by SDS-PAGE gel, and blotted and probed with an anti-ubiquitin antibody (see Figure 3.7). Figure 3.7.a shows the ubiquitinated protein pattern in pollen tube samples with induced SI at three different time-points. The ubiquitination levels were higher with SI samples compared to samples that were pretreated with the inhibitor of caspase-3-like activity, Ac-DEVD-CHO and then SI challenged.

The relative signal intensity of the ubiquitination pattern was measured using Quantity One software (see Figure 3.7.b). Ubiquitination in the *Papaver* pollen that was incubated with the incompatible stigmatic PrsS recombinant proteins increases with the time of SI challenge.

When caspase-3-like activity was inhibited, there was ~20 % less ubiquitination of proteins, however, with the increasing time of SI challenge, the ubiquitination levels increased as well.

a



b

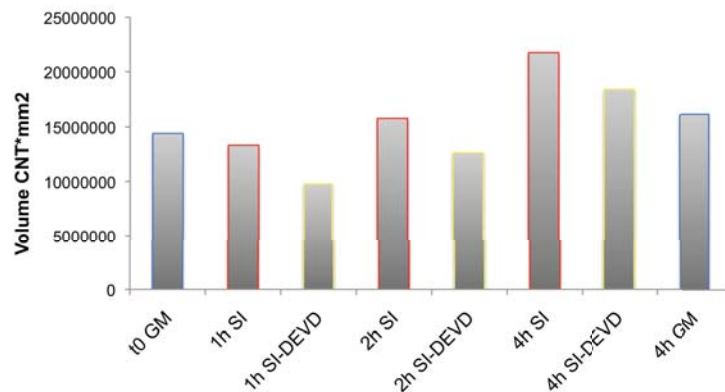


Figure 3.7.: Protein ubiquitination levels in poppy pollen tubes pretreated with an inhibitor of caspase activity (Ac-DEVD-CHO) and SI challenged at three different time points: 1 h, 2 h and 4 h. Untreated pollen tubes germinated in GM are a negative control at t0 and 4 h (blue outline) (a) western blot probed with ubiquitin antibody, tubulin presents a control for equal loading; (b) relative light intensity of ubiquitination levels, blue outline presents untreated control, red outline presents samples with induced SI and yellow outline presents samples pretreated with Ac-DEVD-CHO and then SI induced. (N=1)

The experiment was carried out only once, so a firmer conclusion would require more repeats. However, taken together these data indicate that during SI in incompatible *Papaver* pollen tube increased ubiquitination of yet unknown protein targets occur, which are probably targeted for degradation by the 26S proteasome. This SI-specific ubiquitination of

proteins is connected with the caspase-3-like activity, which, based on previous results, acts upstream or in parallel with the UbP pathway in the incompatible *Papaver* pollen tube.

3.2.8. Involvement of an E3 ligases in *Papaver* SI

The E3 ligase AtPUB17 and its tobacco homologue NtACRE276 were demonstrated to play a functional role in the HR cell death in tobacco and *A. thaliana*, mediated by the resistance proteins (Yang et al., 2006). In a screen for interactors of the ARM domain of PUB17, (Sadanandom et al., 2008) isolated the POB1 protein. AtPOB1 belongs to the family of BTB/POZ transcriptional repressors and is localised in the nucleus during HR. Dr Ari Sadanandom (University of Durham) provided antibodies against PUB17 and POB1 proteins. We wished to investigate further the involvement of UbP pathway in the SI in *Papaver*. If this was the case, there might be some functional homologues of PUB17 and POB1 activated in the *Papaver* pollen tube system, recognized by the antibodies. If the proteins could be identified, we could investigate further their possible involvement in the SI in *Papaver*.

While anti-PUB17 antibody (PUB17 with Mw 83 kDa) did not recognise any specific protein (Figure 3.8.a), anti-POB1 antibody (POB1 with Mw 65 kDa) recognised distinct proteins in poppy pollen tube extracts (Figure 3.8.b).

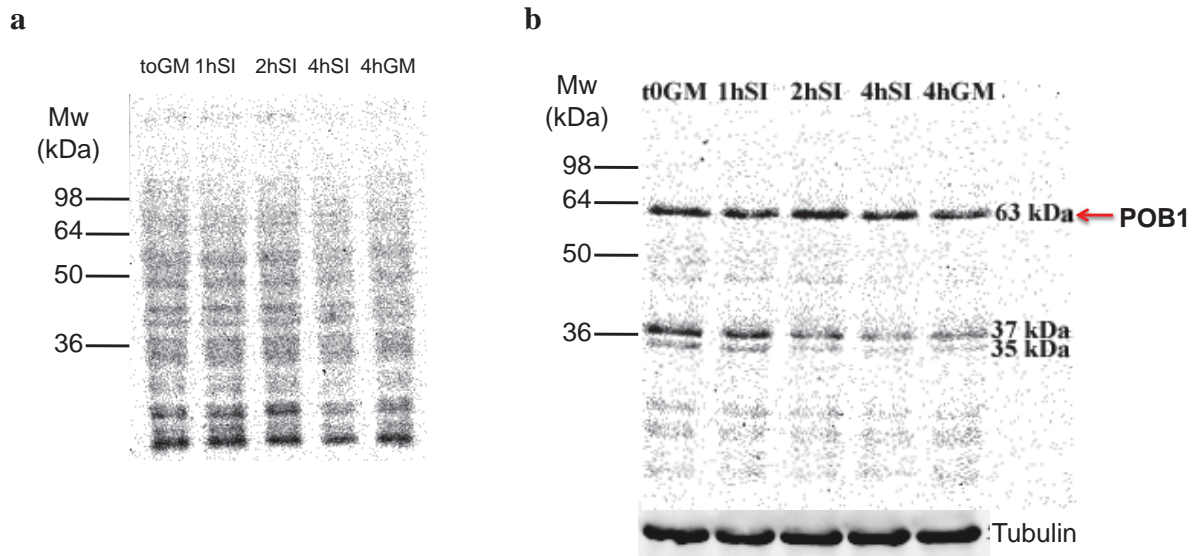


Figure 3.8: Protein expression of putative homologues of AtPUB17 and AtPOB1 E3 ligases during SI in *Papaver* (a) AtPUB17 antibody did not recognise any specific protein homologue at 83 kDa during SI in *Papaver*. (b) AtPOB1 (Mw 65 kDa) recognised a putative homologue at 63 kDa. Another two protein bands at 37 and 35 kDa were recognised by AtPOB1. Decrease of signal with time of SI suggests that SI triggered their degradation. Tubulin was used for equal loading.

PUB17 antibody resulted in a smear, with some weaker bands visible at low molecular weights. Signal intensity of the poppy pollen extract detected with AtPUB17 decreased with the time of SI incubation, but this was also the case with untreated pollen. However, when testing whether the AtPOB1 antibody could recognise an equivalent protein during SI in *Papaver* pollen, we observed a distinct band at 63 kDa and two lower ones at 37 and 35 kDa. Whereas the higher molecular weight band probably corresponds to the POB1 protein (Mw 65 kDa), the lower bands might be degradation products (Figure 3.8.b), suggesting that SI triggers its degradation.

A. thaliana AtPOB1 plants were resistant to virulent bacteria, they accumulated ROS and exhibited HR cell death (A. Sadanandom, personal communication). AtPOB1 represses the expression of genes that regulate defence against pathogen *Pseudomonas* (Sadanandom et al., 2008). If drawing a parallel between HR and SI systems, AtPOB1 homologues recognised by the POB1 antibody could function by repressing genes required for the SI

response. Upon SI, putative poppy POB1 homologues may be targeted for degradation, gene expression is activated and functional SI can occur. Interestingly, AtPOB1 proteins are localised in the nucleus (Sadanandom et al., 2008). Their localisation has not yet been examined in the *Papaver* pollen, however if it is nuclear as well, this could explain their slow degradation, as it is known that DEVDase activity in *Papaver* becomes localised in the vegetative cell and generative nucleus at 5 h SI (Bosch and Franklin-Tong, 2007), although it was rarely observed in the pollen at 1 or 2 h post SI. This could imply that POB1 homologues in *Papaver* might be responsible for repressing caspase-3-like activity in compatible pollen and are being subsequently degraded in incompatible pollen tubes.

3.3. DISCUSSION

Ubiquitin-dependent proteasomal degradation pathway plays a role during SI in *Papaver* pollen and is most likely an important component of *Papaver* SI. In the present study, a pharmacological approach with the proteasome inhibitor MG132 was used to demonstrate the role for UbP pathway. A link between PCD and the UbP pathway in incompatible *Papaver* pollen was also demonstrated. MG132 is a membrane-permeable peptide aldehyde with chymotrypsin-like inhibitory activity. The treatment of poppy pollen with the selective proteasome inhibitor MG132 slightly altered tube morphology and decreased the length of pollen tubes in a concentration-dependent manner.

UbP pathway is involved in kiwifruit pollen tube organization, germination and maintenance of polarized pollen tube growth as ubiquitin and its conjugates were localized

mainly in the apex of pollen tubes (Scoccianti et al., 2003, Speranza et al., 2001). When proteasomal degradation was inhibited by MG132 dramatic changes to the morphology of pollen tube were observed, such as inhibition of pollen tube growth and pollen tube tip swelling and branching, and germination of more than one tube per grain, which was also observed in *Picea* pollen (Scoccianti et al., 2003, Sheng et al., 2006, Speranza et al., 2001). However the effects of the inhibitor were reversible since the removal of inhibitor restored growth. Those effects were not so dramatic in case of *Antirrhinum* pollen, although some pollen tube tips appeared to be swollen (Qiao et al., 2004b). Similar response was observed in *Papaver* pollen germination with severe pollen tube alterations at concentrations of MG132 exceeding 40 μ M. The alterations in pollen tube morphology suggest that UbP activity is required for normal pollen tube growth and development in *Papaver*. As pollen tube growth was affected by MG132 at higher concentrations, 40 μ M concentration was chosen for the experiments on *Papaver* pollen.

It is well established that the UbP pathway, and more precisely E3 ubiquitin ligases play a role in the sporophytic SI (Yee and Goring, 2009, Tantikanjana et al., 2010) and in the S-RNase based gametophytic SI (Meng et al., 2011). MG132 inhibited compatible pollination in *Antirrhinum*, but had little effect on incompatible pollination *in vitro* or *in vivo* (Qiao et al., 2004b). During compatible pollination the level of ubiquitinated S-RNases was significantly higher than during incompatible pollination in *Antirrhinum* and *Petunia* (Hua and Kao, 2006, Qiao et al., 2004b). The S-RNase degradation model was based on these findings. It was postulated that pollen determinant of S-RNase based SI, SLF, specifically detoxifies non-self S-RNases via the UbP pathway allowing compatible pollinations and thus indicating that non-self pollen tubes might have been protected by specific degradation

of non-self S-RNases, while self-S-RNases remained active in self-pollen tubes (Zhang and Xue, 2008, Takayama and Isogai, 2005). The new model of collaborative non-self recognition in S-RNase-based SI, revealed by Kubo et al., (2010) now predicts that there are multiple types of *SLF* genes in pollen and the product of each type of SLF (Sx-SLF) interacts with a subset of non-self S-RNases.

In *Papaver*, the ubiquitination was implicated to play a role during the SI response, rather than during the SC response. In incompatible pollen tube extract, an increased ubiquitination of yet unknown proteins was detected that is connected with the caspase-3-like activity, which acts downstream or in parallel with the UbP pathway.

The 26S proteasomal degradation was also demonstrated to play a role during SI in *Brassica*, where activated SRK targeted E3 U-box ligase ARC1 to the proteasome, thus implicated to mediate the UbP pathway (Stone et al., 2003). Suppression of ARC1 in *Brassica* or incubation of *Brassica* stigmas with the proteasome inhibitors can lead to the breakdown of SI response (Stone et al., 1999, Stone et al., 2003). Following incompatible pollination, ARC1 targets substrate proteins, presumably compatibility factors, and their degradation by the 26S proteasome results in pollen rejection (Samuel et al., 2011).

Ubiquitin-dependent protein degradation is also important during plant-pathogen interactions and plant responses to the environmental factors (Dielen et al., 2010). Vacca et al.,(2007) demonstrated that decreased cell viability due to heat shock (HS) in tobacco BY2 cells was rescued by pretreatment with MG132, showing that the impairment of the proteasome function results in the prevention of cell death. Inhibition of the proteasomal degradation by MG132 also rescued the loss of viability in yeast cells undergoing acetic acid induced PCD (Valenti et al., 2008), and tungsten induced loss of viability in pea root cells (Adamakis et

al., 2011). The inhibition of proteasomal degradation inhibited length of tracheary elements in *Zinnia* cell cultures and also in *A. thaliana* (Zhao et al., 2008). Thus, the examples stated above indicate that proteasomal activity is involved in and is required for cell death in plant cells.

A similar picture was observed in *Papaver* SI, when the viability of incompatible pollen tubes was significantly restored when proteasomal degradation was inhibited by MG132 confirming the involvement of proteasomal degradation in the SI response in *Papaver* pollen. The use of proteasome inhibitors also allowed for the demonstration of the role of proteasomal degradation in PCD.

A direct link between proteasome-dependent degradation and plant PCD was established by Hatsugai et al., (2009). By using caspase-3 inhibitors, proteasome inhibitors and RNAi lines of the proteasome β -subunits, which possess proteolytic activity β 1 (PBA), β 2 (PBB) and β 5 (PBE), they demonstrated that the proteasome was directly involved in bacteria-induced vacuole membrane and plasma membrane fusion and consequently hypersensitive cell death. Moreover, they identified that the proteasomal subunit PBA1 acts as a caspase-3-like enzyme.

The data, presented above confirm that caspase-3-like activity of SI samples was significantly higher compared to that in the untreated control pollen, while caspase-3-like activity of pollen tubes in which proteasomal degradation had been inhibited before induction of SI was significantly decreased although not to same level as control. This demonstrates that caspase-3-like activated PCD in poppy SI requires proteasome activation. Taking into account that the proteasomal subunit PBA1 acts as a caspase-3-like enzyme in *A.*

thaliana, it is tempting to suggest that the same happens in *Papaver* (Hatsugai et al., 2009). This was not tested as this work was conducted before the report by Hatsugai et al., (2009) was published; nevertheless, some parallels can be drawn.

Molecular mechanisms of SI share similarities with the histocompatibility in animals as well as with the hypersensitive response in plant-pathogen incompatible interaction as all these mechanism require high degree of recognition specificity to recognise between self and non-self. Recognition specificity during plant-pathogen response requires highly polymorphic resistance genes, and it involves a specific interaction between receptor at the epidermal cell surface and its cognate peptide ligands from pathogen (Coll et al., 2011). When a microbial pathogen invades the plant tissue, a defence mechanism is initiated in the plant that triggers signalling cascade of downstream events leading to inhibition of growth of plant cells in order to prevent spread of the pathogens. Downstream signalling events are strikingly similar to downstream events during *Papaver* SI: influx in cytosolic calcium, alterations of the actin cytoskeleton, activation of ROS, activation of caspase-like proteins and cell death. Some molecules were also implicated to play a role during SI and pathogen response, such as tobacco *S*-like RNase NE, that share similarities with RNases determining the specificity of the *S*-RNase based SI, inhibited the hyphal elongation of plant pathogens (Hugot et al., 2002, Dodds et al., 1996). Additionally, thioredoxin, that is implicated to negatively regulate *Brassica* SRK in the absence of SCR, was demonstrated to also negatively regulate *Cladosporium fulvum*-9 (Cf-9) (Cabrillac et al., 2001, Rivas et al., 2004). The incompatible interaction between Cf9, a membrane anchored glycoprotein and Avr9, a secreted protein, elicit a hypersensitive response and cell death. The interaction between Avr9 and Cf9 was also used when AtPUB17 protein was identified (Yang et al., 2006). PUB17 is an E3 ligase

that acts as positive regulator of cell death and defense responses in Solanaceae and Brassicaceae (Yang et al., 2006). PUB17 restored functional HR in plants that had HR impaired due to silencing of Cf9 (Yang et al., 2006).

The incompatible interaction between Cf9, a membrane anchored glycoprotein and Avr9, a secreted protein, resulted in cell death. This is similar to the incompatible interaction between the pollen transmembrane protein, PrpS, and secreted stigmatic protein, PrsS, which also results in cell death in *Papaver* pollen. A collaboration with Dr. Ari Sadanandom, resulted in testing anti-PUB17 antibody during SI response in *Papaver*, as well as another E3 ligase, named POB1, that was identified as PUB17 interacting protein (A. Sadanandom, *personal communication*). Using antibodies against AtPOB1 the potential poppy homologues of POB1 were detected and their abundance changed over time, implicating a role for POB1 homologues during *Papaver* SI. Nuclei localised AtPOB1 act as a negative regulator of PCD, as plants that were deficient in POB1 produced spontaneous cell death (Sadanandom et al., 2008). *A. thaliana* AtPOB1 plants were resistant to virulent bacteria, they accumulated ROS and exhibited HR cell death (A. Sadanandom, *personal communication*). AtPOB1 represses the expression of genes that regulate defence against pathogen *Pseudomonas* (Sadanandom et al., 2008). If drawing a parallel between HR and SI systems, AtPOB1 homologues in *Papaver*, recognised by POB1 antibody, could function by repressing genes required for SI response. Interestingly, AtPOB1 proteins are localised in the nucleus (Sadanandom et al., 2008). Their localization was not yet examined in the *Papaver* pollen, however, if it is nuclear as well, this could explain their slow degradation, as it is known that DEVDase activity in *Papaver* peaks at 5 h of SI and becomes localised in the vegetative cell and generative nucleus (Bosch and Franklin-Tong, 2007), while it was rarely observed in the pollen at 1 or 2 h post SI. If POB1-like proteins act as negative regulators of

PCD by inhibiting caspase-3-like enzymes in normal pollen, then their degradation could trigger caspase-3-like activity.

This could implicate that POB1 homologues in *Papaver* might be responsible for repressing caspase-3-like activity in compatible pollen and are being subsequently degraded in incompatible pollen tubes. The identification of POB1 homologues during *Papaver* SI and their further analysis will establish a further evidence for comparison between two mechanisms, SI and HR.

Based on the results obtained, several models were created that could help to explain a link between UbP degradation and caspase-3-like activity in SI-induced PCD in *Papaver* pollen (Figure 3.9-3.10). These models assume that proteasome activation acts in parallel with DEVDase activity, because a decrease in DEVDase activity was observed where the proteasome inhibitor MG132 was used with the SI induced pollen tube protein extracts.

A model presented in Figure 3.9 is based on the discovery by Hatsugai et al., (2009), and it assumes that proteasome contains caspase-3-like activity, as they demonstrated in *A. thaliana* where proteasomal subunit PBA1 is a caspase-3-like enzyme. Although the experiments for this project were conducted before the publication by Hatsugai et al., (2009), some of the results regarding the involvement of the UbP pathway in *Papaver* SI can be explained by this model.

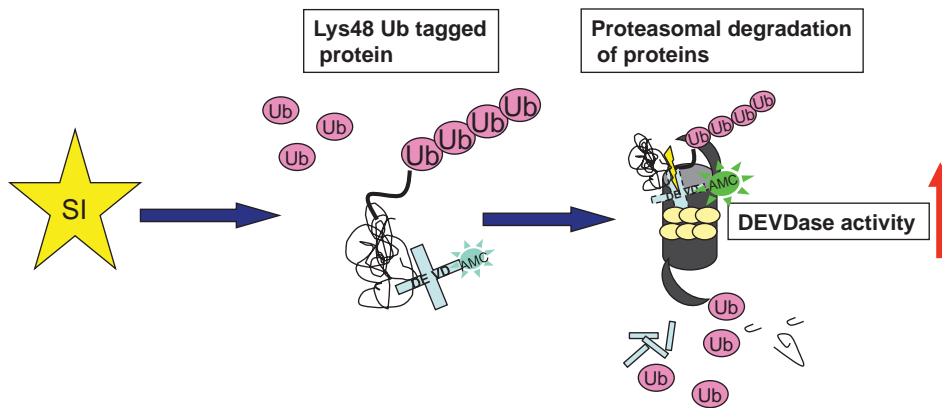


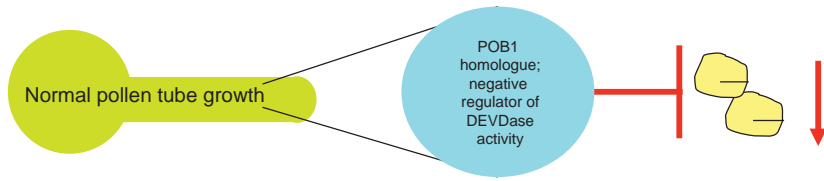
Figure 3.9.: Model of proteasomal degradation and caspase-3-like activation assumes that proteasome contains caspase-3-like activity. During the SI (yellow star) the proteins targeted for degradation are tagged with Ub via Lys48 residue. When the chain is long enough, proteins are degraded by the 26S proteasome and the model assumes that among them are also proteins with DEVD motif, recognised by DEVDases within the proteasome (yellow circles). During an SI we observed an increase in ubiquitinated proteins as well as increase in DEVDase activity. Substrate for caspase-3-like enzymes is represented as a fluorescent probe attached to DEVD tetrapeptide used in caspase-like assays, Ac-DEVD-AMC

The Ac-DEVD-AMC substrate (used for illustration), substrates for caspase-3-like enzymes, and additional unknown proteins, are first tagged by ubiquitin molecules and targeted for the proteasomal degradation. Thus we can explain the increase in ubiquitination levels observed by western blot in SI induced pollen extracts. Once in the proteasome, the catalytic subunit (i.e. caspase-3-like enzyme) cleaves the substrate. When the proteasomal degradation is inhibited by MG132, the decrease in DEVDase activity is observed, which is explained by the model (Figure 3.6. and 3.9). MG132 inhibits proteasomal degradation of short-lived proteins, so it is assumed that proteasomal degradation is not completely inhibited, which would explain why there is not a complete decrease in DEVDase activity (Figure 3.6). In order to test this model we would need to use more specific inhibitors of proteasomal activity, blocking the catalytic subunit, such as Ac-APnLD-CHO (Hatsugai et al., 2009). However, this model cannot explain why there is less ubiquitination in pollen if we inhibit DEVDase activity by Ac-DEVD-CHO before the SI induction (Figure 3.7). If the model is correct, we should observe more ubiquitinated proteins as the proteasomal degradation and

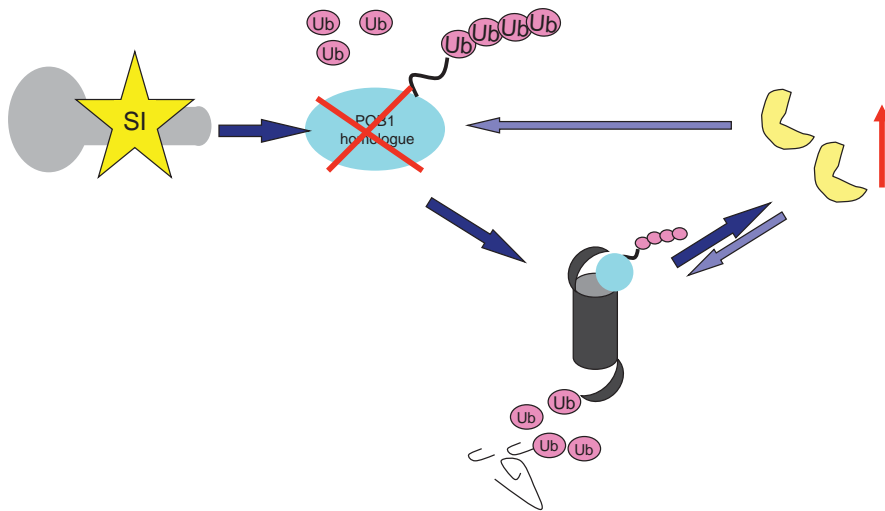
caspase-3-like activation are inhibited, unless the inhibitor Ac-DEVD-CHO only inhibits DEVDase activity and does not affect proteasomal degradation by other catalytic subunits. Hatsugai et al., (2009) demonstrated that during the bacterial infection $\beta 1$ and $\beta 5$ subunits of proteasome with trypsin and chymotrypsin activity also play a role, and that their activity is reduced upon the inhibition of caspase-3-like activity. However, this might not be the case in our model, and therefore, the proteasomal degradation of other proteins that are not substrates for caspase-3 like enzymes might still continue. However, further experiments would be required to confirm any of these predictions.

Another model that could be proposed is based on the discovery by Hatsugai et al., (2009), who reported membrane fusion between the vacuolar membrane and the plasma membrane leading to leakage of vacuolar contents into the apoplast, thereby containing the bacterial infection. The membrane fusion is presumably suppressed by a negative regulator, which is degraded by the 26S proteasome upon bacterial infection. A similar mechanism could function during *Papaver* SI (Figure 3.10). Results obtained with the antibodies against AtPOB1 E3 ligases indicate the existence of a *Papaver* POB1 homologue that is affected by SI (Figure 3.8). AtPOB1 is a negative regulator of PAMP triggered immunity and effector triggered immunity and plays an important role in regulating HR cell death in *A. thaliana* and *N. benthamiana* plants upon fungal infection with *C. fulvum* (A. Sadanandom, personal communication). Taken together, based on the results obtained with the POB1 antibody during SI in *Papaver* pollen and the report by Hatsugai et al., (2009), an additional model was created. This model is set out in Figure 3.10. It presumes the existence of a negative regulator of DEVDase activity, which could be a putative POB homologue.

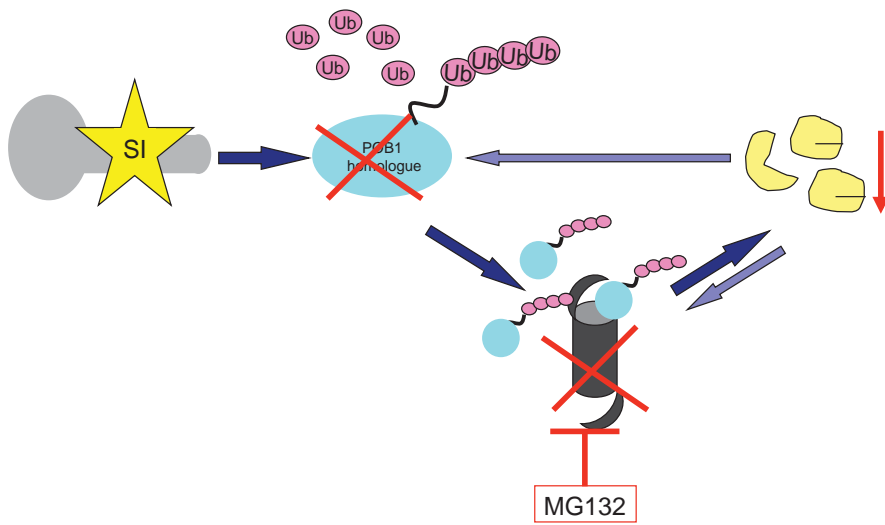
a



b



c



(continues on the next page)

d

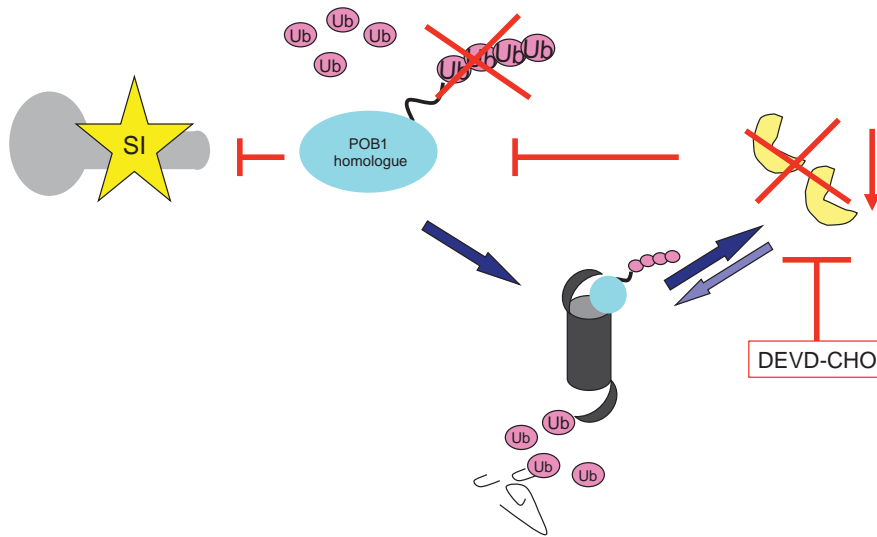


Figure 3.10.: Model that assumes the existence of negative regulator of DEVDase activity, possibly POB1 homologue (a) model assumes that during *Papaver* pollen tube growth, the hypothetical negative regulator of DEVDase activity, possibly POB1 homologue, is regulating the inactivity of DEVDases (b) During SI, negative regulator is tagged by UB through Lys48 residue and targeted for 26S proteasomal degradation and DEVDase activity is increased. Presumably there are also feedback loops between DEVDase activity and proteasomal degradation and DEVDase activity and negative regulator, (c) upon pretreating pollen with proteasomal inhibitor MG132 before SI, the accumulation of Ub is observed as well as decrease in DEVDase activity. Negative regulator is still ubiquitinated but not degraded as proteasomal activity is inhibited (d) when pollen in pretreated with DEVDase inhibitor Ac-DEVD-CHO prior to SI, DEVDase activity is inhibited and this inhibition could feedback to negative regulator, so it is not ubiquitinated anymore. Therefore negative regulator presumes its role and act in concert with DEVDase inhibitor to downregulate DEVDases. Assuming that the proteasomal activity acts upstream of DEVDase activity it is not affected, the degradation of other ubiquitinated proteins targeted during SI is undisturbed.

The model presented in Figure 3.10.a assumes that during normal undisturbed pollen tube growth, DEVDase activity is inhibited by a negative regulator, that could be a *P. rhoeas* POB1 homologue. Upon SI (Figure 3.10.b) the negative regulator is tagged by a chain of ubiquitins, connected by Lys48 and degraded by the 26S proteasome, thus releasing DEVDase activity. The model also assumes a feedback loop between the negative regulator, the 26S proteasome and DEVDase activity. If the proteasomal degradation is inhibited by MG132, then, as known from the results, DEVDase activity is reduced and due to the feedback loop, the ubiquitination of the negative regulator might be reduced, thus re-activating the inhibitor of DEVDase activity (Figure 3.10.c). However, ubiquitination of

other unknown proteins in the pollen tube still occurs but, due to the inhibition of 26S proteasome, their degradation is disabled, therefore the accumulation of ubiquitinated proteins can be observed on a western blot as an increase in ubiquitination signal (Figure 3.5). Upon the addition of the tetrapeptide inhibitor Ac-DEVD-CHO (Figure 3.10.d), the DEVDase activity is decreased, influencing the decrease in ubiquitination of the negative regulator (Figure 3.10.d). However, the proteasomal degradation of ubiquitinated proteins might not be affected, which could explain why the ubiquitination signal of pollen upon SI appeared stronger compared to pollen that was pretreated with Ac-DEVD-CHO before SI induction (Figure 3.7). In order to confirm or disprove this model additional experiments are required which would examine more closely the 26S proteasome activity as well as the POB1 substrate upon inhibition of the DEVDase activity.

Ubiquitination and proteasomal degradation are necessary for normal development of the pollen tube, and for degradation of damaged, outnumbered and unwanted proteins in the cell (Sheng et al., 2010, Sheng et al., 2006, Speranza et al., 2001). They are also strongly involved in the HR of plants to pathogens as well as in other types of SI responses (Dielen et al., 2010, Trujillo and Shirasu, 2010, Chen et al., 2010, Yee and Goring, 2009, Vierstra, 2009). Taken together our data indicate that the proteasomal degradation acts together with, or upstream of, caspase activation and that there is a potential link between caspase activity and proteasomal degradation (see Figure 3.11).

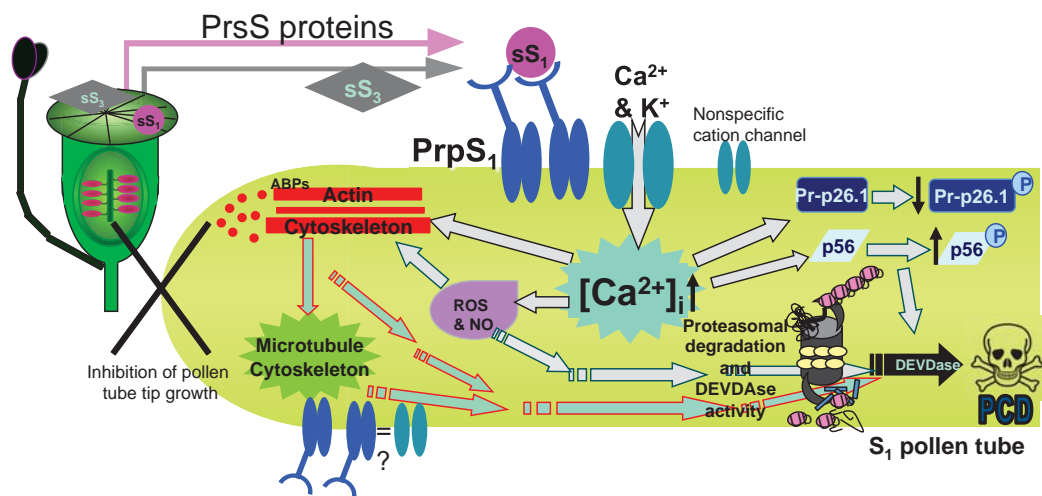


Figure 3.11.: Schematic model of the SI response in *Papaver*. Upon the interaction of secreted stigmatic PrpS proteins and pollen transmembrane protein PrpS, a downstream signalling network is triggered, starting with an increase in K^+ and $[Ca^{2+}]_i$ who is signalling to the inhibition of pyrophosphatase activity and pollen tube tip growth, activation of MAPK, depolymerization of actin and microtubule cytoskeleton and appearance of punctate actin foci, activation of ROS and NO and activation of caspase-like activities, leading to the PCD of the pollen tube. The model presents DEVDase activity that most likely acts in parallel with proteasomal degradation. DEVDases are presented as yellow circles within the proteasome, as identified by Hatsugai et al., (2009).

However, in order to establish a clearer position of the UbP pathway on the SI timeline in *Papaver* pollen, and to draw further parallels between SI and HR, additional experiments would be required investigating proteasome inhibition, finding targets of ubiquitination during SI and specifying the role of the *P. rhoeas* POB1 homologue. In order to specifically elucidate the relationship between proteasome and DEVDases, and to determine whether DEVDase activity is part of the proteasome or acts separately, biochemical and imaging assays should be performed.

Gu et al., (2010) developed a membrane permeable fluorescent probe, MV151, containing a vinyl sulphone reactive group and Bodipy fluorescent group, that bind to the plant proteasome in an activity-dependent manner and could be used for live cell imaging of proteasome activities as well as quantification by protein gels during SI in *Papaver* pollen in

the presence of the proteasome and the DEVDase inhibitor. In this way the proteasome could be also tested for other caspase-like activities. Antibodies against different subunits of the proteasome could also be obtained and tested. (Kisselev et al., 2003) measured different substrate specific sites of the proteasome by using isolated proteasomes from rabbit muscle or yeast. We could adopt this method and analyse a proteasome isolated from *Papaver* pollen for caspase-like activities using inhibitors and fluorescent tagged tetrapeptides using the plate reader during SI. Live cell imaging could be performed using CR(DEVD)₂ probe for DEVDase activity and MV151 probe for proteasome activity (Gu et al., 2010, Bosch and Franklin-Tong, 2007).

By performing biochemical assay of binding DEVDases on the biotinylated column and detecting the protein on a blot with antibody against PBA1, we could initially test whether the observation that the PBA1 subunit of proteasome exhibit DEVDase activity (Hatsugai et al., 2009) is specific for *A. thaliana* leaves or is more general within different plant species. Additionally, the studies of involvement of the UbP pathway during SI in *Papaver* pollen could be tested during SI in *A. thaliana* pollen expressing the *Papaver* pollen determinant PrpS (for details see next chapters). If the transgenic *A. thaliana* model were to produce similar results, then the genetic manipulations and mutations of different components could be performed and tested for response.

In order to identify targets of the proteasomal degradation a pull down assays could also be performed in a similar manner to that described above using biotinylated ubiquitin. The protein band could be excised and subjected to tandem mass spectroscopy (MS) which could reveal the nature of proteins specifically ubiquitinated during SI which are not ubiquitinated in normal untreated pollen.

The role of POB1 should also be analysed more closely. Western analysis using POB1 antibody should be repeated during time progression of the SI. In order to identify a link between putative PrPOB1 and DEVDase activity, POB1 should be also tested using inhibitors of proteasome activity and DEVDase activity. To test the model in Figure 3.10, where POB1 is presented as a negative regulator of SI, it would be interesting to see if it would be identified on MS. The POB1 sequence should be obtained and the protein could be inhibited by using designed POB1 antisense oligonucleotides. If POB1 does act as a negative regulator of SI then an increase in DEVDase activity should be observed even in untreated *Papaver* pollen. It would also be interesting to establish a link between POB1, whose *A. thaliana* and *N. benthamiana* homologues are implicated in plant pathogen responses, and ROS during SI in *Papaver* pollen.

By performing some of the additional experiments, the possible role of ubiquitination and proteasomal degradation should be more firmly linked to the SI in *Papaver* pollen and further parallels should be established in molecular mechanisms of SI and HR.

CHAPTER 4

Investigation of the interaction between PrpS and PrsS

4.1. INTRODUCTION

As mentioned in introduction (section 1.4.3), the recent discovery of PrpS, the *Papaver* pollen *S*-determinant (Wheeler et al., 2009) has identified PrpS as a small, 20 kDa transmembrane protein, associated with the plasma membrane . It represents a novel class of receptor as it has no homology to any known protein in the database (Wheeler et al., 2009). In *Papaver*, SI is comprised of interaction between the secreted stigmatic PrsS proteins that act as a ligand to the receptor on the pollen tube. Identification of PrpS therefore strongly supports the long-standing hypothesis of receptor-ligand – like interaction (Wheeler et al., 2009).

To establish whether PrpS is functionally involved in the SI response, peptides were first tested with *in vitro* SI bioassays. Pollen with the haplotype PrpS₁/PrpS₃ was challenged with the incompatible recombinant stigmatic PrsS₁ and PrsS₃ proteins, which had been incubated with the PrpS₁ peptides. The pollen was ‘rescued’ when peptides were able to block the receptor-ligand type interaction and so far this was the first indication that the predicted extracellular region is involved in recognition and that PrpS might mediate pollen inhibition (Wheeler et al., 2009).

The main aim of this part of the project was to further characterize the binding between PrpS and PrsS in order to demonstrate that PrpS is the pollen *S*-determinant. There are several approaches to characterize and identify regions and residues of protein-protein binding interaction. Some of them, such as mutagenesis, were not possible due to difficulties to transform *Papaver* plants. Other approach that is widely used for protein-protein interaction is yeast-two-hybrid assay. Some preliminary investigations of interaction between PrpS and

PrsS were conducted by Natalie Hadjosif, that identified a large number of false positive interactions as the PrsS proteins seem to auto-activate the system, while PrpS appeared toxic for the cells, presumably due to hydrophobicity of the protein. Considering that PrpS is a transmembrane protein, most likely adopted yeast-two-hybrid screens would be required, such as split-ubiquitin (Iyer et al., 2005). However, due to the time constraints we decided to test the interaction by the slot-blot binding assay, also known as far western assay, by which the protein of interest is bound on the membrane (on the blot) and not separated by electrophoresis as with western blot. The membrane is then incubated with binding partner and the potential interactions detected by specific antibody against binding partner. The far-western technique using peptide arrays is widely used for the mapping of epitopes and for the receptor-ligand interactions (Volkmer et al., 2011). Using peptide array and dot blot assay, a subdomain on *Brassica* stigmatic SRK was identified, that has an important role in binding of the pollen SCR (Kemp and Doughty, 2007). Furthermore, using dot blot assay, they demonstrated an affinity for binding between *Brassica* SRK microsomal membrane proteins and recombinant pollen SCR protein in an *S*-specific manner (Kemp and Doughty, 2007).

We wished to confirm whether one key criteria for the pollen *S*-determinant, which was binding to the pistil *S*-determinant, and the *S*-specific interaction between PrpS and PrsS was investigated. Initially, the secondary structure predictions of PrpS structure were analysed using various transmembrane protein prediction programmes and the extracellular domain was identified as a result of that search. By designing and synthesizing peptides that represent parts of the potential ligand binding domains of the extracellular region of PrpS, we wished to confirm the *S*-specific interaction between PrpS and PrsS *in vitro*.

This study formed a part of the publication (Wheeler et al., 2009) and the review (Wheeler et al., 2010). My contribution was the analysis of the *Papaver* pollen *S*-determinant, PrpS. I analysed the predicted transmembrane structure of the PrpS protein, and demonstrated using far-western ligand-blotting that a predicted extracellular domain interacts in an *S*-specific manner with the stigmatic PrsS proteins. The papers are inserted in the Appendix III.

4.2. RESULTS: The *S*-specific interaction of PrpS and PrsS

4.2.1. Analysis of predicted structure of PrpS

In order to test if the PrsS and PrpS interact, it was first necessary to obtain the predicted structure of the transmembrane protein PrpS.

The majority of membrane protein prediction programmes base their searches on the fact that transmembrane (TM) segments in proteins can be distinguished by continuous stretches of hydrophobic amino acid residues (Krogh et al., 2001, Hirokawa et al., 1998, Tusnády and Simon, 2001). Figure 4.1 shows the structure of the pollen PrpS₁ protein as predicted by the prediction programme TMHMM (<http://www.cbs.dtu.dk/services/TMHMM/>).

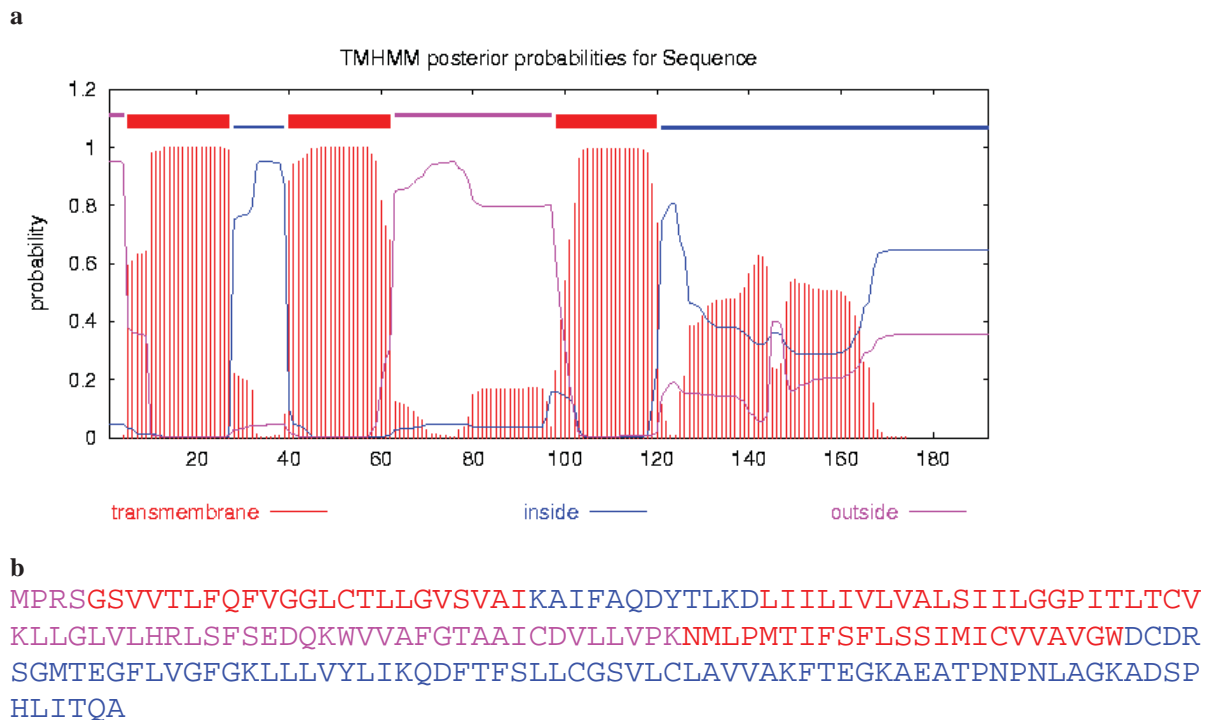


Figure 4.1. Structural prediction of PrpS₁ as predicted by prediction programme TMHMM (**a**) prediction diagram predicts N terminus to be extracellular and C terminus intracellular. Programme predicts 3 TM segments but also shows a hydrophobic tendency between amino acids 125-170, where there is potentially another TM segment. (**b**) amino acid sequence of PrpS₁ with colour-coded amino acids to illustrate extracellular, transmembrane and intracellular regions. Amino acids are colour-coded: pink – extracellular, red – transmembrane, blue – intracellular.

As PrsS proteins are secreted by the stigma it was expected that the interaction would occur on the extracellular part of the PrpS protein, as the extracellular part of the PrpS is exposed to the secreted stigmatic PrsS.

According to the first TMHMM prediction, PrpS₁ has 3 transmembrane domains and an extracellular loop segment, comprised of 35 amino acids, from position 63-97, which seems the most promising site for the interaction with the PrsS proteins (Figure 4.1.b).

The N-terminus of PrpS is possibly a signal peptide and therefore cleaved off (Petersen et al., 2011). The significance of this part of the protein being extracellular is not discussed further, but the work presented here discusses on the central extracellular part of the PrpS protein (35 aa), where the interaction most likely occurs. According to the TMHMM

prediction, 4 overlapping peptides, covering the extracellular domain sequence of extracellular domain, were synthesized by AltaBiosciences (Figure 4.2).

```
Peptide A1: VKLLGLVLHRLSFSE
Peptide A2:           LHRLSFSEDQKWVVA
Peptide A3:           DQKWVVAFGTAAICD
Peptide A4:           TAAICDVLLVPKNML
Scrambled A3 peptide: FTVDVKDCAAAGWQI
```

Figure 4.2.: Amino acid sequence of four overlapping peptides. Peptides represent PrpS₁ extracellular 35aa domain predicted by TMHMM prediction programme and at the bottom scrambled A3 peptide.

Peptide A3 and its randomized version were already used in order to establish the functionality of the PrpS in the SI response. They were first tested for the effect on the SI phenotype (Figure 4.3) (Wheeler et al., 2009).

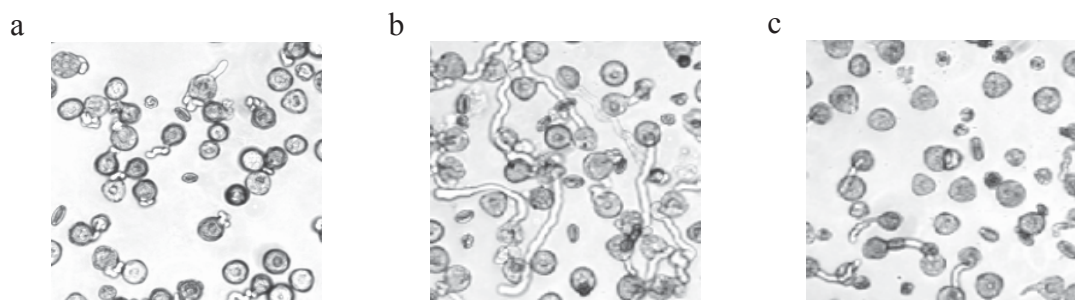


Figure 4.3.: *In vitro* SI bioassay. (a) PrsS proteins were added to pollen and SI reaction occurred – pollen was inhibited; (b) PrsS proteins were added to pollen together with A3 peptide and pollen was “rescued”; (c) when scrambled A3 peptide was added to pollen and SI reaction occurred it indicates that scrambled peptide had no effect and pollen was inhibited (Wheeler et al., 2009).

Figure 4.3.b (work conducted by Kim Osman) illustrates that the addition of the 15-mer peptide A3, corresponding to parts of the predicted extracellular domain of the PrpS₁, rescues pollen tube growth in the competition bioassay with PrsS₁, whereas randomized version had no effect in the bioassay (Figure 4.3.c) (Wheeler et al., 2009). Since the *in vitro* bioassay experiment was carried out (Figure 4.3), two more PrpS alleles had been identified:

PrpS₃ and PrpS₈. Alignment and prediction of their structures, as predicted by TMHMM is presented in Figure 4.4.

```

PrPS1A      MPRSGSVVTLFQFVGGGLCTLLGVSAIKAIFAQDYTLKDLIIILIVLVALSIILGGPITLT 60
PrPS8A      MPRHAIVVHVVFQFLAGFVTLFGSALAIRTVISHPYTLQDLIIFILLFAI AVLVGKYITIT 60
PrPS3A      MPRNRHAIYVFRFLAMFVTLFGVAFLVRIKSHHALTWKDLTAFVVLIVLSVIGGGYVSLM 60
          ***      .: :*:*: . : **:* .: .: :      : * :** :*:*.::: * :.:

PrPS1A      CVKLLGLVLHRLSFSQKQWVAFGTAAICDVLVLPKNMLPMTIFSFLSSIMICVVAAGW 120
PrPS8A      YLKLLGWVLQHLTVTENQKQWVAFGTAVCDVFLVTTNMTPVTSICFLSSIMICVVAAGW 120
PrPS3A      YVQALRWLLQHLHVSENQKQWVAFGTAAICDVLVLPKNMLPMTIFSFLSSIMICVVAAGW 120
          : : * :*: * .: :*:*:*:*:*:*:*:*:*:*. ** . : :. *: : ***** **

PrPS1A      DCDRSGMTEGFLVGFGLKLLLVYLIKQDFTFSLGCVLCLAVVAKFTEGKAEATP-NPNL 179
PrPS8A      DRDRSGMTEGFLIGFGLKLLLVNLIREDCTASVMYGSVLF LAIVAKFTENAVGATPLNPP I 180
PrPS3A      GRDRSGMTEGFFVGFGLKLLLVNLIINLFSGNLPSALF* TGIIVLFLAVVAKLTECADEATS -AARL 179
          . *****:*****: * : : . : : * * * *:***: * ** . . :

PrPS1A      AGKADSPHLITQA 192
PrPS8A      VGHEDSSHRSVEV 193
PrPS3A      VGNADSPCPNEA- 191
          .*: **.

```

Figure 4.4. Clustal W alignment of structural predictions of PrpS₁, PrpS₃ and PrpS₈ as predicted by TMHMM. Amino acids are colour-coded: pink – extracellular, red – transmembrane, blue – intracellular. Identical amino acids are marked with “*”, conserved substitutions with “.” and semi-conserved substitutions with “:”. Clustal W source: <http://www.ebi.ac.uk/Tools/clustalw2/index.html>

As prediction programmes give just predictions, we studied the sequence analysis of all three PrpS alleles using various prediction programmes in order to obtain a more “realistic” picture of the predicted structures.

PrpS sequences were analysed using following transmembrane protein prediction programmes: TMHMM2.0, PredictProtein, SOSUI, HMMTOP, TMpred, TM-Finder, SPLIT 4, ConPred II, Phobius (Hirokawa et al., 1998, Tusnády and Simon, 2001, Krogh et al., 2001, Rost and Liu, 2003, Deber et al., 2001, Juretić et al., 2002, Arai et al., 2004, Käll et al., 2004, Hofmann and Stoffel, 1993). The TMHMM prediction programme, whose prediction was first used to determine structure, is based on the hidden Markov model (Krogh et al., 2001). It incorporates hydrophobicity, charge bias, helix lengths, and grammatical constraints into one model (Krogh et al., 2001). TMHMM success rate in

discriminating soluble from membrane proteins is claimed to be higher than 99 % in proteins without a signal peptide, but it can yield false positives and false negatives (Krogh et al., 2001). Figure 4.5 shows an alignment of PrpS₁ using different prediction programmes. Synthesized peptides that correspond to the extracellular 35 aa segment were designed according to the TMHMM prediction. Two other programmes, SOSUI and PredictProtein predict that part of the “35 aa region” is extracellular and part transmembrane, while the TMPredict and HMMTOP programmes predict this part to be intracellular. All the prediction programmes give very similar topology for PrpS₈ but, surprisingly, they predict an inverted structure with 4 TM segments for PrpS₃.

<u>TMHMM</u>	MPRSGSVVTLFQFVGGLCTLLGVSVAIKAIFAQDYTLKDLIILIVLVALS	50
<u>SOSUI</u>	MPRSGSVVTLFQFVGGLCTLLGVSVAIKAIFAQDYTLKDLIILIVLVALS	50
<u>PredPR</u>	MPRSGSVVTLFQFVGGLCTLLGVSVAIKAIFAQDYTLKDLIILIVLVALS	50
<u>HMMTOP</u>	MPRSGSVVTLFQFVGGLCTLLGVSVAIKAIFAQDYTLKDLIILIVLVALS	50
<u>TMPred</u>	MPRSGSVVTLFQFVGGLCTLLGVSVAIKAIFAQDYTLKDLIILIVLVALS	50
<u>TMfind</u>	MPRSGSVVTLFQFVGGLCTLLGVSVAIKAIFAQDYTLKDLIILIVLVALS	50
<u>SPLIT4</u>	MPRSGSVVTLFQFVGGLCTLLGVSVAIKAIFAQDYTLKDLIILIVLVALS	50
<u>TMHMM</u>	IILGGPITLTCVKLLGLVLHRLSFSSEDQKWVAFGTAAICDVLLVPKNML	100
<u>SOSUI</u>	IILGGPITLTCVKLLGLVLHRLSFSSEDQKWVAFGTAAICDVLLVPKNML	100
<u>PredPR</u>	IILGGPITLTCVKLLGLVLHRLSFSSEDQKWVAFGTAAICDVLLVPKNML	100
<u>HMMTOP</u>	IILGGPITLTCVKLLGLVLHRLSFSSEDQKWVAFGTAAICDVLLVPKNML	100
<u>TMPred</u>	IILGGPITLTCVKLLGLVLHRLSFSSEDQKWVAFGTAAICDVLLVPKNML	100
<u>TMfind</u>	IILGGPITLTCVKLLGLVLHRLSFSSEDQKWVAFGTAAICDVLLVPKNML	100
<u>SPLIT4</u>	IILGGPITLTCVKLLGLVLHRLSFSSEDQKWVAFGTAAICDVLLVPKNML	100
<u>TMHMM</u>	PMTIFSFLSSIMICVAVGWDCDRSGMTEGFLVGFGLLLVYLIKQDFTF	150
<u>SOSUI</u>	PMTIFSFLSSIMICVAVGWDCDRSGMTEGFLVGFGLLLVYLIKQDFTF	150
<u>PredPR</u>	PMTIFSFLSSIMICVAVGWDCDRSGMTEGFLVGFGLLLVYLIKQDFTF	150
<u>HMMTOP</u>	PMTIFSFLSSIMICVAVGWDCDRSGMTEGFLVGFGLLLVYLIKQDFTF	150
<u>TMPred</u>	PMTIFSFLSSIMICVAVGWDCDRSGMTEGFLVGFGLLLVYLIKQDFTF	150
<u>TMfind</u>	PMTIFSFLSSIMICVAVGWDCDRSGMTEGFLVGFGLLLVYLIKQDFTF	150
<u>SPLIT4</u>	PMTIFSFLSSIMICVAVGWDCDRSGMTEGFLVGFGLLLVYLIKQDFTF	150
<u>TMHMM</u>	SLLCGSVLCLAVVAKFTEGKAEATPNPNLAGKADSPHLITQA	192
<u>SOSUI</u>	SLLCGSVLCLAVVAKFTEGKAEATPNPNLAGKADSPHLITQA	192
<u>PredPR</u>	SLLCGSVLCLAVVAKFTEGKAEATPNPNLAGKADSPHLITQA	192
<u>HMMTOP</u>	SLLCGSVLCLAVVAKFTEGKAEATPNPNLAGKADSPHLITQA	192
<u>TMPred</u>	SLLCGSVLCLAVVAKFTEGKAEATPNPNLAGKADSPHLITQA	192
<u>TMfind</u>	SLLCGSVLCLAVVAKFTEGKAEATPNPNLAGKADSPHLITQA	192
<u>SPLIT4</u>	SLLCGSVLCLAVVAKFTEGKAEATPNPNLAGKADSPHLITQA	192

Figure 4.5.: Structural prediction of PrpS₁ using different prediction programmes: TMHMM, SOSUI, PredictProtein, HMMTOP, TMPred, TMFinder and SPLIT4. Amino acids are colour-coded: pink – extracellular, red – transmembrane, blue – intracellular, black – no orientation given.

Membrane-protein topology-prediction methods are typically based on sequence statistics and contain hundreds of parameters that are optimized using known topologies of membrane proteins (Bernsel et al., 2008). Although the predictions differ, they all predict that PrpS has transmembrane helices and the alignment of the PrpS sequences suggests that all three proteins share a similar topology. Predictions indicated 3, 4, 5 or 6 TM domains for PrpS₁ but PrpS most likely has four transmembrane segments, as it is a good number to make a four helix bundle in the membrane. 3 and 5 TM proteins do exist but are rarer (*Dr. A. Lovering, personal communication*). Additional argument for four TM domains is the GxxxG motif that is involved in number of helix oligomers, that is also present in the PrpS₁, PrpS₃ and PrpS₈ sequence toward the C-terminus, and is also aligned with *Drosophilla* protein Flower, for which they demonstrated the formation of a channel (see Appendix I) (Dawson et al., 2002, Senes et al., 2004, Yao et al., 2009). So, if this motif is to potentially play a role in oligomerization in PrpS, then it should be within the fourth TM domain. Also the TMHMM diagram for PrpS₁ in Figure 4.1.a shows a fourth highly hydrophobic region at the C-terminus between aa 125 and 170. At this position there is a predicted TM domain in PrpS₃ and it is highly possible that it is applicable to the other alleles as there are stretches of hydrophobic acids in the TMHMM predicted “intracellular” domain in PrpS₁ and PrpS₈. This area is 39 % identical at the aa level between the three alleles and 74 % similar for PrpS₁ and 78 % similar for PrpS₈. The alignment of these 4 TM domains is such that a loop is extracellular as we have some evidence that it is involved in binding with PrsS (Wheeler et al., 2009), which has extracellular access to PrpS. Based on the predictions of the 4 prediction programmes, cartoon on Figure 4.6 shows 4 different topologies. Interestingly, the PredictProtein prediction shows very similar topology of PrpS₁ to what we think it might be. Peptide A3 is located between aa 77-91. This peptide gave the strongest interaction using

far-western assay as well as competition bioassay. Nevertheless, despite all four programmes presented in Figure 4.6 identifying a major extracellular domain apart of TMHMM on whose prediction the synthesis and design was based, only PredictProtein predicted region of peptide A3 to be extracellular, SOSUI predicts only part of this peptide extracellular and part transmembrane, while HMMTOP predict it intracellular (Figure 4.6). Therefore, we must keep in mind that predictions are just that: predictions and not experimentally defined structures.

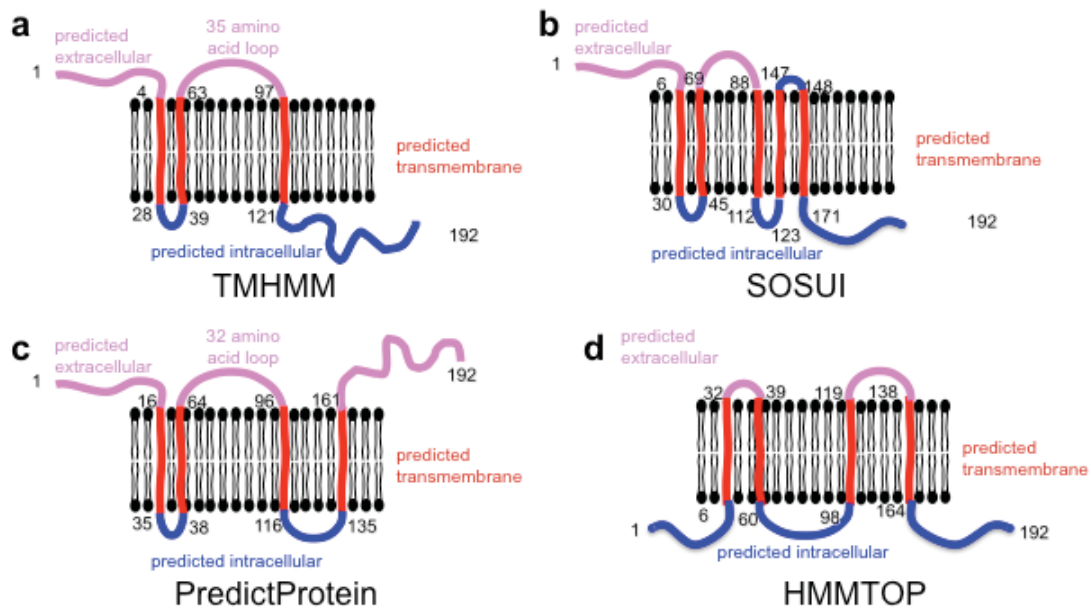


Figure 4.6.: Cartoon of possible structural topologies of PrpS₁ as revealed by different prediction programmes (a) TMHMM, (b) SOSUI, (c) PredictProtein, (d) HMMTOP. Cartoon Colour-coding: pink – extracellular, red – transmembrane, blue – intracellular. Numbers indicate the amino acid residue for PrpS₁.

4.2.2. Binding assays

The aim of this experimental study relating to PrpS was to establish whether the PrpS and PrsS bind each other and whether the binding was *S*-specific. As all the above predictions indicate an extracellular loop segment, we carried out further experiments using the

synthesized 15-mer peptides, spanning over the extracellular domain of PrpS₁. We used the ‘slot-blot’ method, a technique used in molecular biology to detect biomolecules also known as “far western”.

The peptides representing the extracellular domain of PrpS₁ were applied directly to a PVDF membrane and the potential binding between PrpS₁ peptides and recombinant PrsS₁ protein was detected with antibody raised against PrsS₁.

Figure 4.7. shows a representative slot-blot with all the peptides (see also Figure 4.2). From the figure we can see differential binding with all the peptides, except with the peptide A2, which gave no binding. No binding was observed with the scrambled peptide.

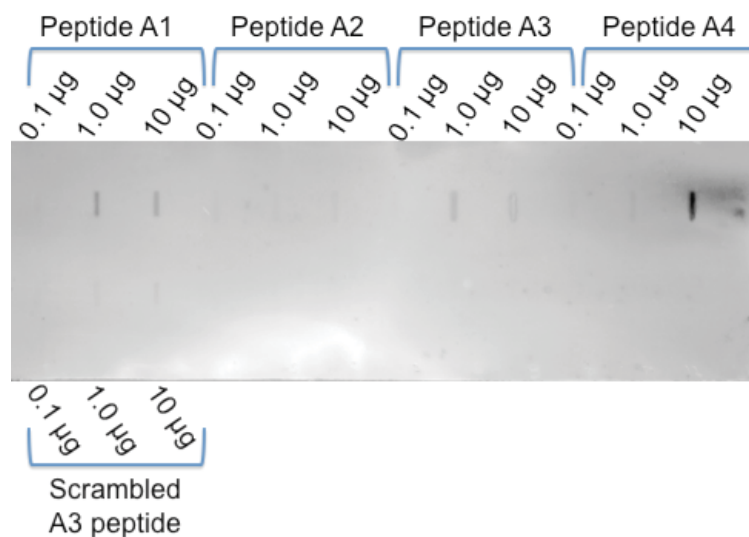


Figure 4.7.: Binding assay with differential loading 10 µg, 1µg and 0.1 µg of peptides A1, A2, A3, A4 and scrambled A3 peptide as control. Binding was detected with anti-PrsS₁ at a concentration of 1:2000.

A problem that was initially observed with the slot-blot assay was relatively high background on the PVDF membrane. In order to reduce the background optimization was required, such as: adding extra washes to the membrane, cleaning up the antibodies and using higher titre of the primary antibody.

The peptide A3 gave positive results with *in vitro* bioassays so it was important to attempt to demonstrate the differential specific binding and allelic specificity. Despite the results in figure 4.7, the work was continued mostly with peptide A3. As the peptides synthesized corresponded to PrpS₁, we attempted to demonstrate the S-specificity of peptide A3 through binding with PrsS₃ and detection with PrsS₃ antibody (see Figure 4.8).

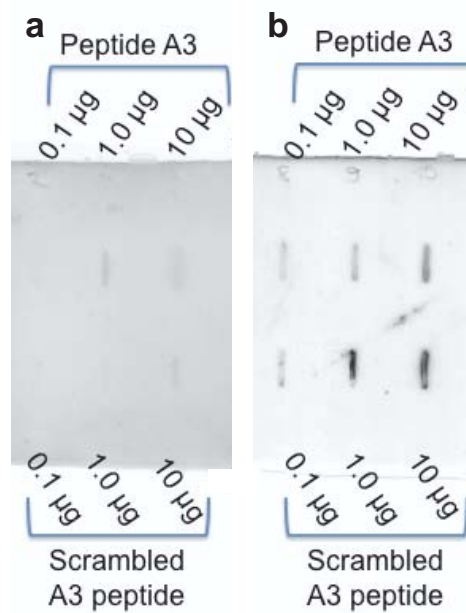


Figure 4.8. Binding assay with differential loading 10 µg, 1µg and 0.1 µg of A3 peptide and scrambled A3 peptide as a control. Peptide A3 designed over PrpS₁ was bound on the membrane, which was then incubated with PrsS proteins. (a) membrane was incubated with PrsS₁ proteins and binding was detected with anti-PrsS₁, (b) membrane was incubated with PrsS₃ proteins and binding detected with anti-PrsS₃ (both at a concentration of 1:2000).

Figure 4.8 shows that the membrane incubated with anti-PrsS₁ gave higher background than the membrane incubated with anti-PrsS₃. The PrsS₁-treated membrane had a clearer signal and differential loading was observed with peptide A3. Although there is a weak signal with 10 µg of scrambled peptide, this disappears when the background is subtracted. On the other hand, the PrsS₃ blot showed an unusual pattern. At the first glance it seems that we have differential loading not only with peptide A3, but also with the scrambled peptide. Both blots were processed at the same time with the same reagents and solutions. The only difference

was in the primary antibodies. Closer inspection showed that there was also some signal in the position of the slots that were empty (i.e. which did not have any peptide loaded). Furthermore, the signal does not seem to be throughout the position of the slot but is confined to the edge. These indentations could also be observed in later blots, but only when detected with anti-PrsS₃ antibody (see representative Figure 4.9).

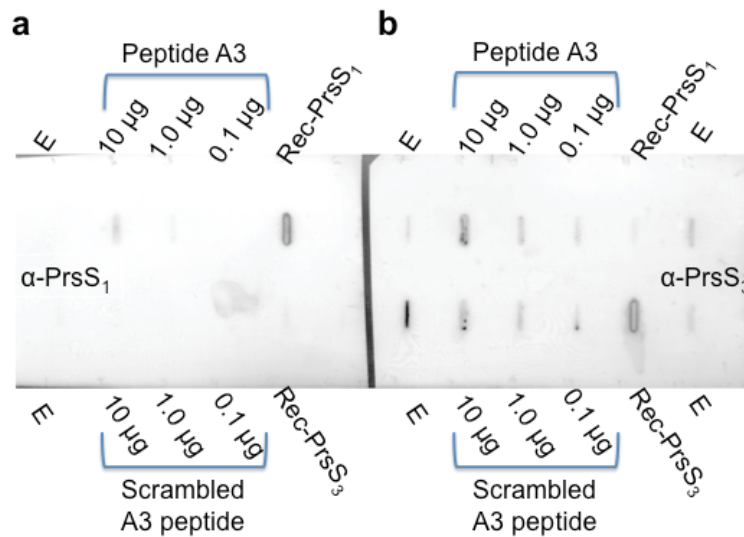


Figure 4.9.: One of many repeated binding assays with differential loading 10 µg, 1 µg and 0.1 µg of A3 peptide and scrambled A3 peptide as a control. Peptide was bound on the membrane, which was then incubated with PrsS proteins. Recombinant PrsS₁ and PrsS₃ were loaded as the control at a concentration of 0.1 µg. (a) following binding, membrane was incubated with PrsS₁ proteins and binding was detected with anti-PrsS₁ (α -PrsS₁; 1:6000), (b) membrane was incubated with PrsS₃ proteins and binding detected with anti-PrsS₃ (α -PrsS₃; 1:500) antibody. E – empty slots.

The blot on Figure 4.9 shows the S-specific binding of A3 peptide with PrsS₁. Differential loading of peptide A3 is demonstrated and no signal with the scrambled peptide. The PrsS₁ antibody specifically recognizes the recombinant PrsS₁ protein and not the recombinant PrsS₃ protein. Several different titres were tested by western blot in order to try to get specific signals. Antibodies were used at concentrations that give an equivalent intensity of signal for 0.1 µg of peptides. Antibodies were also column purified to remove unspecific interactions. The blot probed with the anti-PrsS₃ antibody does not give a straightforward

result. If we focus only on the signals for peptide A3, then we might conclude that we have differential loading. But we can also observe differential binding with the scrambled peptide. Also, the recombinant PrpS₃ protein is recognised specifically by the PrpS₃ antibody, whereas the recombinant PrpS₁ protein gives a very weak signal that can be attributed to the background. If we look at the blot as a whole, then we see quite strong signals in the positions of the empty slots.

All the data so far shows that the anti-PrpS₃ antibody does not bind specifically enough, as it binds to the edges of empty wells and often gave a very high background signal. Furthermore, alleles 1, 3 and 8 have 73 % aa identity in the area of peptide A3 (see Figure 4.10). For this reason we moved the focus of our attention to peptide A1 (Figure 4.2.) where the aa identity between alleles is 27 %, so the region is more variable.

```
PrpS1      KLLGLVLHRLSFSEDQKWVVAFGTAAICDVLLVPK 35
PrpS3      QALRWLLQHLHVSENQKWVIAFGTTAICDVFLATH 35
PrpS8      KLLGWVLQHLTVTENQKWVVAFGTTAVCDVFLVTT 35
           : *   :*:* . :*:*****:*****:*****:*. .
```

Figure 4.10. Clustal W alignment of amino acid sequence of predicted extracellular loop of 3 different alleles of PrpS protein. Identical amino acids are marked with “*”, conserved substitutions with “:” and semi-conserved substitutions with “.”.

In order to test for reciprocal *S*-specific interaction, we chose the area of peptide A1 in PrpS₁ and PrpS₈. Peptide A1 and its corresponding scrambled control from this less similar region of extracellular domain were designed and synthesized by AltaBiosciences (Figure 4.11.).

```
PrpS1 A1 — VKLLGLVLHRLSFSE
ScrPrpS1 — ELGVKLHSLSVLRFL

PrpS8 A1 — LKLLGWVLQHLTVTE
ScrPrpS8 — GLTWLQLKEVHLTVL
```

Figure 4.11. Peptides A1 for PrpS₁ and PrpS₈ and their scrambled versions, synthesized by AltaBiosciences

Peptides were tested using the binding assay for the *S*-specific interaction. The PrpS₁ and PrpS₈ peptides were bound to the membrane and incubated with the corresponding pistil PrsS₁ and PrsS₈ proteins, respectively. Binding was detected with anti-PrsS₁ and anti-PrsS₈ antibodies and can be seen in Figure 4.12.

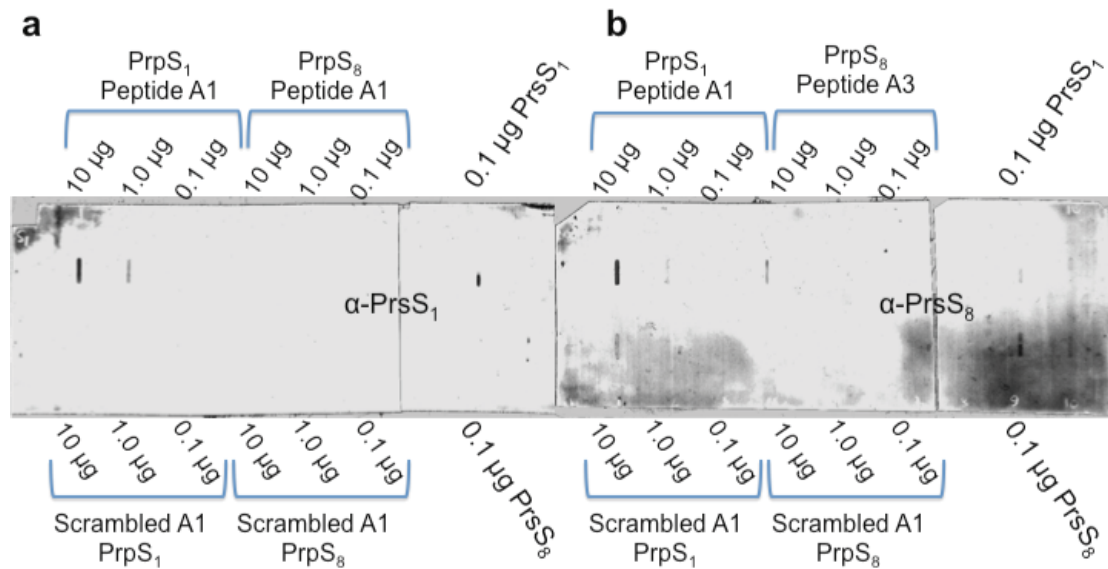


Figure 4.12.: Binding assay between pollen PrpS₁ and PrpS₈ A1 peptides and recombinant stigmatic PrsS₁ and PrsS₈ proteins. Peptides were bound on the membrane at three different concentrations: 10 μ g, 1.0 μ g and 0.1 μ g. The membrane was then incubated with PrsS proteins. Recombinant PrsS₁ and PrsS₈ were loaded as the controls at a concentration of 0.1 μ g. (a) following binding, membrane was incubated with PrsS₁ proteins and binding was detected with anti-PrsS₁ (α -PrsS₁; 1:6000), (b) membrane was incubated with PrsS₈ proteins and binding detected with anti-PrsS₈ (α -PrsS₈; 1:4000) antibody.

We can see from Figure 4.12 the *S*-specific binding between PrpS₁ and PrsS₁ but not between PrpS₈ and PrsS₁. There was no binding detected between the scrambled control peptides and PrsS₁ and very weak binding between 10 μ g of the PrpS₁ A1 scrambled control peptide and PrsS₈. This provides the first formal evidence that PrpS and PrsS interact in an *S*-specific manner.

4.3 DISCUSSION

In this chapter we demonstrated with the binding assay the *S*-specificity for the interaction between PrpS and its ligand PrsS using peptides overlapping the extracellular domain of PrpS. Slot-blot binding assay is one of the commonly used techniques to show for protein-protein interactions (Southwick and Long, 2002). A modified version of slot-blot assay, a dot blot was also used by Kemp and Doughty, (2007), with which they documented binding in a haplotype-specific manner between stigmatic membrane proteins and recombinant SCR protein. Pollen recombinant SCR₂₉ was iodinated before incubation with a membrane with bound stigmatic microsomal membrane proteins from stigmas S₂₉S₂₉ and S₆₃S₆₃ of *Brassica*. They confirmed the *S*-specific binding of SCR₂₉ to S₂₉S₂₉ stigmas with fivefold higher affinity than to stigmatic membrane of different allele (Kemp and Doughty, 2007). Our assay demonstrated in a similar manner the *S*-specific binding between PrsS and PrpS, however, we demonstrated more specifically the binding between the extracellular domain of the transmembrane protein PrpS₁ and the recombinant ligand PrsS₁ and not just binding of a membrane extract with the recombinant protein (Kemp and Doughty, 2007, Wheeler et al., 2009).

Brassica-like SI is triggered upon the interaction between pollen coat protein *S*-locus Cysteine Rich (SCR), that binds to and activates *S*-locus Receptor Kinase (SRK), transmembrane protein encoded in stigmatic papillae (Kachroo et al., 2001, Takayama et al., 2001). *A. thaliana* is already used as a model for *Brassica*-like SI, expressing SRK/SCR gene pairs from *A. lyrata* and *C. grandiflora* (Nasrallah et al., 2002, Nasrallah et al., 2004, Boggs et al., 2009b). Use of this model system and mutagenesis enabled the identification of the 6-7 important amino acid residues in the extracellular domain of the SRK, determining

the specificity of the receptor-ligand interaction (Boggs et al., 2009a). These residues occur in two separate clusters located in the highly polymorphic sites of eSRK and were found on the same position in two variants tested.

The PrpS-PrsS interaction could be also demonstrated using different techniques, such as modified yeast-two-hybrid assays: split-ubiquitin or reverse Ras recruitment system (Stagljar and Fields, 2002). The reverse Ras recruitment system, for example, is based on Ras pathway in yeast. Membrane protein of interest (PrpS) is expressed in the membrane, while the interaction protein (PrsS) is fused to the mRas, that is cytoplasmic. The successful interaction between PrpS-PrsS should then result in the growth of yeast at 36 °C, which is otherwise too high (Stagljar and Fields, 2002). Alternative way to demonstrate PrpS-PrsS protein interaction would be pulldown assays, where PrsS could be immobilized as a bait on a His-column, and used to pull out the PrpS protein in the pollen extract. However, next steps are also the analysis of the PrpS residues that are important for the interaction with PrsS in the extracellular domain, and that are important for the intracellular interaction with yet unknown proteins. Additionally, the detailed analysis of TM domains could provide information's regarding the oligomerization of the protein, or its potential to form a pore or a channel.

CHAPTER 5

Functional analysis *in vitro* of the *Arabidopsis thaliana* expressing *Papaver rhoeas* PrpS₁ and PrpS₃

5.1 INTRODUCTION

As described in the introduction, section 1.4.3., *Papaver rhoeas* avoids self-fertilization on a molecular level by cell-cell specific self-recognition and rejection of self-pollen with transmembrane receptor PrpS, localised in the pollen plasma membrane, that lands on the stigma, which secretes small cysteine-rich proteins PrsS (Wheeler et al., 2009). Such SI interaction in the incompatible *Papaver* pollen triggers the cascade of downstream molecular events in pollen that ultimately lead to the inhibition of pollen tube growth and PCD of pollen tube (Thomas and Franklin-Tong, 2004).

We wished to see if the *Papaver* S-determinants PrpS and PrsS could be functionally transferred to other species, initially to *Arabidopsis thaliana*, triggering *Papaver*-like SI response. This would provide an important model for studying *Papaver* SI, as genetic manipulations are very difficult in *Papaver*, while *A. thaliana* is well amenable to the transformation by *Agrobacterium*, and extensive mutant collections already exist and are commercially available. The functionality of *Papaver* SI in other species could also have a long term potential for the F₁ hybrid breeding in crops. Many agriculturally important species, such as wheat, rye, barley or rice are self-compatible (SC) and for plant breeding and production of hybrids other ways of elimination of self-fertilization are essential, such as manual emasculation of anthers or use of cytoplasmic male sterility (for example very important for rice hybrid breeding) (Dwivedi et al., 2008, Cheng et al., 2007, Pelletier and Budar, 2007). These breeding programmes can be very expensive and lengthy to reach the end result so the stable introduction of SI that would interrupt SC might be positive and useful for future production of F₁ hybrids.




As mentioned above, the first step towards in the research of functionality of PrpS and PrsS in another angiosperm was the transformation into *A. thaliana*, a plant model organism, whose sequenced genome was sequenced (Initiative, 2000). *A. thaliana* is a SC species from the Brassicaceae family, which lost SI through mutation in the male specificity gene *SCR*, while female specificity gene *SRK* remained intact (Tsuchimatsu et al., 2010, Tang et al., 2007).

A. thaliana became the transgenic model of the *Brassica* SI system by transformation with *SRK-SCR* receptor ligand gene pair isolated from self-incompatible crucifers *Arabidopsis lyrata* or *Capsella grandiflora* (Nasrallah et al., 2002, Boggs et al., 2009b, Rea et al., 2010, Nasrallah et al., 2004). Their studies on transgenic *A. thaliana* focused on the analysis of the natural variation for the expression of SI, the evolutionary switch between outbreeding and inbreeding in *A. thaliana*, analysis of residues that determine SI specificity and identification of genes required for SI signalling and potential overlaps with other plant signalling pathways (reviewed in (Rea et al., 2010). Several different accessions of *A. thaliana* were transformed with SRK-SCR gene pair with SI response tested and they identified that not all accessions exhibit same degree of SI and they exhibit different levels of polymorphism at the *S*-locus and the SI modifier loci, leading to conclusion that inbreeding status of *A. thaliana* was probably developed multiple times by independent mutations in different accessions (Sherman-Broyles et al., 2007, Boggs et al., 2009c). *A. thaliana* presents an excellent system to study molecular mechanisms due to easy transformation using *Agrobacterium*, which can be difficult or impossible in some species, for example *Brassica* or in our case, *Papaver*. Transgenic *A. thaliana* expressing SRK-SCR gene pair was used for analysis of residues that are important for SRK specificity and therefore SI response. Site-directed mutagenesis approach was used on polymorphic amino acid residues in the extracellular domain of SRK

and six were identified to mediate the ligand-specific SI activation (Boggs et al., 2009a). Mutational analysis in transgenic *A. thaliana* expressing SRK-SCR also enabled the identification of mutation in RNA-dependent RNA polymerase RDR6, that acts as a negative regulator of SI and causes stigma exertion and simultaneous enhancement of SI, which implicated a broader role for SRK in pistil development (Tantikanjana et al., 2009). Further unexpected results were obtained when crossing *A. thaliana* plants expressing *SRKb-SCRb* genes that exhibit stable SI response with *A. thaliana* strains that contained inactive *PUB17* or *APK1b* genes, which were most similar to *Brassica ARC1* and *MLPK*. Those crosses resulted in unabolished SI response, which means that the role of ARC1 and MLPK might not be as crucial for SI as previously reported (Rea et al., 2010, Kitashiba et al., 2011).

Papaver-based SI *A. thaliana* model was generated by *Agrobacterium*-mediated transformation of the *Papaver S*-determinants into *A. thaliana*. The transformations of *Papaver S*-determinants into *A. thaliana* were carried out by Barend de Graaf (BG plant lines) and Huawen Zou (HZ plant lines). This chapter describes in detail work with transgenic *A. thaliana* lines expressing PrpS₁-GFP (BG16) and PrpS₃-GFP (HZ3) and to lesser extent also 35S:PrpS₁ (BG3). These were the lines that were available and chosen to work on at the start of this project. The constructs are presented in the Table 5.1.

Table 5.1: The cartoon illustrations of the constructs of the poppy SI determinants that were used for *Agrobacterium* mediated transformation into *A. thaliana*.

Gene	Resistance Marker	Name	Construct
PrpS ₁	Kan	BG16	
PrpS ₃	Kan	HZ3	
PrpS ₁	Kan	BG3	

To achieve tissue specific expression of the male *S*-determinants PrpS₁-GFP and PrpS₃-GFP in the pollen of *A. thaliana*, a strong, pollen specific promoter from tobacco, *ntp303*, was used (Weterings et al., 1995). For BG3 line, PrpS₁ expression was cloned under the control of the cauliflower mosaic virus 35S promoter (Hull, 1983) that has a constitutive expression throughout the plant. In order to detect the transformed plant cells, the kanamycin (Kan) resistance cassette was on the T-region of the construct acting as a selection marker. In all lines except BG3, PrpS was expressed as a fusion protein with green fluorescence protein (*GFP*) towards its C-termini.

The results of the study, presented in this chapter, resulted in a publication where I am joint first author. The paper is presented in the Appendix III.

AIMS

Part of this PhD study was the functional analysis of *Papaver* SI in *A. thaliana*. Several approaches were taken: *in vitro* and semi-*in vitro* described here, and *in vivo* (described later in Chapter 6). The initial studies were the characterization and segregation analysis based on the inheritance of the resistance markers Kan and reporter marker GFP of PrpS₁-GFP and PrpS₃-GFP expressing *A. thaliana* lines, and identification of homozygous progenies of transgenic lines with the highest expression of *Papaver* *S*-determinants. The use of the homozygous lines would optimise the reproducibility of the study. Once the highest expressing homozygous lines were identified, the functional analysis studies were conducted. The aim was to conduct *in vitro* studies on transgenic *A. thaliana* pollen expressing PrpS₁-GFP and PrpS₃-GFP fusion protein. We wished to establish whether PrpS-

GFP in *A. thaliana* pollen responded to its cognate stigmatic recombinant proteins in the same manner as *Papaver* pollen. The SI response was induced in transgenic *A. thaliana* pollen expressing PrpS₁-GFP or PrpS₃-GFP and germinating in Petri dishes, with an addition of the cognate recombinant stigmatic PrsS₁ or PrsS₃ proteins. Various responses were analysed, such as: inhibition of pollen tube growth, decrease of pollen viability and the appearance of punctate actin foci. The outline of these experiments is presented on Figure 5.1. The S-specific response was ensured by analysing PrpS-GFP expressing *A. thaliana* pollen upon incubation with biologically inactive incompatible PrsS proteins, treatment with compatible proteins and incubation of wild type Col-0 *A. thaliana* pollen using *Papaver* stigmatic PrsS recombinant proteins.

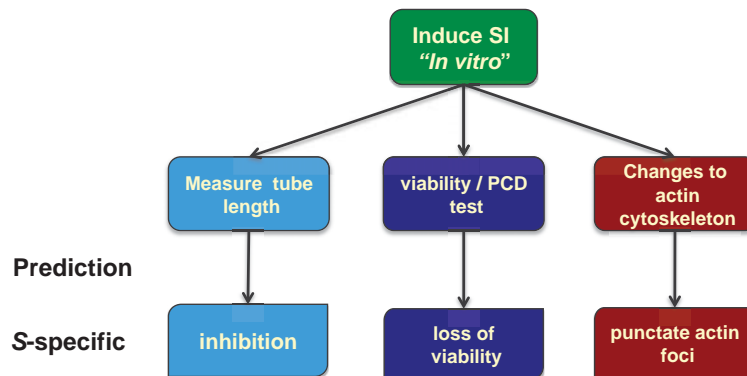


Figure 5.1.: Schematic diagram presenting the outline of the *in vitro* functional analysis experiments. In vitro SI reaction was induced in transgenic *A. thaliana* pollen expressing PrpS₁-GFP or PrpS₃-GFP and the several responses were tested, such as inhibition of pollen tube growth, decrease of viability and the appearance of punctate actin foci.

The inhibition of pollen tubes was analysed by measuring pollen tube length, analysed the organisation of the actin cytoskeleton with the use of rhodamine phalloidin and the viability of pollen tubes at different time points using Evans Blue dye as well as investigated pollen cell death and DEVDase activity of transgenic *A. thaliana* pollen.

5.2 RESULTS

5.2.1. Characterization of *A. thaliana* expressing *Papaver* SI system

At the start of the project, the seeds from up to 30 independent primary transformants of different lines were available: BG16 expressing PrpS₁-GFP, HZ3 expressing PrpS₃-GFP and BG3 expressing PrpS₁ using constitutive 35S promoter, whose characterisation is presented in this chapter and lines HZ1 expressing PrsS₁ and HZ2 expressing PrsS₃ and BG6 expressing whole *S*₁-locus whose characterisation is presented in the next Chapter 6.

Before carrying out the functional characterisation it was necessary to identify the highest expressing individual lines. Although lines were pre-screened on the selection medium, there was the possibility that they did not contain the insert corresponding to the *S*-genes within their genome. Therefore we screened for the plants with inserts by PCR on genomic DNA purified from leaf disks. The T₂ generation of the transgenic *A. thaliana* lines were tested for the presence of the inserts by PCR using genomic DNA as a template. Lines BG16 and HZ3 were tested for the presence of PrpS₁ and PrpS₃ respectively. Once having confirmed if the insert was present, only the plants that showed the insert by PCR were tested if they were expressing the PrpS by reverse transcription-PCR (RT-PCR).

We wished to identify at least two individuals with the highest expression of *Papaver S*-determinants within each transgenic *A. thaliana* line, so the further functional analysis could be accomplished.

5.2.1.1. PrpS expressing *A. thaliana* lines

Seeds of *Arabidopsis::PrpS-GFP* were initially screened on the germination medium MS containing kanamycin. Only the plants containing the PrpS-GFP transgene were expected to survive, so resistant and non-resistant seedlings were counted for segregation analysis. Heterozygous plants were expected to segregate in Mendelian fashion with 3:1 ratio between resistant and non-resistant seedlings, while homozygous plants were expected to be 100% resistant on the kanamycin containing media. Another marker utilised in the analysis of homozygous lines was the reporter gene GFP, expressed in transgenic *A. thaliana* pollen. It was expected that in homozygous lines GFP would be expressing in every pollen grain (100% expression). The results of the segregation analysis are presented in Tables 5.2 and 5.3.

Table 5.2: Segregation of Kan resistance and GFP expression in progenies of transgenic *A. thaliana* lines expressing *Papaver* pollen determinant PrpS₁. Statistical analysis was performed using Chi square analysis (χ^2 value presented). Percentage of GFP expressing pollen is presented as mean value \pm standard error of means (SEM). HO-homozygous.

Line (PrpS ₁ -GFP)	Generation	Kan ^R	Kan ^S	N	Ratio	χ^2 (3:1)	GFP (%) \pm SEM
BG16B# 25	T ₂	202	84	3	2.4:1	2.91	67 \pm 6
BG16B# 25.1	T ₃	248	15	3	16.5:1	52.23	91 \pm 1
BG16B# 25.1-1	T ₄	354	1	8	HO	95.35	97 \pm 1
BG16B# 25.1-2	T ₄	134	0	2	HO	44.67	96 \pm 2
BG16B# 25.1-1.x	T ₅	351	1	10	HO	114.7	100
BG16A# 19	T ₂	291	126	4	2.3:1	6.05	67 \pm 5
BG16A# 19.1	T ₃	353	125	5	2.8:1	0.34	79 \pm 2
BG16A# 19.8	T ₃	152	79	3	1.9:1	10.4	80 \pm 2
BG16A# 19.8-2	T ₄	64	19	2	3.3:1	0.20	66 \pm 1
BG16A# 19.8-3	T ₄	115	10	3	11.5:1	19.27	95 \pm 1
BG16.8#3.1	T ₄	117	85	2	1.4:1	31.4	82 \pm 2
BG16A#13	T ₂	53	7	3	7.6:1	5.69	87 \pm 1
BG16A#13.1	T ₃	84	11	3	7.6:1	9.12	97 \pm 2
BG16A#13.2	T ₃	118	12	3	10:1	17.24	98 \pm 1

With the segregation analysis, the expected Mendelian segregation for the single insert was 3:1 (Kan^R:Kan^S) and the proportion of the GFP expressing pollen in heterozygous line would be 50 % (1:1 Mendelian segregation ratio). Such segregation was observed in many of the analysed PrpS-GFP expressing *A. thaliana* lines but not in all of them. After selfing, the T₃ generations sometimes exhibited ratio ~15:1 (BG16B#25.1, HZ3.1-15) which probably corresponds to the transgene insertion at two independent loci. But with the increased segregation, we also observed an increase in GFP expression in pollen. The GFP expression in pollen of PrpS₁-GFP expressing *A. thaliana* was around 67 % in T₂ BG16B#25 and 91 % in the BG16B#25.1 line with the higher segregation ratio. After another round of selfing the line was homozygous in generation T₄ and also GFP expression in pollen was 97 % at that generation. As the total pollen was counted for the GFP expression, the pollen that was not expressing PrpS₁-GFP exhibited distorted shape under microscope, pollen grains were smaller and it was not viable. Therefore we concluded that line, homozygous for the Kan resistance feature, was also homozygous for the GFP expression, as expected.

However, line BG16A#19 was not yet homozygous for the insert at generation T₄. It shows 3:1 segregation ratio in generation T₂ and T₃ of BG16A#19.1, with 79 % of pollen expressing GFP. However, the T₃ line BG16A#19.8 that was also identified as the highest expressing line (described later in this Chapter), shows segregation ratio of 2:1 with 80 % of pollen expressing PrpS₁-GFP. Although segregation ratio 2:1 seems to be associated with the homozygous lethality (Limanton-Grevet and Jullien, 2001), the T₃ generation of BG16A#19.8 exhibited 3:1 segregation (BG16A#19.8-2) with 66 % GFP expression, and 11.5:1 (BG16A#19.8-3) with 95 % GFP expression in pollen. The higher segregation ratio could be associated with transgene insertion at two loci, possibly linked (Feldmann et al., 1997). Line BG16A#19 was not yet homozygous for the insert at generation T₃, however the

T₃ line BG16A#19.8 was also identified as a highest expressing line (described later in this Chapter). Additionally, the unusual segregation ratio of 1.4:1 was also observed for the T₄ generation of the line BG16.8#3.1, which was also identified to express PrpS₁-GFP in high concentrations, while the 82 % of the pollen was expressing PrpS₁-GFP.

Distorted segregation ratios were observed also in the line BG16A#13, which was added to the experiments later on, due to its very high GFP expression of more than 90 % in generation T₃. Its segregation shows 8:1 in T₁ with very high PrpS₁-GFP pollen expression of 87 % and 8:1 and 10:1 in T₃ with homozygous PrpS₁-GFP pollen expression of 97 % and 98 %, respectively. Such distorted segregation ratios were previously associated with the segregation at the *S*-locus in *Petunia* (Harbord et al., 2000) where distorted segregation ratios of 8:1 or higher were anticipated due to gamethophytic selection of *S*-alleles.

However, in the case of *Papaver S*-transgenes in *A. thaliana*, the location of the insert was not identified. Line BG16A#13 was having homozygous GFP expression in pollen in generation T₃, which did not show any abnormalities, but was still heterozygous for the Kan resistance marker. The explanation for this discrepancy could be that the two markers in line BG16A#13 follow the Mendelian segregation of independent segregation in T₃ generation because the markers are located on the opposite sides of the T-DNA construct so it could be possible for one inserted construct to lose the Kan marker. However, pollen from BG16A#13 exhibited normal germination rates compared to Col-0 and for that reason it was used in some preliminary experiments, such as caspase assays.

For functional analysis the progeny of lines BG16B#25 and BG16A#19 were selected (see also RT-PCR analysis later in this section).

The unusual high segregation ratios most often indicate the segregation of inserts at two linked loci. Whereas the segregation of inserts at two unlinked loci gives 15:1 ratio, the segregation at two linked loci could give rise to segregation ratios $3:1 < x < 15:1$ (Feldmann et al., 1997). If we assume multiple insertion and independent segregation of the separated fusion construct then we would be expecting greater GFP expression than single insert, which is what we observed. The variable transgene expression could also be due to the position effects, meaning that the actively transcribed regions of the genome or a transgene insertion near enhancer elements are more likely to be expressed. Therefore, a few seedlings with the insert near the highly expressed region could give rise to the observed intense expression of GFP (for example line BG16A#13 which exhibited very high GFP expression, while the Kan segregation was heterozygous 8:1 and 10:1 ratios). Another possible reason for distorted segregations of double T-DNA copy could result from epigenetic transgene silencing, which is common for repetitive sequences, potentially as a defence response against foreign DNA (Jorgensen et al., 1996, Muskens et al., 2000, De Buck et al., 2007, Matzke and Matzke, 1998). Double insertion of the gene often arrange as inverted repeats of which many are dominant silencing loci and can repress the expression of homologous genes, associated with increase in DNA methylation (Muskens et al., 2000). The post-transcriptional silencing of genes results from degradation of double stranded RNA (dsRNA) directed DNA methylation and dsRNA induced degradation of homologous RNAs (Muskens et al., 2000)

Table 5.3 presents the results of segregation analysis of PrpS₃-GFP expressing *A. thaliana* lines.

Table 5.3: Segregation of kanamycin resistance and GFP expression in progenies of transgenic *A. thaliana* lines expressing *Papaver* pollen determinant PrpS₃. Statistical analysis was performed using Chi square analysis (χ^2 value presented). Percentage of GFP expressing pollen is presented as mean value \pm SEM. HO–homozygous. N.A.–not analysed.

Line (PrpS ₃ -GFP)	Generation	Kan ^R	Kan ^S	N	Ratio	χ^2 (3:1)	GFP (%) \pm SEM
HZ3.1	T ₁	141	49	2	3:1	0.016	/
HZ3.1-3	T ₂	116	39	2	3:1	0.0022	71 \pm 3
HZ3.1-15	T ₂	169	9	2	19:1	37.8	88 \pm 3
HZ3.1-3.1	T ₃	98	39	2	2.5:1	0.87	83 \pm 3
HZ3.1-15.1	T ₃	272	21	4	13:1	49.7	96 \pm 1
HZ3.1-3.1-x	T ₄	269	28	7	7:1	21.7	96 \pm 1
HZ3.1-15.1-x	T ₄	200	0	8	HO	66.7	98 \pm 1
HZ3.2	T ₁	0	200	2	0:1	600	N.A.
HZ3.3	T ₁	132	54	2	2.4:1	1.61	N.A.
HZ3.4	T ₁	0	100	1	0:1	300	N.A.
HZ3.5	T ₁	96	56	2	1.7:1	11.37	N.A.
HZ3.7	T ₁	46	26	1	1.8:1	4.74	N.A.
HZ3.8	T ₁	53	32	1	1.6:1	7.25	N.A.

In the *A. thaliana* HZ3 line expressing PrpS₃-GFP, the seeds of transformed plants were pooled together so the T₁ do not represent independent primary transformants, but rather plants that were selected on the Kan containing MS medium from the pool of T₀ seeds. Eight of T₁ lines presented in Table 5.3 were grown on the MS-Kan medium, two out of those were Kan sensitive (HZ3.2 and HZ3.4) and only two lines, namely HZ3.1 and HZ3.3 showed the expected 3:1 segregation ratio based on the inheritance of Kan resistance. Lines HZ3.5, HZ3.6 and HZ3.7 show non-Mendelian segregation ratio of 2:1 and were not included in subsequent experiments.

The line HZ3.1 was analysed as well as its subsequent generations (presented on Table 5.3). One progeny of the line, HZ3.1-3 exhibits 3:1 ratio in generation T₂ and T₃, indicating it is still segregating following Mendelian inheritance, while in T₄ it exhibits an abnormal 7:1 segregation ratio. However, despite following the Mendelian rules for Kan resistance gene, the PrpS₃-GFP protein expression is 71 % in T₂ and 83 % in T₃, indicating the 3:1

segregation of PrpS₃-GFP pollen expression. The other progeny of the line 3.1, HZ3.1-15 shows a 19:1 segregation in T₂ with 88 % pollen GFP expression. 13:1 ratio in T₃, which suggests that the PrpS₃-GFP insert might be present at two loci (normally 15:1 Mendelian segregation) and it reached homozygous state by pollen PrpS₃-GFP expression of 96 %. The HZ3.1-15 line reached homozygous state for the both markers (Kan and GFP) in generation T₄. This line was also used in the experiments testing for the functional analysis, while line HZ3.1-3.1 was used only in preliminary tests due to its unusual segregation pattern (3:1 in T₂, 3:1 in T₃, 7:1 in T₄), although the GFP expression in T₄ was complete.

In order to identify lines with the highest expression of the transgene the RT-PCR was used. Initial PCR screening for the presence of PrpS₁ and PrpS₃ inserts was performed on the leaves of young plants, using gene specific primers and flowers of the plants that were positive for the insert were analysed by RT-PCR. Figure 5.2.a present the screening results on BG16 line expressing PrpS₁-GFP, while Figure 5.2.b present HZ3 line expressing PrpS₃-GFP.

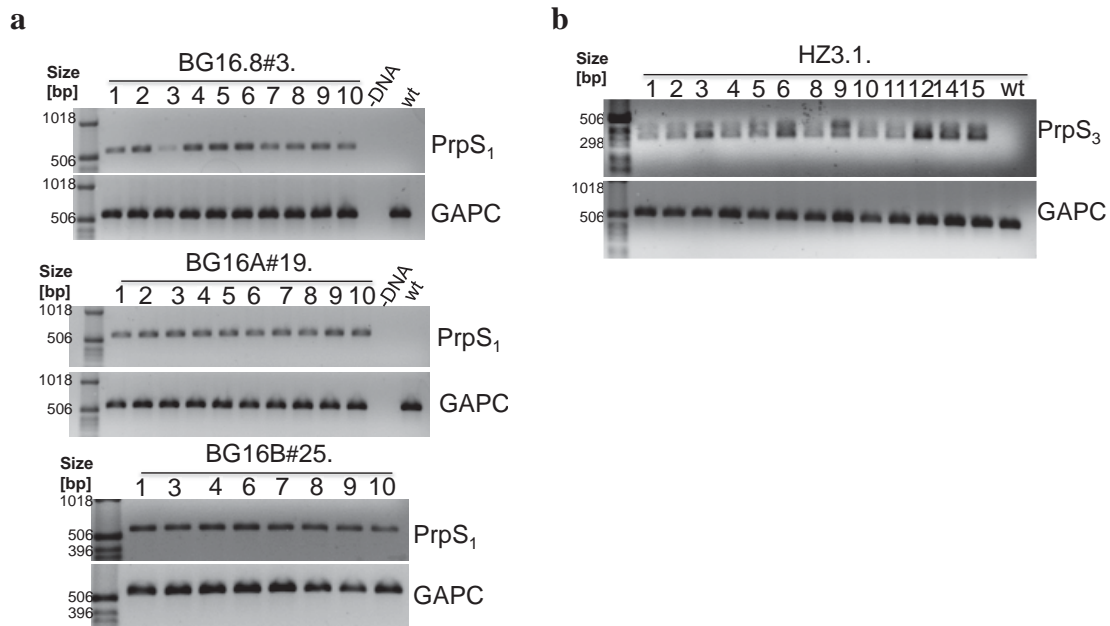


Figure 5.2. (a) PrpS₁ expressing *A. thaliana* plants that were positive for inserts were analysed by the RT-PCR in order to identify the highest expressors (lines BG16.8#3, BG16A#19 and BG16B#25). (b) PrpS₃ expressing *A. thaliana* plants that were positive for inserts were analysed by RT-PCR in order to identify the highest expressors (line HZ3.1). GAPC was used as a standard and is presented at the lower part of each image. Reactions without DNA and with Col-0 DNA were used as a control.

The expression levels were analysed using RT-PCR, which was conducted on the flowers from the same plants used for genotyping and housekeeping gene GAPC was used as a control. Figure 5.2.a shows the results of the RT-PCR analysis on BG16 flowers. PrpS₁ primers were designed to align on 5' and 3' ends of the insert and a size of the obtained product was expected to be 583 bp. BG16B#25 exhibited uniform expression with all the samples analysed, while the expression of the BG16A#19 and BG16.8#3 was less uniform. The RT-PCR analysis was done on PrpS₃ expressing flowers using HZ3.1 line only, with the exception of the samples 7 and 13 (Figure 5.2.b). The reason for HZ3.3 not being analysed by RT-PCR was with time and material constraints at the time. PrpS₃ primers were designed to yield a product of 436 bp. Under the same conditions, wt Col-0 was used as a control but not yielding any product.

It can be observed in Figure 5.2.b that PCR product of PrpS₃ gene resulted in double band. There could be a series of technical reasons for doublets in the gel, from the different concentrations between the forward and reverse primers, different annealing temperatures, to non-homogeneous distribution of the dye between molecules (Carlsson et al., 1995). However, technical issues were taken into the account and no problems were found with primers or melting temperatures. Primers were also used in genotyping PCR reaction where they produce normal single band. The DNA electrophoresis was repeated using 1 % agarose gel and running under lower currents for longer time but with the same result. In the process of transformation cDNA of PrpS₃ was used; however the PCR bands presented in the Figure 5.2.b were obtained from RNA so this could likely be a splicing variants. PrpS₁ and PrpS₈ were already demonstrated to produce splice variants but not PrpS₃ (Hadjiosif, 2008). The expression of PrpS₃ was not uniform with all the flowers, six flowers exhibited higher expression than the rest. Further selection of 5 samples was made initially, by quantifying the intensity of the bands using ImageJ software (see Figure 5.3) as the highest expressing lines were desired for the functional analysis.

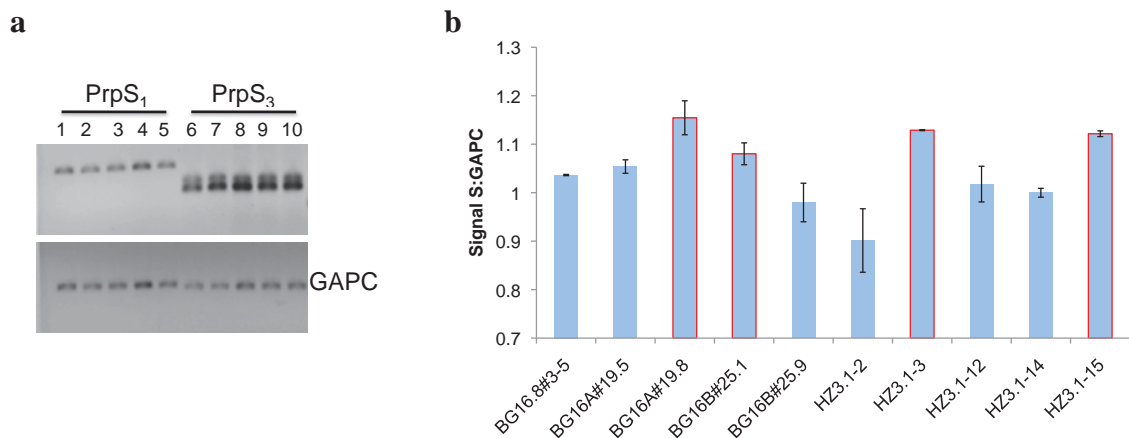


Figure 5.3.: (a) Top 5 highest expressing PrpS₁ and PrpS₃, and the corresponding GAPC control. Legend: 1-BG16.8#3.5, 2-BG16A#19.5, 3-BG16A#19.8, 4-BG16B#25.1, 5-BG16B#25.9, 6-HZ3.1-2, 7-HZ3.1-3, 8-HZ3.1-13, 9-HZ3.1-14, 10-HZ3.1-15. (b) Column chart presenting ratio between transgene signal and GAPC signal. Quantification was performed using ImageJ software. Highest expressors outlined in red.

cDNA samples of plants BG16.8#3.5, BG16A#19.5, BG16A#19.8, BG16B#25.1 and BG16B#25.9 from PrpS₁ expressing flowers, and HZ3.1.2, HZ3.1.3, HZ3.1.12, HZ3.1.14 and HZ3.1.15 from PrpS₃ expressing flowers were further re-analysed on the DNA gel and compared to GAPC control (Figure 5.3.a).

In order to get some idea of the quantification of expression of the transgene, the peak band intensity was measured using ImageJ software for each sample and its GAPC control (Figure 5.3.b). From each transgenic line, two plants with the highest expression identified by intensity ratio were used in subsequent functional experiments. The apparent lines with the highest expression of the transgene were: BG16A#19.8 and BG16B#25.1 expressing PrpS₁-GFP, HZ3.1-3 and HZ3.1-15 expressing PrpS₃-GFP, however lines BG16B#25.1 and HZ3.1-15 exhibited higher and homozygous expression of GFP (see Tables 5.2 and 5.3). The progeny of these plants were used in further experiments to determine whether the PrpS-GFP was functional when expressed in *A. thaliana* pollen. Family tree of the PrpS₁ and PrpS₃ expressing lines BG16 and HZ3 are presented in the Appendix II.

Since the RT-PCR results showed that mRNA was present in the pollen of transgenic *A. thaliana* expressing PrpS₁-GFP, we tried to confirm the PrpS₁ expression at the protein level in BG16 pollen. For this aim we extracted proteins in two different buffers suitable for the extraction of transmembrane (TM) proteins: first buffer was 2x extraction buffer for TM proteins and second buffer was additionally optimised for extraction of TM proteins (*personal communication with Andy Lovering*). Proteins were extracted with a buffer with high Glycerol and Triton X-100 concentrations, and the sample was not boiled prior to loading on SDS-PAGE, as proteins are likely to aggregate during boiling. After the transfer of the gel onto the membrane, the blot was incubated in stripping buffer for short time before

detection with antibodies (see Materials and Methods). Proteins were separated by western blotting and detected using alkaline phosphatase (Figure 5.4).

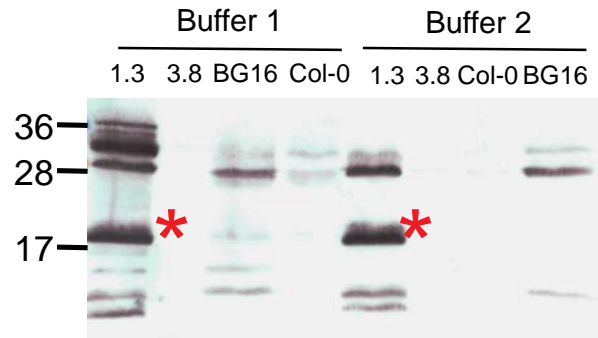


Figure 5.4.: Western blot analysis of pollen extract from BG16 pollen expressing PrpS₁ and controls, using two different extraction buffers. Buffer 1 (left side) was 2x extraction buffer and buffer 2 (right side) was optimised for extraction of TM proteins (with increased Glycerol and Triton X-100 concentrations; samples were not boiled prior to loading on a membrane; after the transfer, the blot was incubated in stripping buffer before detection with antibodies; see Materials and Methods). As controls were used *A. thaliana* non-transgenic Col-0 pollen extract, as positive control was used *Papaver* S₁S₃ pollen extract and as negative control *Papaver* S₃S₈ pollen extract. Samples were loaded on the membrane in duplicates, and after blotting the membrane was incubated in stripping buffer at 55 °C for 15 min before the incubation with antibodies. Primary antibody used was rat polyclonal anti-PrpS₁ (60C) in 1:1000 concentration and secondary was anti-rat-AP in 1:5000 concentration. PrpS₁ in *Papaver* extract is indicated by red star.

In *Papaver* S₁ and S₃ (S₁S₃) pollen extract several bands could be observed with both extraction buffers, but extraction buffer 2 gave clearer result. PrpS₁ size should be ~20 kDa so the lower strong band correspond to it. However, bands in *Papaver* S₁S₃ pollen extract were also detected at ~ 28 kDa mark, very strong at 30 kD and weaker at 36 kDa, The upper band could correspond to PrpS dimer. In BG16 pollen extract, we could observe bands at higher molecular weight ~ 28 and 30 kDa with the 28 kDa band being more intense than 30 kDa. There were also some weaker bands at ~10 kDa.

If PrpS forms multimers, this could indicate toward its potential function as a channel as there are some reports of the small receptors that multimerize in order to form a channel, for example small and novel transmembrane protein named Flower identified in *Drosophila* nervous system (Yao et al., 2009). Flower so far offers most analogies to PrpS proteins

although they do not share much sequence homology but rather a topological similarity. And since the Flower function has been established and demonstrated to multimerize and form a Ca^{2+} channel, this might be a possibility for PrpS as well. However, in order to confirm the dimer or multimer using western blot further optimization might be required.

5.2.2. *In vitro* functional analysis of *Papaver* SI determinants in transgenic *Arabidopsis thaliana in vitro*

As described earlier several PrpS₁-GFP and PrpS₃-GFP expressing transgenic *A. thaliana* lines were selected for further functional analysis: BG16B#25.1-1 and BG16A#25.1-1.x expressing PrpS₁-GFP, and HZ3.1-3.1, HZ3.1-15.1 and HZ3.1-15.1-x expressing PrpS₃-GFP. Lines segregated 3:1 with respect for the Kan resistance marker in heterozygous state and were expected to segregate 50 % for GFP expression. When they reached homozygous state they were completely resistant to Kan and exhibited 100 % GFP expression. Transgene mRNA expression was analysed using RT-PCR and the above selected lines were selected for their high expression.

Pollen from transgenic *A. thaliana* expressing *Papaver* SI pollen S-determinant, PrpS, was used in functional analysis. The semi-*in vitro* SI approach was adopted from the poppy SI system. *A. thaliana* pollen expressing PrpS₁-GFP or PrpS₃-GFP germinated in the petri dish to which control or SI reactions were induced by the addition of recombinant stigmatic PrsS proteins (see Figure 5.5). Control reactions were comprised of untreated pollen, pollen that was treated with heat denatured (i.e. biologically inactive) incompatible stigmatic proteins and compatible stigmatic proteins, while incompatible reaction was comprised of incubating

PrpS₁-GFP and PrpS₃-GFP expressing *A. thaliana* pollen with PrsS₁ and PrsS₃ stigmatic recombinant proteins, respectively (see Figure 5.5).

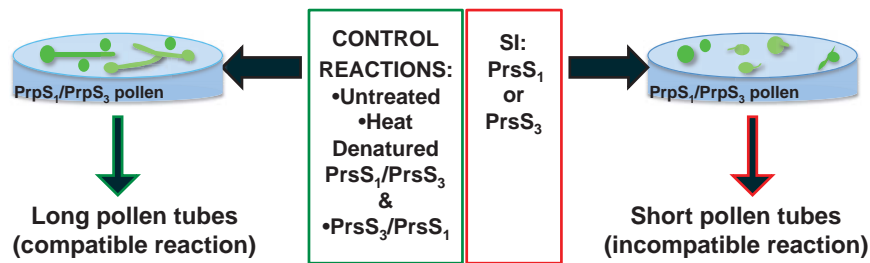


Figure 5.5.: Schematic diagram of the SI experiment *in vitro*. If PrsS₁ or PrsS₃ recombinant proteins are applied to *Arabidopsis* pollen expressing PrpS₁-GFP or PrpS₃-GFP (right side, red outline) there is the genetic match between pistil and pollen determinant and the result is incompatible interaction with inhibited pollen tube growth. Control reactions (left side, outlined with green) were comprised of untreated pollen, grown in GM only, of pollen incubated with inactivated heat denatured incompatible PrsS proteins or with compatible PrsS proteins. Compatible control reactions resulted in growth of pollen tubes.

The aim was to investigate whether characteristic features from *Papaver* SI could be observed in *A. thaliana* pollen expressing PrpS-GFP. Therefore, following SI induction *in vitro* the *S*-specific inhibition of pollen tube growth, the alterations of actin cytoskeleton, pollen viability and PCD were examined in PrpS-GFP expressing *A. thaliana* pollen (Geitmann et al., 2000, Thomas and Franklin-Tong, 2004, Jordan et al., 2000). A preliminary investigation was conducted on the response of *A. thaliana* mesophyll protoplasts using line BG3 expressing 35S::PrpS₁ and Col-0 transformed with 35S:: PrpS-GFP upon the incubation with recombinant stigmatic PrsS proteins.

5.2.2.1. *S*-specific inhibition of transgenic *A. thaliana* pollen tube growth

The inhibition of transgenic pollen tubes was analysed upon the induced SI response in pollen of transgenic *A. thaliana* lines BG16B#25.1-1 expressing PrpS₁-GFP, and HZ3.1-15.1 expressing PrpS₃-GFP. *A. thaliana* BG16B#25.1-1 and BG16B#25.1-2, and HZ3.1-15.1 and

HZ3.1-3.1 pollen along with untransformed control and *Papaver* S₁ and S₃ control pollen were pre-germinated for 1 h prior to the induction of SI and controls. Analysis was conducted by measuring the length of pollen tubes after overnight incubation (details in Materials and Methods section). *Papaver* S₁S₃ pollen was used as a control and was incubated in GM only (untreated – UT) or had induced SI reaction. *A. thaliana* untransformed pollen, also used as a control, was incubated in GM (UT) or with stigmatic recombinant PrsS₁ or PrsS₃ proteins. *A. thaliana* transgenic pollen expressing PrpS₁-GFP or PrpS₃-GFP was incubated in GM only (UT), had induced SI reaction by applying active PrsS₁ recombinant stigmatic proteins to PrpS₁-GFP pollen or PrsS₃ proteins to PrpS₃-GFP expressing pollen, while the control reactions comprised incubation with heat denatured (hd) PrsS proteins and compatible PrsS proteins. Pollen was pre-germinated for 1 h before the SI or controls were induced, as described above, and was then left to incubate for 20 h (overnight). Results of pollen tube length measurements are presented in Figure 5.6.

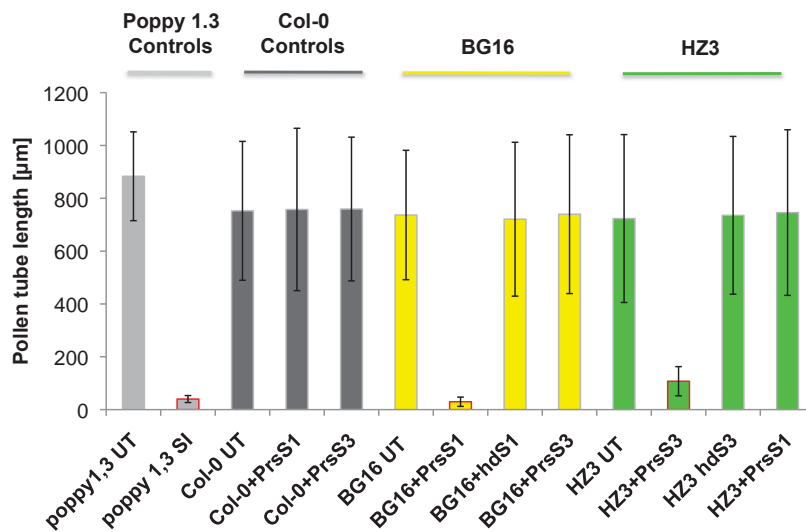


Figure 5.6: *A. thaliana* pollen tube inhibition graph presenting pollen tube length in μm . First two bars in light gray represent *Papaver* pollen control untreated (UT) and treated with recombinant PrsS₁/PrsS₃ proteins (SI), red outline. Next three bars in dark grey represent Arabidopsis Col-0 pollen control UT, and treated recombinant PrsS₁ and PrsS₃, respectively. Next four bars in yellow represent BG16 pollen expressing PrpS₁-GFP: BG16 –UT, treated with recombinant PrsS₁ (SI), red outline. BG16 pollen was also treated with heat-denatured (hd) PrsS₁ and with PrsS₃ as a control. Last four bars in green represent HZ3 pollen expressing PrpS₃-GFP: HZ3 – UT, and treated with recombinant PrsS₃ (SI), red outline. HZ3 pollen was also treated with hd PrsS₃ and PrsS₁ as a control. Error bars represent \pm standard deviation of mean. N=6 repeats for *A. thaliana* and N=3 for poppy; n=20 tubes measured.

Untreated and SI *Papaver* pollen were used as controls. The average length of the *Papaver* pollen tubes grown in GM was $883 \pm 168 \mu\text{m}$ while the length of pollen tubes with induced SI was $40 \pm 13 \mu\text{m}$, which was about 96 % shorter (N=3, n=20 pollen tubes, $P = 1.2 \times 10^{-43}$, ***). The untreated *A. thaliana* (UT) pollen tubes reached average length of $753 \pm 263 \mu\text{m}$ and were 15 % shorter compared to the poppy control pollen tube length (N=6; n=20 tubes; $P = 5.2 \times 10^{-3}$; **). However, when Col-0 pollen was treated with recombinant stigmatic PrsS₁ ($758 \pm 307 \mu\text{m}$; $P = 0.87$; N.S.) or PrsS₃ ($759 \pm 272 \mu\text{m}$; $P = 0.89$; N.S.), they had no effect compared to the untreated pollen grown in GM only.

BG16B#25.1-1 pollen, which expresses PrpS₁-GFP fusion protein, grown in GM only was not significantly different compared to the untreated Col-0 control ($737 \pm 245 \mu\text{m}$; $P = 0.73$; N.S.) but when it was challenged with incompatible PrsS₁ proteins (see Figure 5.6, yellow bars outlined with red line), the pollen tube length exhibited 96 % decrease compared to the

BG16 UT ($30 \pm 18 \mu\text{m}$; $P=5.2 \times 10^{-66}$; ***). To determine whether the PrsS₁ protein without its biological activity could induce this decrease, we inactivated PrsS₁ by heat denaturing for 5 min. The pollen tube length of BG16B#25.1-1 treated with biologically inactivated PrsS₁ was not significantly different from the UT BG16 pollen and was 96 % longer than the pollen treated with biologically active PrsS₁ ($721 \pm 291 \mu\text{m}$; $P=0.75$, N.S. compared to BG16-UT and $P=7.3 \times 10^{-58}$, *** compared to BG16-PrsS₁). This indicates that biologically active PrsS₁ was required for the inhibition of pollen tube growth. To assess whether any active PrsS protein was able to inhibit the pollen tube of transgenic *A. thaliana* pollen expressing PrpS₁-GFP or if the inhibition was S-specific, the BG16B#25.1-1 pollen was incubated with PrsS₃ proteins. The resulting length of pollen tubes indicate that the PrsS₃ proteins had no effect on the BG16 pollen tubes since they were not significantly different to the BG16-UT and highly significantly longer than the BG16 pollen incubated with incompatible PrsS₁ ($740 \pm 301 \mu\text{m}$; $P=0.95$, N.S. compared to BG16-UT and $P=4.1 \times 10^{-58}$, *** compared to BG16-PrsS₁). This demonstrates that PrpS₁-GFP expressing *A. thaliana* pollen was inhibited in an S-specific manner.

The experiment was repeated with HZ3.1-15.1 line, whose pollen expresses PrpS₃-GFP fusion protein. When HZ3.1-15.1 pollen was grown in GM, it was not significantly different compared to the Col-0 UT ($723 \pm 318 \mu\text{m}$; $P=0.58$; N.S.). To examine the SI inhibition of pollen tube growth, the PrpS₃-GFP pollen was challenged with PrsS₃ stigmatic proteins (Figure 5.6 green bar outlined with red line) and the pollen was 85 % shorter compared to the HZ3 UT ($108 \pm 55 \mu\text{m}$; $P=5.5 \times 10^{-47}$; ***). HZ3.1-15.1 pollen, treated with heat-denatured (biologically inactive) PrsS₃ protein was not significantly different from UT pollen ($736 \pm 299 \mu\text{m}$; $P=0.81$, N.S. compared to HZ3-UT), but was significantly longer than the SI challenged

pollen, treated with biologically active PrsS₃ ($P=7.6 \times 10^{-54}$, *** compared to HZ3+PrsS₃). The HZ3 pollen was also incubated with PrsS₁ proteins and the resulting length of pollen tubes indicates that the PrsS₁ proteins had no effect on the HZ3 pollen tubes. Pollen tubes incubated with PrsS₁ were not significantly different to the HZ3-UT and highly significantly longer to the HZ3 pollen incubated with incompatible PrsS₃ ($746 \pm 314 \mu\text{m}$; $P=0.66$, N.S. compared to HZ3-UT and $P=4.7 \times 10^{-53}$, *** compared to HZ3-PrsS₃). This demonstrates that PrpS₃-GFP expressing *A. thaliana* pollen was inhibited in an *S*-specific manner.

Together, these data demonstrate that the inhibition of the PrpS₁-GFP expressing pollen tube growth in selected BG16 lines by recombinant PrsS₁ proteins or PrpS₃-GFP expressing pollen in selected HZ3 lines by recombinant PrsS₃ proteins acts in an *S*-specific manner and requires biologically active PrsS₁ or PrsS₃ proteins, respectively. Pollen tube inhibition assays that were carried on transgenic *A. thaliana* pollen expressing PrpS₁-GFP or PrpS₃-GFP proteins challenged with PrsS₁ or PrsS₃ recombinant proteins show that inhibition occurred very rapidly. Inhibited incompatible *A. thaliana* pollen tubes were very short which was expected and pollen tube inhibition was complete. With *Papaver* SI the arrest of the “incompatible” pollen tube growth is one of the first events upon the interaction of PrpS and incompatible PrsS protein, which is crucial for successful prevention of fertilization.

This *S*-specific inhibition response of transgenic *A. thaliana* pollen expressing *Papaver* PrpS proteins by PrsS proteins suggests that poppy male *S*-determinant, PrpS, is functional in *A. thaliana*.

5.2.2.2. PrpS-PrsS interaction stimulates formation of punctate actin foci in transgenic *A. thaliana* pollen

The results in previous section 5.4.2 confirmed that the *Arabidopsis* transgenic pollen expressing *Papaver* PrpS-GFP was inhibited in an *S*-specific manner by the addition of the recombinant stigmatic PrsS proteins. The formation of the punctate actin foci is one of the hallmark features of SI response in *Papaver* as actin cytoskeleton is a very early target for the SI signals (Snowman et al., 2002, Geitmann et al., 2000, Snowman et al., 2000, Poulter et al., 2010a). Therefore, in order to provide further evidence that the observed inhibition of *A. thaliana* pollen tube length was due to an SI response, we explored other key poppy SI-like events in *A. thaliana* pollen. We investigated whether actin filament modification was also observed in *A.thailana* PrpS-GFP expressing pollen when treated with PrsS recombinant proteins.

We initiated the analysis of actin cytoskeleton in pollen of the transgenic *A. thaliana* lines BG16B#25.1-1 expressing PrpS₁-GFP, and HZ3.1-15.1 expressing PrpS₃-GFP, after 3 h SI challenge. BG16B#25.1-1 was incubated with recombinant stigmatic PrsS₁ proteins and HZ3.1-15.1 with PrsS₃ proteins. Controls consisted of untreated (UT) Col-0 and transgenic pollen; transgenic *A. thaliana* pollen treated with heat denatured (hd) recombinant proteins or compatible recombinant proteins, as with previous assay.

Untransformed *A. thaliana* Col-0 pollen, grown in GM only, had a visible array of F-actin filaments in pollen grains and pollen tubes (Figure 5.7.a) and the results also demonstrate that actin filaments in nontransgenic Col-0 pollen were not disturbed upon the addition of recombinant PrsS₁ (Figure 5.7.b).

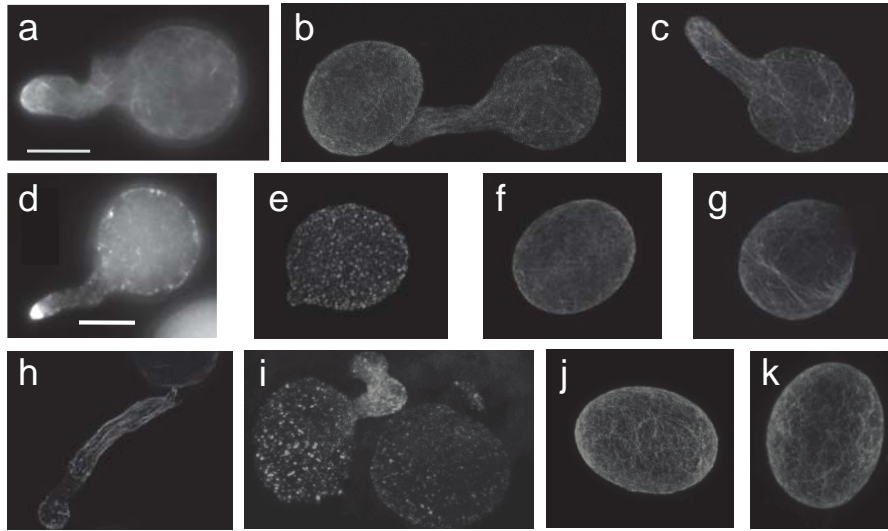


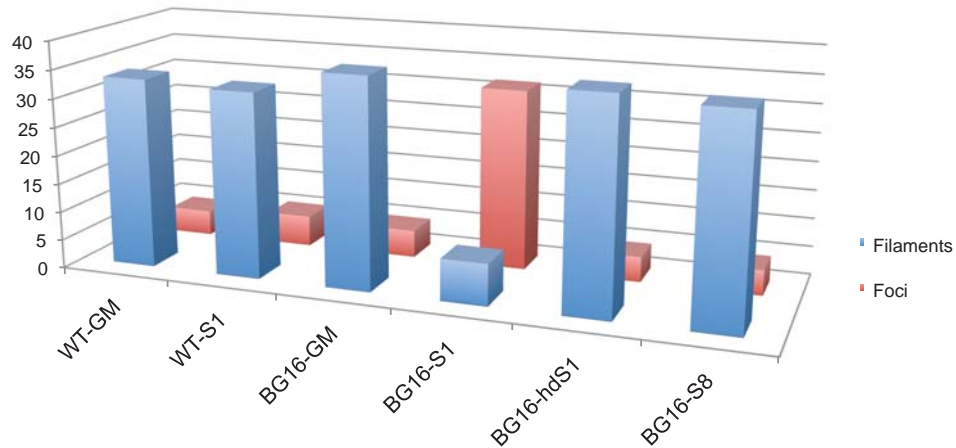
Figure 5.7: Rhodamine Phalloidin stained actin in *A. thaliana* pollen (a) Col-0 untreated, (b) Col-0 treated with PrsS₁, (c) BG16 untreated, (d, e) BG16 treated with PrsS₁, (f) BG16 treated with heat denatured PrsS₁, (g) BG16 treated with PrsS₈, (h) HZ3 untreated, (i) HZ3 treated with PrsS₃, (j) HZ3 treated with heat denatured PrsS₃, (k) HZ3 treated with PrsS₁. Scale represents 10 μm. Figures were imaged using the confocal microscopy by Katie Wilkins (except a & d, which were imaged by epifluorescence microscopy).

Filamentous actin arrays were also observed in the unchallenged pollen of transgenic line BG16 expressing PrpS₁-GFP (Figure 5.7.c) or HZ3 expressing PrpS₃-GFP (Figure 5.7.h). Characteristic punctate actin foci were observed in BG16 pollen that was incubated with PrsS₁ proteins (Figures 5.7.d&e) and HZ3 pollen challenged with PrsS₃ proteins (Figure 5.7.i). Foci were not present in any of the controls where incompatible and heat inactivated PrsS proteins were added (Figures 5.7.f & j) or when compatible PrsS control was applied (Figures 5.7.g & k). Taken together these data demonstrate that *A. thaliana* PrpS₁-GFP and PrpS₃-GFP expressing pollen exhibit the *S*-specific appearance of punctate actin foci, a hallmark feature of poppy SI.

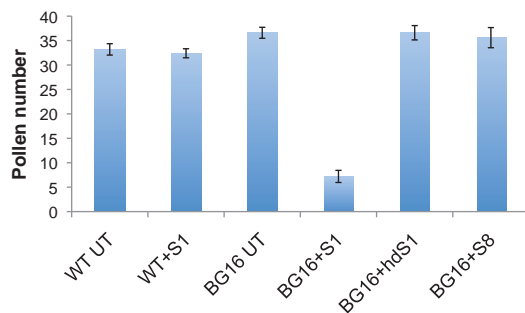
A. thaliana BG16B#25.1-1 pollen expressing PrpS₁-GFP was examined for the presence of actin filaments or punctate actin foci (see Figure 5.8) in order to quantify the *S*-specific appearance of foci observed under the microscope. Figure 5.8.a clearly shows that actin

filaments (blue bars) are predominant in all control treatments, while SI challenge on PrpS₁-GFP expressing pollen exhibit mostly punctate actin foci (red bars). Taking into account only scored pollen with clearly visible actin structures, 88 % of the untreated non transgenic Col-0 pollen samples exhibit filamentous actin, which was not affected if Col-0 pollen was challenged with PrsS₁ proteins (85 % filaments; P=0.46). Scoring filaments, BG16B#25.1-1 untreated pollen exhibited 88 % actin filaments (P=0.97 compared to Col-0 untreated; N=250), while BG16B#25.1-1 that was incubated with biologically inactivated PrsS₁ or compatible PrsS₈ exhibited 89 % actin filaments (P=0.78 and P=0.85, respectively, compared to BG16 untreated, N=250), indicating that biologically active PrsS₁ only are required for the alterations in actin cytoskeleton. Quantification also revealed that SI challenge of BG16 with PrsS₁ resulted in 81 % of pollen exhibiting punctate actin foci (Figure 5.8.c), which represents a highly significant 558 % increase compared to untreated BG16 pollen (P=8.9x10⁻⁴⁵; N=250).

a



b



c

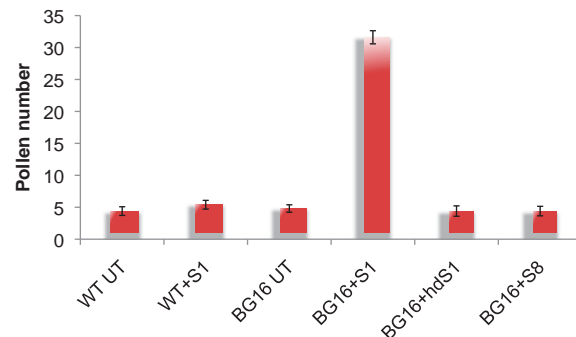


Figure 5.8.: Quantification of actin foci and filaments in PrpS₁-GFP expressing pollen. **(a)** actin foci (red bars) and filaments (blue bars) presented on the same graph; **(b)** quantification of actin filaments; **(c)** quantification of actin foci. N=5, n=50; Error bars represent ± St. Error of means.

None of the non-transgenic controls or BG16 controls with inactivated incompatible proteins or compatible proteins showed actin foci pattern and were not significantly different from the untreated pollen in which foci are mostly observed. Together these data demonstrate the highly significant presence of punctate actin foci, specifically in SI challenged transgenic *A. thaliana* BG16B#25.1-1 pollen, expressing PrpS₁-GFP. These data demonstrate that there is an *S*-specific interaction between biologically active PrsS₁ and PrpS₁-GFP, leading to the alterations of actin cytoskeleton in PrpS₁-GFP expressing *A. thaliana* pollen, that result in the appearance of punctate actin foci. Therefore a key characteristic of poppy SI was observed in transgenic *A. thaliana* pollen, indicating that PrpS₁-GFP transgene is functional in *A. thaliana*.

5.2.2.3. Evidence for PCD in the *A. thaliana* transgenic pollen upon SI challenge

5.2.2.3.1. Pollen viability is decreased in an *S*-specific manner upon interaction between PrpS-GFP expressing *A. thaliana* pollen and recombinant stigmatic PrsS

We were interested to examine whether the interaction between *Papaver* pollen and pistil determinants affected Arabidopsis pollen viability. It has been shown in *Papaver* that the *S*-specific interaction between PrpS and PrsS decreases pollen viability and triggers PCD (Thomas and Franklin-Tong, 2004). The pollen viability in *Papaver* was analysed using FDA, which becomes fluorescent when taken up by metabolically active–viable–pollen (Breeuwer et al., 1995). However, we were unable to use the same drug in *A. thaliana* as it was not possible to distinguish between FDA signal of viable pollen and GFP signal of pollen expressing PrpS-GFP fusion protein. Therefore, we used the low toxicity non-permeating azo-compound dye Evans Blue (Shigaki and Bhattacharyya, 1999). Dye penetrated in non-viable cells, so they appear dark blue when inspected by the microscope, while it was excluded from viable cells with intact membrane so they appeared colourless.

Lines of PrpS₁-GFP and PrpS₃-GFP expressing *A. thaliana* pollen (BG16B#25.1-1 and BG16B#25.1-2, and HZ3.1-15.1 and HZ3.1-3.1) were used as for measuring pollen tube length and pollen was collected and treated as with previous experiments. Viability of pollen was inspected at three time points: 0 h, 8 h and 24 h by adding 0.05 % Evans Blue to the sample. Dye was left to incubate for 10 min and washed with GM before pollen viability was assessed (see Figure 5.9). In poppy SI DNA fragmentation indicating PCD was measured after 8 h (Thomas and Franklin-Tong, 2004) although the maximum DNA fragmentation was observed at 14 h post SI (Jordan et al., 2000). *A. thaliana* pollen tubes

grew slower than *Papaver* with the optimized germination rates reported after 16 h, so we chose to investigate viability at 24 h post-SI.

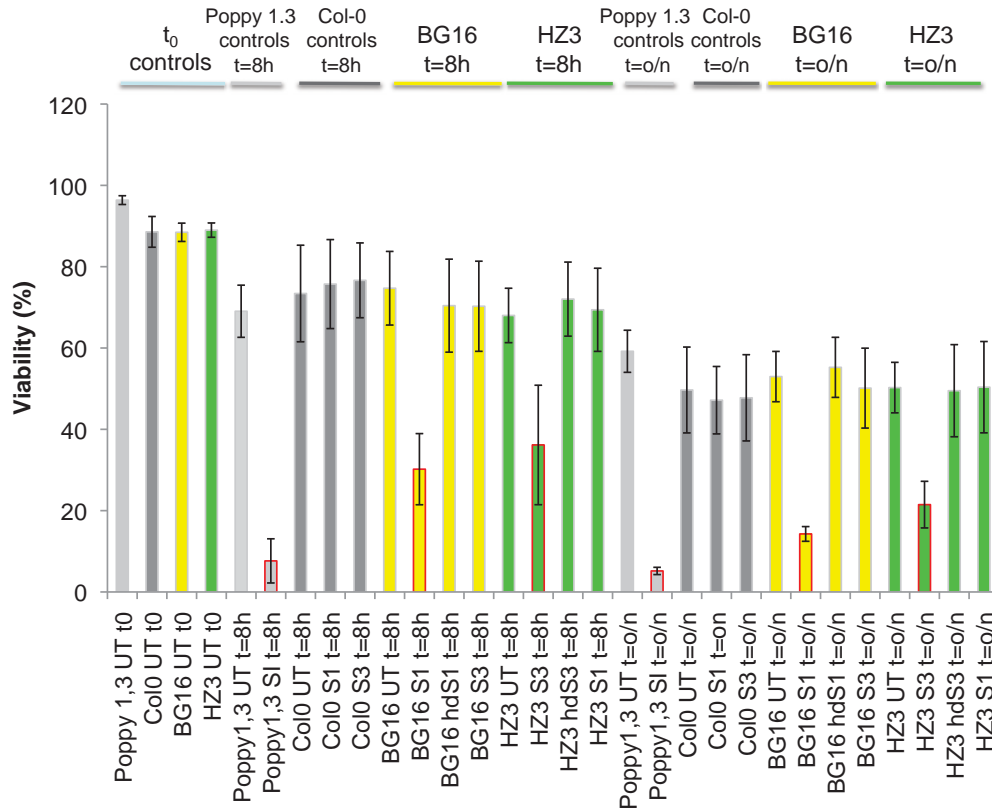


Figure 5.9.: Viability (%) of *A. thaliana* transgenic pollen BG16 (yellow bars) and HZ3 (green bars) along with Col-0 (dark gray bars) and *Papaver* pollen control (light gray bars) at 0 h, 8 h and 24 h. Pollen was incubated with GM only (UT), with incompatible PrsS₁ proteins for BG16 pollen or PrsS₃ proteins for HZ3 pollen (SI, red outline), with heat-denatured PrsS proteins and with compatible PrsS₁ for BG16 pollen and PrsS₃ for HZ3 pollen. Error bars represent standard deviation of mean. N=5 repeats (N=3 for poppy), n=117±21 pollen counted.

The initial viability of the untreated *A. thaliana* non-transgenic Col-0 pollen at t₀ was 89±4 % (P=3.6x10⁻² compared to poppy UT). The viability of Col-0 pollen decreased by 17 % after 8 h. The PrsS proteins did not have any effect on the viability of untransformed pollen, viability of pollen treated with PrsS₁ for 8 h was 76±11 % (P=0.71 compared to Col-0 t=8 h) and viability of Col-0 treated with PrsS₃ for 8 h was 77±9 % (P=0.83 compared to Col-0 t=8 h).

In control *Papaver* pollen from S₁S₃ plants, the incubation with incompatible PrsS₁PrsS₃ proteins for 8 h resulted in highly significant 90 % decreased viability compared to the *Papaver* pollen that was incubated in GM for 8 h (P=4.3x10⁻¹⁹ compared to *Papaver* S₁S₃ UT t=8 h). With longer incubation time (24 h total), the viability of the control pollen decreased. Untreated S₁S₃ *Papaver* pollen exhibited 59±5 % viability, which is 39 % less than at 8 h but viability of S₁S₃ *Papaver* pollen incubated with PrsS₁ and PrsS₃ proteins did not significantly change compared to the 8h incubation 6±1 % (P=2.3x10⁻⁵¹ compared to *Papaver* S₁S₃ UT; ***). *A. thaliana* untreated non-transgenic control Col-0 pollen exhibited 50±11 % viability after 24 h incubation. The viability of Col-0 incubated with PrsS₁ or PrsS₃ for 24 h was not significantly different from the untreated Col-0 (P=0.72 and P=0.78, respectively).

Viability of transgenic BG16 pollen (expressing PrpS₁-GFP) grown in GM only was initially around 88±2 % (P=0.98 compared to Col-0 UT t₀; N.S.). After 8 h, the viability decreased for 16 % and reached 75±9 % (P=0.83 compared to Col-0 UT t=8h). When BG16 pollen was challenged with PrsS₁ proteins for 8 h, a significant decrease in viability to 30±9 % (P=2.9x10⁻¹⁰ compared to BG16 UT t=8 h) was observed. The heat-denatured PrsS₁ protein had no effect on BG16 pollen after 8 h incubation (viability 70±11 %; P=0.50 compared to BG16 UT t=8 h) nor did active PrsS₃ protein (viability 70±11 %; P=0.48 compared to BG16 UT t=8 h). The viability of BG16 pollen that was incubated overnight in the GM decreased by 29 % and reached 53±6 % of viability (total decrease in 24 h was 40 %) but was not significantly different from the Col-0 UT control at the same incubation time (P=0.64). Significant decrease in viability was observed when BG16 pollen was incubated with PrsS₁ proteins for 24 h with 14±2 % of viability (P=6.9x10⁻⁹ compared to the BG16 UT t=24 h). The decrease in viability compared to the untreated BG16 control was 73 % and 53 %

compared to the BG16 pollen incubated with PrsS₁ proteins for 8 h only. This could suggest that the cell death response in *A. thaliana* pollen is somewhat slower compared to *Papaver* pollen. The response was *S*-specific and observed only with active PrsS₁ proteins as incubation of BG16 with heat-denatured PrsS₁ or PrsS₃ for 24 h had no significant effect on pollen compared to the untreated BG16 control (P=0.75 and P=0.69, respectively).

Viability of PrpS₃-GFP expressing transgenic pollen HZ3 exhibited similar results to the observed from BG16. HZ3 grown in GM exhibited an initial viability of 89±2 % (P=0.92 compared to Col-0 UT t₀; N.S.). After 8 h, the viability decreased by 24 % and reached 69±7 % (P=0.40 compared to Col-0 UT t=8 h). The incubation of HZ3 pollen with recombinant PrsS₃ proteins for 8 h caused a significant decrease of viability to 36±14 % (P=6.5x10⁻⁶ compared to HZ3 UT t=8 h). Only active PrsS₃ protein had an effect on the viability of HZ3 pollen. After 8 h incubation with heat-denatured PrsS₃ protein, the viability was 72±9 % (P=0.53 compared to HZ3 UT t=8 h). No effect on viability was observed when the HZ3 pollen was incubated in the presence of active PrsS₁ proteins that decreased viability of BG16 pollen (viability 69±10 %; P=0.83 compared to HZ3 UT t=8 h). After overnight incubation in GM the viability of HZ3 pollen decreased for further 26 % and reached 50±6 % (total decrease in 24 h was 44 %) but was not significantly different from the Col-0 UT control at t=24 h (P=0.93). With incompatible reaction between HZ3 pollen and recombinant PrsS₃ proteins, the significant decrease in viability was observed after 24 h incubation as it reached 21±6 % (P=2.2x10⁻⁵ compared to the HZ3 UT t=24 h). The decrease in viability compared to the untreated HZ3 pollen incubated in GM for 24 h was 57 %, while further decrease compared to incompatible incubation of HZ3 pollen with PrsS₃ for 8 h was 40 %. As with BG16 pollen, the response was *S*-specific and observed only with active PrsS₃

proteins. The incubation of HZ3 with heat inactivated PrsS₃ or active PrsS₁ for 24 h had no significant effect on pollen compared to the HZ3 control grown in GM only (P=0.75 and P=0.69, respectively).

The SI-induced decrease of viability in pollen from BG16B#25.1-1 line expressing PrpS₁-GFP and HZ3.1-15.1 line expressing PrpS₃-GFP, by the addition of the recombinant stigmatic PrsS₁ or PrsS₃, respectively, indicates that the *S*-specific interaction between PrsS and PrpS is functional and results in cell death of transgenic pollen.

5.2.2.3.2. Decrease of pollen viability involving DEVDase activity

A key downstream event after the *S*-specific interaction between the stigmatic PrsS proteins and pollen receptor PrpS in *Papaver*, is the activation of the caspase-like proteins ending up with the PCD of pollen (Thomas and Franklin-Tong, 2004). The PCD in *Papaver* was demonstrated with assays measuring DNA fragmentation, and with the use of caspase-3 specific tetrapeptide inhibitor Ac-DEVD-CHO, which abolished PCD (Thomas and Franklin-Tong, 2004, Jordan et al., 2000). Hence, we investigated whether DEVD-ase activity plays any role in the *S*-specific decrease of viability observed in transgenic *A. thaliana* lines BG16B#25.1-1.1, BG16B#25.1-1.5 and BG16B#25.1-1.7, expressing PrpS₁-GFP and HZ3.1-15.1-1, HZ3.1-15.1-6 and HZ3.1-15.1-12, expressing PrpS₃-GFP. Transgenic *A. thaliana* homozygous pollen from T₄ generation plant lines was used for the experiment. *A. thaliana* plants from lines BG16B#25.1-1.1 and BG16B#25.1-1.7 were used as a source for PrpS₁-GFP pollen, and lines HZ3.1-15.1-1 and HZ3.1-15.1-5 for PrpS₃-GFP pollen. PrpS₁-GFP and PrpS₃-GFP expressing *A. thaliana* pollen, and controls *Papaver* S₁S₃

pollen and *A. thaliana* untransformed Col-0 pollen were pretreated with the inhibitor of DEVDase activity, tetrapeptide Ac-DEVD-CHO, before the induction of SI by the addition of recombinant stigmatic PrsS proteins. Additional control was comprised of pollen incubated in GM only (untreated – UT) or pollen that had induced SI reaction. Viability of pollen was investigated at two time points: 0h and 8h by adding 0.05 % Evans Blue solution to the sample. The results of these assays are presented in the Figure 5.10. When comparing percentages of viability between treatments, the control was assumed a 100 % activity.

A. thaliana non-transgenic pollen germinated in GM (UT) exhibited 90 ± 4 % viability at t_0 and was only 1 % higher than viability of untreated *Papaver* pollen at t_0 ($P=0.79$ compared to poppy UT). After 8 h incubation the viability of Col-0 pollen decreased by 28 % having 65 ± 4 % of viable pollen. The pretreatment with tetrapeptide Ac-DEVD-CHO did not have any effect on the non-transgenic pollen; viability was 62 ± 6 % ($P=0.66$ compared to Col-0 UT pollen $t=8$ h). PrsS proteins did not have any effect on the viability of the Col-0 control pollen, viability of pollen treated with PrsS₁ for 8 h was 65 ± 4 % ($P=0.95$ compared to Col-0 UT $t=8$ h) and viability of Col-0 treated with PrsS₃ for 8 h was 66 ± 6 % ($P=0.98$ compared to Col-0 UT $t=8$ h).

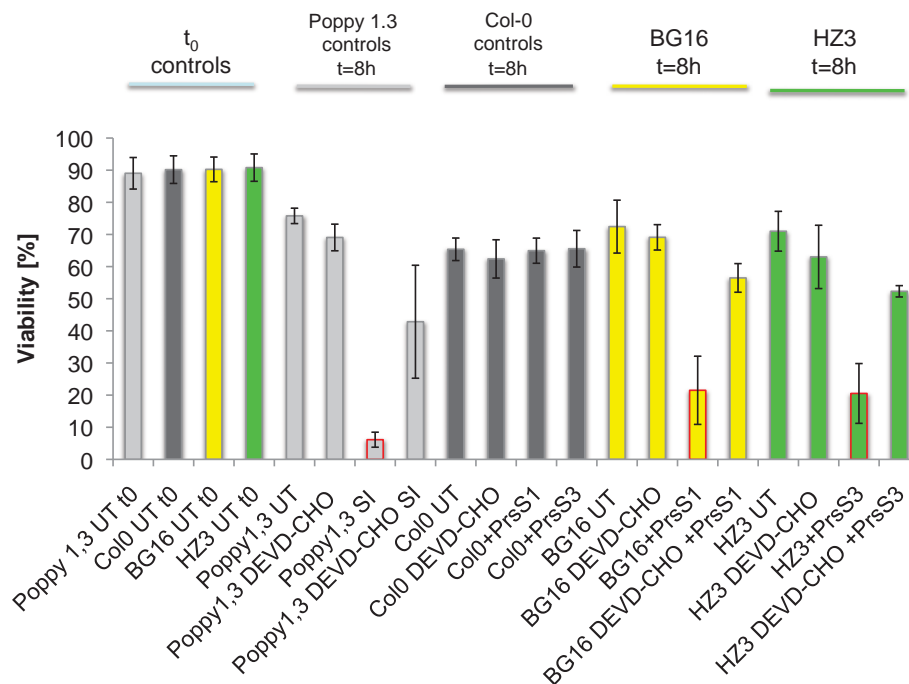


Figure 5.10. Viability (%) of Ac-DEVD-CHO pretreated *A. thaliana* transgenic pollen BG16B#25.1-1.1 and BG16B#25.1-1.7 (yellow bars), and HZ3.1-15.1-1 and HZ3.1-15.1-5 (green bars) along with Col-0 (dark gray bars) and *Papaver* S1S3 (light gray bars) pollen control at t=0 and t=8 h. Pollen was incubated in GM only (UT) or in caspase-3 inhibitor, tetrapeptide Ac-DEVD-CHO as control. SI was induced with incompatible PrsS proteins (red outline), while the bar after the outlined one represent pollen that was pretreated with Ac-DEVD-CHO inhibitor before SI was induced. Error bars represent standard deviation of mean. N=3 repeats; n=145±16 pollen counted.

The viability of untreated control S₁S₃ *Papaver* pollen decreased after 8 h incubation to 76±2 % while pollen that was pretreated with the caspase inhibitor Ac-DEVD-CHO for an hour and then incubated for 8 h exhibited 69±4 % viability (P=0.29 compared to S₁S₃ *Papaver* UT control t=8 h). The incompatible challenge on *Papaver* pollen decreased the viability to 6±2 % (P=1.3x10⁻²³ compared to *Papaver* S₁S₃ UT t=8 h). However, viability was not lost when pollen was pretreated with caspase-3 inhibitor Ac-DEVD-CHO before induction of SI but significantly increased viability that was 43±18 % (P=1.6x10⁻⁹ compared to S₁S₃ *Papaver* SI t=8 h).

Initial viability of transgenic pollen expressing PrpS₁-GFP grown in GM only was around 90±4 % (P=0.98 compared to Col-0 UT t₀). After 8h, the viability decreased by 20 % and

was 72 ± 8 % ($P=0.28$ compared to Col-0 UT $t=8$ h). The pretreatment of BG16 pollen with tetrapeptide Ac-DEVD-CHO did not significantly affect the viability (69 ± 4 %, $P=0.60$ compared to BG16 UT $t=8$ h). SI challenge of BG16B#25.1-1.1 and BG16B#25.1-1.7 pollen with PrsS₁ proteins for 8 h caused a significant decrease of viability to 22 ± 11 % ($P=5.3 \times 10^{-13}$ compared to BG16 UT $t=8$ h), but viability increased significantly by 162 % when PrsS₁-challenged BG16 pollen was pretreated with inhibitor Ac-DEVD-CHO (57 ± 4 %; $P=4 \times 10^{-7}$ compared to BG16 SI $t=8$ h).

Similar viabilities were observed in HZ3.1-15.1-1 and HZ3.1-15.1-5 pollen expressing PrpS₃-GFP. Initial viability of HZ3 pollen was 91 ± 4 % ($P=0.88$ compared to Col-0 UT t_0). After 8 h, the viability decreased for 22 % and reached 71 ± 6 % ($P=0.39$ compared to Col-0 UT $t=8$ h). When HZ3 pollen was pretreated with tetrapeptide Ac-DEVD-CHO, the viability was not significantly affected (63 ± 10 %, $P=0.23$ compared to HZ3 UT $t=8$ h). Challenge of PrpS₃-GFP expressing pollen with stigmatic recombinant PrsS₃ proteins for 8 h caused a significant decrease of viability to 21 ± 9 % ($P=7.8 \times 10^{-13}$ compared to HZ3 UT $t=8$ h); however, viability increased significantly by 155 % if SI challenged HZ3 pollen was pretreated with inhibitor Ac-DEVD-CHO (52 ± 2 %; $P=3 \times 10^{-6}$ compared to HZ3 SI $t=8$ h).

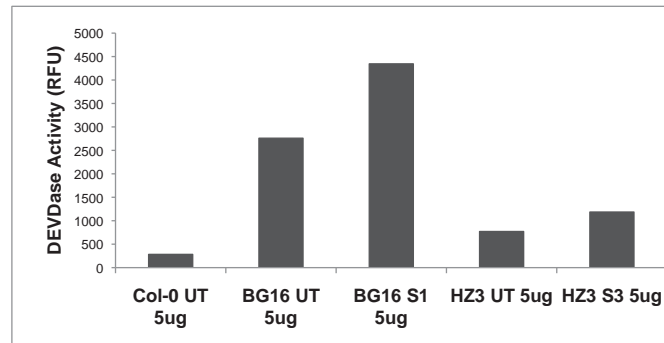
Taken together, these data demonstrate that PrsS triggers cell death in PrpS-GFP expressing pollen in an *S*-specific manner. Moreover, the cell death involves DEVDase activity and indicates that PCD might be triggered in incompatible *A. thaliana* pollen expressing PrpS₁-GFP or PrpS₃-GFP fusion protein when incubated with the cognate recombinant stigmatic PrsS proteins.

5.2.2.4. PCD in *A. thaliana* transgenic pollen expressing PrpS-GFP

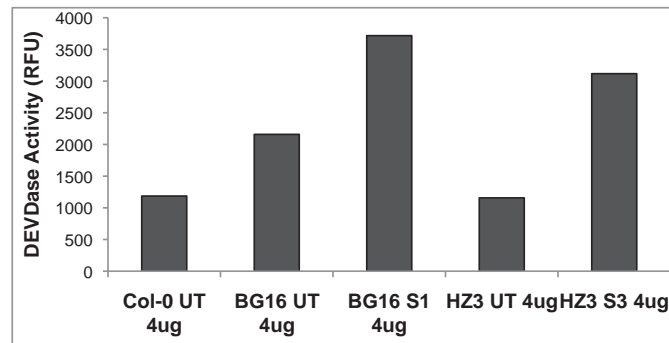
As described in previous section, the viability of transgenic *A. thaliana* pollen expressing male PrpS₁-GFP or PrsS₃-GFP was reduced in an S-specific manner upon treatment with the recombinant stigmatic PrsS proteins. In order to ascertain whether the poppy SI response is fully functional in *A. thaliana*, analysis of PCD was addressed. Therefore, we initiated studies to analyse SI-induced PCD in transgenic *A. thaliana* pollen expressing PrpS₁-GFP and PrpS₃-GFP by attempting to measure caspase-3-like DEVDase activity more directly using the caspase-3 specific fluorogenic tetrapeptide Ac-DEVD-AMC. The stimulation of several specific caspase-like activities was demonstrated using caspase activity assays (Bosch and Franklin-Tong, 2007). They were based on measuring the release of the fluorophore from the specific peptide substrate tetrapeptide, e.g. caspase-3 optimal tetrapeptide recognition motif is DEVD. Substrate used in the fluorometric assay has DEVD conjugated to the fluorescent probe AMC (Ac-DEVD-AMC). The fluorescence can be detected upon cleavage of the AMC from the DEVD peptide by caspase-3-like proteins. Assays measuring caspase-like activity in *Papaver* pollen were optimised to use 10 µg of the total pollen protein extract in the assay. Due to the miniature size of *A. thaliana* flowers which produce less pollen compared to *Papaver* flowers and the fact that pollen required fresh collection every day, preliminary experiments were carried out on *A. thaliana* pollen, in order to investigate whether the caspase activity could be reliably measured with less than 10 µg of total *A. thaliana* pollen protein extract. In order to use the same concentration of pollen protein extract as it was used with *Papaver* pollen, the method was not suitable for *A. thaliana* pollen, as the pollen collection from *A. thaliana* flowers was very time consuming.

Figure 5.11 shows initial preliminary data using 3, 4 and 5 μg protein extract that encouraged us to pursue this assay further.

a



b



c

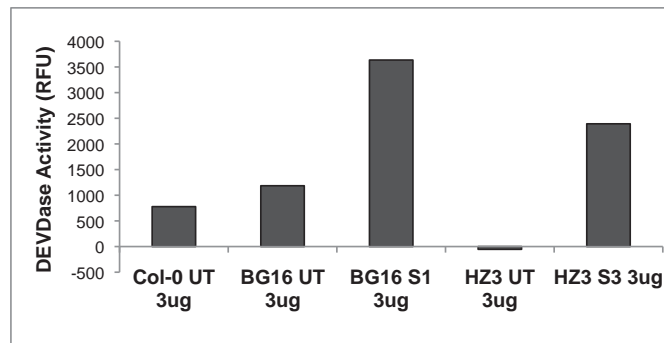


Figure 5.11.: DEVDase activity of protein extract from BG16B#25.1-1 and HZ3.1-15.1 pollen that was incubated with GM only (UT), or had induced SI by addition of recombinant stigmatic PrsS₁ (BG16 S1) and PrsS₃ (HZ3 S3) proteins, respectively. Non-transgenic Col-0 incubated in GM only (UT) was used as a control (far left bar). (a) 5 μg of pollen extract; (b) 4 μg of pollen extract and (c) 3 μg of pollen extract.

Preliminary results in Figure 5.11 suggested that DEVDase activity in SI-induced samples of transgenic *A. thaliana* pollen expressing PrpS₁-GFP and PrpS₃-GFP was detected and

increased compared to the control sample, even when using the substrate in concentration as low as 3 μ g. Since the protein concentration of our loaded pollen extract in the assay was on the lower limit of detection, this means that any changes in the very sensitive *A. thaliana* pollen balance appeared enhanced in the caspase assay.

In order to examine whether SI interaction in *A. thaliana* transgenic pollen triggered PCD, we used another approach and pretreated pollen with the tetrapeptide inhibitor Ac-DEVD-CHO before the induction of SI and measurement of caspase-like activity. *A. thaliana* transgenic homozygous T₄ generation plant lines BG16B#25.1-1.1 and BG16B#25.1-1.7 were used as a source for PrpS₁-GFP pollen, and lines HZ3.1-15.1-1 and HZ3.1-15.1-5 for PrpS₃-GFP pollen; pollen from untransformed Col-0 was used as control. Pollen was pretreated with 100 μ M tetrapeptide inhibitor, Ac-DEVD-CHO and SI was induced by the addition of incompatible recombinant stigmatic PrsS proteins: PrsS₁ proteins added to PrpS₁-GFP expressing pollen and PrsS₃ proteins to PrpS₃-GFP expressing pollen. Controls comprised of transgenic and untransformed pollen that was untreated, incubated with the inhibitor Ac-DEVD-CHO only or incubated with PrsS₁ or PrsS₃ recombinant stigmatic proteins.

The caspase-3-like activity measurements are presented in Figure 5.12.

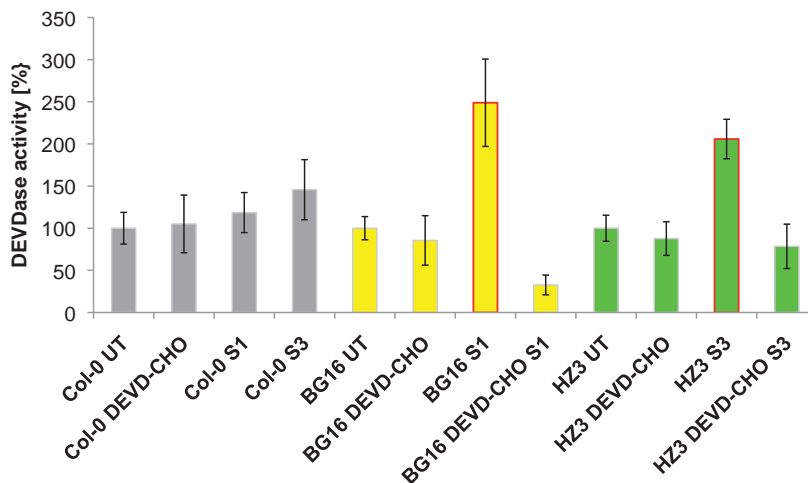


Figure 5.12: DEVDase activity in *A. thaliana* pollen with induced SI or pretreated with inhibitor Ac-DEVD-CHO prior to induction of SI. Grey bars correspond to untransformed Col-0 control that was untreated or incubated with Ac-DEVD-CHO or stigmatic PrsS₁ and PrsS₃ proteins. BG16B#25.1-1.1 and BG16B#25.1-1.7 pollen (represented by yellow bars) was challenged with incompatible PrsS₁ (BG16 S1) and was also pretreated with inhibitor Ac-DEVD-CHO prior to induction of SI (BG16 DEVD-CHO S1). Control was comprised of untreated BG16 pollen (BG16 UT) and BG16 pollen incubated with inhibitor only (BG16 DEVD-CHO). HZ3.1-15.1-1 and HZ3.1-15.1-5 pollen (represented by green bars) was challenged with incompatible PrsS₃ (HZ3 S3) and was also pretreated with inhibitor Ac-DEVD-CHO prior to induction of SI (HZ3 DEVD-CHO S3). Control was comprised of untreated HZ3 pollen (HZ3 UT) and HZ3 pollen incubated with inhibitor only (HZ3 DEVD-CHO). Error bars are \pm SEM.

(n=8 for BG16 DEVD-CHO, HZ3 UT, HZ3 DEVD-CHO. HZ3 S3, HZ3 DEVD-CHO S3 n=7 for Col-0 UT, Col-0 S1, BG16 UT, BG16 S1, BG16 DEVD-CHO S1 n=6 for Col-0 DEVD-CHO, Col-0 S3)

The cleavage of Ac-DEVD-AMC by SI-activated caspase-3-like proteins in *A. thaliana* transgenic pollen was significantly increased by 150 ± 52 % in BG16 PrsS₁ treated pollen (yellow bar, $P=0.04$, *) and by 106 ± 23 % in HZ3 PrsS₃ treated pollen (green bar, $P=0.003$, **). Pretreatment of pollen tubes with the tetrapeptide inhibitor significantly reduced the SI-induced DEVDase activity in BG16 pollen by 87 ± 12 % ($P=0.009$, **) and by 62 ± 23 % in HZ3 pollen ($P=0.003$, **). As shown in Figure 5.12, control treatment of *A. thaliana* pollen with tetrapeptide inhibitor Ac-DEVD-CHO had no significant effect on the DEVDase activity of pollen ($P=0.90$ for Col-0 pollen, grey bars; $P=0.67$ for BG16 pollen, yellow bars and $P=0.63$ for HZ3 pollen, green bars).

These data together presents the first evidence for activation of a caspase-3-like activity in PrpS₁-GFP and PrpS₃-GFP expressing *A. thaliana* pollen upon induction of SI. The PrsS induced PCD demonstrates that PrpS₁-GFP and PrpS₃-GFP are functional in *A. thaliana*.

We also wished to characterize the DEVDase activity by adding the tetrapeptide inhibitor Ac-DEVD-CHO to the pollen extracts in the assay to see if we could bring down the levels of DEVDase activity. SI was stimulated in *A. thaliana* transgenic pollen PrpS₁-GFP and PrpS₃-GFP and untransformed Col-0 control by the addition of stigmatic recombinant PrsS proteins. Following 5 h incubation, when maximal DEVDase activity was exhibited in *Papaver* pollen (Bosch and Franklin-Tong, 2007), the *A. thaliana* pollen protein extracts were made. To test the effect of caspase inhibitor on the substrate cleavage, 50 μ M peptide inhibitor Ac-DEVD-CHO inhibitor was added to the assay and DEVDase activity was measured (Figure 5.13).

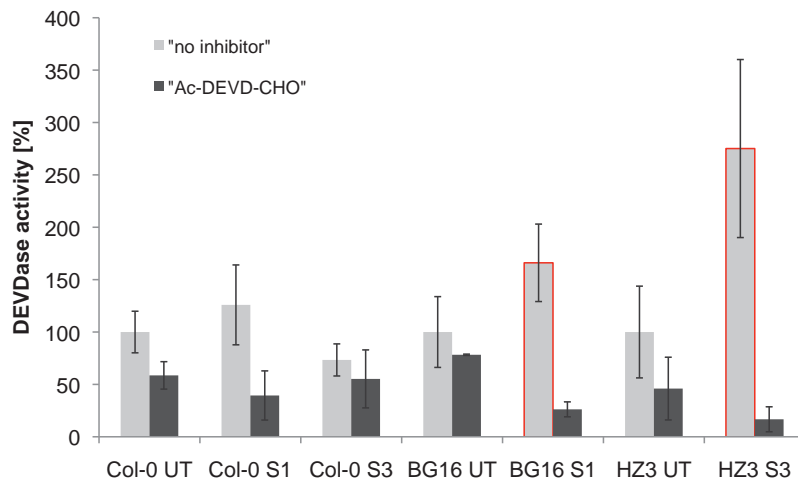


Figure 5.13.: Effect of DEVDase inhibitor on the SI induced caspase-like activity. Light grey bars present DEVDase activity in *A. thaliana* BG16B#25.1-1 and HZ3.1-15.1 pollen challenged with PrsS₁ and PrsS₃ proteins, respectively (SI challenge outlined by red line). Non-transgenic Col-0 pollen with the same challenge was used as a control. Dark grey bars show DEVDase activity of pollen extract with the additions of Ac-DEVD-CHO inhibitor in the assay. N=3 repeats. Error bars present \pm St. Error of means.

Results in Figure 5.13 show the increase of DEVDase activity by 66 % in PrpS₁-GFP expressing pollen challenged with PrsS₁ and increase by 175 % in PrpS₃-GFP expressing pollen challenged with PrsS₃. Despite the increase, the results of this preliminary experiment were not significantly different from the untreated controls (P= 0.47 for PrpS₁ and 0.21 for PrpS₃). However, when the inhibitor Ac-DEVD-CHO was used in the assay, the activity was reduced, indicating the activated caspase-3-like DEVDase activity. DEVDase activity was decreased significantly with the addition of the inhibitor Ac-DEVD-CHO in PrpS₁-GFP and PrpS₃-GFP expressing pollen that had SI induced, indicating that the PrsS-PrpS interaction stimulates high DEVDase activity in transgenic *A. thaliana* pollen.

As our data indicate, DEVDase activity could be decreased, however, the results were not significant. Experiment was repeated only three times so it might be possible that with more repeats and higher protein concentration we could observe significant response.

5.2.3. *A. thaliana* mesophyll protoplasts expressing PrpS₁

The previous sections demonstrated that PrpS₁-GFP and PrpS₃-GFP were functional in pollen of transgenic *A. thaliana*. Preliminary experiments were conducted to explore whether *Papaver* PrpS₁ receptor could be functional in other tissues as well. This would demonstrate that for a functional SI response, just PrpS and PrsS were required, while the downstream components required for the characteristic SI response were already present in the host cell.

These initial preliminary studies were done using *A. thaliana* mesophyll protoplasts as they offer versatile cell-based system. Initially, *A. thaliana* BG3, stable transformant line was used, expressing PrpS₁ under the control of 35S promoter. Using RT-PCR the presence of PrpS₁ mRNA was confirmed in three weeks old BG3 seedlings, however, the signal for

expression of the functional protein using western blot was not possible to detect. However, if the protein was expressed than it should be somehow responding to the recombinant PrsS₁. We attempted a series of experiments trying to capture the response between two determinants: immunolocalisation, viability and caspase activity assay, but no response was detected. There could be various reasons for this:

1. PrpS₁ protein might not be expressed in high enough levels in BG3 protoplasts and young seedlings.
2. If it was expressed it might not be properly folded and therefore not functional.
3. It might be expressed in a very low concentration and it might not be expressed in all the cells of seedlings.

Therefore we decided to use a system of transient DNA expression in *A. thaliana* non-transgenic Col-0 mesophyll protoplasts. We transfected Col-0 protoplasts with 35S:PrpS₁-GFP, so the transfected protoplasts could be visualised by detecting GFP reporter gene and the response to PrsS₁ would be anticipated. Following transfection protocol (see materials and methods) we isolated Col-0 protoplasts and transfected them with 35S:PrpS₁-GFP. The transfection rates were very low, between 10-19 %, however the GFP signal was observed and detected (see Figure 5.14).

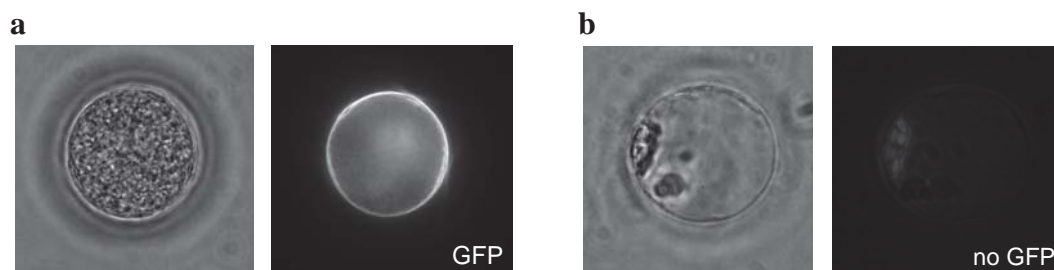


Figure 5.14: GFP expression in Col-0 protoplasts transformed with 35S:PrpS₁-GFP. (a) protoplasts expressing GFP on the right, left is brightfield image; (b) protoplasts with no GFP expression on the image on the right, left represents brightfield image of the same protoplast. The experiment was done together with Dr. Javier-Andres Juarez-Diaz.

Using transformed Col-0 protoplasts we measured the viability of Col-0 35S:PrpS₁-GFP protoplasts that were incubated with recombinant PrsS₁ proteins at three time points: t₀, 24h and 48h. As a control we used Col-0 protoplasts transfected with H₂O. The preliminary experiment was repeated twice and viability was measured using 0.05 % Evans Blue. Results are presented on Figure 5.15.

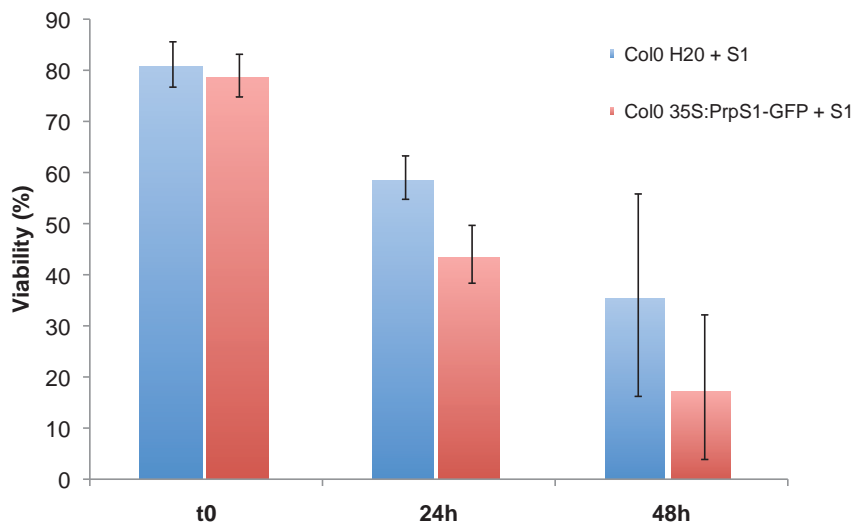


Figure 5.15: Viability of *A. thaliana* Col-0 protoplasts transfected with 35S:PrpS₁-GFP (red bars) and H₂O control (blue bars), incubated with recombinant PrsS₁. Error bars represent \pm St. Deviation. N=2

At t₀ the viability of Col0 - 35S:PrpS₁-GFP and H₂O control was around 80 %. After 24h the average viability of the control was 60 \pm 4 % and the viability of PrpS₁-GFP expressing protoplasts was 44 \pm 6 %. The viability after 48h was 36 \pm 20 % for the control and 18 \pm 14 % for the transfected protoplasts, which was 50 % less than the control.

The preliminary experiments indicate the S-specific reduction of the viability of PrpS₁-GFP expressing protoplasts upon PrsS₁ incubation. However, for more reliable and firmer conclusion, the experiments should be repeated several times.

The protoplasts were not difficult to produce but were extremely sensitive to any sort of stress from the environment and often the transformation rates were not high. So in order to

produce high quality protoplasts continuously, the protocol should be optimised further to suit the needs of our experiment (Yoo et al., 2007, Wu et al., 2009). The preliminary work has so far confirmed our hypothesis that PrpS₁-GFP could be expressed and potentially functional in other tissue. However, further work would be required on this area to provide strong, conclusive evidence. Experiments for interaction between PrpS₁-GFP expressed protoplasts and recombinant PrsS₁ proteins should be conducted, such as: examination of actin structures (preliminary experiments pointed at the problem of overlapping red signal of chloroplasts in protoplasts and rhodamine-phalloidin stained actin), changes in the viability, involvement of the caspase-like activity, examination of PCD. Protoplast system could also be used to study interaction between PrpS and PrsS.

5.3 DISCUSSION

The studies presented here demonstrate that the PrpS proteins can be functional when expressed in *A. thaliana*. Experiments focused on the use of semi-*in vitro* system by growing transgenic *A. thaliana* pollen expressing PrpS-GFP and challenging it with incompatible stigmatic recombinant PrsS proteins. Several aspects were examined, which will be discussed here.

5.3.1 Alterations to the actin cytoskeleton

In this study we have established the presence of the punctate actin foci in *A. thaliana* pollen tube expressing PrpS-GFP after 3 h challenge with incompatible PrsS recombinant protein.

Actin cytoskeleton is of vital importance for normal pollen tube growth. During the SI process in *Papaver rhoeas*, it undergoes through rapid and dramatic alterations (Geitmann et al., 2000, Snowman et al., 2002, Poulter et al., 2008, Poulter et al., 2010a). First changes of actin depolymerisation were observed as early as 1-2 min (Snowman et al., 2002) and after 3 h stable punctate actin foci were observed (Geitmann et al., 2000, Snowman et al., 2002).

Results presented in this study show that controls challenged with compatible or heat denatured PrsS proteins resulted in the same display of bundled actin filaments as untreated BG16 pollen or as non-transgenic pollen. It was also demonstrated that PrsS proteins, that were added to the untransformed pollen had no effect on the actin cytoskeleton. Although some intermediate actin structures (filaments-foci) or no structures at all were also observed, their presence was significantly lower than the filaments. The restriction of the staining technique was mostly in uneven staining of the large heterogeneous pollen population. Although the sample was mixed when the staining (or permeabilization, fixative, or treatment) was added, the pollen settled to the bottom of the tube, and consequently each of the pollen grains and tubes were unevenly exposed to the media. Mixed pollen population was unavoidable, as we needed to collect enough pollen to compensate for its losses during the washing steps of the protocol. Great precaution was taken with the experimental procedure and with collecting the same stage flowers from healthy *A. thaliana* plants.

The cytoskeleton in *A. thaliana* pollen tubes was only disturbed upon the challenge of PrpS₁ or PrpS₃ expressing pollen with its cognate incompatible PrsS₁ or PrsS₃ recombinant protein, respectively. Foci were quantified in PrpS₁ expressing BG16 pollen where they were present in majority of all analysed pollen. This suggests that functional interaction between biologically active PrsS protein and its cognate PrpS receptor was required for the disruption of the actin cytoskeleton in pollen. Therefore, the punctate actin foci that we observed in the

transgenic *A. thaliana* model upon the interaction between PrpS₁-GFP and PrsS₁ represents an important landmark in exploring *Papaver* SI system in other species.

The next step with the actin cytoskeleton would be to characterise the temporal dynamics, composition and formation of the punctate actin foci in order to investigate how closely it resembles the well-characterised poppy SI response, where reorganisations are observed as early as 1-2 min post SI. Another aspect of SI induced actin cytoskeleton remodelling, that was not investigated in this study, were the ABPs involved in regulating these modifications, such as CAP and ADF, and were demonstrated and analysed in *Papaver* pollen (Poulter et al., 2010a). It would be also interesting to know whether there was a crosstalk between microtubules and microfilaments (Poulter et al., 2008) and also link between actin depolymerization and PCD (Thomas et al., 2006) should be explored further in incompatible *A. thaliana* pollen.

Our studies, conducted in transgenic *A. thaliana*, a model for *Papaver* SI, reported for the first time, that reorganisations of the actin cytoskeleton occurred upon PrsS interaction with PrpS-GFP in *A. thaliana* and the appearance of characteristic punctate actin foci was confirmed. In a self compatible *A. thaliana*, that is a more closely related to Brassicaceae than Papaveraceae, this might seem surprising but it suggests, that just PrpS and PrsS are required for the SI response. However, the recent advances in the research on the SI induced actin reorganisations in different systems suggest, that there might be a parallel between the mechanistically different SI systems and that the SI systems could be more conserved than known so far, which would put our research of two evolutionary distant species into perspective (Liu et al., 2007c, Iwano et al., 2007, Wang et al., 2010, Poulter et al., 2011).

5.3.2. Decrease of viability involving DEVDase activity

Pollen viability was examined in PrpS₁ and PrpS₃ expressing *A. thaliana* pollen, and in non-transgenic pollen and *Papaver* S₁ and S₃ pollen that were used as a control, using Evans Blue dye due to the overlap of the signal from FDA stain and GFP in transgenic pollen tubes. However, many investigations on PCD processes in plants utilize Evans Blue dye as a tool to assess cell death levels, for example, the investigation of the kiss-of-death (KOD)-induced PCD or UV and H₂O₂ induced PCD in *A. thaliana* (He et al., 2007b, Blanvillain et al., 2011). Evans Blue dye quenches the fluorescent GFP signal, therefore the imaging of Evans Blue staining and corresponding GFP fluorescence of the same pollen tube was not possible. The GFP expression would be very informative, especially initially, with the pollen from the heterozygous lines, where we could directly compare the GFP fluorescence in PrpS-GFP expressing pollen and how it is affected during the interaction between PrpS and PrsS.

Papaver pollen viability decreased to 7 % as previously reported by (Jordan et al., 2000), while the viability of *A. thaliana* pollen decreased to 30 %, which was significant decrease. The compatible stigmatic PrsS recombinant proteins had no effect on the integrity of transgenic pollen membrane. We also established that only biologically active incompatible PrsS₁ (with BG16 pollen) or PrsS₃ (with HZ3 pollen) proteins can trigger the decrease in the membrane integrity as heat denatured version did not affect pollen viability, which remained same as in untreated pollen. So, the decrease in the membrane integrity of pollen and therefore loss of viability occurred in an S-specific manner upon the interaction between PrpS-GFP and PrsS.

We examined viability after 24 h incubation. Control pollen viability was around 50 %, while the viability of SI induced PrpS₁-GFP or PrpS₃-GFP pollen decreased for further 50

% . Lower viability in pollen from homozygous lines was expected earlier, considering rapid inhibition of pollen tubes and homozygous state of pollen used. There can be several possible explanations for this: *A. thaliana* pollen could retain membrane integration and therefore viability for longer period of time, suggesting that the “SI” in *A. thaliana* is acting slower. On the other hand, data, that 50 % of control pollen tubes remained viable for 24 h was not surprising as (Fan et al., 2001) also reported that *A. thaliana* pollen tubes exhibit clear cytoplasmic streaming after 24 h incubation and even 36 h, although not all pollen tubes were healthy. In conclusion, our data presented indicate that *S*-specific interaction between PrpS and PrsS results in cell death of transgenic *A. thaliana* pollen expressing PrpS₁-GFP and PrpS₃-GFP fusion proteins, respectively.

Thomas and Franklin-Tong, (2004) reported for the first time that SI interaction in *Papaver* triggers PCD. They pretreated incompatible pollen with DEVDase inhibitor and measured pollen tube length. They demonstrated that Ac-DEVD-CHO alleviates pollen tube inhibition that is consequence of SI response and that pollen tube growth was recovered with the use of the caspase-3 inhibitor. Our results also indicate, that the SI induced decrease in viability could provide a link with DEVDase activity in *A. thaliana* pollen. PrpS₁-GFP or PrpS₃-GFP expressing *A. thaliana* pollen was challenged with PrsS₁ or PrsS₃, respectively, and stimulated SI response, which resulted in significantly decreased pollen viability. When pollen was pretreated with the inhibitor of the caspase-3 activity, Ac-DEVD-CHO, the viability was significantly higher in BG16 and HZ3 *A. thaliana* pollen. The results confirmed that poppy PrpS can be functional in *A. thaliana* pollen at least “*in vitro*”.

5.3.3. PCD in *A. thaliana* transgenic pollen

The data presented in the Section 5.4. indicates, that *Arabidopsis* transgenic pollen expressing PrpS₁-GFP or PrpS₃-GFP fusion proteins triggered PCD upon SI interaction. We analysed SI-mediated PCD in transgenic *A. thaliana* pollen further by investigating the role of the caspase-3-like activity. Jordan et al., (2000) demonstrated DNA degradation in incompatible *Papaver* pollen and the complete evidence for the PCD was provided by (Thomas and Franklin-Tong, 2004) with the study utilising caspase-3 inhibitor Ac-DEVD-CHO. In their study they also demonstrated SI-specific release of cytochrome-c into cytosol from mitochondria and PARP cleavage activity. Bosch and Franklin-Tong, (2007) took investigations of PCD in *Papaver* further. They widened their investigation by examining the involvement of other caspase-like activities in *Papaver* SI. They also provided a temporal profile on the caspase-3-like activity by imaging live cell activity with the use of specific probe CR-(DEVD)₂. The caspase-like activities in their study were measured by utilising a specific fluorescent probes, attached on the tetrapeptide, specific for caspase cleavage. In addition to DEVDase activity, VEIDase, LEVDase and YVADase activities were also identified (Bosch and Franklin-Tong, 2007, Bosch et al., 2010).

We investigated PCD in *A. thaliana* pollen by measuring DEVDase activity upon cleavage of the AMC tagged tetrapeptide DEVD (Ac-DEVD-AMC) and identified caspase-3-like activity that was highly increased when the transgenic pollen expressing PrpS₁-GFP or PrpS₃-GFP was incubated with PrsS₁ or PrsS₃ recombinant proteins. This activity was alleviated when pollen was pretreated with caspase-3 inhibitor Ac-DEVD-CHO prior to the SI induction. However, the basal DEVDase activity was observed in the control pollen and

for firmer statistical data the experiment should be repeated with higher pollen protein concentration.

In order to confirm that the transgenic *A. thaliana* system, expressing *Papaver* PrpS proteins, has the same downstream elements as poppy pollen, analysis of other caspase-like activities that were identified in *Papaver* would be beneficial (Bosch and Franklin-Tong, 2007, Bosch et al., 2010). For the investigation of the detailed temporal profile of caspase-3-like activity in incompatible transgenic *A. thaliana* pollen, live cell imaging could be applied using probe CR(DEVD)₂.

Characterization and functional analysis of transgenic *A. thaliana*, presented in this chapter, has confirmed that *Papaver* S-locus determinants can be transformed into *A. thaliana* and that hallmark features of *Papaver* SI are exhibited in *A. thaliana* pollen expressing fusion proteins PrpS-GFP. The demonstrated hallmark features, that were observed upon *in vitro* SI challenge of *A. thaliana* pollen expressing PrpS-GFP and cognate stigmatic PrsS recombinant protein, were pollen tube growth inhibition, formation of punctate actin foci, decrease of viability and increase in DEVDase activity.

Until recently, SI induced alterations to actin cytoskeleton, production of ROS and PCD were characteristic for SI in *Papaver*, but recently they were reported from another SI system – S-RNase induced SI in *Pyrus pyrifolia* pollen (Liu et al., 2007c, Wang et al., 2010). The SI induced alterations to actin cytoskeleton were not reported so far in the *Brassica* pollen upon SI interaction, however the study conducted by (Iwano et al., 2007) reported the SI induced actin alterations in the stigmatic papillae cells in *Brassica*. These data indicates that downstream events of SI, such as the alterations to the actin cytoskeleton, ROS production

and PCD, might be more conserved in different species than known so far, despite the evolutionary difference between the species. A possible hypothesis is that downstream events observed in *Papaver* upon the incompatible interaction between PrpS and PrsS (e.g. Ca^{2+} influx and signaling, alterations to actin cytoskeleton and PCD) are the conserved and “primitive” signalling mechanisms that were used in response to convey a message and form a quick inhibitory response in plant cells. Plant-pathogen interaction and SI are examples of such stressful situations where a response to prevent the further growth of the cell is required very quickly. So it is possible that these mechanisms were used initially in many Angiosperms and *Papaver* kept it in this “basic” form to prevent self-fertilization, while other species evolved and refined ways by adding other signalling components to achieve the same result. However, that basic mechanism might be still conserved in plants and might be utilized again upon the interaction between cognate PrpS-PrsS pair. It would be interesting to know more specifically if this receptor-ligand interaction could work in plant somatic cells as well or maybe even in mammalian cells and it would be also interesting to see with other components of receptor-ligand signalling (e.g. SCR-SRK in *Brassica*) if they also trigger this basic response leading to inhibition of cell growth and cell death in other species. If the poppy SI-like mechanism of self-pollen inhibition in *A. thaliana* could be demonstrated as well *in vivo*, it would be very useful tool for further studies related to SI. The *Papaver* SI-like system would be useful to initiate studies in crop species as it would represent a novel way to prevent self-fertilization, which is an obstacle for successful plant breeding.




CHAPTER 6

**Functional analysis *in vivo* of transgenic *A. thaliana*
expressing *Papaver* S-determinants, PrsS and PrpS**

6.1 INTRODUCTION

Papaver female *S*-determinant PrsS gene and whole *S_I*-locus were introduced into *A. thaliana* using *Agrobacterium* transformation. The transformation of the *S_I*-locus was carried out by Barend de Graaf (line BG6) and transformation of PrsS₁ and PrsS₃ by Huawen Zou (lines HZ1 and HZ2). This chapter describes the characterization of transgenic *A. thaliana* lines expressing PrsS₁ (HZ1), PrsS₃ (HZ2) and *S_I*-locus as well as *in vivo* functional analysis using PrsS₁ and PrsS₃ expressing plants and pollen from transgenic *A. thaliana* expressing PrpS₁-GFP and PrpS₃-GFP, described in previous chapter. The constructs are presented in Table 6.1.

Table 6.1: Cartoon illustrates the constructs of the poppy SI determinants that were used for *Agrobacterium* mediated transformation into *A. thaliana*.

Gene	Resistance Marker	Name	Construct
PrsS ₁	Basta	HZ1	
PrsS ₃	Basta	HZ2	
<i>S_I</i> -locus	Kan	BG6	

To achieve tissue specific expression of the female *S*-determinants PrsS₁ and PrsS₃ Stig1 promoter from *N.tabacum* was used and for expression of *S_I*-locus native poppy promoter was used. Kanamycin (Kan) resistance cassette was used as a selection marker with *S_I*-locus expressing transformants BG6 and Basta resistance was used for selection of the PrsS expressing *A. thaliana*.

In order to analyse PrsS expressing transgenic *A. thaliana* lines *in vivo* and semi *in vitro* approaches were used. *Papaver*-like SI was analysed *in vivo* in *A. thaliana* in order to determine whether *Papaver* *S*-genes can be fully functional in *A. thaliana*. The functionality of the inserted PrsS and PrpS in *A. thaliana* were tested *in vivo* by pollinations assays and crosses for seed set. For this, T₃ generation of transgenic *A. thaliana* lines HZ1.1-3.1 and HZ1.8-2.1 flowers expressing PrsS₁, and HZ2.6-1.1 and HZ2.13-5.1 expressing PrsS₃ were used as females, and lines BG16B#25.1-1 and HZ3.1-15.1, expressing PrpS₁ and PrpS₃, respectively, were used as pollen donors. Scheme of crosses can be seen on Figure 6.1. Incompatible response was expected with PrsS₁ expressing stigma that was pollinated with PrpS₁-GFP expressing pollen, and PrsS₃ expressing stigma, pollinated with PrpS₃-GFP expressing pollen. Controls were comprised of compatible crosses, e.g. PrsS₁ stigma pollinated with PrpS₃ pollen or PrsS₃ stigma pollinated with PrpS₁ pollen. Pollen functionality was tested by using Col-0 stigma as female, and PrpS₁ or PrpS₃ expressing pollen as male, while the receptiveness of the PrsS₁ or PrsS₃ expressing stigmas was tested by pollinations with Col-0 pollen. Following the emasculation and pollination, stigmas were either collected in aniline blue for the analysis of pollen tube growth or left to develop on the plant for the analysis of the seed set.

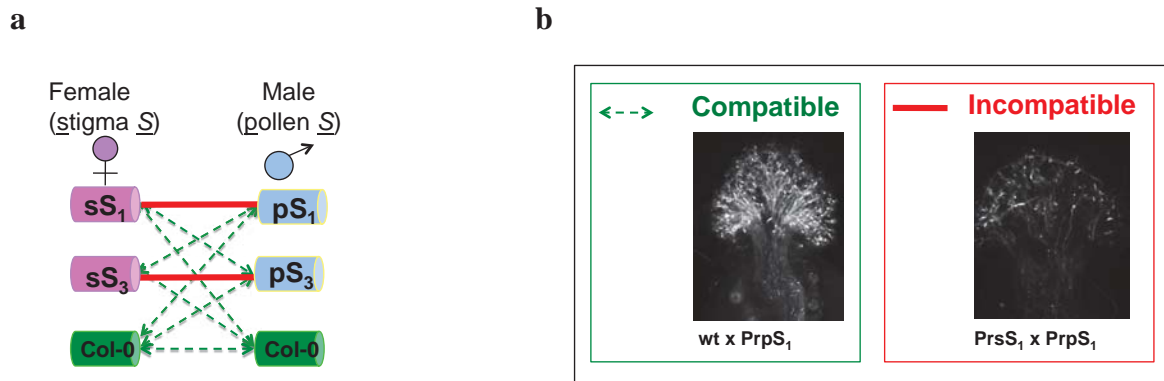


Figure 6.1.: (a) Scheme of combination of crosses in transgenic *A. thaliana* expressing different *Papaver S*-determinants. Transgenic lines expressing female determinants (PrsS) are labelled in pink (lines HZ1.8-2.1 and HZ1.1-3.1 expressing PrsS₁, and HZ2.6-1.1 and HZ2.13-5.1 expressing PrsS₃), lines expressing male determinants (PrpS) are in blue (lines BG16#25.1-1, BG16#25.1-1.1 and BG16#19.8-3 expressing PrpS₁, and lines HZ3.1-15.1, HZ3.1-15.1-1 and HZ3.1-3.1-2 expressing PrpS₃), while non-transgenic Col-0 is in green. Predicted incompatible crosses are connected with solid red line and predicted compatible crosses are connected with thinner dashed green line (b) illustration of the predicted outcome in the pollen tube growth, stained with aniline blue. Compatible cross is outlined with green, incompatible cross is outlined with red.

When conducting emasculations, the stage of stigma was crucial. The stigma had to be mature with the anthers just below the upper part of gynoecium so that it was not in contact with the self-pollen. This was normally achieved in stage 12, which was described by Smyth et al., (1990), as the stage where petals level with stamen. (Nasrallah et al., 2002) also reported that transgenic *A. thaliana*, ecotype Colombia, exhibiting *A.lyrata* SRKb/SCRb, was exhibiting transient SI that varied with the age of flowers. Young flowers in stage 12 and older flowers in late stage 14 were self-compatible, whereas stigmas in stage 13 and early 14 exhibited SI.

For our assays, pollen free stigmas were collected at the stage 12, when stigmas were receptive but before the pollen grains were mature. For pollination assays, following emasculations, pistils were excised and placed on a layer of 0.5 % agar to mature over night. The following day, stigmas reached the optimal biological stage 13 (or early stage 14) and they were manually pollinated with hundreds of pollen grains obtained from the mature post-anthesis flowers from PrpS-GFP expressing plants (or controls) and collected in aniline blue

16 h after pollination. For the seed set analysis, pistils were left on the plant to develop the siliques, which were collected before shedding seeds.

6.2. RESULTS

6.2.1. Characterization of *A. thaliana* expressing *Papaver* PrsS determinants

The primary goal was to analyse the PrsS expression of transgenic *A. thaliana* lines expressing PrsS₁, PrsS₃ or PrsS₈ under the control of Stig1 promoter. It was expected that the promoter would direct specific expression of PrsS at high levels in stigmatic tissue. No reporter gene was tagged with the PrsS, so the analysis relied upon the segregation of the resistance marker Basta and on the PCR analysis.

Seedlings of *Arabidopsis*::PrsS were initially screened by spraying Basta and only the plants containing the PrsS transgene were expected to survive. For the segregation analysis, seedlings were grown in MS medium containing Basta (see Materials & Methods) and resistant and non-resistant seedlings were counted. Heterozygous plants were expected to segregate in Mendelian fashion, while homozygous plants were expected to be 100 % resistant on the Basta containing media. The aim of the analysis was to identify the homozygous PrsS-expressing *A. thaliana* lines with the highest expression of the transgene.

PCR screening for the presence of inserts was performed initially on the leaves of young plants, using gene specific primers, as described in the Materials and Methods. The plants that were positive for the insert were selected for the analysis of the transcript by RT-PCR.

Figure 6.2. presents the RT-PCR results on HZ1 line expressing PrsS₁ and HZ2 line expressing PrsS₃.

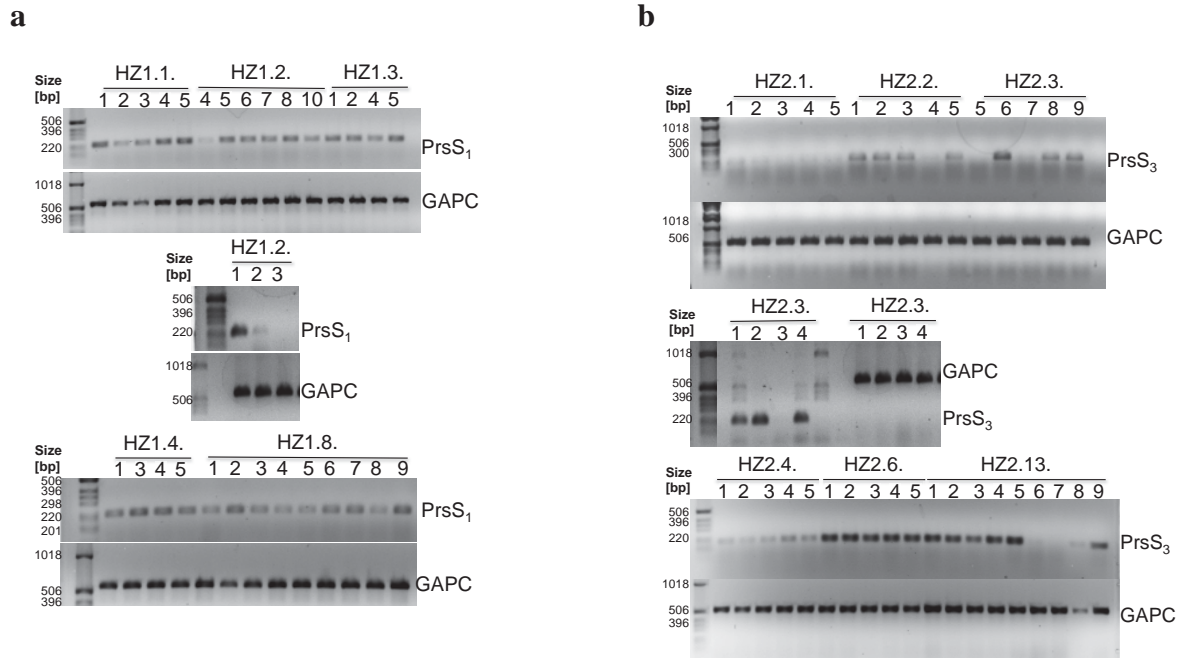


Figure 6.2.: (a) PrsS₁-expressing plants that were positive for inserts were analysed by RT-PCR to identify the highest expressers (lines HZ1.1, HZ1.2, HZ1.3, HZ1.4, HZ1.8). (b) PrsS₃-expressing plants that were positive for inserts were analysed by RT-PCR to identify the highest expressers (lines HZ2.1, HZ2.2, HZ2.3, HZ2.4, HZ2.6, HZ2.13). With the RT-PCR reactions GAPC was used as a standard (lower part of each image). Reactions with Col-0 DNA and without DNA were used as a negative control.

PrsS₁ insert was detected in 55 progenies out of 65, which showed a ~6:1 segregation ratio. The PCR product size with designed primers was 225 bp. The RT-PCR analysis was performed on 33 progenies with the insert confirmed by PCR on genomic DNA (Figure 6.2.a). Transcription of the PrsS genes were lower compared to the GAPC used as standard, and in the line HZ1.2.3, no band was detected, which could mean that the plant was not expressing PrsS₁ or that the expression was below the level of detection.

With the PCR genotyping of 38 plants for PrsS₃ insert in transgenic *A. thaliana*, 33 were found to be expressing *PrsS₃* transgene which resulted in a ~ 6:1 segregation ratio. The

product size using primers was 196 bp, which is as expected. Flowers from all the plants were analysed by RT-PCR for the relative expression of PrsS₃ (Figure 6.2.b).

The functional analysis was only performed on the highest expressing PrsS₁ and PrsS₃ expressing lines HZ1 and HZ2, so the further selection of 5 samples was made initially, by quantifying the intensity of the bands using ImageJ software (see Figure 6.3). cDNA samples of plants HZ1.1-1, HZ1.1-2, HZ1.1-3, HZ1.3-5 and HZ1.8-2 from PrsS₁ expressing flowers, and HZ2.6-1, HZ2.6-2, HZ2.6-5, HZ2.13-5 and HZ2.13-8 from PrsS₃ expressing flowers were further re-analysed on the DNA gel and compared to the GAPC control (Figure 6.3.a).

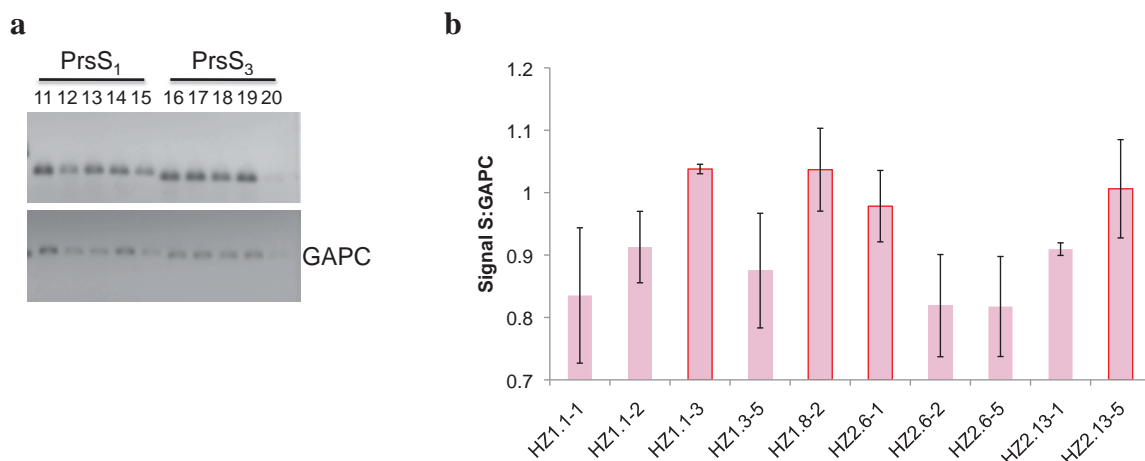


Figure 6.3.: (a) Top 5 highest expressing PrsS₁ and PrsS₃ plants, and the corresponding GAPC control (bottom). Legend: 11-HZ1.1-1, 12-HZ1.1-2, 13-HZ1.1-3, 14-HZ1.3-5, 15-HZ1.8-2, 16-HZ2.6-1, 17- HZ2.6-2, 18-HZ2.6-5, 19-HZ2.13-5, 20-HZ2.13-8. (b) Column chart presenting ratio between transgene signal of PrsS and GAPC signal. Quantification was performed using ImageJ software. The highest expressors outlined in red.

In order to quantify the expression of the transgene, the peak band intensity was measured using ImageJ software for each sample and its GAPC control (Figure 6.3.b). From each transgenic line, two plants with the highest expression identified by the intensity ratio were used in subsequent functional experiments. The apparent highest expressing lines were:

HZ1.1.-3 and HZ1.8-2 expressing PrsS₁, and HZ2.6-1 and HZ2.13-5 expressing PrsS₃. The progeny of these plants were used in further experiments to determine whether the PrsS was functional when expressed in *A. thaliana* stigma and the family trees are presented in the Appendix II.

Basta selection by spraying was used initially and later the Basta herbicide was used as a selection with the MS medium. To confirm the homozygous lines by Basta resistance in the medium, only lines that were chosen as the highest expressors were selected (Figure 6.3.). Those were lines HZ1.1.-3 and HZ1.8-2 expressing PrsS₁, and HZ2.6-1 and HZ2.13-5 expressing PrsS₃. The results of the segregation analysis are presented in Tables 6.2 and 6.3.

Table 6.2: Segregation of Basta resistance in progenies of transgenic *A. thaliana* lines expressing *Papaver* stigma determinant PrsS₁. Statistical analysis was performed using Chi square analysis. HO – homozygous

Seeds (PrsS ₁)	Generation	Basta ^R	Basta ^S	N	Ratio	χ^2 (3:1)
HZ1.1	T ₁	16	2	1	8:1	1.85
HZ1.1-3	T ₂	19	1	1	19:1	4.27
HZ1.1-3.1	T ₃	63	0	2	HO	21
HZ1.1-3.1-x	T ₄	76	0	2	HO	25.3
HZ1.8	T ₁	6	5	1	1.2:1	2.45
HZ1.8-2	T ₂	31	0	1	HO	10.3
HZ1.8-2.1	T ₃	61	0	2	HO	20.3
HZ1.8-2.1-x	T ₄	75	0	2	HO	25

Table 6.3: Segregation of Basta resistance in progenies of transgenic *A. thaliana* lines expressing *Papaver* stigma determinant PrsS₃. Statistical analysis was performed using Chi square analysis. HO - homozygous

Line (PrsS ₃)	Generation	Basta ^R	Basta ^S	N	Ratio	χ^2 (3:1)
HZ2.6	T ₁	15	6	1	2.5:1	0.14
HZ2.6-1	T ₂	11	6	1	1.8:1	0.96
HZ2.6-1.1	T ₃	47	12	2	3.9:1	0.68
HZ2.6-1.1-x	T ₄	81	12	2	7:1	7.3
HZ2.13	T ₁	15	4	1	3.8:1	0.16
HZ2.13-5	T ₂	11	0	1	HO	3.67
HZ2.13-5.1	T ₃	46	2	2	23:1	11.1
HZ2.13-5.1-x	T ₄	59	0	2	HO	19.7

The expected 3:1 segregation ratio (Basta^R:Basta^S) based on the inheritance of Basta resistance was observed only in T₁ (HZ2.6) and T₃ (HZ2.6-1.1) generation of PrsS₃ expressing *A. thaliana* (Table 6.3). In PrsS₁ expressing *A. thaliana* (Table 6.2.) it was not observed. Instead, the analysed HZ1.1 line exhibited distorted Mendelian 8:1 segregation ratio in T₁ generation (Table 6.2) and its progeny showed 19:1 ratio in T₂ generation. The line became homozygous for Basta in generation T₃. Segregation ratio of 7:1 was also observed in T₄ generation of HZ2.6-1.1.

(Page and Grossniklaus, 2002) reported that 7:1 segregation ratio is expected for the recessive mutants obtained by seed mutagenesis. However, we did not mutagenise the seeds. Another possibility (Rudolph, 1966) could be that 7:1 segregation might result from the 15:1 ratio distorted due to the lethality dependent on PrsS expression, and in next generation of HZ1.1-3 we observed increased segregation ratio, meaning we could have the insertion at two loci.

The other line selected for PrsS₁ expression showed 1:1 segregation ratio in T₁, but interestingly exhibited homozygous state already from generation T₂ onwards. HZ2.6 and HZ2.13 lines analysed showed the expected Mendelian segregation ratio 3:1 in T₁ generation. However, line HZ2.6 exhibits non-Mendelian ratios in subsequent generations: 2:1 ratio in generation T₂, 4:1 ratio in T₃ and very distorted ratio 7:1 in generation T₄. On the other hand, in the line HZ2.13 the segregation of resistance seems equally unstable, changing from generation to generation. It shows homozygous expression in T₂ and T₄ but ratio 23:1 in generation T₃. *A. thaliana* transgenic lines that were selected for further analysis based on the expression of the transcript analysed by RT-PCR were HZ1.1-3 and HZ1.8-2 expressing PrsS₁, and lines expressing PrsS₃ were HZ2.6-1 and HZ2.13-5.

Since the RT-PCR showed that PrsS₁ mRNA was specifically present in HZ1 flowers, we wished to confirm the PrsS₁ protein presence using western blot, however, it was impossible to detect any PrsS₁ signal using the 20-50 µg total protein extract and only PrsS₁ recombinant protein, expressed in *E. coli*, resulted in a very strong band (data not shown). Considering the RT-PCR detection of the PrsS₁ mRNA transcripts in transgenic *A. thaliana* flowers, the PrsS₁ protein are expressed at extremely low levels that are below detection using western blot, or the protein is not properly expressed or folded. In any case, this could explain some of the results described later in section 6.2.4 .

6.2.2. *S₁*-locus expressing *A. thaliana* line

Another important construct that was generated by Barend de Graaf included the whole *S₁*-locus from *Papaver* (both, PrpS₁ and PrsS₁ determinants at the same time) and was coupled with endogenous *Papaver* promoters for PrpS₁ and PrsS₁ (see Table 6.1). Segregation of the Kan resistance was investigated in the progeny of T₁ generation of *A. thaliana* line BG6 expressing the whole *S₁*-locus (Table 6.4).

Table 6.4.: Segregation of the kanamycin resistance in progenies of transgenic *A. thaliana* lines expressing *Papaver S₁*-locus. Statistical analysis was performed using Chi square analysis.

Line (S ₁ -locus)	Generation	Kan ^R	Kan ^S	N	Ratio	χ^2 (3:1)
BG6.1	T ₁	47	20	1	2.35:1	0.84
BG6.2	T ₁	24	22	1	1.1:1	12.8
BG6.3	T ₁	0	50	1	0:1	150
BG6.4	T ₁	0	50	1	0:1	150
BG6.5	T ₁	71	25	1	3:1	0.056
BG6.6	T ₁	0	52	1	0:1	150
BG6.7	T ₁	27	11	1	2.5:1	0.32
BG6.8	T ₁	18	32	1	0.5:1	40.6
BG6.9	T ₁	19	48	1	0.2:1	103.2
BG6.10	T ₁	4	21	1	0.2:1	46.4
BG6.11	T ₁	11	34	1	0.3:1	61.3
BG6.12	T ₁	2	48	1	0.04:1	134.4
BG6.13	T ₁	8	28	1	0.3:1	53.5
BG6.14	T ₁	16	34	1	0.5:1	49.3
BG6.15	T ₁	32	27	1	1.2:1	13.6
BG6.16	T ₁	34	16	1	2.1:1	1.31
BG6.17	T ₁	38	12	1	3:1	0.027
BG6.18	T ₁	0	57	1	0:1	150
BG6.19	T ₁	41	16	1	3:1	0.29
BG6.20	T ₁	1	47	1	0.02:1	136
BG6.21	T ₁	32	21	1	1.5:1	6.04
BG6.22	T ₁	35	19	1	1.8:1	2.99
BG6.23	T ₁	0	54	1	0:1	150
BG6.24	T ₁	0	50	1	0:1	150
BG6.25	T ₁	0	53	1	0:1	150
BG6.26	T ₁	27	29	1	1:1	21.4
BG6.27	T ₁	12	38	1	0.3:1	69.4
BG6.28	T ₁	38	21	1	1.8:1	3.53

In total, 28 original primary transformants were analysed. Seven were Kan sensitive and did not survive the selection process. The other lines exhibited various segregation ratios: four exhibited the 3:1 segregation ratio (BG6.5, BG6.7, BG6.17 and BG6.19), five lines exhibited a ratio of 2:1 (BG6.1, BG6.7, BG6.16, BG6.22 and BG6.28), only five lines exhibited the expected segregation ratio of 1:1 (BG6.2, BG6.14, BG6.15, BG6.21 and BG6.26) and seven lines exhibited a ratio of less than 0.5:1 (BG6.9, BG6.10, BG6.11, BG6.12, BG6.13, BG6.20

and BG6.27). As previously mentioned, the expected segregation ratio in fully functional BG6 line would be 1:1. If the plants were heterozygous then 50 % of pollen would be expected to express PrpS₁ and 50 % of pollen would be wt and only the wt pollen would be allowed to grow through the stigma and successfully fertilize the ovules. The pollen expressing PrpS₁ would be expected to be inhibited upon landing on the stigma expressing PrsS₁. Therefore, the expectation of a 1:1 segregation ratio, but it was found that only ~20 % of all BG6 plants exhibited this ratio.

Some plants expressing S₁-locus were analysed by RT-PCR using PrpS₁ and PrsS₁ primers. Initially, only two samples (randomly chosen showing 3:1 and 0.2:1 ratio) were analysed using PrpS₁ and PrsS₁ primers in the reaction simultaneously (Figure 6.4.a). The PrsS₁ band was detected upon analysis on the DNA gel but PrpS₁ product was not visualised. The RT-PCR was repeated using more samples with different segregation ratios, including the expected 1:1, and the primers were used in separate reactions (e.g PrsS₁ primers were used with an aliquot of RNA in one reaction, and another aliquot of RNA was used in the RT-PCR reaction using PrpS₁ primers, see Figure 6.4.b) but no PrpS₁ band was visualised and identified when analysing the PCR product by electrophoresis.

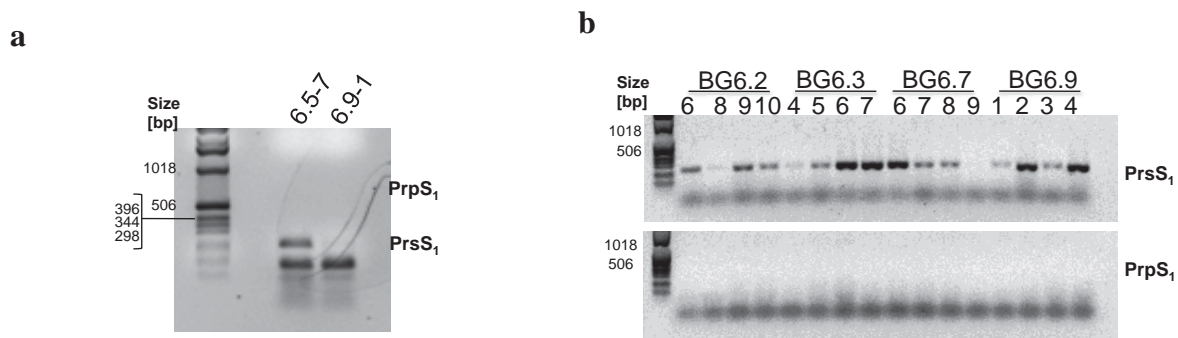


Figure 6.4.: RT-PCR expression analysis on BG6 flowers expressing whole S_1 -locus using Prp S_1 and Prs S_1 primers (a) trial analysis on samples BG6.5-7 and BG6.9-1 (top band Prp S_1 , bottom band Prs S_1) (b) analysis on samples BG6.2, BG6.3, BG6.7 and BG6.9 (top band Prs S_1 , bottom band Prp S_1).

The RNA extraction and RT-PCR test was repeated again by colleague Javier-Andres Juarez-Diaz, using primers designed over different area on Prp S_1 (Prp S_1 a.n. primers), different set of pipettes and different work space but with the same result: Prp S_1 mRNA could not be amplified from BG6 samples.

Since the RT-PCR analysis could not be used in order to identify lines with the highest transgene expression, seed set analysis was performed on all the lines from the BG6 family expressing S_1 -locus

6.2.3. *Papaver* pollen growth in the presence of stigmatic extract of *A. thaliana* expressing Prs S_1 and Prs S_3

Previous chapter presenting “*in vitro*” results demonstrated that *Papaver* PrpS proteins were functional when expressed in *A. thaliana*. The functional SI response was achieved through the interaction between recombinant stigmatic PrsS proteins and PrpS-GFP receptor expressed in *A. thaliana*. As the stigmatic PrsS proteins were also transformed to *A. thaliana*, with targeted expression in the stigma, we wished to investigate whether stigmatic PrsS proteins were functional when expressed in *A. thaliana*. To *Papaver* S_1S_3 pollen

growing in petridishes we added the stigmatic protein extract derived from transgenic *A. thaliana* flowers expressing PrsS₁ and PrsS₃ proteins, respectively. Transgenic *A. thaliana* T₄ generation plant lines were characterized homozygous in previous section, and were used for the experiment. *A. thaliana* plants from lines HZ1.1-3.1-x and HZ1.8-2.1-x were used as a source for PrsS₁ expressing stigmas, and lines HZ2.6-1.1-x and HZ2.13-5.1-x for PrpS₃ expressing stigma.

Employing this semi-*in vitro* system, “incompatible” pollen (*Papaver* S₁ and S₃ pollen incubated with stigmatic HZ1 and HZ2 extracts) should be inhibited, while pollen tube length of the control pollen (*Papaver* S₂ and S₄ pollen incubated with HZ1 and HZ2 extracts) should not be affected by the PrsS₁ and PrsS₃ expressing flower extracts. HZ1 and HZ2 stigmatic extracts were added to *Papaver* PrpS₁/PrpS₃ and PrpS₂/PrpS₄ pollen. As a positive control we induced SI response in *Papaver* pollen with recombinant stigmatic PrsS₁ and PrsS₃. In order to affirm that the effect of the PrsS expressing *A. thaliana* stigmas was due to PrsS proteins and not to other soluble proteins present in *A. thaliana* stigmatic tissue, we also challenged *Papaver* PrpS₁/PrpS₃ pollen with *A. thaliana* untransformed Col-0 stigmatic extract and left them to grow in GM only (untreated, UT). Additional controls were the heat denatured (hd) stigmatic extracts from HZ1 and HZ2 flowers and from Col-0 flower, in order to ensure that the response was due to the biologically active PrsS proteins. The S-specificity control was comprised of *Papaver* PrpS₂/PrpS₄ pollen that was incubated with stigmatic extracts from HZ1 expressing PrsS₁ and HZ2 flowers expressing PrsS₃ (i.e. a compatible allelic combinations).

Pollen was left to incubate with proteins overnight and pollen tubes were imaged and measured after 20 h incubation. *Papaver* PrpS₁/PrpS₃ pollen was inhibited by the addition of *A. thaliana* HZ1 and HZ2 stigmatic extract (Figure 6.5.e), although not as strongly as pollen

challenged with incompatible recombinant PrsS₁ and PrsS₃ proteins (Figure 6.5.b). Moreover, some pollen tube tips were affected by the HZ1 and HZ2 stigmatic extracts and some developed extremely swollen tubes and bulbous tips (Figure 6.5.e). When pollen was incubated with wild type stigmatic extracts (Figure 6.5.c) or with heat denatured HZ1&HZ2 extract (Figure 6.5.f), pollen tubes were not inhibited. There were some pollen tube tips slightly swollen, however, to lesser extent than pollen incubated with the HZ1 and HZ2 stigmatic extracts. Long pollen tubes without swollen tips were observed when HZ1&HZ2 stigmatic extracts were incubated with *Papaver* S₂S₄ pollen (Figure 6.5.i).

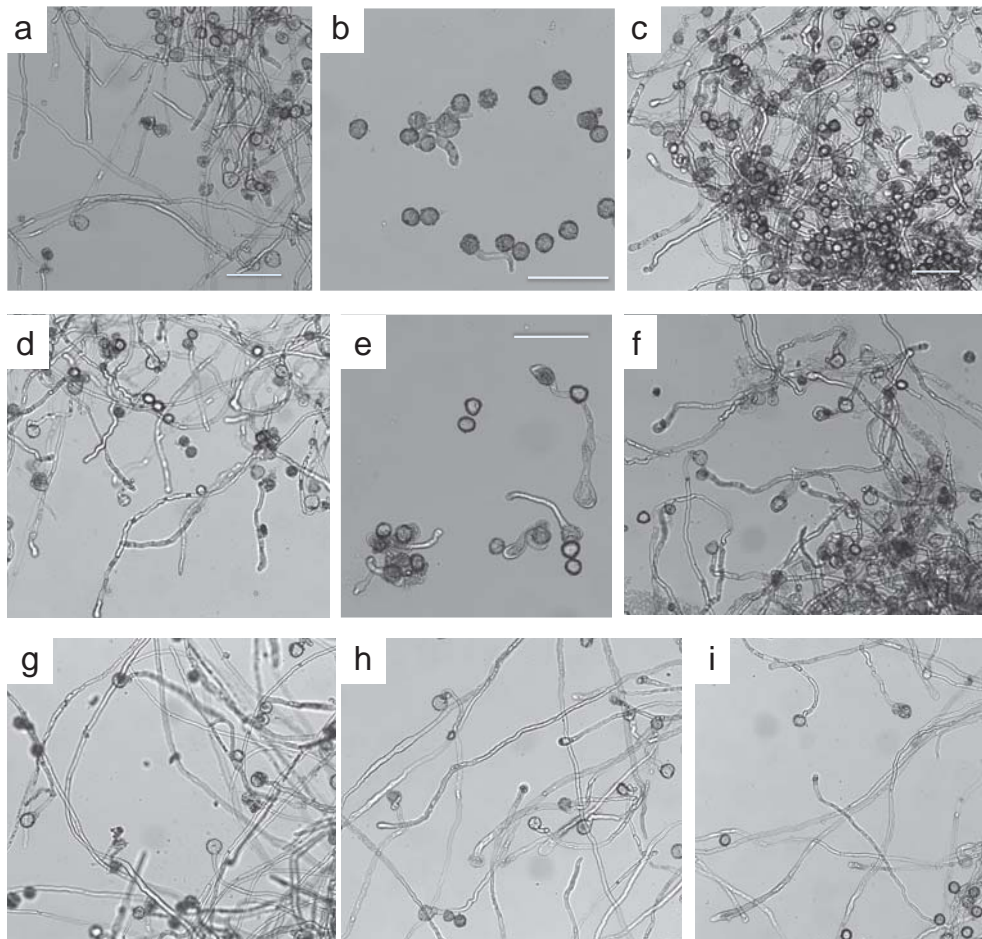


Figure 6.5: Images of *Papaver* pollen tubes incubated with stigmatic protein extracts from transgenic *A. thaliana* flowers: HZ1.1-3.1-x and HZ1.8-2.1-x flowers expressing PrsS₁, and HZ2.6-1.1-x and HZ2.13-5.1-x (a) UT *Papaver* S₁S₃ pollen; (b) *Papaver* S₁S₃ pollen incubated with recombinant PrsS₁ and PrsS₃; (c) *Papaver* S₁S₃ pollen incubated with Col-0 stigmatic extract; (d) *Papaver* S₁S₃ pollen incubated with hd Col-0 stigmatic extract; (e) *Papaver* S₁S₃ pollen incubated with HZ1&HZ2 stigmatic extract; (f) *Papaver* S₁S₃ pollen incubated with hd HZ1&HZ2 stigmatic extract; (g) *Papaver* S₂S₄ pollen UT; (h) *Papaver* S₂S₄ pollen with Col-0 stigmatic extract; (i) *Papaver* S₂S₄ with HZ1&HZ2 stigmatic extract. Scale bar represents 100 μ m.

In order to quantify the observed effects of *A. thaliana* stigmatic extracts on *Papaver* pollen we measured pollen tube length and tip diameter (see Figure 6.6). Figure 6.6.a presents the mean length of *Papaver* pollen tubes, incubated with *A. thaliana* stigmatic proteins.

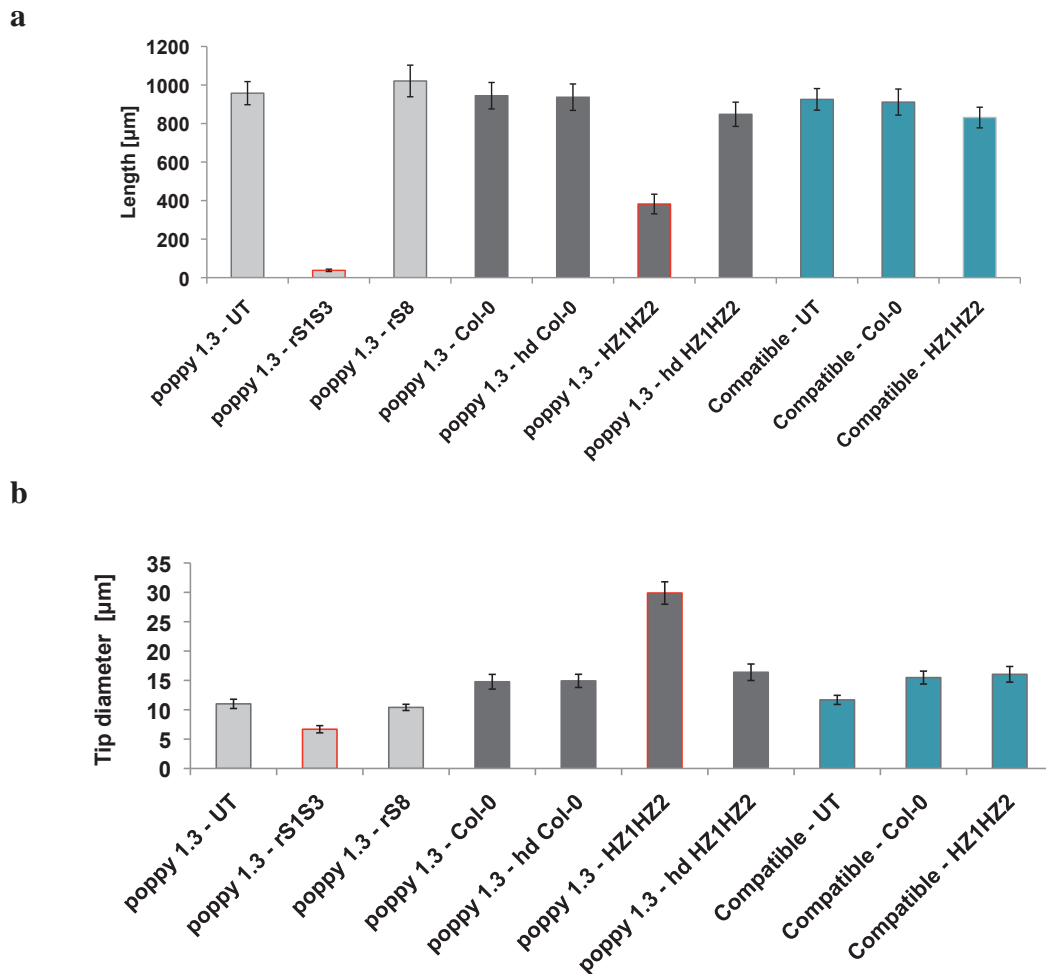


Figure 6.6: Quantification of *Papaver* pollen tube length and tip diameter upon incubation with *A. thaliana* stigmatic protein extracts (Col-0 – untransformed *A. thaliana* stigmatic protein extract, HZ1HZ2 – PrsS₁ and PrsS₃ expressing *A. thaliana* stigmatic protein extracts) and controls (a) average pollen tube length and (b) average tube tip diameter. S₁S₃ *Papaver* pollen untreated and recombinant stigmatic controls are presented with light grey bars, pollen incubated with *A. thaliana* stigmatic proteins and controls are presented with dark grey bars, while control S₂S₄ pollen is presented in teal bars. Red outline indicates incompatible interaction between pollen and pistil determinant. Error bars represent \pm St.Deviation. UT – untreated, rS8 – recombinant PrsS₈; hd – heat denatured. Some of these experiments were conducted by Javier-Andres Juarez-Diaz.

Unchallenged PrsS₁/PrsS₃ *Papaver* pollen tube length was $958 \pm 60 \mu\text{m}$, while length of pollen with recombinant PrsS₁ and PrsS₃ proteins added was $38 \pm 6 \mu\text{m}$ ($P = 2.7 \times 10^{-108}$),

N=80), which is only 4 % of untreated control. The pollen tube length of *Papaver* incubated with stigmatic protein extract from PrsS₁ and PrsS₃ expressing *A. thaliana* flowers, was reduced significantly by 60 % compared to the UT control ($P=1.1 \times 10^{-61}$, N=80) or to pollen incubated with non-transgenic stigmatic extract ($945 \pm 69 \mu\text{m}$, $P=1.3 \times 10^{-56}$, N=80), reaching average length of $380 \pm 51 \mu\text{m}$. The tip diameter of pollen incubated with stigmatic protein extract from HZ1 and HZ2 *A. thaliana* flowers (Figure 6.6.b) was significantly increased with $30 \pm 2 \mu\text{m}$ compared to $11 \pm 1 \mu\text{m}$ for untreated pollen ($P=1.9 \times 10^{-74}$, N=80) or $15 \pm 1 \mu\text{m}$ for pollen incubated with Col-0 protein extract ($P=7.0 \times 10^{-57}$, N=80). Untreated compatible poppy PrsS₂/PrsS₄ pollen reached the length of $925 \pm 56 \mu\text{m}$, which was comparable to untreated PrsS₁/PrsS₃ pollen ($P=0.25$; N=60). The length of PrsS₂/PrsS₄ pollen treated with Col-0 stigmatic extract was $911 \pm 68 \mu\text{m}$, which was not different to Col-0 treated PrsS₁/PrsS₃ pollen ($P=0.35$, N=60). However, the length of “compatible” poppy pollen incubated with HZ1 and HZ2 stigmatic extracts was $831 \pm 54 \mu\text{m}$, which was significantly different compared to HZ1 and HZ2 incubation of PrsS₁/PrsS₃ pollen ($P=1.5 \times 10^{-35}$, N=60). Quantification also revealed the significant difference between tips of compatible PrsS₂/PrsS₄ pollen incubated with HZ1 and HZ2 stigmatic extracts, with diameter of $16 \pm 1 \mu\text{m}$ and HZ1&HZ2 incubated S₁S₃ pollen ($P=3.7 \times 10^{-42}$).

These data demonstrate PrsS₁ and PrsS₃ stigmatic proteins that were expressed in *A. thaliana* stigmas under stigma specific Stig1 promoter, had an inhibitory effect on PrsS₁/PrsS₃ *Papaver* pollen in an S-specific manner. However, the interaction causes not only *Papaver* pollen tube inhibition but also some other morphological changes, like tube swelling.

6.2.4 *Papaver* SI *in vivo* in transgenic *Arabidopsis thaliana*

6.2.4.1 Pollination assays in transgenic *A. thaliana* expressing *Papaver* PrsS and PrpS

Incompatible crosses and controls were examined with a microscope. Figure 6.7 shows analysis of the highest PrsS₁ expressing *A. thaliana* lines HZ1.1-3.1 and HZ1.8-2.1. Crosses for the aniline blue staining of the pollen tube growth were conducted on *A. thaliana* plants fourteen times in total. Pollination tests were initially conducted on T₂ plants, and after the highest expressing lines were identified on T₃ plants (see Figure 6.7).

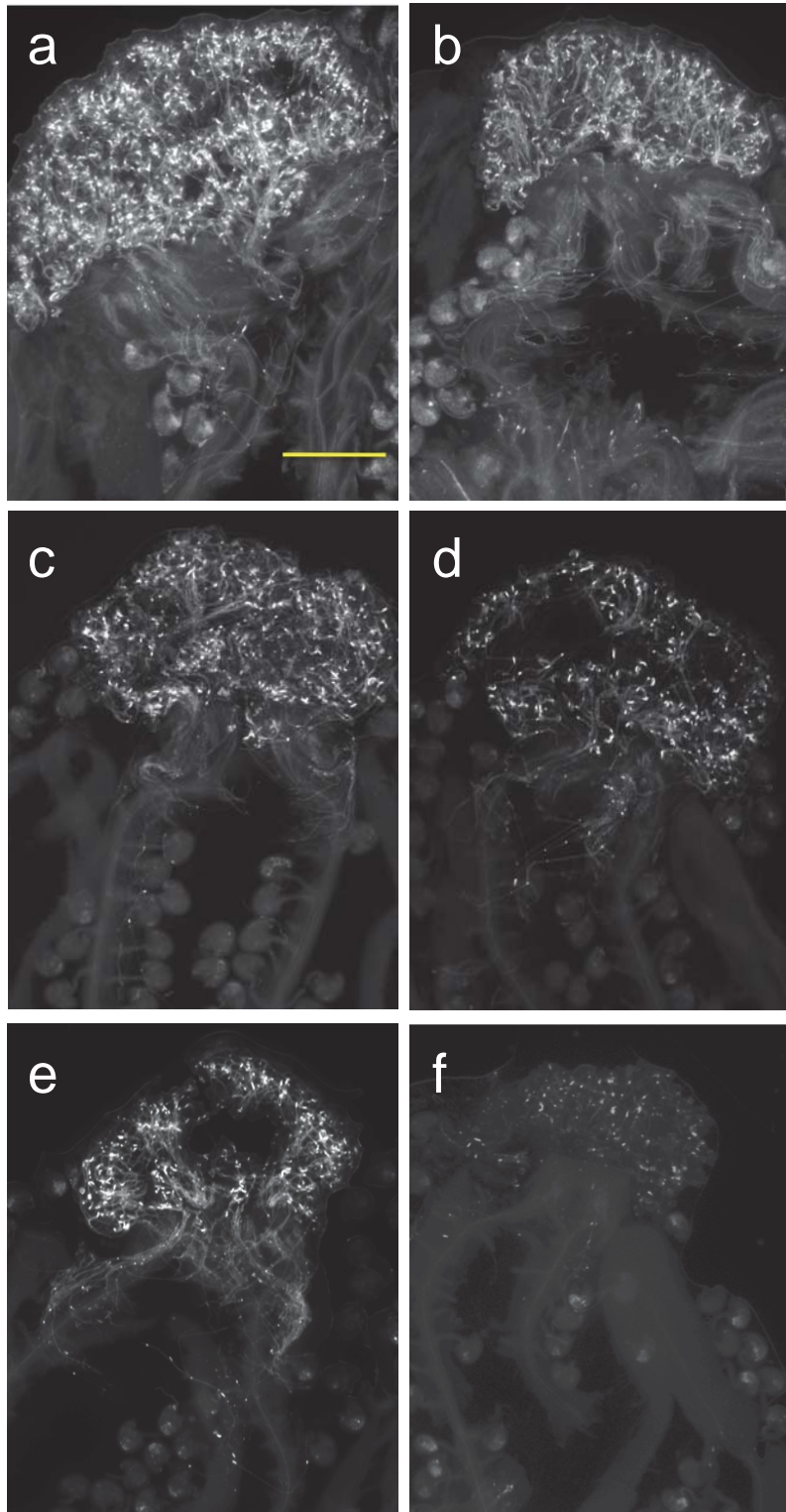


Figure 6.7.: Aniline blue staining of crosses with PrsS₁ expressing *A. thaliana* stigmas. (a) HZ1.1-3.1 x BG16#25.1-1 (PrsS₁ x PrpS₁), (b) HZ1.1-3.1 x HZ3.1-15.1 (PrsS₁ x PrsS₃), (c) HZ1.1-3.1 x HZ1.1-3.1 (PrsS₁ x PrsS₁); (d) HZ1.1-3.1 x Col-0 (PrsS₁ x Col-0); (e) HZ1.8-2.1 x BG16#25.1-1 (PrsS₁ x PrpS₁); (f) HZ1.8-2.1 x Col-0 (PrsS₁ x Col-0). Scale represents 500 μ m.

Few crosses resulted in reduced pollen tube growth but generally the incompatible crosses resulted in long pollen tube growth through the style, which could indicate that the plants were heterozygous. More likely, the pollen tube growth could be due to the weak or 'leaky' SI response. The incompatible crosses HZ1.1-3.1 x BG16#25.1-1 and HZ1.8-2.1 x BG16#25.1-1, presented in Figures 6.7.a and 6.7.e, respectively, show long pollen tube growth, which was comparable to the control and compatible pollinations. Control crosses confirmed that HZ1.1-3.1 and HZ1.8-2.1 flowers were receptive and functional (Figures 6.7.c, d & f) but did not exhibit full SI.

Preliminary investigation also examined the pollination of PrpS₃ expressing HZ2.13-5.1 and HZ2.6-1.1 flowers (see Figure 6.8) by PrpS₃ expressing HZ3.1-15.1 and non-transgenic or compatible control.

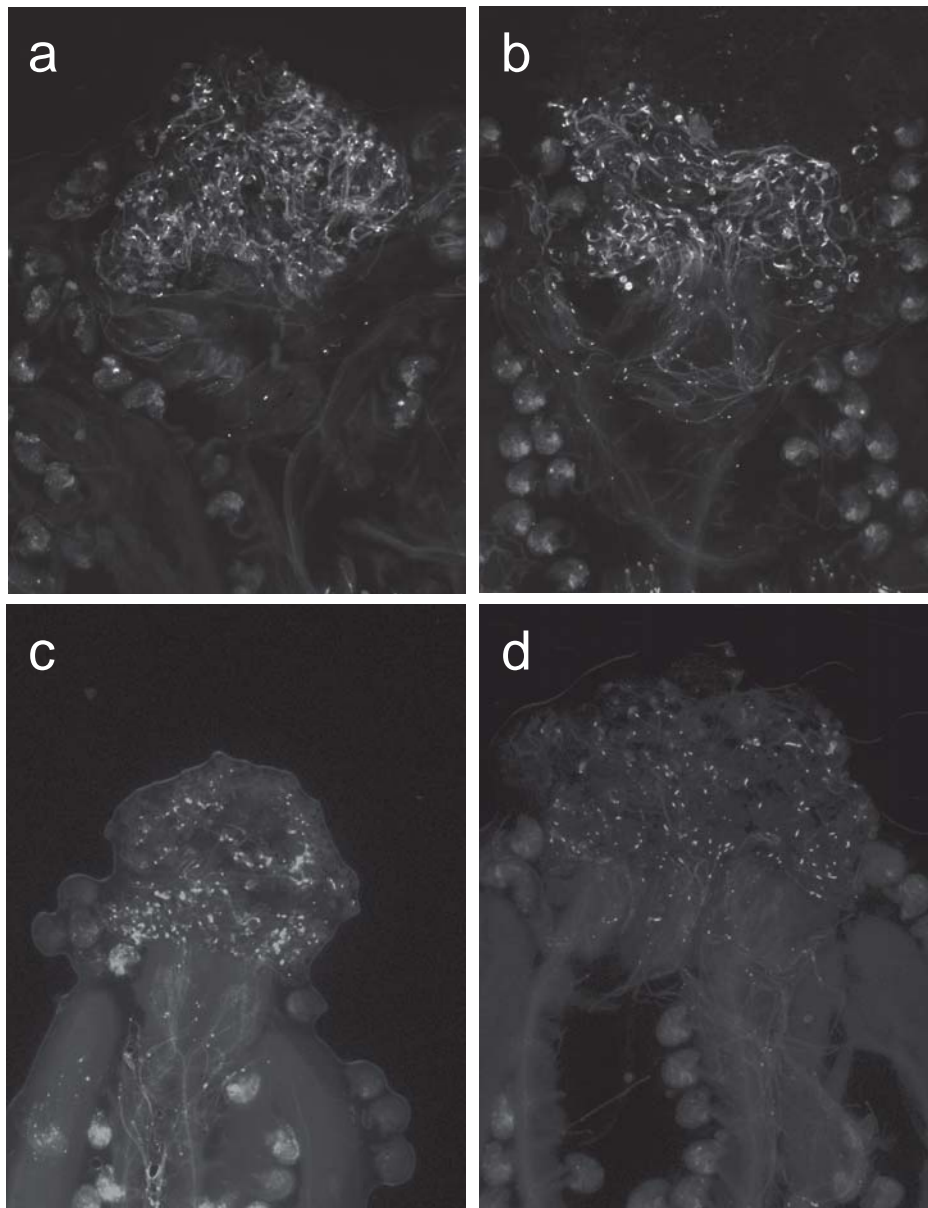


Figure 6.8: Aniline blue staining of crosses with PrsS₃ expressing *A. thaliana* stigmas. **(a)** HZ2.13-5.1 x HZ3.1-15.1 (PrsS₃ x PrpS₃) **(b)** HZ2.13-5.1 x Col-0 (PrsS₃ x Col-0); **(c)** HZ2.6-5.1 x HZ3.1-15.1 (PrsS₃ x PrpS₃); **(d)** HZ2.6-5.1 x BG16#25.1-1 (PrsS₃ x PrpS₁).

Incompatible crosses of HZ2.13-5.1 x HZ3.1-5.1 and HZ2.6-5.1 x HZ3.1-15.1, presented on figure 6.8.a and 6.8.c, respectively, exhibited compatible phenotype as there were numerous pollen tubes growing down the style.

In order to characterize the pollinations in greater detail, more systematic and quantitative analysis was proposed. However, the PrsS₁ protein signal was not detected using western blot analysis on the PrsS₁ expressing stigmatic extracts, despite the RT-PCR analysis confirmed the presence of PrsS₁ mRNA. There could be several reasons that there was no protein detected by western blot. It is possible that PrsS₁ protein was not correctly translated, not correctly targeted or it was expressed at very low concentration that was below the level of detection by western blot analysis. Therefore the inhibition of PrpS₁-GFP pollen *in vivo* did not occur. However, the results of incubation of *Papaver* S₁S₃ pollen with HZ1 and HZ2 stigmatic protein extracts indicated, that HZ1 and HZ2 expressing PrsS₁ and PrsS₃, respectively could be functional. The total protein concentration within that experiments was 100 µg mL⁻¹ but we could not quantify what proportion (if any) of that concentration was represented by properly folded, active PrsS proteins. The inhibition of *Papaver* pollen was observed, but at the same time also pollen tube swelling which could indicate that the PrsS proteins were possibly not properly folded or at very low concentration. There was also possibility that the insertion of the PrsS by transformation in *A. thaliana* caused some other transient stigmatic phenotype that could not be observed visually but affected the total stigmatic protein concentration. And finally the stoichiometry of the SI response, i.e. number of molecules of receptor and ligand required for the SI response to be triggered, also remains unknown.

6.2.4.2 Seed set analysis in transgenic *A. thaliana* expressing *Papaver* PrsS and PrpS

Seed set analysis was conducted in parallel on transgenic *A. thaliana* lines to test *Papaver* SI *in vivo*. HZ1.1-3.1 and HZ1.8-2.1 plants expressing PrsS₁ and HZ2.6-1.1 and HZ2.13-5.1 plants, expressing PrsS₃ were emasculated and pollinated with selected pollen donor to obtain: incompatible cross, reciprocal cross or other allele specific controls (see Materials and Methods). Siliques were left on the plant to develop seeds before they were collected and measured with the seed set counted. However, not all the crosses were successful, hence the discrepancy in the number of fertilized siliques.

Figure 6.9.a presents the seed set from all the individual incompatible crosses (Figure 6.9.a, red outline, yellow bars for PrsS₁ x PrpS₁ and light green bars for PrsS₃ x PrpS₃) and controls. Certain incompatible crosses resulted in smaller silique size and lower seed set (HZ1.8-2.1 x BG16A#19.8-3, HZ2.6-1.1 x HZ3.1-15.1 and HZ2.6-1.1 x HZ3.1-15.1-1), however, the majority of incompatible crosses resulted in the normal seed set, compared to compatible reciprocal crosses. Crosses were performed by Steve Price.

In order to analyze the female expressors (PrsS₁ expressing lines HZ1.1-3.1 or HZ1.8-2.1 and PrsS₃ expressing lines HZ2.6-1.1 or HZ2.13-5.1) as pollen acceptors and pollen donors, the silique length and seed set data of incompatible pollinations with the same PrsS expressing line was joined (Figure 6.9.b, red outline) and its reciprocal control for individual PrsS expressing lines (see Figure 6.9.b).

The incompatible crosses with PrsS₁ expressing *A. thaliana* stigma HZ1.1-3.1 and PrpS₁-GFP expressing BG16 pollen resulted in 29.1±12.9 seeds and silique length 16.3±2.1 mm (n=14), and were 43 % compared to its reciprocal cross with 41.6±16.2 seeds and silique

length 17.0 ± 2.4 mm ($n=11$) (see Figure 6.3.3.b, yellow bars). The seed set of this incompatible cross ($\text{PrsS}_1 \times \text{PrpS}_1$) was also 17 % when compared to the cross with Col-0 ($\text{HZ1.1-3.1} \times \text{Col-0}$), which resulted in 34 seeds ($n=1$) but 18 % higher when compared to the compatible cross $\text{HZ1.1-3.1} \times \text{HZ3}$ with 23.9 ± 8.6 seeds and silique length 14.1 ± 1.9 mm ($n=5$). PrsS_1 expressing HZ1.8.2-1 plants crossed with incompatible PrpS_1 -GFP expressing BG16 had on average 19 % higher seed set with 34.5 ± 14.3 seeds and silique length 15.1 ± 2.7 mm ($n=13$) when compared with HZ1.1-3.1 , and as well 30 % higher seed set than its reciprocal control $\text{BG16} \times \text{HZ1.8-2.1}$ with 24.7 ± 12.1 seeds and silique length 13.1 ± 3.8 mm ($n=5$). When incompatible HZ1.8-2.1 cross ($\text{PrsS}_1 \times \text{PrpS}_1$) was compared to the compatible control $\text{HZ1.8-2.1} \times \text{HZ3}$, the compatible seed set was 18 % lower with 28.3 ± 11.4 seeds and silique length 12.8 ± 2.8 mm ($n=5$). These data indicates that incompatible cross was not completely functional, indicating that transgenic *A. thaliana* might not be expressing PrsS at high enough levels.

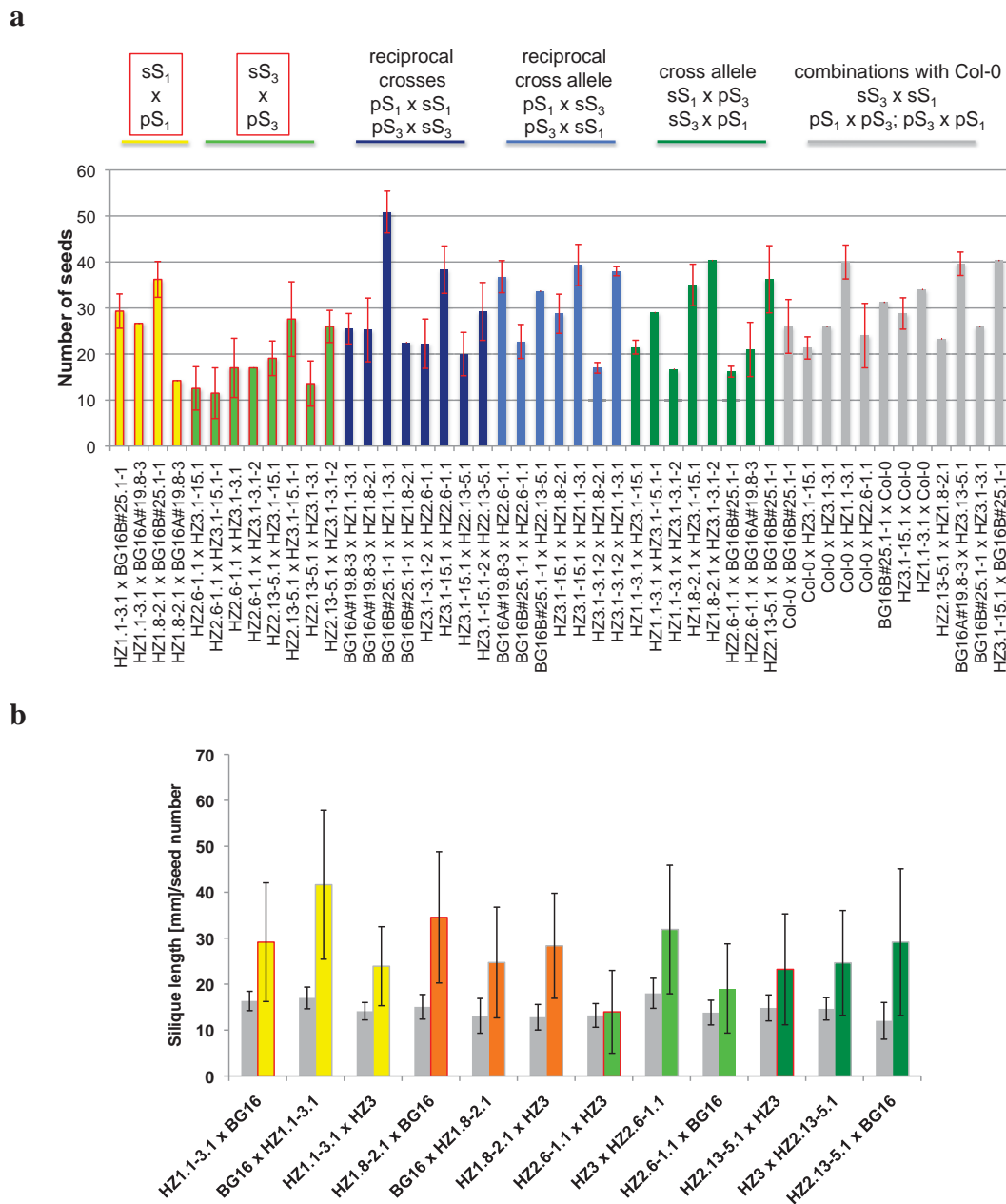


Figure 6.9.: (a) Seed set of all the incompatible crosses and controls; yellow bars, red outline: incompatible crosses $PrsS_1 \times PrpS_1$, spring green bars, red outline: incompatible crosses $PrsS_3 \times PrpS_3$, dark blue bars: reciprocal crosses: $PrpS_1 \times PrsS_1$ and $PrpS_3 \times PrsS_3$, light blue bars compatible reciprocal crosses: $PrpS_1 \times PrsS_3$ and $PrpS_3 \times PrsS_1$, dark green bars compatible controls: $PrsS_1 \times PrpS_3$ and $PrsS_3 \times PrpS_1$, grey bars: various control crosses including Col-0. Error bars \pm St. Error. (b) Joined data of a same $PrsS_1$ expressing plant line with incompatible crosses (red outline on bars), its reciprocal crosses and compatible controls. Yellow bars: pooled HZ1.1-3.1 data, orange bars: pooled HZ1.8-2.1 data, spring green bars: joined HZ2.6-1.1 data and dark green bars: joined HZ2.13-5.1 data. Grey bars represent average silique length. Error bars \pm Standard Deviation.

$PrsS_3$ expressing flowers HZ2.6-1.1 that were crossed with incompatible $PrpS_3$ -GFP expressing HZ3 pollen had an average seed set of 14.0 ± 9.0 seeds and silique length 13.2 ± 2.6

mm (n=11), which is ~130 % lower than its reciprocal crosses HZ3 x HZ2.6-1.1 with 31.9±14.0 seeds and silique length 18±3.3 mm (n=10). The seed set of compatible control HZ2.6-1.1 x BG16 was 36 % higher with 19.1±9.7 seeds and silique length of 13.8±2.7 mm (n=6). Another set of incompatible crosses with PrsS₃ expressing flower HZ2.13-5.1 x HZ3 was 6 % lower with 23.2±12.1 and silique length 14.8±2.8 mm (n=21), compared to its reciprocal cross HZ3 x HZ2.13-5.1 with 24.6±11.4 seeds and silique length 14.6±2.4 mm (n=8) and 25 % lower compared to the compatible cross HZ2.12-5.1 x BG16 with 29.1±16 seeds and silique length of 12±4 mm (n=7).

Taken together, the analysed seed set data indicate that the incompatible PrpS combinations might have an effect on the PrsS₁ expressing line HZ1.1-3.1 and PrsS₃ expressing line HZ2.6-1.1. However, the incompatible pollinations should not result in any seed set, so the result observed could be due to leaky phenotype, very weak expression as discussed above, or does not work at all.

6.2.4.3 Seed set and silique length of the F₁ progeny from incompatible crosses

Seeds from incompatible crosses of *A. thaliana* expressing *Papaver PrsS* and *PrpS-GFP* genes were tested for germination and seed set after self-pollination in F₁ generation. 30 seeds from each of the following crosses were selected: HZ1.1-3.1 x BG16#25.1-1 (PrsS₁ x PrpS₁), HZ1.8-2.1 x BG16#25.1-1 (PrsS₁ x PrpS₁), reciprocal cross BG16#25.1-1 x HZ1.8-2.1 (PrpS₁ x PrsS₁), HZ2.6-1.1 x HZ3.1-15.1-1 (PrsS₃ x PrpS₃) and HZ2.13-5.1 x HZ3.1-15.1 (PrsS₃ x PrpS₃), and germinated on MS media with double selection Kan and Basta. If the transfer of the genetic material occurred then the resulting seeds would be resistant to

Basta that was inherited through maternal side, and to Kan that was inherited through the paternal side by pollination. Because the parents used were homozygous, all the seeds were expected to survive the selection. If the incompatible cross would have been successful then no seeds would have been expected, however, seeds resulted from all the crosses so it would as well be possible that seeds would be sterile in the case of incompatible cross.

The Mendelian segregation (live to dead ratio) of F₁ seedlings from cross HZ1.1-3.1 x BG16#25.1-1 (PrsS₁ x PrpS₁) was 23:7 (3:1). The F₁ seedlings resulting from incompatible cross HZ1.8-2.1 x BG16#25.1-1 (PrsS₁ x PrpS₁) exhibited segregation 5:25 (0.2:1) with the first repeat and 7:23 (or 0.3:1) with the second repeat on double selection media. F₁ from reciprocal cross BG16#25.1-1 x HZ1.8-2.1 (PrpS₁ x PrsS₁) resulted in 2:1 segregation ratio. Segregation ratios of F₁ seedlings in case of incompatible crosses with PrsS₃-expressing stigmas were as follows: HZ2.6-1.1 x HZ3.1-15.1 (PrsS₃ x PrpS₃) resulted in one surviving seedling and exhibited a segregation ratio of 1:30 (or 0.03:1), and HZ2.13-5.1 x HZ3.1-15.1 (PrsS₃ x PrpS₃) exhibited a 26:4 ratio (or 6.5:1) with first repeat, and a 14:16 ratio (or ~ 1:1) with the second repeat. *A. thaliana* non-transformed control germinated only on MS media without any selections and did not germinate on double selection media.

These data indicates that both determinants (PrsS and PrpS) are present in the F₁ seeds, therefore it would be expected that self-fertilization is prevented in those plants if both PrsS and PrpS are functional in *A. thaliana*.

Surviving F₁ seedlings were planted in soil and left to self-fertilize following which the seed set was counted and silique length was measured.

From each F₁ line 5 plants were chosen and 10 siliques measured on each plant, except in the case of the first repeat of HZ1.8-2.1 x BG16#25.1-1 (2 plants) and HZ2.6-1.1 x HZ3.1-15.1

(1 plant only) as they were the only plants surviving after selection on plate and growth in pots. Seed set of F₁ plants derived from incompatible crosses is presented on Figure 6.10.

Self-fertilized *A. thaliana* Col-0 plants had 54±7.4 seeds (n=50 siliques measured in total). F₁ plants resulting from HZ1.1-3.1 x BG16#25.1-1 that exhibited 3:1 segregation ratio had the seed set of 37.8±11.9, which is significantly lower compared to Col-0 seed set (n=50; P=1.4*10⁻¹²). Seed set of F₁ plants resulting from cross HZ1.8-2.1 x BG16#25.1-1 (PrsS₁ x PrpS₁) with the segregation of 0.2:1 was 17.9±5.3 (n=20, P=7.3*10⁻³⁰ compared to Col-0) for the first repeat and 21.8±5.4 (n=50, P=4.9*10⁻⁴⁴ compared to Col-0) for the second repeat, both repeats were significantly lower compared to Col-0 self seed set. Reciprocal cross BG16#25.1-1 x HZ1.8-2.1 (PrsS₁ x PrpS₁) with 2:1 segregation ratio gave 47.8±9 seeds, which is significantly higher compared to seed set resulting from incompatible cross (n=50; P=3.1*10⁻⁴ compared to Col-0, P=3.8*10⁻²¹ compared to its incompatible cross, repeat 1 and P=1.5*10⁻³¹ compared to its incompatible cross, repeat 2).

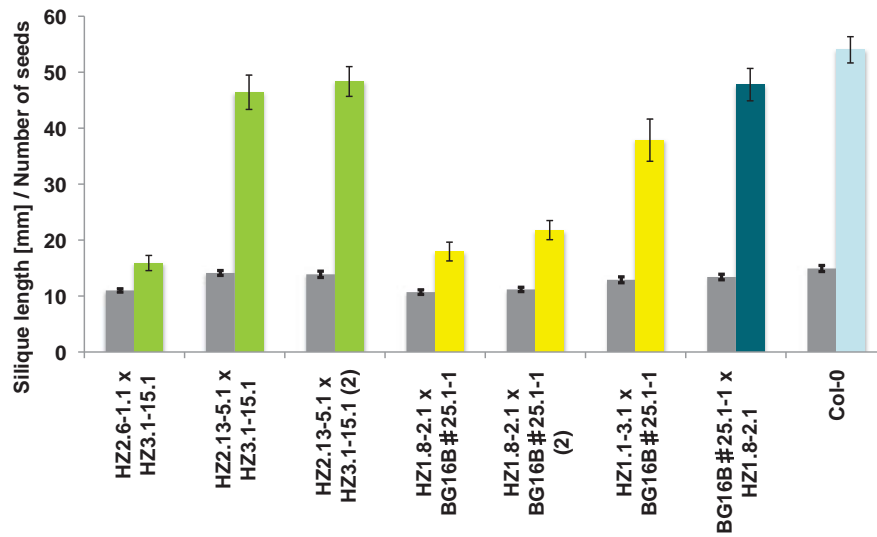


Figure 6.10: Siliqua length (grey bars) and seed set of surviving F₁ seedlings. Green bars PrsS₃ expressing stigmas used as females, yellow bars PrsS₁ expressing stigmas used as females in original cross, teal bar, reciprocal cross with BG16#25.1-1 used as a female and light blue bar Col-0 control. n=10 siliques; N=5 plants (except in case of the first repeat of HZ1.8-2.1 x BG16#25.1-1 (N=2 plants) and HZ2.6-1.1 x HZ3.1-15.1 (N=1 plant)). Error bars represent ± St. error.

Seed set from F₁ plants derived from HZ2.6-1.1 x HZ3.1-15.1 (PrsS₃ x PrpS₃) cross was 15.9±4.2 seeds and is significantly lower compared to Col-0 self-seed set, which was 54±7.4 (n=10, P=1.2*10⁻¹⁶). On the other hand, seed set from F₁ plants that were derived from HZ2.13-5.1 x HZ3.1-15.1 cross was 46.4±9.7 seeds for repeat 1, (n=50) and 48.3±8.4 seeds for the repeat 2 (n=50). Both these values were not significantly different from the Col-0. F₁ with the lowest seed set number were from plant lines deriving from crosses HZ1.8-2.1 x BG16#25.1-1 and HZ2.6-1.1 x HZ3.1-15.1.

Taken together, these data indicate that incompatible crosses HZ1.8-2.1 x BG16#25.1-1 (PrsS₁ x PrpS₁) and HZ2.6-1.1 x HZ3.1-15.1 (PrsS₃ x PrpS₃) displayed the strongest SI phenotype. However, the F₁ progeny resulting from these crosses exhibited distorted Mendelian segregation based on the seed germination on Kan and Basta MS media. Maternal PrsS expressing line HZ1.8-2.1 was homozygous, while the HZ2.6-1.1 line was

exhibiting ~4:1 segregation. The distorted and very low segregation could be due to reduced transmission through the male or female gametes and insertional inactivation of a gene expressed postmeiotically that is essential for the male and female gametophytic development or to epigenetic gene silencing and DNA methylation (Howden et al., 1998, Finnegan, 2004, Muskens et al., 2000).

In order to identify whether the PrsS was expressing correctly and to analyse the possibility of the reduced transmission through male or female gametes, the F₁ seeds should have been plated in a double selection medium (Basta and Kan) as well as a single selection media (Basta or Kan).

The *in vivo* results provided in this and previous sections lead to conclusion that PrsS was not functional in transgenic *A. thaliana* lines, due to low expression of the transgene and possible other effects that depend on the insertion of the transgene.

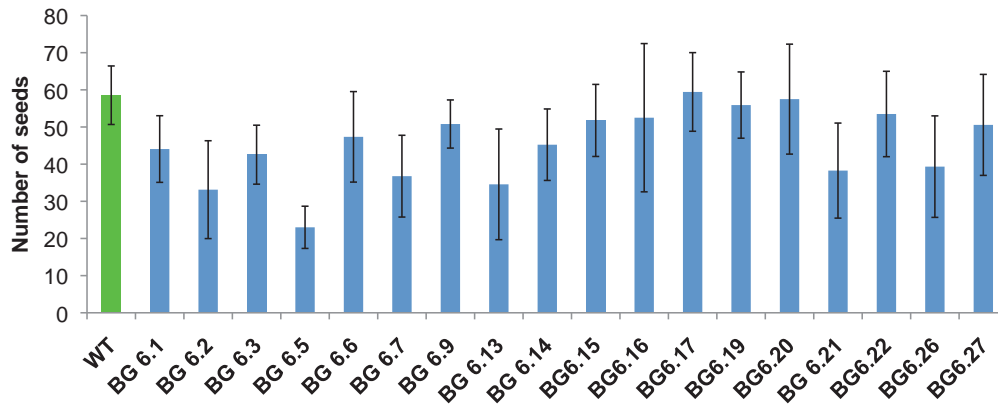
6.2.5. Investigating the function of the whole *Papaver* S₁ locus in transgenic *A. thaliana*

Transgenic *A. thaliana* line BG.6 expressing whole S₁-locus (described in previous section with segregation analysis) was systematically analysed in generation T₂. The *in vivo* analysis measured silique length and seed set. Results, presented in Figure 6.11 (a –seed set and b – silique length) show that majority of lines exhibit highly significantly reduced seed set, compared to non-transformed control.

A. thaliana non-transformed control had 58.6±7.9 seeds (n=30) and 13 lines out of 18 (72 %) exhibit lower seed set. The lines with the highest seed set reduction also exhibited decreased

silique length (11 lines, line BG6.14 and BG6.15 exhibited lower seed set but not lower silique length).

a



b

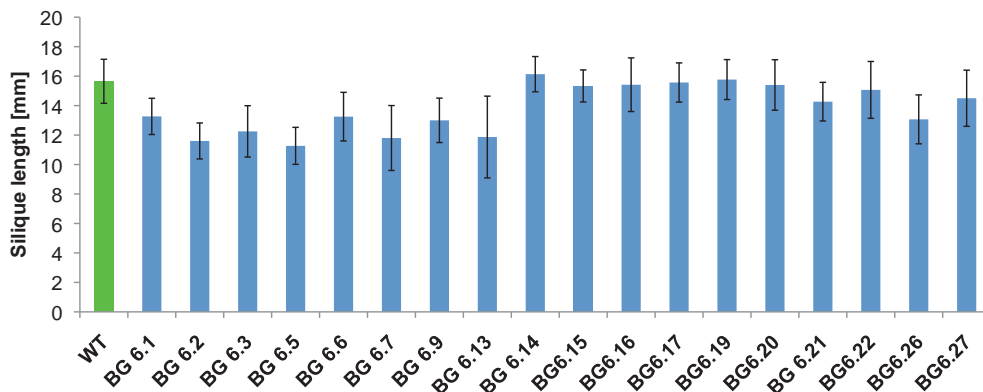


Figure 6.11.: Analysis of SI *in vivo* in *S_I*-locus expressing transgenic *A. thaliana* line BG6 (blue bars) and non-transgenic Col-0 control (green bar). **(a)** Seed set number and **(b)** Silique length. Error bars represent \pm standard deviation. N=10 siliques; N=3 plants (in total 30 siliques counted for each sample).

The plant line with the most affected seed set was BG6.5 (Figure 6.11.a), which had 23 ± 5.7 seeds ($n=30$, $P=1.5 \cdot 10^{-32}$ compared to Col-0) and it exhibited a 3:1 Mendelian segregation ratio for Kan insert. The lines that had seed set not significantly different from Col-0 were BG6.16 (exhibiting 2:1 segregation), BG6.17 (exhibiting 3:1 segregation), BG6.19 (exhibiting 3:1 segregation) and BG6.20 (exhibiting segregation $<1:1$). These implicate that the seed set number was not consistent with the segregation ratios, indication that there were

post-translational modifications, errors in gamete transmission or epigenetic gene silencing occurring.

In order to investigate the plant phenotype further, seed set of some plants was analysed in generation T_3 after selfing. Plants were selected based on their low or fertility expression in generation T_2 . Those plants were BG6.1 with 44.1 ± 9.0 seeds ($n=30$, $P=1.2 \times 10^{-09}$ compared to Col-0; $\sim 3:1$ segregation ratio), BG6.2 that had 33.1 ± 13.2 seeds ($n=30$, $P=6.7 \times 10^{-14}$ compared to Col-0; 1:1 segregation ratio), BG6.5 with 23 ± 5.7 seeds (3:1 segregation ratio). BG6.9, which had 50.8 ± 6.4 seeds ($n=30$, $P=2.6 \times 10^{-05}$ compared to Col-0; 0.2:1 segregation ratio) was chosen as a test control.

Figure 6.12 presents analysis of seed set on T_3 generation of transgenic plants expressing S_1 -locus after self-pollination. Within each sub-line, 10 siliques were measured from 3 different plants.

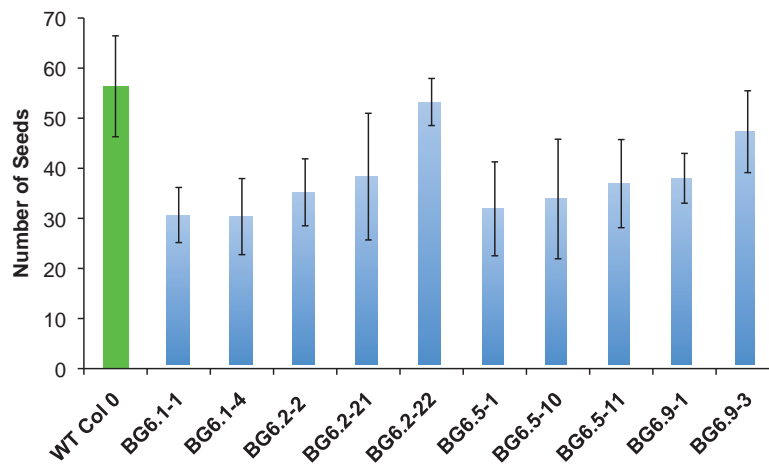


Figure 6.12: Seed set analysis on the T_3 generation of S_1 -locus expressing *A. thaliana* BG6 plants (blue bars) and non-transgenic Col-0 control (green bar). Error bars represent \pm standard deviation.

If the reduced seed set was due to the functionality of the S_1 -locus, then it would be expected than in the next generation after selfing, plant fertility would be severely affected. The highest degree of seed set reduction or possibly non-fertile seeds, was expected in the case of

BG6.5 plants as they exhibited lowest seed set in generation T₂. As the seeds were heterozygous in T₂ generation with 3:1 segregation ratio, only the non-transgenic pollen would be able to pollinate S₁ expressing stigmas and such seeds would not germinate on the MS with Kan selection marker. Therefore, the seed set in generation T₂ was not expected to survive another round of selection if the SI system would be strongly exhibited.

However, results on figure 6.12 indicate that the plants are displaying various degrees of seed set reduction compared to non-transgenic plants. If we take BG6.5 plants for example, in generation T₃ we counted 31.9±9.4 seeds in plant sub-line BG6.5-1 (n=30; P=8.3*10⁻¹⁴), 33.9±11.9 seeds in BG6.5.10 (n=30; P=9.4*10⁻¹¹) and 36.9±8.8 seeds in BG6.5-11 (n=30; P=7.2*10⁻¹¹). In fact, they actually exhibited higher seed set number than the parental plant BG6.5 in generation T₂. Lower seed set than parental line was observed in sub-line BG6.1, where 30.7±5.5 seeds were counted in BG6.1-1 plants (n=30, P=9.6*10⁻¹⁸) and 30.4±7.6 seeds in BG6.1-4 (n=20, P=7.1*10⁻¹⁴). Unusual pattern can also be observed with BG6.2 plants, where plant BG6.2-22 exhibit the highest seed set number 53.2±4.1 (n=30; P=0.13), which is not significant from the Col-0, although the BG6.2 line was the only one exhibiting expected segregation of the inserted whole S₁-locus, 1:1. The other BG6.2 sub lines are highly significantly different from Col-0 and from its sister line (BG6.2-2 and BG6.2-10). The sub-line BG6.9 also shows reduced seed set compared to Col-0, although the fertility reduction was comparable between the two sub-lines. BG6.9-1 had 38±4.9 seeds (n=30; P=1.6*10⁻¹²) while BG6.9-3 had 47.3±8.2 seeds (n=20; P=1*10⁻⁰³). So, this data could indicate that the S₁-locus might be functional when transformed into *A. thaliana*, however, some further detailed analysis for the presence of PrpS₁ and PrsS₁ transgene and transcript is required in order to confirm that.

In order to analyse SI on transgenic *A. thaliana* expressing S_1 -locus further, a preliminary analysis of BG6 self-pollination was attempted and representative images presented on figure 6.13. For representation, only two lines were chosen: BG6.2-2, which exhibited reduced seed set and line BG6.22-2, whose seed set was not significantly different from non-transgenic.

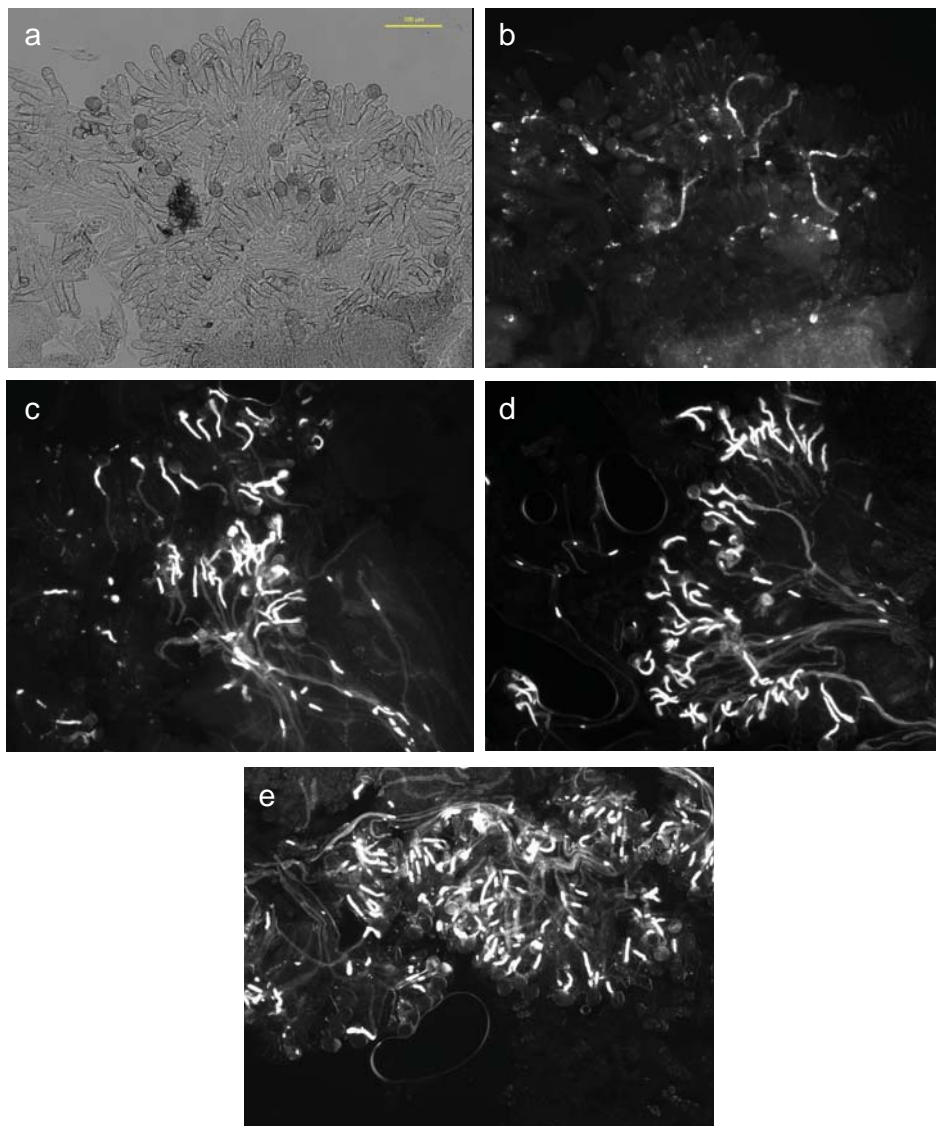


Figure 6.13.: Aniline blue staining analysis of self-pollination and control pollination of non-transgenic Col-0 on BG6 flowers (a) BG6.2-2 x BG6.2-2 – brightfield image; (b) BG6.2-2 x BG6.2-2 ; (c) BG6.2-2 x Col-0; (d) BG6.2-22 x BG6.2-22; (e) BG6.2-22 x Col-0. Scale represents 100 μ m.

Figure 6.13.b shows that the inhibition of self-pollen occurred to some degree, but was not 100 % (see figure 6.13.a). The rejection is not due to the non-receptive BG6.2-2 stigma, as can be seen on figure 6.13.c, as the pollination with Col-0 leads to development of long pollen tubes. On the other hand, self pollination of BG6.2-22, that exhibited normal seed set also exhibit 'compatible' self-pollination (Figure 6.13.d), which is comparable to the pollination with Col-0 pollen (Figure 6.13.e).

Due to the small size of analysed samples no firm conclusions could be made. The reduction of the seed production and decreased self-pollination in some BG6 lines, could indicate that the locus is functional. In order to analyse S_I -locus expressing *A. thaliana* lines (and therefore functionality of *Papaver* SI in *A. thaliana*) further, a more detailed analysis would be required, including systematic RT-PCR analysis and pollination assays.

6.3 DISCUSSION

Preliminary *in vivo* analysis of transgenic *A. thaliana* expressing stigmatic PrsS₁ (HZ1) and PrsS₃ (HZ2), pollen PrpS₁ (BG16) and PrpS₃ (HZ3) or S_I -locus (BG6) revealed that incompatible phenotype was not so easy to obtain. Some lines and crosses exhibited a reduced pollen tube growth, especially at the beginning of investigations. However, with time and experience it became obvious that age of plant and stage of stigma were crucial for this analysis. If plants were too old and producing more than 50 % of their siliques, then their stigmas, despite the right biological stage, were not fully receptive, and the pollen was not germinating well, even on the receptive stigmas. (Nasrallah et al., 2002) illustrates the right biological stage of stigma and also demonstrates that maturity of pollen is very

important. They collected stigmas from stage 12, stage 13, early stage 14 (14E) and late stage 14 (14L) buds of transgenic *A. thaliana*, ecotype Colombia, expressing SRKb/SCRb. Stigmas were then pollinated with self or cross pollen. The results show that stigmas in the stage 12 or stage 14L allowed all the pollen to grow, regardless whether it was self (and therefore should be incompatible) or cross (compatible) pollen. However, in stage 13 and 14E, when stigmas reached their optimal biological stage, self-pollen was rejected and its growth inhibited (Nasrallah et al., 2002). As briefly described at the beginning of the result chapter, we emasculated buds in the stage 12, excised the stigmas and place them in 0.5 % agar where they were left to mature for 20-24 h before pollination. According to (Smyth et al., 1990), stage 12 lasts for 12 h in total so our pollinations were done in stage 13 (which lasts for 6 h) or early stage 14 (stage 14 lasts 18 h), when stigmas were not only receptive but should as well have maximum expression of PrsS. This technique differs from the other labs where they emasculated buds on plants and immediately pollinated them (Nasrallah et al., 2002). As *A. thaliana* pollen germinates well on stigma, the stigmas were collected for pollination assays after 2 h (Nasrallah et al., 2002). Despite the fast *in vivo* pollen germination, that takes ~15 minutes in *A. thaliana* (Boavida et al., 2005), we left pollen to germinate on stigma for 16 h, which was the optimal identified time for germination of *A. thaliana* flowers *in vitro* (Boavida and McCormick, 2007). This time-point was used for pollination assays in transgenic *A. thaliana* expressing *Papaver* genes as we did not know if, and what role the temporal expression of *Papaver* genes plays in *A. thaliana in vivo* pollen tube growth.

Nasrallah et al., (2002) demonstrated, that SI phenotype in transgenic *A. thaliana* expressing *Brassica S*-determinants was developmentally regulated. The temporal analysis on the expression of the *Papaver* female *S*-determinant, PrsS, was initially detected two days

preanthesis, increased at one day preanthesis and remained high for several days after flower opening (Foote et al., 1994). In *Papaver*, inhibition of incompatible pollen occurs very quickly on the stigmatic papillae, within minutes of pollination (Franklin-Tong et al., 2002), so the same was expected to occur in *A. thaliana* expressing PrsS or whole S_I -locus. *In vitro* pollen tube inhibition and viability assay in transgenic *A. thaliana* expressing *Papaver* pollen determinant PrpS demonstrated that the significant decrease of pollen viability occurred as quick as 2 h after incompatible pollen challenge (data not shown), and incompatible pollen tubes were inhibited and very short, comparable to the inhibited *Papaver* pollen tubes. Very informative were also the results of actin analysis where PrpS-expressing pollen was challenged with incompatible recombinant PrsS proteins. Actin foci were present mostly in *A. thaliana* pollen grains or grains with very short tubes, indicating that inhibition occurred very rapidly upon the SI interaction as no pollen tubes were observed, which was comparable to the *Papaver* SI response. Therefore it was expected that *in vivo* analysis of pollination of PrsS-expressing *A. thaliana* stigmas with its cognate PrpS-GFP pollen expressing *A. thaliana* would confirm the rapid inhibition of pollen on the stigma surface and show no or very little penetration of pollen through the stigma surface. The results obtained *in vivo* showed no inhibition of the incompatible pollen tube growth through PrsS expressing stigmas and such incompatible pollinations resulted in fertile seed set, indicating that there is no or very low expression of PrsS. Although the mRNA for PrsS was detected using RT-PCR on stage 13 flowers, the transcript levels of PrsS were lower compared to PrpS, and the PrsS protein was not detected using western blotting. Very low expression of PrsS could be explained by translation of low levels of mRNA into protein that was expressed below critical threshold in flowers; however, it was also possible that protein was not translated properly.

In vivo pollination assay and crosses for the seed set had a low reproducibility rate, as it was very difficult to assure the same conditions. It was impossible to cross-pollinate flowers with the same amount of pollen each time, and number of pollen was of great importance to ensure reproducibility and accuracy for the seed set data. To ensure that comparable crosses or repeats were pollinated with the same pollen mix of pollen from several different flowers was used. Pistils were also very susceptible to any sort handling damage that occurred mostly during the emasculation stage and this was the reason why there are less repeats of certain crosses.

With pollination assays, emasculated stigmas in early stage 13 were excised and placed in Elisa plate with 0.5 % agar, where they were left to mature, pollinated and finally collected in aniline blue containing tube. If there was any degree of pollen rejection and inhibition on incompatible crosses, then it was possible that inhibited pollen fell off the stigma or was washed away when stigma was placed in an eppendorf tube with aniline blue. Masters student Stephanie Smith, who continued with the pollination experiments, solved this issue with a temporarily “compartmentalised” microscope slide where stigmas were loaded before staining. With this technique, the visualisation of stigmas included total pollen used for pollination as in incompatible situation none got washed away or was lost as it fell of the stigma. However, no incompatible pollinations were observed due to low or no expression of PrsS in transgenic *A. thaliana*.

Intriguing results were obtained when PrsS₁ and PrsS₃ expressing *A. thaliana* stigmas were used to incubate *Papaver* S₁ and S₃ pollen. Pollen inhibition was observed in an S-specific manner and in addition also pollen tube tip swelling. This indicates that transgenic PrsS expressing *A. thaliana* stigmas are expressing PrsS protein, but most likely in low

concentrations as many stigmas were used for the stigmatic extract. It could also be possible that proteins are not properly folded or some other components of the stigmatic extract caused the *Papaver* pollen tube tip swelling, although the later explanation seems unlikely as non-transgenic Col-0 stigmatic extract was used as a control and no such dramatic pollen tube tip swelling was observed with it. Also, if the protein is not folded correctly we would not be expecting to observe such a response, as it was demonstrated *in vitro* (See Chapter 5) that heat denatured recombinant PrsS proteins had no effect on growth of pollen tubes.

Following successful *in vitro* analysis on PrpS expressing *A. thaliana* pollen, it was anticipated that *in vivo* analysis, although preliminary, might indicate stronger level of inhibition in incompatible pollinations. Most likely, the problem lies within the expression levels of PrsS in stigma. For successful incompatible response, the expression level of stigmatic gene is crucial and it was also demonstrated in the case of transgenic *A. thaliana* expressing *Brassica SRK* genes in the model of transgenic SI *A. thaliana* (Bi et al., 2000, Nasrallah et al., 2002, Boggs et al., 2009b). In transgenic *A. thaliana* expressing *Brassica* SI they solved the problem by transforming the SI system from more closely related SI *Arabidopsis lyrata* and *Capsella grandiflora* (Nasrallah et al., 2002, Boggs et al., 2009b, Nasrallah et al., 2007). In this light, the expression of the stigmatic genes in *A. thaliana* seems more problematic than expression of pollen genes. However, the proteins that are being utilised in *Papaver*-like transgenic *A. thaliana* SI model and *Brassica*-like transgenic model are completely different. In *Papaver*, PrsS are small globular, secreted stigmatic proteins, while in *Brassica* the stigmatic S-receptor kinase, SRK, is a single-pass transmembrane protein kinase. Structurally the proteins are very different, so the problem of

successful expression of foreign stigmatic genes in *A. thaliana* probably lies with the incorrect processing of the stigmatic determinants or in a weak expression.

The stigmas used for the *in vivo* experiments were homozygous but even if diploid stigmas would be heterozygous for PrsS, this would mean that they still contain one copy of the *PrsS* gene. When such flower is crossed with pollen that is homozygous for PrpS, the outcome of an incompatible cross should be 100 % pollen inhibited (PrsS expressing stigma x PrpS pollen), if we assume, that pollen inhibition occurs on the stigmatic surface. The seeds of such cross (F₁ progeny) would therefore be able to survive the Basta and Kan selection. So if incompatible crosses between PrsS and PrpS expressing *A. thaliana* lines (HZ1 x BG16 or HZ2 x HZ3) would be successful, then there would be no seed produced as the pollen should be inhibited on the surface of the stigma or at least very early as it would grow through the style. However, our crosses between PrsS and PrpS determinant of the cognate *S*-haplotype resulted in pollen tubes growing thorough the style and fertilizing the ovaries. The analysis of F₁ generation seedlings arriving from some of the incompatible crosses presented in this section showed various segregation phenotype and seed set. The segregation was analysed on a double selection media, using both, Kan and Basta. Only the seedlings expressing both, PrsS and PrpS, could survive and it was therefore expected that surviving seedlings would have reduced seed set as a result of simultaneous expression of both, PrsS and PrpS. This was true for most of the analysed F₁ lines. Significantly different seed set from Col-0 plants were observed in F₁ plants deriving from cross between HZ1.1-3.1 x BG16#25.1-1, HZ1.8-2.1 x BG16#25.1-1 and HZ2.6-1.1 x HZ3.1-15.1 but not from two crosses of HZ2.13-5.1 x HZ3.1-15.1, whose seed set was not significantly different from Col-0. For more complete analysis the presence of the genes should be analysed by RT-PCR and the seeds from F₁

progeny should be grown on individual selection media in order to give us more information about the nature of parental expression. It would also be important to perform Southern analysis in order to investigate number of inserts present as well as study the protein expression by Western analysis and immunolocalization. The lowest seed set was observed in F₁ derived from HZ1.8-2.1 x BG16#25.1-1 (17.9±5 seeds) and HZ2.6-1.1 x HZ3.1-15.1 (15.9±4.2 seeds), which could indicate that these two have the highest expression of PrsS₁ or PrsS₃, respectively, and those lines would therefore be the most interesting for the future *in vivo* analysis of *Papaver* SI in transgenic *A. thaliana*.

Nevertheless, the *in vivo* data suggest that we ended with a “leaky” PrsS phenotype and despite all the above possibilities, the PrsS expression is very low (probably below the level required for inhibition) or the protein is not being properly folded. In order to obtain a more complete picture of PrsS expression in *A. thaliana*, the repeat of transformation with highly active stigma-specific promoter Stig1 from *N.tabacum* would be proposed or transformation with another stigma-specific promoter, such as SLG promoter from *Brassica* (Thorsness et al., 1993, Goldman et al., 1994).

Preliminary analysis of *A. thaliana* BG6 lines expressing whole *S₁*-locus revealed that majority of lines exhibited a significantly reduced seed set after self-pollination, while seed set of some lines was not affected after self-pollination (BG6.16, BG6.17, BG6.19 and BG6.20). If the transgenic BG6 *A. thaliana* were homozygous, then the seed set would not be expected. Therefore the poppy SI (using the *S₁*-locus) was probably leaky in *A. thaliana*. Most probably the problem lies within the protein expression levels as the protein translation is coupled with the endogenous promoter (the PrpS₁ in BG16 is coupled with a strong

ntp303 promoter, hence the high and strong expression). However, the RT-PCR analysis that was so far conducted on a limited number of BG6 samples, resulted in only PrsS mRNA present, and not PrpS; so the pollen seed set could also indicate that pollinations are due to the Col-0 phenotype of pollen (heterozygous) and that the reduced seed set occurred for different reasons. The place of insertion on the genome and the number of inserted copies, were also unknown and this might well be the contributing factor to the reduced fertility. Transgenic BG6 lines expressing whole S_1 -locus require further detailed analysis. The RT-PCR analysis should be systematically carried on all the lines from BG6 plants, screening the PrsS and PrpS expression, as we cannot be certain whether the reduction of seeds was due to the functional SI.

The transgenic *A. thaliana* model for *Brassica* SI did not express the whole *S*-locus, but the functional SRK-SCR gene pairs (Nasrallah et al., 2004). If the whole *Papaver* *S*-locus could be transferred to and be functional in a such an evolutionary distant species as *A. thaliana*, as was demonstrated for pollen determinant PrpS, then this could provide an information into evolution of SI. It would demonstrate a possible signalling mechanism being conserved in *A. thaliana* that would probably open up a further debate not only about the evolution SI but also about the evolution of other recognition systems, such as plant-pathogen. Furthermore, this system could be used for plant breeding in a production of F1 hybrids where self-compatibility poses a problem that needs to be overcome. Furthermore, this *Papaver*-like SI system could potentially be also linked to different promoters for expression in somatic plant cells or even mammalian cells in order to use it as a potential inducible switch to trigger PCD, which would be of great interest with mammalian cancer cells. And most importantly, the *A. thaliana* model exhibiting *Papaver*-like SI would represent a helpful and valuable tool

in studying the SI events on a detailed molecular level, as it would enable the crosses with various other lines of interest or analysis by mutations of various events, from the details of interaction between PrsS and PrpS to PCD.

CHAPTER 7

GENERAL DISCUSSION

The studies presented in this thesis cover the analysis of the initial events of SI, the interaction between the stigmatic *S*-determinant, PrsS and pollen *S*-determinant, PrpS, the preliminary investigation into the involvement of the ubiquitin-proteasomal pathway during SI, and *in vitro* and *in vivo* analysis of transgenic *A. thaliana*, expressing *Papaver* *S*-determinants.

Papaver SI model in Figure 7.1. summarizes the SI events including the *S*-specific interaction between PrpS and PrsS (presented in Chapter 4, published in Wheeler et al., 2009) and the model of UbP degradation pathway connected to DEVDase activity (presented in Chapter 3). The involvement of UbP pathway in *Papaver* SI is discussed in details in Chapter 3 and not dealt here.

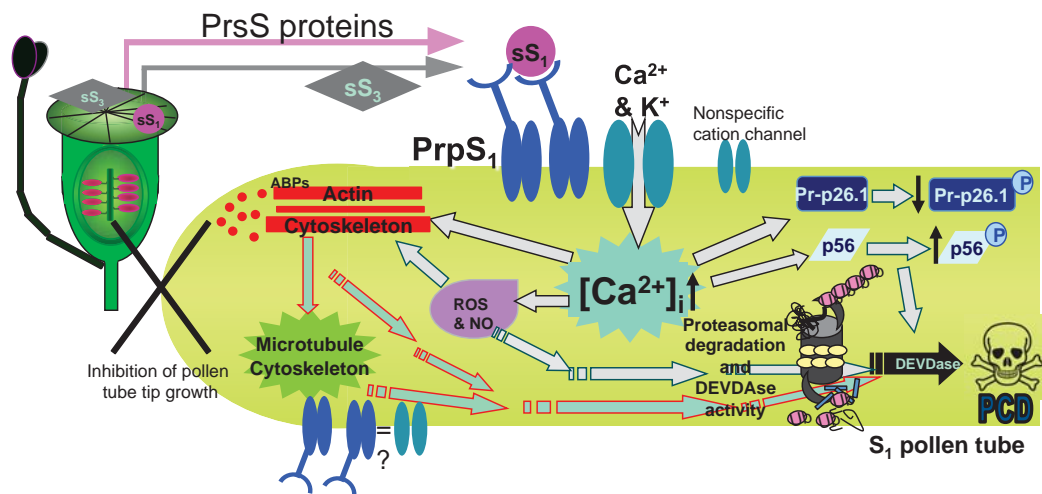


Figure 7.1.: Schematic model of the SI response in *Papaver*. Upon the interaction of secreted stigmatic PrsS proteins and pollen transmembrane protein PrpS, a downstream signalling network is triggered, starting with an increase in K^+ and $[Ca^{2+}]_i$ who is signalling to the inhibition of pyrophosphatase activity and pollen tube tip growth, activation of MAPK, depolymerization of actin and microtubule cytoskeleton and appearance of punctate actin foci, activation of ROS and NO and activation of caspase-like activities, leading to the PCD of the pollen tube. The model presents DEVDase activity that most likely acts in parallel with proteasomal degradation. DEVDases are presented as yellow circles within the proteasome, as identified by Hatsugai et al., (2009).

7.1. *Papaver* S-determinant interactions

SI in *Papaver* is achieved when incompatible pollen grains land on the stigma where it is recognized and discriminated from the genetically different pollen, and selectively inhibited. The stigmatic secreted PrpS proteins mediate this recognition and rejection, and act as a signalling ligand for the pollen transmembrane protein, PrpS (Foote et al., 1994, Wheeler et al., 2009). The discovery of PrpS as the pollen determinant of the SI response in *Papaver* represented a breakthrough in the SI research and the long sought missing link required for the recognition and rejection of the incompatible pollen.

The results presented in this thesis demonstrate the S-specific binding between PrpS and PrsS using the far western blot and the peptides designed to mimic the extracellular domain. The extracellular domain was predicted to be positioned between TM 2 and 3 using a variety of prediction programmes and was proposed to be the interacting region for the secreted ligand PrsS (Wheeler et al., 2009). The binding was further indicated when the peptides designed over the extracellular domain, alleviated the incompatible pollen inhibition when added to the *in vitro* bioassay (Wheeler et al., 2009). The far western method is well established and widely used for determining protein interaction sites in receptor-ligand interaction as well as the use of the synthetic peptides (Volkmer et al., 2011). Far western approach was used to confirm many protein-protein interactions, for example, to demonstrate the interaction in plant-pathogen system between rice Pi-ta receptor and host AVR-Pita protein (Jia et al., 2000) or to identify the S-specific interaction between stigmatic microsomal fraction and recombinant SCR in *Brassica* (Kemp and Doughty, 2007).

The PrpS represents a novel transmembrane protein and shares no homology to any other protein, so the exact mechanism of the perception is not yet known. PrpS could be part of a greater multimeric complex where it could play a role of the *S*-specific signal perception protein but not the downstream transduction. An example of such complex is CLV complex where LRR RLKs CLV1 and CLV2 dimerize in order to form a receptor complex (Clark et al., 1995, Jeong et al., 1999). CLV1 binds the CLV3 derived CLE ligand through its extracellular domain and functions in stem cell specification (Clark et al., 1995, Clark, 2001, Stahl and Simon, 2005, Ogawa et al., 2008). CLV1 and CLV3 are expressed only in the central zone of SAM (Clark et al., 1997, Fletcher et al., 1999). Below the central zone a control zone is located where another protein, implicated in SAM is expressed. Transcription factor WUSCHEL (WUS) forms a feedback network with CLV (Schoof et al., 2000). WUS upregulates CLV3 when the number of stem cells is low, while CLV3 binds to CLV1 and downregulates WUS when the stem cells are in abundance (Reddy and Meyerowitz, 2005). If PrpS forms a part of a larger protein complex, it is yet unknown. However, the *S*-protein binding protein (SBP) was previously identified that apparently binds to the PrpS, but not in the *S*-specific manner (Hearn et al., 1996). The connection between PrpS and SBP is not yet analysed as no protein or gene has yet been identified for SBP. Alternatively, the PrpS could perceive and transduce a signal on its own. Some analogies might be drawn between the *Drosophilla* protein Flower (Yao et al., 2009) or the mammalian CRAC calcium channel (Luik et al., 2008) and PrpS. Protein Flower is TM protein with 4 predicted TM domains and is involved in the endocytosis of the synaptic vesicles. It displays properties of Ca²⁺ channel: negatively charged aminoacids in the TM domains, which play a key role in the ion selectivity. Similar to Flower, the 4 TM protein CRAC/Orai also carries negatively charged aminoacids in the TM domains and multimerizes to form a channel. In this process each

monomer contributes one TM domain with the negatively charged amino acid to the pore (Yao et al., 2009, Prakriya et al., 2006). Flower proteins also form multimers and are thus able to form a calcium channel by which it controls Ca^{2+} influx (Yao et al., 2009). Protein alignment of PrpS proteins revealed a conserved glutamic acid residue at position 75. This region is mostly predicted to be extracellular in PrpS₁ and PrpS₈, and intracellular in PrpS₃, although some prediction programmes also gave inverted predictions, but none predicted a TM domain. Concluding from the analysis conducted, this region is involved in the PrpS interaction (Wheeler et al., 2009). Interestingly, this glutamic acid residue is also conserved with Flower protein, when PrpS and Flower are aligned, although in Flower the region is predicted TM. The negatively charged amino acids appear to be crucial in the TM domains for the formation of the voltage-gated calcium channels. Alignment of PrpS proteins revealed a total of 7 conserved negatively charged amino acids: three glutamic acids (E75, E129 and E168), and three aspartic acids (D39, D90, and D123) with some being the candidates for the potential pore formation. An additional motif that is well known to be involved in the protein oligomerization and formation of the membrane channel is the GxxxG motif (Dawson et al., 2002, Senes et al., 2004, McClain et al., 2003). *Helicobacter pylori* vacuolating toxin can form an anion-selective membrane channel as it contains three tandem GxxxG motifs, characteristic for TM dimerization and membrane channel formation (McClain et al., 2003). The PrpS alignment revealed two conserved tandem GxxxG motifs at positions 126 and 130, with the first one also conserved in Flower. This region is also not predicted to be part of a TM domain but is the long cytoplasmic tail. More detailed analysis of the residues suggests a fourth TM domain, so the motif is most likely part of the fourth TM domain. The GxxxG motif at position 126 also contains a conserved glutamic acid residue.

Taken together, PrpS *S*-specifically recognizes the PrsS proteins and it most likely acts as a receptor. One of the first downstream events following the interaction is the increase in the cytosolic calcium (Franklin-Tong et al., 1993, Franklin-Tong et al., 2002), and it was also demonstrated that the SI activates ligand-gated nonspecific cation conductance (Wu et al., 2011), so the PrpS might form a channel, composed of PrpS multimers or a channel complex where it would form a subunit. This is something that is currently being investigated in the Franklin-Tong's lab.

7.2 Functional analysis of *Papaver rhoeas* self-incompatibility in transgenic *Arabidopsis thaliana*

We initiated studies to see whether the *Papaver* SI system might be functionally transferable to other plant species and studies in this thesis describe the successful interspecific transfer of the *Papaver* pollen determinants of SI, PrpS, to SC *A. thaliana*. Several transgenic *A. thaliana* lines were created, expressing the PrpS fused to the GFP: PrpS₁-GFP and PrpS₃-GFP, and stigmatic *S*-determinants PrsS₁ and PrsS₃ under the control of pollen and stigma specific promoters, respectively, and lines expressing whole *S_I* locus or PrpS₁, under the control of the native promoter and constitutive 35S promoter, respectively. Our results “*in vitro*” revealed an *S*-specific inhibition of the PrpS-GFP expressing transgenic *A. thaliana* pollen tube growth by recombinant PrsS, and key hallmark features for *Papaver* SI: loss of pollen viability, appearance of actin foci and increase in DEVDase activity. These data suggest that PrpS expressed in evolutionary very distantly related species *A. thaliana*, is functional and that only PrpS and PrsS are required for a fully functional SI response in *A. thaliana* pollen, where all the required components for the pollen tube inhibition are present.

However, preliminary *in vivo* assay demonstrated that PrsS exhibits weaker expression in *A. thaliana* flowers. Although the full SI response was not demonstrated *in vivo*, we observed significant inhibition of *Papaver* pollen with protein extract from PrsS expressing *A. thaliana* stigmas, leading to the conclusion of low expression of PrsS in transgenic *A. thaliana*.

Our study represents the first such study of transforming *A. thaliana* with the GSI determinants. Transformation of *A. thaliana* by determinants of *Brassica* SI is already developed by Nassrallah lab and studies on *A. thaliana* expressing functional intact or chimeric SRK/SCR pairs are underway to identify the mechanism of SI and to elucidate components of pollen-pistil signalling (Tantikanjana et al., 2010, Nasrallah et al., 2002, Rea et al., 2010). *SRK-SCR* receptor-ligand gene pair used for the studies of *Brassica* SI were isolated from the SI crucifers *Arabidopsis lyrata* or *Capsella grandiflora*, and the SI analysed by performing crosses between them (Nasrallah et al., 2002, Boggs et al., 2009b, Rea et al., 2010, Nasrallah et al., 2004). Although *Brassica* model of SI in *A. thaliana* took several years to develop and optimize, it now represents invaluable system for the studies of the mechanism of SI and pollen-pistil interactions, as well as evolutionary aspects of SI (Nasrallah et al., 2002, Nasrallah et al., 2004, Rea et al., 2010). The transgenic *A. thaliana* expressing SRK-SCR gene pair was used for example for the analysis of the residues important for the SRK specificity and therefore the SI response. Site-directed mutagenesis approach was used on the polymorphic aminoacid residues in the extracellular domain of SRK and six were identified as crucial for ligand-specific SI activation (Boggs et al., 2009a). Although in *Papaver* we have identified the extracellular domain of PrpS₁, required for the SI response, and 15 aa domain that is crucial for the interaction with PrsS₁, it was so far impossible to narrow down the S-specificity to the individual amino acids. The transgenic *A.*

thaliana pollen expressing PrpS is a model for *Papaver*-like SI that now enables the possibility to investigate the specific residues within PrpS, determining the specificity of the ligand binding interaction or protein multimerization.

Papaver belongs to the basal order in the lineage Ranunculales, diverged very early in the history of eudicots (Allen and Hiscock, 2008). The evolutionary distance between Ranunculales and Brassicales, lineage where belongs *A. thaliana*, is estimated to 140 million years (Bell et al., 2010). This suggests that *Papaver* SI response pre-dates other SSI mechanism as well as other GSI and it may represent the ancestral state of SI. It is also possible that SSI system evolved from the SC species originating from the GSI ancestors (Allen and Hiscock, 2008). Although *A. thaliana* operated *Brassica*-type of SI and it diverged from *A. lyrata* ~10 million years ago (Hu et al., 2011), the transfer of the *Papaver* pollen *S*-determinant was functional. *A. thaliana* pollen had the cellular machinery required to elicit a *S*-specific pollen rejection upon the PrpS-PrsS interaction. This could indicate that an ancestral SI mechanism, operating in *Papaver* might still be conserved in other species, although they evolved more complex mechanisms of SI (for review see McClure et al., (2011), Tantikanjana et al., (2010)) but might have kept basic components and recruited this mechanism for different purposes. The recent advances of the research on the SI induced actin reorganisations in different SI systems suggest, that there could be a link between the mechanistically different SI systems and the SI could be more conserved than known so far (Liu et al., 2007c, Iwano et al., 2007, Wang et al., 2010, Poulter et al., 2010a).

The preliminary analysis to investigate whether the *Papaver*-like SI response could be induced in any plant tissue was tested using *A. thaliana* leaf mesophyll protoplasts, and the results so far confirmed the functionality of the PrpS-PrsS system.

Ca^{2+} is mediating downstream events of SI, observed in incompatible *Papaver* pollen tube, however, it is also a well known and conserved secondary messenger in other plant species, mammals and also bacteria, relaying the signals, perceived by the receptors on the cell surface to target molecules in the cytosol (Shemarova and Nesterov, 2005, Ma and Berkowitz, 2007). It is very important, for example, for the signal transduction during plant-pathogen interactions, as Ca^{2+} increase is one of the first steps during plant immune response to the PTI and ETI, signalling to the PCD. Considering many similarities between SI and HR as well as animal histocompatibility, such as aforementioned Ca^{2+} signalling to phosphorylation of target proteins, alterations to the cytoskeleton, activation of ROS and induction of the DEVDase activities leading to PCD, might indicate that these targets are ancient and conserved, and it would be interesting to investigate the evolutionary connection between them.

CHAPTER 8

REFERENCES

- ADAMAKIS, I.-D. S., PANTERIS, E. & ELEFThERIOU, E. P. 2011. The fatal effect of tungsten on *Pisum sativum* L. root cells: indications for endoplasmic reticulum stress-induced programmed cell death. *Planta*, 234, 21-34.
- ALLEN, A. M. & HISCOCK, S. J. 2008. Evolution and Phylogeny of Self-Incompatibility Systems in Angiosperms. In: V.E.FRANKLIN-TONG (ed.) *Self-Incompatibility in Flowering Plants*. Springer-Verlag Berlin Heidelberg.
- AMIEN, S., KLIWER, I., MÁRTON, M. L., DEBENER, T., GEIGER, D., BECKER, D. & DRESSELHAUS, T. 2010. Defensin-Like ZmES4 Mediates Pollen Tube Burst in Maize via Opening of the Potassium Channel KZM1. *PLoS Biol*, 8, e1000388.
- ARAI, M., MITSUKE, H., IKEDA, M., XIA, J.-X., KIKUCHI, T., SATAKE, M. & SHIMIZU, T. 2004. ConPred II: a consensus prediction method for obtaining transmembrane topology models with high reliability. *Nucleic Acids Res*, 32, W390-3.
- ASTRÖM, H. 1997. *The structure and function of Tobacco pollen tube cytoskeleton*, University of Helsinki, Finland.
- BECRAFT, P. W., STINARD, P. S. & MCCARTY, D. R. 1996. CRINKLY4: A TNFR-like receptor kinase involved in maize epidermal differentiation. *Science*, 273, 1406-9.
- BELENGHI, B., SALOMON, M. & LEVINE, A. 2004. Caspase-like activity in the seedlings of *Pisum sativum* eliminates weaker shoots during early vegetative development by induction of cell death. *J Exp Bot*, 55, 889-897.
- BELL, C. D., SOLTIS, D. E. & SOLTIS, P. S. 2010. The age and diversification of the angiosperms re-revisited. *Am J Bot*, 97, 1296-303.
- BERNSEL, A., VIKLUND, H., FALK, J., LINDAHL, E., VON HEIJNE, G. & ELOFSSON, A. 2008. Prediction of membrane-protein topology from first principles. *PNAS*, 105, 7117-81.
- BI, Y. M., BRUGIÈRE, N., CUI, Y., GORING, D. R. & ROTHSTEIN, S. J. 2000. Transformation of Arabidopsis with a *Brassica* SLG/SRK region and ARC1 gene is not sufficient to transfer the self-incompatibility phenotype. *Mol Gen Genet*, 263, 648-54.
- BLANVILLAIN, R., YOUNG, B., CAI, Y.-M., HECHT, V., VAROQUAUX, F., DELORME, V., LANCELIN, J.-M., DELSENY, M. & GALLOIS, P. 2011. The Arabidopsis peptide kiss of death is an inducer of programmed cell death. *The EMBO Journal*, 30, 1173-83.
- BOAVIDA, L. C. & MCCORMICK, S. 2007. TECHNICAL ADVANCE: Temperature as a determinant factor for increased and reproducible in vitro pollen germination in *Arabidopsis thaliana*. *The Plant Journal*, 52, 570-582.
- BOAVIDA, L. C., VIEIRA, A. M., BECKER, J. D. & FEIJÓ, J. A. 2005. Gametophyte interaction and sexual reproduction: how plants make a zygote. *Int J Dev Biol*, 49, 615-32.
- BOGGS, N. A., DWYER, K. G., NASRALLAH, M. E. & NASRALLAH, J. B. 2009a. *In Vivo* Detection of Residues Required for Ligand-Selective Activation of the S-Locus Receptor in Arabidopsis. *Current Biology*, 1-6.
- BOGGS, N. A., DWYER, K. G., SHAH, P., MCCULLOCH, A. A., BECHSGAARD, J., SCHIERUP, M. H., NASRALLAH, M. E. & NASRALLAH, J. B. 2009b. Expression of Distinct Self-Incompatibility Specificities in *Arabidopsis thaliana*. *Genetics*, 182, 1313-1321.
- BOGGS, N. A., NASRALLAH, J. B. & NASRALLAH, M. E. 2009c. Independent S-Locus Mutations Caused Self-Fertility in *Arabidopsis thaliana*. *PLoS Genet*, 5, e1000426.

- BOLLER, T. & FELIX, G. 2009. A renaissance of elicitors: perception of microbe-associated molecular patterns and danger signals by pattern-recognition receptors. *Annual review of plant biology*, 60, 379-406.
- BONNEAU, L., GE, Y., DRURY, G. E. & GALLOIS, P. 2008. What happened to plant caspases? *J Exp Bot*, 59, 491-499.
- BORÉN, M., HÖGLUND, A.-S., BOZHKOVA, P. & JANSSON, C. 2006. Developmental regulation of a VEIDase caspase-like proteolytic activity in barley caryopsis. *Journal of Experimental Botany*, 57, 3747-53.
- BOSCH, M., CHEUNG, A. Y. & HEPLER, P. K. 2005. Pectin methylesterases, a regulator of pollen tube growth. *Plant Physiology*, 138, 1334-1346.
- BOSCH, M. & FRANKLIN-TONG, V. E. 2007. Temporal and spatial activation of caspase-like enzymes induced by self-incompatibility in *Papaver* pollen. *Proc Natl Acad Sci USA*, 104, 18327-32.
- BOSCH, M., POULTER, N. S., PERRY, R. M., WILKINS, K. A. & FRANKLIN-TONG, V. E. 2010. Characterization of a legumain/vacuolar processing enzyme and YVADase activity in *Papaver* pollen. *Plant Mol Biol*, 74, 381-93.
- BOU DAHER, F., CHEBLI, Y. & GEITMANN, A. 2009. Optimization of conditions for germination of cold-stored *Arabidopsis thaliana* pollen. *Plant Cell Rep*, 28, 347-57.
- BOZHKOVA, P. V., FILONOVA, L. H., SUAREZ, M. F., HELMERSSON, A., SMERTENKO, A. P., ZHIVOTOVSKY, B. & VON ARNOLD, S. 2004. VEIDase is a principal caspase-like activity involved in plant programmed cell death and essential for embryonic pattern formation. *Cell Death and Differentiation*, 11, 175-182.
- BRADFORD, M. 1976. A rapid and sensitive method for quantitation of microgram quantities of protein utilizing the principle of protein-dye-binding. *Anal Biochem*, 72, 248-254.
- BRAND, U., FLETCHER, J. C., HOBE, M., MEYEROWITZ, E. M. & SIMON, R. 2000. Dependence of stem cell fate in *Arabidopsis* on a feedback loop regulated by CLV3 activity. *Science*, 289, 617-619.
- BREEUWER, P., DROCOURT, J. L., BUNSCHOTEN, N., ZWIETERING, M. H., ROMBOUITS, F. M. & ABEE, T. 1995. Characterization of uptake and hydrolysis of fluorescein diacetate and carboxyfluorescein diacetate by intracellular esterases in *Saccharomyces cerevisiae*, which result in accumulation of fluorescent product. *Applied and Environmental Microbiology*, 61, 1614.
- CABRILLAC, D., COCK, J. M., DUMAS, C. & GAUDE, T. 2001. The S-locus receptor kinase is inhibited by thioredoxins and activated by pollen coat proteins. *Nature*.
- CAI, G. & CRESTI, M. 2009. Organelle motility in the pollen tube: a tale of 20 years. *J Exp Bot*, 60, 495-508.
- CANALES, C., BHATT, A. M., SCOTT, R. & DICKINSON, H. 2002. EXS, a putative LRR receptor kinase, regulates male germline cell number and tapetal identity and promotes seed development in *Arabidopsis*. *Curr Biol*, 12, 1718-27.
- CAPRON, A., GOURGUES, M., NEIVA, L. S., FAURE, J.-E., BERGER, F., PAGNUSSAT, G., KRISHNAN, A., ALVAREZ-MEJIA, C., VIELLE-CALZADA, J.-P., LEE, Y.-R., LIU, B. & SUNDARESAN, V. 2008. Maternal control of male-gamete delivery in *Arabidopsis* involves a putative GPI-anchored protein encoded by the LORELEI gene. *Plant Cell*, 20, 3038-49.
- CARLSSON, C., JONSSON, M. & AKERMAN, B. 1995. Double bands in DNA gel electrophoresis caused by bis-intercalating dyes. *Nucleic Acids Res*, 23, 2413-20.

- CHANG, L. F. & KARIN, M. 2001. Mammalian MAP kinase signalling cascades. *Nature*, 410, 37-40.
- CHARPENTEAU, M., JAWORSKI, K., RAMIREZ, B. C., TRETYN, A., RANJEVA, R. & RANTY, B. 2004. A receptor-like kinase from *Arabidopsis thaliana* is a calmodulin-binding protein. *Biochem J*, 379, 841-8.
- CHEN, G., ZHANG, B., ZHAO, Z., SUI, Z., ZHANG, H. & XUE, Y. 2010. 'A life or death decision' for pollen tubes in S-RNase-based self-incompatibility. *J Exp Bot*, 61, 2027-2037.
- CHENG, S.-H., ZHUANG, J.-Y., FAN, Y.-Y., DU, J.-H. & CAO, L.-Y. 2007. Progress in research and development on hybrid rice: a super-domesticated in China. *Annals of botany*, 100, 959-66.
- CHEUNG, A. Y., BOAVIDA, L. C., AGGARWAL, M., WU, H. M. & FEIJO, J. A. 2010. The pollen tube journey in the pistil and imaging the in vivo process by two-photon microscopy. *J Exp Bot*, 61, 1907-1915.
- CHEUNG, A. Y. & WU, H. M. 1999. Arabinogalactan proteins in plant sexual reproduction. *Protoplasma*, 208, 87-98.
- CHEUNG, A. Y. & WU, H. M. 2008. Structural and signaling networks for the polar cell growth machinery in pollen tubes. *Annual review of plant biology*, 59, 547-72.
- CHEVALIER, D., BATOUX, M., FULTON, L., PFISTER, K., YADAV, R. K., SCHELLENBERG, M. & SCHNEITZ, K. 2005. STRUBBELIG defines a receptor kinase-mediated signaling pathway regulating organ development in Arabidopsis. *Proc Natl Acad Sci USA*, 102, 9074-9.
- CHICHKOVA, N. V., GALIULLINA, R. A., TALIANSKY, M. E. & VARTAPETIAN, A. B. 2008. Tissue disruption activates a plants caspase-like protease with TATD cleavage specificity. *Plant Stress*, 2, 89-95.
- CHICHKOVA, N. V., KIM, S. H., TITOVA, E. S., KALKUM, M., MOROZOV, V. S., RUBTSOV, Y. P., KALININA, N. O., TALIANSKY, M. E. & VARTAPETIAN, A. B. 2004. A plant caspase-like protease activated during the hypersensitive response. *Plant Cell*, 16, 157-71.
- CHICHKOVA, N. V., SHAW, J., GALIULLINA, R. A., DRURY, G. E., TUZHIKOV, A. I., KIM, S. H., KALKUM, M., HONG, T. B., GORSHKOVA, E. N., TORRANCE, L., VARTAPETIAN, A. B. & TALIANSKY, M. 2010. Phytaspase, a relocatable cell death promoting plant protease with caspase specificity. *Embo Journal*, 29, 1149-1161.
- CHISHOLM, S. T., COAKER, G., DAY, B. & STASKAWICZ, B. J. 2006. Host-microbe interactions: shaping the evolution of the plant immune response. *Cell*, 124, 803-814.
- CHO, S. K., LARUE, C. T., CHEVALIER, D., WANG, H., JINN, T.-L., ZHANG, S. & WALKER, J. C. 2008. Regulation of floral organ abscission in *Arabidopsis thaliana*. *Proc Natl Acad Sci USA*, 105, 15629-34.
- CHOW, B. & MCCOURT, P. 2006. Plant hormone receptors: perception is everything. *Genes & Development*, 20, 1998-2008.
- CHRISTOFFERSON, D. E. & YUAN, J. 2010. Necroptosis as an alternative form of programmed cell death. *Current Opinion in Cell Biology*, 22, 263-8.
- CLARK, S. E. 2001. Cell signalling at the shoot meristem. *Nat Rev Mol Cell Biol*, 2, 276-84.
- CLARK, S. E., RUNNING, M. P. & MEYEROWITZ, E. M. 1995. CLAVATA3 is a specific regulator of shoot and floral meristem development affecting the same processes as CLAVATA1. *Development*, 121, 2057-2067.

- CLARK, S. E., WILLIAMS, R. W. & MEYEROWITZ, E. M. 1997. The CLAVATA1 gene encodes a putative receptor kinase that controls shoot and floral meristem size in Arabidopsis. *Cell*, 89, 575-85.
- CLOUSE, S. D. 2011. Brassinosteroid Signal Transduction: From Receptor Kinase Activation to Transcriptional Networks Regulating Plant Development. *Plant Cell*, 23, 1219-30.
- COFFEEN, W. C. & WOLPERT, T. J. 2004. Purification and characterization of serine proteases that exhibit caspase-like activity and are associated with programmed cell death in *Avena sativa*. *Plant Cell*, 16, 857-73.
- COLL, N. S., EPPLE, P. & DANGL, J. L. 2011. Programmed cell death in the plant immune system. *Cell Death and Differentiation*, 1-10.
- COLL, N. S., VERCAMMEN, D., SMIDLER, A., CLOVER, C., VAN BREUSEGEM, F., DANGL, J. L. & EPPLE, P. 2010. Arabidopsis type I metacaspases control cell death. *Science*, 330, 1393-7.
- COOPERMAN, B., BAYKOV, A. & LAHTI, R. 1992. Evolutionary conservation of the active site of soluble inorganic pyrophosphatase. *Trends in biochemical sciences*, 17, 262-266.
- CRAIG, A., EWAN, R., MESMAR, J., GUDIPATI, V. & SADANANDOM, A. 2009. E3 ubiquitin ligases and plant innate immunity. *Journal of Experimental Botany*, 60, 1123-32.
- CRUZ-GARCIA, F., NATHAN HANCOCK, C., KIM, D. & MCCLURE, B. 2005. Styler glycoproteins bind to S-RNase in vitro. *The Plant journal* 42, 295-304.
- DANGL, J. L. & JONES, J. D. 2001. Plant pathogens and integrated defence responses to infection. *Nature*, 411, 826-33.
- DANON, A., ROTARI, V. I., GORDON, A., MAILHAC, N. & GALLOIS, P. 2004. Ultraviolet-C overexposure induces programmed cell death in Arabidopsis, which is mediated by caspase-like activities and which can be suppressed by caspase inhibitors, p35 and Defender against Apoptotic Death. *J Biol Chem*, 279, 779-87.
- DAWSON, J. P., WEINGER, J. S. & ENGELMAN, D. M. 2002. Motifs of serine and threonine can drive association of transmembrane helices. *J Mol Biol*, 316, 799-805.
- DE BUCK, S., PECK, I., DE WILDE, C., MARJANAC, G., NOLF, J., DE PAEPE, A. & DEPICKER, A. 2007. Generation of Single-Copy T-DNA Transformants in Arabidopsis by the CRE/loxP Recombination-Mediated Resolution System. *Plant Physiology*, 145, 1171-1182.
- DE GRAAF, B. H. J., RUDD, J. J., WHEELER, M. J., PERRY, R. M., BELL, E. M., OSMAN, K., FRANKLIN, F. C. H. & FRANKLIN-TONG, V. E. 2006. Self-incompatibility in *Papaver* targets soluble inorganic pyrophosphatases in pollen. *Nature*, 444, 490-3.
- DE SMET, I., VASSILEVA, V., DE RYBEL, B., LEVESQUE, M. P., GRUNEWALD, W., VAN DAMME, D., VAN NOORDEN, G., NAUDTS, M., VAN ISTERDAEL, G., DE CLERCQ, R., WANG, J. Y., MEULI, N., VANNESTE, S., FRIML, J., HILSON, P., JURGENS, G., INGRAM, G. C., INZE, D., BENFEY, P. N. & BEECKMAN, T. 2008. Receptor-Like Kinase ACR4 Restricts Formative Cell Divisions in the Arabidopsis Root. *Science*, 322, 594-597.
- DEBER, C. M., WANG, C., LIU, L. P., PRIOR, A. S., AGRAWAL, S., MUSKAT, B. L. & CUTICCHIA, A. J. 2001. TM Finder: a prediction program for transmembrane protein segments using a combination of hydrophobicity and nonpolar phase helicity scales. *Protein Sci*, 10, 212-9.

- DEL POZO, O. & LAM, E. 1998. Caspases and programmed cell death in the hypersensitive response of plants to pathogens. *Current Biology*, 8, 1129-1132.
- DHARMASIRI, N., DHARMASIRI, S. & ESTELLE, M. 2005. The F-box protein TIR1 is an auxin receptor. *Nature*, 435, 441-5.
- DICKMAN, M. B., PARK, Y. K., OLTERS DORF, T., LI, W., CLEMENTE, T. & FRENCH, R. 2001. Abrogation of disease development in plants expressing animal antiapoptotic genes. *PNAS*, 98.
- DIELEN, A.-S., BADA OUI, S., CANDRESSE, T. & GERMAN-RETANA, S. 2010. The ubiquitin/26S proteasome system in plant-pathogen interactions: a never-ending hide-and-see game. *Molecular Plant Pathology*, 11, 293-308.
- DIXIT, R., RIZZO, C., NASRALLAH, M. & NASRALLAH, J. 2001. The brassica MIP-MOD gene encodes a functional water channel that is expressed in the stigma epidermis. *Plant Mol Biol*, 45, 51-62.
- DODD, A. N., KUDLA, J. & SANDERS, D. 2010. The language of calcium signaling. *Annual review of plant biology*, 61, 593-620.
- DODDS, P. N., CLARKE, A. E. & NEWBIGIN, E. 1996. Molecular characterization of an S-like RNase of *Nicotiana glauca* that is induced by phosphate starvation. *Plant Mol. Biol.*, 31, 227-38.
- DONG, W., NOWARA, D. & SCHWEIZER, P. 2006. Protein polyubiquitination plays a role in basal host resistance of barley. *Plant Cell*, 18, 3321-31.
- DREHER, K. & CALLIS, J. 2007. Ubiquitin, hormones and biotic stress in plants. *Annals of Botany*, 99, 787-822.
- DWIVEDI, S., PEROTTI, E. & ORTIZ, R. 2008. Towards molecular breeding of reproductive traits in cereal crops. *Plant Biotechnology Journal*, 6, 529-59.
- ENTANI, T., IWANO, M., SHIBA, H., CHE, F. S., ISOGAI, A. & TAKAYAMA, S. 2003. Comparative analysis of the self-incompatibility (S-) locus region of *Prunus mume*: identification of a pollen-expressed F-box gene with allelic diversity. *Genes to Cells*, 8, 203-213.
- ESCOBAR-RESTREPO, J.-M., HUCK, N., KESSLER, S. A., GAGLIARDINI, V., GHEYSELINCK, J., YANG, W.-C. & GROSSNIKLAUS, U. 2007. The FERONIA receptor-like kinase mediates male-female interactions during pollen tube reception. *Science*, 317, 656-660.
- ETCHELLS, J. P. & TURNER, S. R. 2010. The PXY-CLE41 receptor ligand pair defines a multifunctional pathway that controls the rate and orientation of vascular cell division. *Development*, 137, 767-74.
- FAN, L. M., WANG, Y. F., WANG, H. & WU, W. H. 2001. In vitro Arabidopsis pollen germination and characterization of the inward potassium currents in Arabidopsis pollen grain protoplasts. *J Exp Bot*, 52, 1603-14.
- FEIJÓ, J. A. 2010. The mathematics of sexual attraction. *J Biol*, 9, 18.
- FEIJÓ, J. A., SAINHAS, J., HOLDAWAY-CLARKE, T., CORDEIRO, M. S., KUNKEL, J. G. & HEPLER, P. K. 2001. Cellular oscillations and the regulation of growth: the pollen tube paradigm. *Bioessays*, 23, 86-94.
- FELDMANN, K. A., COURY, D. A. & CHRISTIANSON, M. L. 1997. Exceptional segregation of a selectable marker (KanR) in Arabidopsis identifies genes important for gametophytic growth and development. *Genetics*, 147, 1411-1422.
- FILONOVA, L. H., BOZHKO V, P. V., BRUKHIN, V. B., DANIEL, G., ZHIVOTOVSKY, B. & VON ARNOLD, S. 2000. Two waves of programmed cell death occur during

- formation and development of somatic embryos in the gymnosperm, Norway spruce. *Journal of Cell Science*, 113 Pt 24, 4399-411.
- FINNEGAN, J. A. M., D. 2004. Transgene inactivation – plants fight back. *Nature Biotechnology*, 12, 883-888.
- FISHER, K. & TURNER, S. 2007. PXY, a receptor-like kinase essential for maintaining polarity during plant vascular-tissue development. *Curr Biol*, 17, 1061-6.
- FLETCHER, J. C., BRAND, U., RUNNING, M. P., SIMON, R. & MEYEROWITZ, E. M. 1999. Signaling of cell fate decisions by CLAVATA3 in Arabidopsis shoot meristems. *Science*, 283, 1911-4.
- FLETCHER, J. C. & MEYEROWITZ, E. M. 2000. Cell signaling within the shoot meristem. *Curr Opin Plant Biol*, 3, 23-30.
- FOOTE, H. C., RIDE, J. P., FRANKLIN-TONG, V. E., WALKER, E. A., LAWRENCE, M. J. & FRANKLIN, F. C. 1994. Cloning and expression of a distinctive class of self-incompatibility (S) gene from *Papaver rhoeas* L. *Proc Natl Acad Sci USA*, 91, 2265-9.
- FRANKLIN-TONG, V. E., DROBAK, B. K., ALLAN, A. C., WATKINS, P. & TREWAVAS, A. J. 1996. Growth of pollen tubes of *Papaver rhoeas* is regulated by a slow-moving calcium wave propagated by inositol 1,4,5-trisphosphate. *Plant Cell*, 8, 1305-1321.
- FRANKLIN-TONG, V. E., HACKETT, G. & HEPLER, P. K. 1997. Ratio-imaging of Ca²⁺ in the self-incompatibility response in pollen tubes of *Papaver rhoeas*. *Plant Journal*, 12, 1375-1386.
- FRANKLIN-TONG, V. E., HOLDAWAY-CLARKE, T. L., STRAATMAN, K. R., KUNKEL, J. G. & HEPLER, P. K. 2002. Involvement of extracellular calcium influx in the self-incompatibility response of *Papaver rhoeas*. *Plant J*, 29, 333-45.
- FRANKLIN-TONG, V. E., RIDE, J. P. & FRANKLIN, F. C. H. 1995. Recombinant stigmatic self-incompatibility (S-) protein elicits Ca²⁺ transient in pollen of *Papaver rhoeas*. *The Plant Journal*, 9, 299-307.
- FRANKLIN-TONG, V. E., RIDE, J. P., READ, N. D., TREWAVAS, A. J. & FRANKLIN, F. C. H. 1993. The self-incompatibility response in *Papaver rhoeas* is mediated by cytosolic free calcium. *The Plant Journal*, 4, 163-177.
- FU, Y. 2010. The actin cytoskeleton and signaling network during pollen tube tip growth. *Journal of Integrative Plant Biology*, 52, 131-7.
- FU, Y., WU, G. & YANG, Z. 2001. Rop GTPase-dependent dynamics of tip-localized F-actin controls tip growth in pollen tubes. *J Cell Biol*, 152, 1019-1032.
- GEITMANN, A. 2010. How to shape a cylinder: pollen tube as a model system for the generation of complex cellular geometry. *Sex Plant Reprod*, 23, 63-71.
- GEITMANN, A., FRANKLIN-TONG, V. E. & EMONS, A. C. 2004. The self-incompatibility response in *Papaver rhoeas* pollen causes early and striking alterations to organelles. *Cell Death Differ*, 11, 812-22.
- GEITMANN, A., SNOWMAN, B. N., EMONS, A. M. & FRANKLIN-TONG, V. E. 2000. Alterations in the actin cytoskeleton of pollen tubes are induced by the self-incompatibility reaction in *Papaver rhoeas*. *Plant Cell*, 12, 1239-51.
- GIFFORD, J. L., WALSH, M. P. & VOGEL, H. J. 2007. Structures and metal-ion-binding properties of the Ca²⁺-binding helix-loop-helix EF-hand motifs. *Biochem J*, 405, 199-221.

- GIFFORD, M. L., ROBERTSON, F. C., D.C., S. & INGRAM, G. C. 2005. ARABIDOPSIS CRINKLY4 Function, Internalization, and Turnover Are Dependent on the Extracellular Crinkly Repeat Domain. *Plant Cell*, 17, 1154-1166.
- GLICKMAN, M. 2000. Getting in and out of the proteasome. *Seminars in Cell and Developmental Biology*, 11, 149-158.
- GÖHRE, V., SPALLEK, T., HÄWEKER, H., MERSMANN, S., MENTZEL, T., BOLLER, T., DE TORRES, M., MANSFIELD, J. W. & ROBATZEK, S. 2008. Plant pattern-recognition receptor FLS2 is directed for degradation by the bacterial ubiquitin ligase AvrPtoB. *Curr Biol*, 18, 1824-32.
- GOLDMAN, M. H., GOLDBERG, R. B. & MARIANI, C. 1994. Female sterile tobacco plants are produced by stigma-specific cell ablation. *EMBO J*, 13, 2976-84.
- GOLDRAIJ, A., KONDO, K., LEE, C. B., HANCOCK, C. N., SIVAGURU, M., VAZQUEZ-SANTANA, S., KIM, S., PHILLIPS, T. E., CRUZ-GARCIA, F. & MCCLURE, B. 2006. Compartmentalization of S-RNase and HT-B degradation in self-incompatible *Nicotiana*. *Nature*, 439, 805-10.
- GÓMEZ-GÓMEZ, L. & BOLLER, T. 2000. FLS2: An LRR Receptor-like Kinase Involved in the Perception of the Bacterial Elicitor Flagellin in Arabidopsis. *Molecular cell*, 5, 1003-1011.
- GRILL, E. & CHRISTMANN, A. 2007. Botany. A plant receptor with a big family. *Science*, 315, 1676-7.
- GROBE, K., BECKER, W. M., SCHLAAK, M. & PETERSEN, A. 1999. Grass group I allergens (beta expansins) are novel, papain-related proteinases. *European Journal of Biochemistry*, 263, 33-40.
- GROLL, M., SCHELLENBERG, B., BACHMANN, A. S., ARCHER, C. R., HUBER, R., POWELL, T. K., LINDOW, S., KAISER, M. & DUDLER, R. 2008. A plant pathogen virulence factor inhibits the eukaryotic proteasome by a novel mechanism. *Nature*, 452, 755-8.
- GROSS, P. & AP REES, T. 1986. Alkaline inorganic pyrophosphatase and starch synthesis in amyloplasts. *Planta*, 167, 140-145.
- GROVE, M. D., SPENCER, G. F., ROHWEDDER, W. K., MANDAVA, N., WORLEY, J. F., WARTHEN, J. D., STEFFENS, G. L., FLIPPEN-ANDERSON, J. L. & COOK, J. C. 1979. Brassinolide, a plant growth-promoting steroid isolated from *Brassica napus* pollen. *Nature*, 281, 216-217.
- GU, C., KOŁODZIEJEK, I., MISAS-VILLAMIL, J., SHINDO, T., COLBY, T., VERDOES, M., RICHAU, K. H., SCHMIDT, J., OVERKLEEF, H. S. & VAN DER HOORN, R. A. L. 2010. Proteasome activity profiling: a simple, robust and versatile method revealing subunit-selective inhibitors and cytoplasmic, defense-induced proteasome activities. *The Plant journal : for cell and molecular biology*, 62, 160-70.
- GUNAWARDENA, A. H. L. A. N., GREENWOOD, J. S. & DENGLER, N. G. 2004. Programmed cell death remodels lace plant leaf shape during development. *Plant Cell*, 16, 60-73.
- HACKAUF, B. & WEHLING, P. 2005. Approaching the self-incompatibility locus Z in rye (*Secale cereale* L.) via comparative genetics. *Theor Appl Genet*, 110, 832-45.
- HADJIOSIF, N. E. 2008. *Functional characterisation of PrPS, a pollen S locus specific gene that is required for the self-incompatibility reaction in Papaver rhoeas*, PhD Thesis, University of Birmingham.

- HARA, K., KAJITA, R., TORII, K. U., BERGMANN, D. C. & KAKIMOTO, T. 2007. The secretory peptide gene EPF1 enforces the stomatal one-cell-spacing rule. *Genes & Development*, 21, 1720-5.
- HARA, K., YOKOO, T., KAJITA, R., ONISHI, T., YAHATA, S., PETERSON, K. M., TORII, K. U. & KAKIMOTO, T. 2009. Epidermal cell density is autoregulated via a secretory peptide, EPIDERMAL PATTERNING FACTOR 2 in Arabidopsis leaves. *Plant Cell Physiol*, 50, 1019-31.
- HARBORD, R. M., NAPOLI, C. A. & ROBBINS, T. P. 2000. Segregation distortion of T-DNA markers linked to the self-incompatibility (S) locus in *Petunia hybrida*. *Genetics*, 154, 1323-1333.
- HATSUGAI, N., IWASAKI, S., TAMURA, K., KONDO, M., FUJI, K., OGASAWARA, K., NISHIMURA, M. & HARA-NISHIMURA, I. 2009. A novel membrane fusion-mediated plant immunity against bacterial pathogens. *Genes Dev*, 23, 2496-506.
- HATSUGAI, N., KUROYANAGI, M., YAMADA, K., MESHI, T., TSUDA, S., KONDO, M., NISHIMURA, M. & HARA-NISHIMURA, I. 2004. A plant vacuolar protease, VPE, mediates virus-induced hypersensitive cell death. *Science*, 305, 855-8.
- HE, P., SHAN, L. & SHEEN, J. 2007a. Elicitation and suppression of microbe-associated molecular pattern-triggered immunity in plant-microbe interactions. *Cell Microbiology*, 9, 1385-1396.
- HE, R., DRURY, G. E., ROTARI, V. I., GORDON, A., WILLER, M., TABASUM, F., WOLTERING, E. J. & GALLOIS, P. 2007b. Metacaspase-8 modulates programmed cell death induced by UV and H₂O₂ in Arabidopsis. *Journal of Biological Chemistry*, 283, 774-783.
- HE, X. & KERMODE, A. R. 2003. Proteases associated with programmed cell death of megagametophyte cells after germination of white spruce (*Picea glauca*) seeds. *Plant Mol. Biol.*, 52, 729-744.
- HEARN, M. J., FRANKLIN, F. C. H. & RIDE, J. P. 1996. Identification of a membrane glycoprotein in pollen of *Papaver rhoeas* which binds stigmatic self-incompatibility (S-) proteins. *The Plant Journal*, 9, 467-475.
- HEPLER, P. K., VIDALI, L. & CHEUNG, A. Y. 2001. Polarized cell growth in higher plants. *Annu Rev Cell Dev Biol*, 17, 159-87.
- HERSHKO, A. & CIECHANOVER, A. 1998. The ubiquitin system. *Annu Rev Biochem*, 67, 425-79.
- HESLOP-HARRISON, J. 1975. Incompatibility and the pollen-stigma interaction. *Ann. Rev. Plant Physiol*, 26, 403-425.
- HIGASHIYAMA, T. 2002. The synergid cell: attractor and acceptor of the pollen tube for double fertilization. *J Plant Res*, 115, 149-60.
- HIGASHIYAMA, T. 2010. Peptide Signaling in Pollen-Pistil Interactions. *Plant and Cell Physiology*, 51, 177-189.
- HIRAKAWA, Y., SHINOHARA, H., KONDO, Y., INOUE, A., NAKANOMYO, I., OGAWA, M., SAWA, S., OHASHI-ITO, K., MATSUBAYASHI, Y. & FUKUDA, H. 2008. Non-cell-autonomous control of vascular stem cell fate by a CLE peptide/receptor system. *Proc Natl Acad Sci USA*, 105, 15208-13.
- HIROKAWA, T., BOON-CHIENG, S. & MITAKU, S. 1998. SOSUI: classification and secondary structure prediction system for membrane proteins. *Bioinformatics*, 14, 378-9.
- HISCOCK, S. & KÜES, U. 1999. Cellular and molecular mechanisms of sexual incompatibility in plants and fungi. *International review of cytology*, 193, 165-295.

- HISCOCK, S. J. & ALLEN, A. M. 2008. Diverse cell signalling pathways regulate pollen-stigma interactions: the search for consensus. *New Phytologist*, 179, 286-317.
- HOFIUS, D., SCHULTZ-LARSEN, T., JOENSEN, J., TSITSIGIANNIS, D. I., PETERSEN, N. H. T., MATTSSON, O., JORGENSEN, L. B., JONES, J. D. G., MUNDY, J. & PETERSEN, M. 2009. Autophagic components contribute to hypersensitive cell death in Arabidopsis. *Cell*, 137, 773-783.
- HOFMANN, K. & STOFFEL, W. 1993. TMbase - A database of membrane spanning proteins segments. *Biol. Chem. Hoppe-Seyler*, 374, 166.
- HOLDAWAY-CLARKE, T. L., FEIJÓ, J. A., HACKETT, G. R., KUNKEL, J. G. & HEPLER, P. K. 1997. Pollen tube growth and the intracellular cytosolic calcium gradient oscillate in phase while extracellular calcium influx is delayed. *Plant Cell*, 9, 1999-2010.
- HOWDEN, R., PARK, S. K., MOORE, J. M., ORME, J., GROSSNIKLAUS, U. & TWELL, D. 1998. Selection of T-DNA-tagged male and female gametophytic mutants by segregation distortion in Arabidopsis. *Genetics*, 149, 621-31.
- HU, T. T., PATTYN, P., BAKKER, E. G., CAO, J., CHENG, J.-F., CLARK, R. M., FAHLGREN, N., FAWCETT, J. A., GRIMWOOD, J., GUNDLACH, H., HABERER, G., HOLLISTER, J. D., OSSOWSKI, S., OTTILAR, R. P., SALAMOV, A. A., SCHNEEBERGER, K., SPANNAGL, M., WANG, X., YANG, L., NASRALLAH, M. E., BERGELSON, J., CARRINGTON, J. C., GAUT, B. S., SCHMUTZ, J., MAYER, K. F. X., VAN DE PEER, Y., GRIGORIEV, I. V., NORDBORG, M., WEIGEL, D. & GUO, Y.-L. 2011. The *Arabidopsis lyrata* genome sequence and the basis of rapid genome size change. *Nat Genet*, 43, 476-81.
- HUA, Z. & KAO, T.-H. 2006. Identification and characterization of components of a putative *Petunia S*-locus F-box-containing E3 ligase complex involved in S-RNase-based self-incompatibility. *Plant Cell*, 18, 2531-53.
- HUA, Z.-H., FIELDS, A. & KAO, T.-H. 2008. Biochemical models for S-RNase-based self-incompatibility. *Mol Plant*, 1, 575-85.
- HUANG, J., ZHAO, L., YANG, Q. & XUE, Y. 2006. AhSSK1, a novel SKP1-like protein that interacts with the S-locus F-box protein SLF. *Plant J*, 46, 780-93.
- HUGOT, K., PONCHET, M., MARAIS, A., RICCI, P. & GALIANA, E. 2002. A tobacco S-like RNase inhibits hyphal elongation of plant pathogens. *Mol Plant Microbe Interact*, 15, 243-50.
- HULL, R. A. C., S.N. 1983. Replication of cauliflower mosaic virus DNA. *Sci. Prog. Oxf.*, 68, 403-422.
- HUNT, L. & GRAY, J. E. 2009. The signaling peptide EPF2 controls asymmetric cell divisions during stomatal development. *Curr Biol*, 19, 864-9.
- HUSSEY, P. J., KETELAAR, T. & DEEKS, M. J. 2006. Control of the actin cytoskeleton in plant cell growth. *Annual Review in Plant Biology*, 57, 109-125.
- IKEDA, S., NASRALLAH, J. B., DIXIT, R., PREISS, S. & NASRALLAH, M. E. 1997. An aquaporin-like gene required for the *Brassica* self-incompatibility response. *Science*, 276, 1564-1566.
- INITIATIVE, A. G. 2000. Analysis of the genome sequence of the flowering plant *Arabidopsis thaliana*. *Nature*, 408, 796-815.
- ITO, Y., NAKANOMYO, I., MOTOSE, H., IWAMOTO, K., SAWA, S., DOHMAE, N. & FUKUDA, H. 2006. Dodeca-CLE peptides as suppressors of plant stem cell differentiation. *Science*, 313, 842-5.

- IVANOV, R., FOBIS-LOISY, I. & GAUDE, T. 2010. When no means no: guide to Brassicaceae self-incompatibility. *Trends in Plant Science*.
- IVANOV, R. & GAUDE, T. 2009. Brassica self-incompatibility: a glimpse below the surface. *Plant Signal Behav*, 4, 996-8.
- IWANO, M., ENTANI, T., SHIBA, H., KAKITA, M., NAGAI, T., MIZUNO, H., MIYAWAKI, A., SHOJI, T., KUBO, K., ISOGAI, A. & TAKAYAMA, S. 2009. Fine-Tuning of the Cytoplasmic Ca²⁺ Concentration Is Essential for Pollen Tube Growth. *Plant Physiol*, 150, 1322-1334.
- IWANO, M., SHIBA, H., MATOBA, K., MIWA, T., FUNATO, M., ENTANI, T., NAKAYAMA, P., SHIMOSATO, H., TAKAOKA, A., ISOGAI, A. & TAKAYAMA, S. 2007. Actin Dynamics in Papilla Cells of *Brassica rapa* during Self- and Cross-Pollination. *Plant Physiol*, 144, 72-81.
- IYER, K., BÜRKLE, L., AUERBACH, D., THAMINY, S., DINKEL, M., ENGELS, K. & STAGLJAR, I. 2005. Utilizing the Split-Ubiquitin Membrane Yeast Two-Hybrid System to Identify Protein-Protein Interactions of Integral Membrane Proteins *Science*, 2005, p13.
- JACKSON, P., ELDRIDGE, A., FREED, E., FURSTENTHAL, L., HSU, J. Y., K, K. B. & REIMANN, J. D. 2000. The lore of the RINGs: substrate recognition and catalysis by ubiquitin ligases. *Trends in cell biology*, 10, 429-439.
- JAILLAIS, Y., HOTHORN, M., BELKHADIR, Y., DABI, T., NIMCHUK, Z. L., MEYEROWITZ, E. M. & CHORY, J. 2011. Tyrosine phosphorylation controls brassinosteroid receptor activation by triggering membrane release of its kinase inhibitor. *Genes & Development*, 25, 232-7.
- JEONG, S., TROTOCHAUD, A. E. & CLARK, S. E. 1999. The Arabidopsis CLAVATA2 gene encodes a receptor-like protein required for the stability of the CLAVATA1 receptor-like kinase. *Plant Cell*, 11, 1925-34.
- JIA, G., LIU, X., OWEN, H. A. & ZHAO, D. 2008. Signaling of cell fate determination by the TPD1 small protein and EMS1 receptor kinase. *PNAS*, 105, 2220-2225.
- JIA, Y., MCADAMS, S. A., BRYAN, G. T., HERSHEY, H. P. & VALENT, B. 2000. Direct interaction of resistance gene and avirulence gene products confers rice blast resistance. *The EMBO Journal*, 19, 4004-14.
- JOHNSON-BROUSSEAU, S. A. & MCCORMICK, S. 2004. A compendium of methods useful for characterizing Arabidopsis pollen mutants and gametophytically-expressed genes. *Plant J*, 39, 761-75.
- JONES, A. M. & ASSMANN, S. M. 2004. Plants: the latest model system for G-protein research. *EMBO Rep*, 5, 572-8.
- JONES, J. D. G. & DANGL, J. L. 2006. The plant immune system. *Nature*, 444, 323-329.
- JORDAN, N. D., FRANKLIN, F. C. & FRANKLIN-TONG, V. E. 2000. Evidence for DNA fragmentation triggered in the self-incompatibility response in pollen of *Papaver rhoeas*. *Plant J*, 23, 471-9.
- JORDAN, N. D., KAKEDA, K., CONNER, A., RIDE, J. P., FRANKLIN-TONG, V. E. & FRANKLIN, F. C. 1999. S-protein mutants indicate a functional role for SBP in the self-incompatibility reaction of *Papaver rhoeas*. *Plant J*, 20, 119-25.
- JORGENSEN, R. A., CLUSTER, P. D., ENGLISH, J., QUE, Q. & NAPOLI, C. A. 1996. Chalcone synthase cosuppression phenotypes in *Petunia* flowers: comparison of sense vs. antisense constructs and single-copy vs. complex T-DNA sequences. *Plant Mol. Biol.*, 31, 957-973.

- JUÁREZ-DÍAZ, J. A., MCCLURE, B., VÁZQUEZ-SANTANA, S., GUEVARA-GARCÍA, A., LEÓN-MEJÍA, P., MÁRQUEZ-GUZMÁN, J. & CRUZ-GARCÍA, F. 2006. A novel thioredoxin h is secreted in *Nicotiana glauca* and reduces S-RNase in vitro. *J Biol Chem*, 281, 3418-24.
- JURETIĆ, D., ZORANIĆ, L. & ZUCIĆ, D. 2002. Basic charge clusters and predictions of membrane protein topology. *J Chem Inf Comput Sci*, 42, 620-32.
- KACHROO, A., SCHOPFER, C. R., NASRALLAH, M. E. & NASRALLAH, J. B. 2001. Allele-specific receptor-ligand interactions in *Brassica* self-incompatibility. *Science*, 293, 1824-6.
- KAKEDA, K., JORDAN, N. D., CONNER, A., RIDE, J. P., FRANKLIN-TONG, V. E. & FRANKLIN, F. C. 1998. Identification of residues in a hydrophilic loop of the *Papaver rhoeas* S protein that play a crucial role in recognition of incompatible pollen. *Plant Cell*, 10, 1723-32.
- KÄLL, L., KROGH, A. & SONNHAMMER, E. L. L. 2004. A combined transmembrane topology and signal peptide prediction method. *J Mol Biol*, 338, 1027-36.
- KAO, T.-H. & TSUKAMOTO, T. 2004. The molecular and genetic bases of S-RNase-based self-incompatibility. *Plant Cell*, 16 Suppl, S72-S83.
- KATSIR, L., SCHILMILLER, A. L., STASWICK, P. E., HE, S. Y. & HOWE, G. A. 2008. COI1 is a critical component of a receptor for jasmonate and the bacterial virulence factor coronatine. *Proc Natl Acad Sci USA*, 105, 7100-5.
- KAUR, J. & BACHHAWAT, A. K. 2009. A modified Western blot protocol for enhanced sensitivity in the detection of a membrane protein. *Analytical Biochemistry*, 384, 348-9.
- KEMP, B. P. & DOUGHTY, J. 2007. S cysteine-rich (SCR) binding domain analysis of the *Brassica* self-incompatibility S-locus receptor kinase. *New Phytologist*, 175, 619-629.
- KEPINSKI, S. & LEYSER, O. 2005. The Arabidopsis F-box protein TIR1 is an auxin receptor. *Nature*, 435, 446-51.
- KIM, H. S., JUNG, M. S., LEE, K., KIM, K. E., YOO, J. H., KIM, M. C., KIM, D. H., CHO, M. J. & CHUNG, W. S. 2009. An S-locus receptor-like kinase in plasma membrane interacts with calmodulin in Arabidopsis. *FEBS Lett*, 583, 36-42.
- KIM, M., AHN, J.-W., JIN, U.-H., CHOI, D., PAEK, K.-H. & PAI, H.-S. 2003. Activation of the Programmed Cell Death Pathway by Inhibition of Proteasome Function in Plants. *Journal of Biological Chemistry*, 278, 19406-19415.
- KIM, S. T., ZHANG, K., DONG, J. & LORD, E. M. 2006. Exogenous free ubiquitin enhances lily pollen tube adhesion to an in vitro stylar matrix and may facilitate endocytosis of SCA. *Plant Physiol*, 142, 1397-411.
- KINOSHITA, T., CAÑO-DELGADO, A., SETO, H., HIRANUMA, S., FUJIOKA, S., YOSHIDA, S. & CHORY, J. 2005. Binding of brassinosteroids to the extracellular domain of plant receptor kinase BRI1. *Nature*, 433, 167-71.
- KISSELEV, A. F., GARCIA-CALVO, M., OVERKLEEF, H. S., PETERSON, E., PENNINGTON, M. W., PLOEGH, H. L., THORNBERRY, N. A. & GOLDBERG, A. L. 2003. The caspase-like sites of proteasomes, their substrate specificity, new inhibitors and substrates, and allosteric interactions with the trypsin-like sites. *J Biol Chem*, 278, 35869-77.
- KISSELEV, A. F. & GOLDBERG, A. L. 2001. Proteasome inhibitors: from research tools to drug candidates. *Chem Biol*, 8, 739-58.

- KITASHIBA, H., LIU, P., NISHIO, T., NASRALLAH, J. B. & NASRALLAH, M. E. 2011. Functional test of *Brassica* self-incompatibility modifiers in *Arabidopsis thaliana*. *Proceedings of the National Academy of Sciences*, 108, 18173-18178.
- KLAAS, M., YANG, B., BOSCH, M., THOROGOOD, D., MANZANARES, C., ARMSTEAD, I. P., FRANKLIN, F. C. H. & BARTH, S. 2011. Progress towards elucidating the mechanisms of self-incompatibility in the grasses: further insights from studies in *Lolium*. *Annals of Botany*, 108, 677-85.
- KOLODZIEJEK, I., MISAS-VILLAMIL, J. C., KASCHANI, F., CLERC, J., GU, C., KRAHN, D., NIESSEN, S., VERDOES, M., WILLEMS, L. I., OVERKLEEF, H. S., KAISER, M. & VAN DER HOORN, R. A. L. 2011. Proteasome activity imaging and profiling characterizes bacterial effector syringolin A. *Plant Physiol*, 155, 477-89.
- KOMANDER, D. 2009. The emerging complexity of protein ubiquitination. *Biochem Soc Trans*, 37, 937-53.
- KORTHOOT, H. A., BERECKI, G., BRUIN, W., VAN DUIJN, B. & WANG, M. 2000. The presence and subcellular localization of caspase 3-like proteinases in plant cells. *FEBS Letters*, 475, 139-144.
- KROEMER, G., GALLUZZI, L., VANDENABEELE, P., ABRAMS, J., ALNEMRI, E. S., BAEHRECKE, E. H., BLAGOSKLONNY, M. V., EL-DEIRY, W. S., GOLSTEIN, P., GREEN, D. R., HENGARTNER, M., KNIGHT, R. A., KUMAR, S., LIPTON, S. A., MALORNI, W., NUÑEZ, G., PETER, M. E., TSCHOPP, J., YUAN, J., PIACENTINI, M., ZHIVOTOVSKY, B., MELINO, G. & 2009, N. C. O. C. D. 2009. Classification of cell death: recommendations of the Nomenclature Committee on Cell Death 2009. *Cell Death and Differentiation*, 16, 3-11.
- KROGH, A., LARSSON, B., VON HEIJNE, G. & SONNHAMMER, E. L. 2001. Predicting transmembrane protein topology with a hidden Markov model: application to complete genomes. *Journal of Molecular Biology*, 305, 567-580.
- KROJ, T., RUDD, J., NÜRNBERGER, T., GÄBLER, Y., LEE, J. & SCHEEL, D. 2003. Mitogen-activated protein kinases play an essential role in oxidative burst-independent expression of pathogenesis-related genes in parsley. *Journal of Biological Chemistry*, 278, 2256-2264.
- KUBO, K., ENTANI, T., TAKARA, A., WANG, N., FIELDS, A. M., HUA, Z. H., TOYODA, M., KAWASHIMA, S., ANDO, T., ISOGAI, A., KAO, T. & TAKAYAMA, S. 2010. Collaborative Non-Self Recognition System in S-RNase-Based Self-Incompatibility. *Science*, 330, 796-799.
- KUREPA, J. & SMALLE, J. A. 2008. Structure, function and regulation of plant proteasomes. *Biochimie*, 90, 324-35.
- KUROYANAGI, M., YAMADA, K., HATSUGAI, N., KONDO, M., NISHIMURA, M. & HARA-NISHIMURA, I. 2005. Vacuolar processing enzyme is essential for mycotoxin-induced cell death in *Arabidopsis thaliana*. *J Biol Chem*, 280, 32914-20.
- KURUP, S., RIDE, J. P., JORDAN, N. D., FLETCHER, G., FRANKLIN-TONG, V. E. & FRANKLIN, F. C. H. 1998. Identification and cloning of related self-incompatibility *S*-genes in *Papaver rhoas* and *Papaver nudicaule*. *Sexual Plant Reproduction*, 11, 192-198.
- LAI, Z., MA, W. S., HAN, B., LIANG, L. Z., ZHANG, Y. S., F, H. G. & XUE, Y. B. 2002. An F-box gene linked to the self-incompatibility (*S*) locus of *Antirrhinum* is expressed specifically in pollen and tapetum. *Plant Molecular Biology*, 50, 29-42.

- LEE, D. H. & GOLDBERG, A. L. 1998. Proteasome inhibitors: valuable new tools for cell biologists. *Trends Cell Biol*, 8, 397-403.
- LEE, H. S., HUANG, S. & KAO, T. 1994. S proteins control rejection of incompatible pollen in *Petunia inflata*. *Nature*, 367, 560-3.
- LI, S., SAMAJ, J. & FRANKLIN-TONG, V. E. 2007. A Mitogen-Activated Protein Kinase Signals to Programmed Cell Death Induced by Self-Incompatibility in *Papaver* Pollen. *Plant Physiol*, 145, 236-245.
- LIGTERINK, W., KROJ, T., NIEDEN, U., HIRT, H. & SCHEEL, D. 1997. Receptor-mediated activation of a MAP kinase in pathogen defense of plants. *Science*, 276, 2054-2057.
- LIMANTON-GREVET, A. & JULLIEN, M. 2001. Agrobacterium-mediated transformation of *Asparagus officinalis*- molecular and genetic analysis of transgenic plants. *Molecular Breeding*, 141-150.
- LINCOLN, J. E., RICHAEL, C., OVERDUIN, B., SMITH, K., BOSTOCK, R. & GILCHRIST, D. G. 2002. Expression of the antiapoptotic baculovirus p35 gene in tomato blocks programmed cell death and provides broad-spectrum resistance to disease. *PNAS*, 99, 15217-15221.
- LIU, B., MORSE, D. & CAPPADOCIA, M. 2009. Compatible Pollinations in *Solanum chacoense* Decrease Both S-RNase and S-RNase mRNA. *PLoS One*, 4, 5774.
- LIU, C., APODACA, J., DAVIS, L. & RAO, H. 2007a. Proteasome inhibition in wild-type yeast *Saccharomyces cerevisiae* cells. *Biotech.*, 42, 158-162.
- LIU, X., YUE, Y., LI, B., NIE, Y., LI, W., WU, W.-H. & MA, L. 2007b. A G protein-coupled receptor is a plasma membrane receptor for the plant hormone abscisic acid. *Science*, 315, 1712-6.
- LIU, Z.-Q., XU, G.-H. & ZHANG, S.-L. 2007c. *Pyrus pyrifolia* stylar S-RNase induces alterations in the actin cytoskeleton in self-pollen and tubes in vitro. *Protoplasma*, 232, 61-7.
- LOCKSHIN, R. A. & ZAKERI, Z. 2004. John Wiley & Sons.
- LORD, E. M. & RUSSELL, S. D. 2002. The mechanisms of pollination and fertilization in plants. *Annu Rev Cell Dev Biol*, 18, 81-105.
- LUIK, R. M., WANG, B., PRAKRIYA, M., WU, M. M. & LEWIS, R. S. 2008. Oligomerization of STIM1 couples ER calcium depletion to CRAC channel activation. *Nature*, 454, 538-42.
- MA, W. & BERKOWITZ, G. A. 2007. The grateful dead: calcium and cell death in plant innate immunity. *Cell Microbiol*, 9, 2571-2585.
- MALHÓ, R. 2006. *The pollen tube: a model system for cell and molecular biology studies*.
- MALHÓ, R., READ, N. D., PAIS, M. S. & TREWAVAS, A. J. 1994. Role of cytosolic free calcium in the reorientation of pollen tube growth. *The Plant Journal*, 5, 331-341.
- MALHO, R. & TREWAVAS, A. J. 1996. Localized apical increases of cytosolic free calcium control pollen tube orientation. *The Plant Cell*, 8, 1935-1949.
- MÁRTON, M. L., CORDTS, S., BROADHVEST, J. & DRESSELHAUS, T. 2005. Micropylar pollen tube guidance by egg apparatus 1 of maize. *Science*, 307, 573-576.
- MATSUBAYASHI, Y. 2003. Ligand-receptor pairs in plant peptide signaling. *J Cell Sci*, 116, 3863-70.
- MATSUBAYASHI, Y. & SAKAGAMI, Y. 2006. Peptide hormones in plants. *Annual review of plant biology*, 57, 649-74.

- MATTON, D. P., MAES, O., LAUBLIN, G., XIKE, Q., BERTRAND, C., MORSE, D. & CAPPADOCIA, M. 1997. Hypervariable domains of self-incompatibility RNases mediate allele-specific pollen recognition. *Plant Cell*, 9, 1757-1766.
- MATZKE, A. J. & MATZKE, M. A. 1998. Position effects and epigenetic silencing of plant transgenes. *Curr Opin Plant Biol*, 1, 142-8.
- MAYFIELD, J. A. & PREUSS, D. 2000. Rapid initiation of *Arabidopsis* pollination requires the oleosin-domain protein GRP17. *Nature cell biology*, 2, 128-130.
- MCCLAIN, M. S., IWAMOTO, H., CAO, P., VINION-DUBIEL, A. D., LI, Y., SZABO, G., SHAO, Z. & COVER, T. L. 2003. Essential Role of a GXXXG Motif for Membrane Channel Formation by *Helicobacter pylori* Vacuolating Toxin. *Journal of Biological Chemistry*, 278, 12101-12108.
- MCCLURE, B. 2006. New views of S-RNase-based self-incompatibility. *Curr Opin Plant Biol*, 9, 639-46.
- MCCLURE, B. 2009. Darwin's foundation for investigating self-incompatibility and the progress toward a physiological model for S-RNase-based SI. *Journal of Experimental Botany*, 60, 1069-1081.
- MCCLURE, B., CRUZ-GARCÍA, F. & ROMERO, C. 2011. Compatibility and incompatibility in S-RNase-based systems. *Annals of Botany*, 108, 647-58.
- MCCLURE, B. A. & FRANKLIN-TONG, V. E. 2006. Gametophytic self-incompatibility: understanding the cellular mechanisms involved in "self" pollen tube inhibition. *Planta*, 224, 233-45.
- MCCLURE, B. A., HARING, V., EBERT, P. R., ANDERSON, M. A. & SIMPSON, R. J. 1989. Style self-incompatibility gene products of *Nicotiana glauca* are ribonucleases. *Nature*, 342, 955-957.
- MCCLURE, B. A., MOU, B., CANEVASCINI, S. & BERNATZKY, R. 1999. A small asparagine-rich protein required for S-allele-specific pollen rejection in *Nicotiana glauca*. *Proc Natl Acad Sci USA*, 96, 13548-13553.
- MENG, X., SUN, P. & KAO, T.-H. 2011. S-RNase-based self-incompatibility in *Petunia inflata*. *Annals of Botany*, 108, 637-46.
- MICHARD, E., ALVES, F. & FEIJO, J. A. 2009. The role of ion fluxes in polarized cell growth and morphogenesis: the pollen tube as an experimental paradigm. *International Journal of Developmental Biology*, 53, 1609-1622.
- MITTLER, R., VANDERAUWERA, S., GOLLERY, M. & VAN BREUSEGEM, F. 2004. Reactive oxygen gene network of plants. *Trends Plant Sci*, 9, 490-8.
- MLEJNEK, P. & PROCHAZKA, S. 2002. Activation of caspase-like proteases and induction of apoptosis by isopentenyladenosine tobacco BY-2 cells. *Planta*, 215, 158-166.
- MOSCATELLI, A. & IDILLI, A. I. 2009. Pollen tube growth: a delicate equilibrium between secretory and endocytic pathways. *Journal of Integrative Plant Biology*, 51, 727-39.
- MURASE, K., SHIBA, H., IWANO, M., CHE, F.-S., WATANABE, M., ISOGAI, A. & TAKAYAMA, S. 2004. A membrane-anchored protein kinase involved in *Brassica* self-incompatibility signaling. *Science*, 303, 1516-9.
- MUSKENS, M. W., VISSERS, A. P., MOL, J. N. & KOOTER, J. M. 2000. Role of inverted DNA repeats in transcriptional and post-transcriptional gene silencing. *Plant Mol Biol*, 43, 243-60.
- NAKAUNE, S., YAMADA, K., KONDO, M., KATO, T., TABATA, S., NISHIMURA, M. & HARA-NISHIMURA, I. 2005. A vacuolar processing enzyme, δ VPE, is involved

- in seed coat formation at the early stage of seed development. *The Plant Cell* 17, 876-887.
- NASRALLAH, J. B. 2002. Recognition and rejection of self in plant reproduction. *Science*, 296, 305-8.
- NASRALLAH, J. B. 2005. Recognition and rejection of self in plant self-incompatibility: comparisons to animal histocompatibility. *Trends Immunol*, 26, 412-8.
- NASRALLAH, J. B., LIU, P., SHERMAN-BROYLES, S., SCHMIDT, R. & NASRALLAH, M. E. 2007. Epigenetic mechanisms for breakdown of self-incompatibility in interspecific hybrids. *Genetics*, 175, 1965-1973.
- NASRALLAH, M. E., LIU, P. & NASRALLAH, J. B. 2002. Generation of Self-Incompatible *Arabidopsis thaliana* by Transfer of Two *S* Locus Genes from *A. lyrata*. *Science*, 297, 247-249.
- NASRALLAH, M. E., LIU, P., SHERMAN-BROYLES, S., BOGGS, N. A. & NASRALLAH, J. B. 2004. Natural variation in expression of self-incompatibility in *Arabidopsis thaliana*: implications for the evolution of selfing. *Proc Natl Acad Sci USA*, 101, 16070-4.
- NIMCHUK, Z., EULGEM, T., HOLT, B. F. & DANGL, J. L. 2003. Recognition and response in the plant immune system. *Annual Review of Genetics*, 37, 579-609.
- OBERST, A., BENDER, C. & GREEN, D. R. 2008. Living with death: the evolution of the mitochondrial pathway of apoptosis in animals. *Cell Death and Differentiation*, 15, 1139-46.
- OGAWA, M., SHINOHARA, H., SAKAGAMI, Y. & MATSUBAYASHI, Y. 2008. Arabidopsis CLV3 peptide directly binds CLV1 ectodomain. *Science*, 319, 294.
- OH, M.-H., WANG, X., KOTA, U., GOSHE, M. B., CLOUSE, S. D. & HUBER, S. C. 2009. Tyrosine phosphorylation of the BRI1 receptor kinase emerges as a component of brassinosteroid signaling in Arabidopsis. *Proc Natl Acad Sci USA*, 106, 658-63.
- OH, M.-H., WANG, X., WU, X., ZHAO, Y., CLOUSE, S. D. & HUBER, S. C. 2010. Autophosphorylation of Tyr-610 in the receptor kinase BAK1 plays a role in brassinosteroid signaling and basal defense gene expression. *Proc Natl Acad Sci USA*, 107, 17827-32.
- OHASHI-ITO, K., ODA, Y. & FUKUDA, H. 2010. Arabidopsis VASCULAR-RELATED NAC-DOMAIN6 directly regulates the genes that govern programmed cell death and secondary wall formation during xylem differentiation. *Plant Cell*, 22, 3461-73.
- OKUDA, S., TSUTSUI, H., SHIINA, K., SPRUNCK, S., TAKEUCHI, H., YUI, R., KASAHARA, R. D., HAMAMURA, Y., MIZUKAMI, A., SUSAKI, D., KAWANO, N., SAKAKIBARA, T., NAMIKI, S., ITOH, K., OTSUKA, K., MATSUZAKI, M., NOZAKI, H., KUROIWA, T., NAKANO, A., KANAOKA, M. M., DRESSELHAUS, T., SASAKI, N. & HIGASHIYAMA, T. 2009. Defensin-like polypeptide LUREs are pollen tube attractants secreted from synergid cells. *Nature*, 458, 357-61.
- PAGE, D. R. & GROSSNIKLAUS, U. 2002. The art and design of genetic screens: *Arabidopsis thaliana*. *Nat Rev Genet*, 3, 124-36.
- PALANIVELU, R., BRASS, L., EDLUND, A. F. & PREUSS, D. 2003. Pollen tube growth and guidance is regulated by POP2, an Arabidopsis gene that controls GABA levels. *Cell*, 114, 47-59.
- PARK, S. Y., JAUH, G. Y., MOLLET, J. C., ECKARD, K. & M, L. E. 2000. A lipid transfer-like protein is necessary for lily pollen tube adhesion to an in vitro stylar matrix. *The Plant Cell* 12, 151-163.

- PELLETIER, G. & BUDAR, F. 2007. The molecular biology of cytoplasmically inherited male sterility and prospects for its engineering. *Curr Opin Biotechnol*, 18, 121-5.
- PETERSEN, T. N., BRUNAK, S., VON HEIJNE, G. & NIELSEN, H. 2011. SignalP 4.0: discriminating signal peptides from transmembrane regions. *Nature Methods*, 8, 785-786.
- PISZCZEK, E. & WOJCIECH, G. 2007. Caspase-like proteases and their role in programmed cell death in plants. *Acta Physiol Plant*, 29, 391-398.
- POTOCKÝ, M., JONES, M. A., BEZVODA, R., SMIRNOFF, N. & ŽÁRSKÝ, V. 2007. Reactive oxygen species produced by NADPH oxidase are involved in pollen tube growth. *New Phytologist*, 174, 742-751.
- POULTER, N. S., BOSCH, M. & FRANKLIN-TONG, V. E. 2011. Proteins implicated in mediating self-incompatibility-induced alterations to the actin cytoskeleton of *Papaver* pollen. *Annals of botany*, 1-17.
- POULTER, N. S., STAIGER, C. J., RAPPOPORT, J. Z. & FRANKLIN-TONG, V. E. 2010a. Actin-binding proteins implicated in the formation of the punctate actin foci stimulated by the self-incompatibility response in *Papaver*. *Plant Physiol*, 152, 1274-83.
- POULTER, N. S., VATOVEC, S. & FRANKLIN-TONG, V. E. 2008. Microtubules are a target for self-incompatibility signaling in *Papaver* pollen. *Plant Physiol*, 146, 1358-67.
- POULTER, N. S., WHEELER, M. J., BOSCH, M. & FRANKLIN-TONG, V. E. 2010b. Self-incompatibility in *Papaver*: identification of the pollen S-determinant PrpS. *Biochem Soc Trans*, 38, 588-92.
- PRADO, A. M., COLAÇO, R., MORENO, N., SILVA, A. C. & FEIJÓ, J. A. 2008. Targeting of pollen tubes to ovules is dependent on nitric oxide (NO) signaling. *Molecular Plant*, 1, 703-714.
- PRAKRIYA, M., FESKE, S., GWACK, Y., SRIKANTH, S., RAO, A. & HOGAN, P. G. 2006. Orai1 is an essential pore subunit of the CRAC channel. *Nature*, 443, 230-3.
- QIAO, H., WANG, F., ZHAO, L., ZHOU, J., LAI, Z., ZHANG, Y., ROBBINS, T. P. & XUE, Y. 2004a. The F-box protein AhSLF-S2 controls the pollen function of S-RNase based self-incompatibility. *The Plant Cell*, 16, 2307-2322.
- QIAO, H., WANG, H., ZHAO, L., ZHOU, J., HUANG, J., ZHANG, Y. & XUE, Y. 2004b. The F-Box protein AhSLF-S2 physically interacts with S-RNases that may be inhibited by the ubiquitin/26S proteasome pathway of protein degradation during compatible pollination in *Antirrhinum*. *The Plant Cell*, 16, 582-595.
- QIN, Y., LEYDON, A. R., MANZIELLO, A., PANDEY, R., MOUNT, D., DENIC, S., VASIC, B., JOHNSON, M. A. & PALANIVELU, R. 2009. Penetration of the Stigma and Style Elicits a Novel Transcriptome in Pollen Tubes, Pointing to Genes Critical for Growth in a Pistil. *PLoS Genet*, 5, e1000621.
- REA, A. C., LIU, P. & NASRALLAH, J. B. 2010. A transgenic self-incompatible *Arabidopsis thaliana* model for evolutionary and mechanistic studies of crucifer self-incompatibility. *Journal of Experimental Botany*, 61, 1897-1906.
- REDDY, G. V. & MEYEROWITZ, E. M. 2005. Stem-cell homeostasis and growth dynamics can be uncoupled in the *Arabidopsis* shoot apex. *Science*, 310, 663-7.
- RIVAS, S., ROUGON-CARDOSO, A., SMOKER, M., SCHAUSER, L., YOSHIOKA, H. & JONES, J. D. G. 2004. CITRX thioredoxin interacts with the tomato Cf-9 resistance protein and negatively regulates defence. *The EMBO Journal*, 23, 2156-65.

- ROSEBROCK, T. R., ZENG, L., BRADY, J. J., ABRAMOVITCH, R. B., XIAO, F. & MARTIN, G. B. 2007. A bacterial E3 ubiquitin ligase targets a host protein kinase to disrupt plant immunity. *Nature*, 448, 370-4.
- ROST, B. & LIU, J. 2003. The PredictProtein server. *Nucleic Acids Res*, 31, 3300-4.
- RUDD, J. J., FRANKLIN, F., LORD, J. M. & FRANKLIN-TONG, V. E. 1996. Increased phosphorylation of a 26-kD pollen protein is induced by the self-incompatibility response in *Papaver rhoeas*. *Plant Cell*, 8, 713-724.
- RUDD, J. J., OSMAN, K., FRANKLIN, F. C. H. & FRANKLIN-TONG, V. E. 2003. Activation of a putative MAP kinase in pollen is stimulated by the self-incompatibility (SI) response. *FEBS Lett*, 547, 223-7.
- RUDOLPH, T. D. Year. Segregation for chlorophyll deficiencies and other phenodeviants in the X1 and the X2 generations of irradiated jack pine. *In: Joint Proceedings of the Second Genetics Workshop of the Society of American Foresters and the Seventh Lake States Forest Tree Improvement Conference, May 22 1966.* 18-23.
- SADANANDOM, A., MESMAR, J., YANG, C., EWAN, R., CARR, C. & O'DONNELL, E. 2008. The cell death regulator AtPUB17 directly interacts with the BTB/ POZ domain transcriptional repressor, AtBTB1 to control disease resistance in plants. *Comparative Biochemistry and Physiology, Part A*, 1-2.
- SAMUEL, M. A., CHONG, Y. T., HAASEN, K. E., ALDEA-BRYDGES, M. G., STONE, S. L. & GORING, D. R. 2009. Cellular pathways regulating responses to compatible and self-incompatible pollen in *Brassica* and *Arabidopsis* stigmas intersect at Exo70A1, a putative component of the exocyst complex. *Plant Cell*, 21, 2655-71.
- SAMUEL, M. A., TANG, W., JAMSHED, M., NORTHEY, J., PATEL, D., SMITH, D., SIU, M., MUENCH, D. G., WANG, Z.-Y. & GORING, D. R. 2011. Proteomic analysis of *Brassica* stigmatic proteins following the self-incompatibility reaction reveals a role for microtubule dynamics during pollen responses. *Molecular & cellular proteomics* : MCP [Online]. Available: http://www.ncbi.nlm.nih.gov/entrez/query.fcgi?db=pubmed&cmd=Retrieve&dopt=AbstractPlus&list_uids=21890472 [Accessed Sep 1].
- SCHEER, J. M. & RYAN, C. A. 2002. The systemin receptor SR160 from *Lycopersicon peruvianum* is a member of the LRR receptor kinase family. *Proc Natl Acad Sci USA*, 99, 9585-90.
- SCHOOF, H., LENHARD, M., HAECKER, A., MAYER, K. F., JÜRGENS, G. & LAUX, T. 2000. The stem cell population of *Arabidopsis* shoot meristems is maintained by a regulatory loop between the CLAVATA and WUSCHEL genes. *Cell*, 100, 635-44.
- SCHOPFER, C. R., NASRALLAH, M. E. & NASRALLAH, J. B. 1999. The male determinant of self-incompatibility in *Brassica*. *Science*, 286, 1697-700.
- SCHWESSINGER, B. & ZIPFEL, C. 2008. News from the frontline: recent insights into PAMP-triggered immunity in plants. *Current Opinion in Plant Biology*, 11, 389-395.
- SCOCCIANI, V., OVIDI, E., TADDEI, A. R., TIEZZI, A., CRINELLI, R., GENTILLINI, L. & SPERANZA, A. 2003. Involvement of the ubiquitin/proteasome pathway in the organisation and polarised growth of kiwifruit pollen tubes. *Sex Plant Reprod*, 16, 123-133.
- SENES, A., ENGEL, D. E. & DEGRADO, W. F. 2004. Folding of helical membrane proteins: the role of polar, GxxxG-like and proline motifs. *Curr Opin Struct Biol*, 14, 465-79.
- SERRANO, I., IRENE, S., PELLICCIONE, S., SALVATORE, P., OLMEDILLA, A. & ADELA, O. 2010. Programmed-cell-death hallmarks in incompatible pollen and

- papillar stigma cells of *Olea europaea* L. under free pollination. *Plant Cell Rep*, 29, 561-72.
- SHEMAROVA, I. V. & NESTEROV, V. P. 2005. Evolution of mechanisms of Calcium signaling: the role of Calcium ions in signal transduction in prokaryotes. *Journal of Evolutionary Biochemistry and Physiology*, 41, 12-7.
- SHENG, X., HU, Z., LU, H., WANG, X., BALUSKA, F., SAMAJ, J. & LIN, J. 2006. Roles of the Ubiquitin/Proteasome Pathway in Pollen Tube Growth with Emphasis on MG132-Induced Alterations in Ultrastructure, Cytoskeleton, and Cell Wall Components. *Plant Physiol*, 141, 1578-1590.
- SHENG, X.-Y., DONG, X.-L., ZHANG, S.-S., JIANG, L.-P., ZHU, J. & WANG, L. 2010. Mitochondrial dynamics and its responds to proteasome defection during *Picea wilsonii* pollen tube development. *Cell Biochem. Funct.*, 28, 420-5.
- SHERMAN-BROYLES, S., BOGGS, N., FARKAS, A., LIU, P., VREBALOV, J., NASRALLAH, M. E. & NASRALLAH, J. B. 2007. S-locus genes and the evolution of self-fertility in *Arabidopsis thaliana*. *Plant Cell*, 19, 94-106.
- SHI, Y. 2002. Mechanisms of caspase activation and inhibition during apoptosis. *Molecular cell*, 9, 459-470.
- SHIGAKI, T. & BHATTACHARYYA, M. K. 1999. Color coding the cell death status of plant suspension cells. *BioTechniques*, 26, 1060-2.
- SHIMOSATO, H., YOKOTA, N., SHIBA, H., IWANO, M., ENTANI, T., CHE, F.-S., WATANABE, M., ISOGAI, A. & TAKAYAMA, S. 2007. Characterization of the SP11/SCR high-affinity binding site involved in self/nonself recognition in *Brassica* self-incompatibility. *Plant Cell*, 19, 107-17.
- SHIU, S.-H., KARLOWSKI, W. M., PAN, R., TZENG, Y.-H., MAYER, K. F. X. & LI, W.-H. 2004. Comparative analysis of the receptor-like kinase family in Arabidopsis and rice. *Plant Cell*, 16, 1220-34.
- SHIU, S. H. & BLEECKER, A. B. 2001. Receptor-like kinases from Arabidopsis form a monophyletic gene family related to animal receptor kinases. *Proc Natl Acad Sci USA*, 98, 10763-8.
- SHPAK, E. D., MCABEE, J. M., PILLITTERI, L. J. & TORII, K. U. 2005. Stomatal patterning and differentiation by synergistic interactions of receptor kinases. *Science*, 309, 290-3.
- SIJACIC, P., WANG, X., SKIRPAN, A. L., WANG, Y., DOWD, P. E., MCCUBBIN, A. G., HUANG, S. & KAO, T.-H. 2004. Identification of the pollen determinant of S-RNase-mediated self-incompatibility. *Nature*, 429, 302-305.
- SMALLE, J. & VIERSTRA, R. D. 2004. The ubiquitin 26S proteasome proteolytic pathway. *Annual review of plant biology*, 55, 555-90.
- SMYTH, D. R., BOWMAN, J. L. & MEYEROWITZ, E. M. 1990. Early flower development in Arabidopsis. *Plant Cell*, 2, 755-67.
- SNOWMAN, B. N., GEITMANN, A., CLARKE, S. R., STAIGER, C. J., FRANKLIN, F. C. H., EMONS, A. M. C. & FRANKLIN-TONG, V. E. 2000. Signalling and the Cytoskeleton of Pollen Tubes of *Papaver rhoeas*. *Annals of botany*, 85, 49-57.
- SNOWMAN, B. N., KOVAR, D. R., SHEVCHENKO, G., FRANKLIN-TONG, V. E. & STAIGER, C. J. 2002. Signal-mediated depolymerization of actin in pollen during the self-incompatibility response. *Plant Cell*, 14, 2613-26.
- SOUTHWICK, A. M. & LONG, S. R. 2002. Heterologous expression to assay for plant lectins or receptors. *Plant Molecular Biology Reporter*, 20, 27-41.

- SPARTZ, A. K. & GRAY, W. M. 2008. Plant hormone receptors: new perceptions. *Genes & Development*, 22, 2139-48.
- SPENCER, S. L. & SORGER, P. K. 2011. Measuring and modeling apoptosis in single cells. *Cell*, 144, 926-39.
- SPERANZA, A., SCOCCIANTI, V., CRINELLI, R., CALZONI, G. L. & MAGNANI, M. 2001. Inhibition of proteasome activity strongly affects kiwifruit pollen germination. Involvement of the ubiquitin/proteasome pathway as a major regulator. *Plant Physiol*, 126, 1150-61.
- STAGLJAR, I. & FIELDS, S. 2002. Analysis of membrane protein interactions using yeast-based technologies. *Trends Biochem Sci*, 27, 559-63.
- STAHL, Y. & SIMON, R. 2005. Plant stem cell niches. *Int J Dev Biol*, 49, 479-89.
- STAHL, Y., WINK, R. H., INGRAM, G. C. & SIMON, R. 2009. A Signaling Module Controlling the Stem Cell Niche in Arabidopsis Root Meristems. *Current Biology*, 19, 909-914.
- STEIN, J., HOWLETT, B., BOYES, D., NASRALLAH, M. E. & NASRALLAH, J. B. 1991. Molecular cloning of a putative receptor protein kinase gene encoded at the self-incompatibility locus of *Brassica oleracea*. *PNAS*, 88, 8816-8820.
- STEIN, J. C., DIXIT, R., NASRALLAH, M. E. & NASRALLAH, J. B. 1996. SRK, the stigma-specific *S* locus receptor kinase of *Brassica*, is targeted to the plasma membrane in transgenic tobacco. *Plant Cell*, 8, 429-445.
- STENNICKE, H. R. & SALVESEN, G. S. 2000. Caspases-controlling intracellular signals by protease zymogen activation. *Biochemica et Biophysica Acta* 1477, 299-306.
- STENVIK, G.-E., TANDSTAD, N. M., GUO, Y., SHI, C.-L., KRISTIENSEN, W., HOLMGREN, A., CLARK, S. E., AALEN, R. B. & BUTENKO, M. A. 2008. The EPIP peptide of INFLORESCENCE DEFICIENT IN ABSCISSION is sufficient to induce abscission in arabidopsis through the receptor-like kinases HAESA and HAESA-LIKE2. *Plant Cell*, 20, 1805-17.
- STEWMAN, S. F., JONES-RHOADES, M., BHIMALAPURAM, P., TCHERNOOKOV, M., PREUSS, D. & DINNER, A. R. 2010. Mechanistic insights from a quantitative analysis of pollen tube guidance. *Bmc Plant Biology*, 10, 32.
- STONE, S. L., ANDERSON, E. M., MULLEN, R. T. & GORING, D. R. 2003. ARC1 Is an E3 Ubiquitin Ligase and Promotes the Ubiquitination of Proteins during the Rejection of Self-Incompatible *Brassica* Pollen. *The Plant Cell*, 15, 885-898.
- STONE, S. L., ARNOLDO, M. & GORING, D. R. 1999. A breakdown of *Brassica* self-incompatibility in ARC1 antisense transgenic plants. *Science*, 286, 1729-1731.
- STRATFORD, S., BARNES, W., HOHORST, D. L., SAGERT, J. G., COTTER, R., GOLUBIEWSKI, A., SHOWALTER, A. M., MCCORMICK, S. & BEDINGER, P. 2001. A leucine-rich repeat region is conserved in pollen-exensin-like (Pex) proteins in monocots and dicots. *Plant Mol. Biol.*, 46, 43-56.
- SUNDSTRÖM, J. F., VACULOVA, A., SMERTENKO, A. P., SAVENKOV, E. I., GOLOVKO, A., MININA, E., TIWARI, B. S., RODRIGUEZ-NIETO, S., ZAMYATNIN, A. A., VALINEVA, T., SAARIKETTU, J., FRILANDER, M. J., SUAREZ, M. F., ZAVIALOV, A., STAHL, U., HUSSEY, P. J., SILVENNIONEN, O., SUNDBERG, E., ZHIVOTOVSKY, B. & BOZHKO, P. V. 2009. Tudor staphylococcal nuclease is an evolutionarily conserved component of the programmed cell death degradome. *Nat Cell Biol*, 11, 1347-1354.
- SUZUKI, G., KAI, N., HIROSE, T., FUKUI, K., NISHIO, T., TAKAYAMA, S., ISOGAI, A., WATANABE, M. & HINATA, K. 1999. Genomic organization of the *S* locus:

- identification and characterization of genes in SLG/SRK region of S9 haplotype of *Brassica campestris* (syn. *rapa*). *Genetics*, 153, 391.
- SWANSON, R., EDLUND, A. F. & PREUSS, D. 2004. Species specificity in pollen-pistil interactions. *Annu. Rev. Genet.*, 38, 793-818.
- TAKAYAMA, S. & ISOGAI, A. 2005. Self-Incompatibility in Plants. *Annu. Rev. Plant Biol.*, 56, 467-489.
- TAKAYAMA, S., SHIBA, H., IWANO, M., SHIMOSATO, H., CHE, F. S., KAI, N., WATANABE, M., SUZUKI, G., HINATA, K. & ISOGAI, A. 2000. The pollen determinant of self-incompatibility in *Brassica campestris*. *Proc Natl Acad Sci USA*, 97, 1920-5.
- TAKAYAMA, S., SHIMOSATO, H., SHIBA, H., FUNATO, M., CHE, F. S., WATANABE, M., IWANO, M. & ISOGAI, A. 2001. Direct ligand-receptor complex interaction controls *Brassica* self-incompatibility. *Nature*, 413, 534-538.
- TANG, C. L., TOOMAJIAN, C., SHERMAN-BROYLES, S., PLAGNOL, V., GUO, Y. L., HU, T. T., CLARK, R. M., NASRALLAH, J. B., WEIGEL, D. & NORDBORG, M. 2007. The evolution of selfing in *Arabidopsis thaliana*. *Science*, 317, 1070-1072.
- TANG, W., KELLEY, D., EZCURRA, I., COTTER, R. & MCCORMICK, S. 2004. LeSTIG1, an extracellular binding partner for the pollen receptor kinase LePRK1 and LePRK2, promotes pollen tube growth *in vitro*. *The Plant Journal*, 39, 343-353.
- TANTIKANJANA, T., NASRALLAH, M. E. & NASRALLAH, J. B. 2010. Complex networks of self-incompatibility signaling in the Brassicaceae. *Current Opinion in Plant Biology*, 13, 520-6.
- TANTIKANJANA, T., RIZVI, N., NASRALLAH, M. E. & NASRALLAH, J. B. 2009. A dual role for the *S*-locus receptor kinase in self-incompatibility and pistil development revealed by an *Arabidopsis* *rd6* mutation. *Plant Cell*, 21, 2642-54.
- THOMAS, S. G. & FRANKLIN-TONG, V. E. 2004. Self-incompatibility triggers programmed cell death in *Papaver* pollen. *Nature*, 429, 305-309.
- THOMAS, S. G., HUANG, S., LI, S., STAIGER, C. J. & FRANKLIN-TONG, V. E. 2006. Actin depolymerization is sufficient to induce programmed cell death in self-incompatible pollen. *J Cell Biol*, 174, 221-9.
- THORSNESS, M. K., KANDASAMY, M. K., NASRALLAH, M. E. & NASRALLAH, J. B. 1993. Genetic Ablation of Floral Cells in *Arabidopsis*. *Plant Cell*, 5, 253-261.
- TRUJILLO, M., ICHIMURA, K., CASAIS, C. & SHIRASU, K. 2008. Negative regulation of PAMP-triggered immunity by an E3 ubiquitin ligase triplet in *Arabidopsis*. *Curr Biol*, 18, 1396-401.
- TRUJILLO, M. & SHIRASU, K. 2010. Ubiquitination in plant immunity. *Curr Opin Plant Biol*, 13, 402-8.
- TSUCHIMATSU, T., SUWABE, K., SHIMIZU-INATSUGI, R., ISOKAWA, S., PAVLIDIS, P., STÄDLER, T., SUZUKI, G., TAKAYAMA, S., WATANABE, M. & SHIMIZU, K. K. 2010. Evolution of self-compatibility in *Arabidopsis* by a mutation in the male specificity gene. *Nature*, 464, 1342-1346.
- TUSNÁDY, G. E. & SIMON, I. 2001. The HMMTOP transmembrane topology prediction server. *Bioinformatics*, 17, 849-50.
- UEGUCHI-TANAKA, M., ASHIKARI, M., NAKAJIMA, M., ITOH, H., KATOH, E., KOBAYASHI, M., CHOW, T.-Y., HSING, Y.-I. C., KITANO, H., YAMAGUCHI, I. & MATSUOKA, M. 2005. GIBBERELLIN INSENSITIVE DWARF1 encodes a soluble receptor for gibberellin. *Nature*.

- UPDEGRAFF, E. P., ZHAO, F. & PREUSS, D. 2009. The extracellular lipase EXL4 is required for efficient hydration of Arabidopsis pollen. *Sex Plant Reprod*, 22, 197-204.
- USHIJIMA, K., SASSA, H., DANDEKAR, A. M., GRADZIEL, T. M., TAO, R. & HIRANO, H. 2003. Structural and transcriptional analysis of the self-incompatibility locus of almond: identification of a pollen-expressed F-box gene with haplotype-specific polymorphism. *The Plant Cell*, 15, 771-781.
- VACCA, R. A., VALENTI, D., BOBBA, A., DE PINTO, M. C., MERAFINA, R. S., DE GARA, L., PASSARELLA, S. & MARRA, E. 2007. Proteasome function is required for activation of programmed cell death in heat shocked tobacco Bright-Yellow 2 cells. *FEBS Lett*, 581, 917-22.
- VALENTI, D., VACCA, R. A., GUARAGNELLA, N., PASSARELLA, S., MARRA, E. & GIANNATTASIO, S. 2008. A transient proteasome activation is needed for acetic acid-induced programmed cell death to occur in *Saccharomyces cerevisiae*. *FEMS Yeast Research*, 8, 400-4.
- VAN DEN BURG, H. A., TSITSIGIANNIS, D. I., ROWLAND, O., LO, J., RALLAPALLI, G., MACLEAN, D., TAKKEN, F. L. & JONES, J. D. 2008. The F-box protein ACRE189/ACIF1 regulates cell death and defense responses activated during pathogen recognition in tobacco and tomato. *The Plant Cell*, 20, 697-719.
- VAN DOORN, W. G., BEERS, E. P., DANGL, J. L., FRANKLIN-TONG, V. E., GALLOIS, P., HARA-NISHIMURA, I., JONES, A. M., KAWAI-YAMADA, M., LAM, E., MUNDY, J., MUR, L. A. J., PETERSEN, M., SMERTENKO, A., TALIANSKY, M., VAN BREUSEGEM, F., WOLPERT, T., WOLTERING, E., ZHIVOTOVSKY, B. & BOZHKO, P. V. 2011. Morphological classification of plant cell deaths. *Cell Death and Differentiation*, 18, 1241-1246.
- VAN DOORN, W. G. & WOLTERING, E. J. 2005. Many ways to exit? Cell death categories in plants. *Trends Plant Sci*, 10, 117-22.
- VANOOSTHUYSE, V., TICHTINSKY, G., DUMAS, C., GAUDE, T. & COCK, J. M. 2003. Interaction of calmodulin, a sorting nexin and kinase-associated protein phosphatase with the *Brassica oleracea* S locus receptor kinase. *Plant Physiol*, 133, 919-29.
- VERCAMMEN, D., VAN DE COTTE, B., DE JAEGER, G., EECKHOUT, D., CASTEELS, P., VANDEPOELE, K., VANDENBERGHE, I., VAN BEEUMEN, J., INZÉ, D. & VAN BREUSEGEM, F. 2004. Type II metacaspases Atmc4 and Atmc9 of *Arabidopsis thaliana* cleave substrates after arginine and lysine. *J Biol Chem*, 279, 45329-36.
- VERT, G., NEMHAUSER, J. L., GELDNER, N., HONG, F. & CHORY, J. 2005. Molecular mechanisms of steroid hormone signaling in plants. *Annu Rev Cell Dev Biol*, 21, 177-201.
- VIDALI, L., ROUNDS, C. M., HEPLER, P. K. & BEZANILLA, M. 2009. Lifeact-mEGFP reveals a dynamic apical F-actin network in tip growing plant cells. *PLoS One*, 4, e5744.
- VIERSTRA, R. D. 2003. The ubiquitin/26S proteasome pathway, the complex last chapter in the life of many plant proteins. *Trends Plant Sci*, 8, 135-42.
- VIERSTRA, R. D. 2009. The ubiquitin-26S proteasome system at the nexus of plant biology. *Nat Rev Mol Cell Biol*, 10, 385-97.

- VOGES, D., ZWICKL, P. & BAUMEISTER, W. 1999. The 26S proteasome: a molecular machine designed for controlled proteolysis. *Annual Review of Biochemistry*, 68, 1015-1068.
- VOLKMER, R., KRETZSCHMAR, I. & TAPIA, V. 2011. Mapping receptor-ligand interactions with synthetic peptide arrays: Exploring the structure and function of membrane receptors. *European Journal of Cell Biology* [Online]. Available: http://www.ncbi.nlm.nih.gov/entrez/query.fcgi?db=pubmed&cmd=Retrieve&dopt=AbstractPlus&list_uids=21561681.
- WALKER, E. A., RIDE, J. P., KURUP, S., FRANKLIN-TONG, V. E., LAWRENCE, M. J. & FRANKLIN, F. C. 1996. Molecular analysis of two functional homologues of the S3 allele of the *Papaver rhoeas* self-incompatibility gene isolated from different populations. *Plant Mol Biol*, 30, 983-994.
- WALKER, J. C. & ZHANG, R. 1990. Relationship of a putative receptor protein kinase from maize to the S-locus glycoproteins of *Brassica*. *Nature*, 345, 743-6.
- WANG, C.-L., WU, J., XU, G.-H., GAO, Y.-B., CHEN, G., WU, J.-Y., WU, H.-Q. & ZHANG, S.-L. 2010. S-RNase disrupts tip-localized reactive oxygen species and induces nuclear DNA degradation in incompatible pollen tubes of *Pyrus pyrifolia*. *Journal of Cell Science*, 123, 4301-4309.
- WANG, C.-L., XU, G.-H., JIANG, X.-T., CHEN, G., WU, J., WU, H.-Q. & ZHANG, S.-L. 2009a. S-RNase triggers mitochondrial alteration and DNA degradation in the incompatible pollen tube of *Pyrus pyrifolia* *in vitro*. *The Plant Journal* 57, 220-229.
- WANG, F., ZHU, D., HUANG, X., LI, S., GONG, Y., YAO, Q., FU, X., FAN, L.-M. & DENG, X. W. 2009b. Biochemical insights on degradation of Arabidopsis DELLA proteins gained from a cell-free assay system. *Plant Cell*, 21, 2378-90.
- WANG, X. 2004. Lipid signaling. *Curr Opin Plant Biol*, 7, 329-36.
- WATANABE, N. & LAM, E. 2011. *Arabidopsis* Metacaspase 2d Is a Positive Mediator of Cell Death Induced during Biotic and Abiotic Stresse. *Plant J*, 66, 969-982.
- WETERINGS, K., SCHRAUWEN, J., WULLEMS, G. & TWELL, D. 1995. Functional dissection of the promoter of the pollen-specific gene NTP303 reveals a novel pollen-specific, and conserved cis-regulatory element. *Plant J*, 8, 55-63.
- WHEELER, M. J. 2001. *An investigation into the molecular genetics and cytogenetics of self-incompatibility in Papaver Rhoeas L.*, PhD thesis, Univeristy of Birmingham.
- WHEELER, M. J., DE GRAAF, B. H. J., HADJIOSIF, N., PERRY, R. M., POULTER, N. S., OSMAN, K., VATOVEC, S., HARPER, A., FRANKLIN, F. C. H. & FRANKLIN-TONG, V. E. 2009. Identification of the pollen self-incompatibility determinant in *Papaver rhoeas*. *Nature*, 459, 992-5.
- WHEELER, M. J., VATOVEC, S. & FRANKLIN-TONG, V. E. 2010. The pollen S-determinant in *Papaver*: comparisons with known plant receptors and protein ligand partners. *J Exp Bot*, 61, 2015-2025.
- WILKINS, K. A., BANCROFT, J., BOSCH, M., INGS, J., SMIRNOFF, N. & FRANKLIN-TONG, V. E. 2011. Reactive oxygen species and nitric oxide mediate actin reorganization and programmed cell death in the self-incompatibility response of *Papaver*. *Plant Physiol*, 156, 404-16.
- WOLTERING, E. J. 2010. Death proteases: alive and kicking. *Trends in Plant Science*, 15, 185-188.
- WOLTERS-ARTS, M., VAN DER WEERD., L., VAN AELST, A. C., VAN AS, H. & MARIANI, C. 2002. Water-conducting properties of lipids during pollen hydration. *Plant, Cell and Environment*, 25, 513-519.

- WU, F.-H., SHEN, S.-C., LEE, L.-Y., LEE, S.-H., CHAN, M.-T. & LIN, C.-S. 2009. Tape-Arabidopsis Sandwich - a simpler Arabidopsis protoplast isolation method. *Plant Methods*, 5, 16-26.
- WU, J., WANG, S., GU, Y., ZHANG, S., PUBLICOVER, S. J. & FRANKLIN-TONG, V. E. 2011. Self-incompatibility in *Papaver rhoeas* activates nonspecific cation conductance permeable to Ca²⁺ and K⁺. *Plant Physiol*, 155, 963-73.
- YADAV, R. K., FULTON, L., BATOUX, M. & SCHNEITZ, K. 2008. The Arabidopsis receptor-like kinase STRUBBELIG mediates inter-cell-layer signaling during floral development. *Developmental Biology*, 323, 261-70.
- YAKUNIN, A. F. & HALLENBECK, P. C. 1998. A luminol/iodophenol chemiluminiscent detection system for western immunoblot. *Analytical Biochemistry*, 258, 146-149.
- YANG, C. W., GONZÁLEZ-LAMOTHE, R., EWAN, R. A., ROWLAND, O., YOSHIOKA, H., SHENTON, M., YE, H., O'DONNELL, E., JONES, J. D. G. & SADANANDOM, A. 2006. The E3 ubiquitin ligase activity of Arabidopsis PLANT U-BOX17 and its functional tobacco homolog ACRE276 are required for cell death and defense. *The Plant Cell* 18, 1084-1098.
- YANG, L., JI, W., ZHU, Y., GAO, P., LI, Y., CAI, H., BAI, X. & GUO, D. 2010. GsCBRLK, a calcium/calmodulin-binding receptor-like kinase, is a positive regulator of plant tolerance to salt and ABA stress. *Journal of Experimental Botany*, 61, 2519-33.
- YANG, S.-L., JIANG, L., PUAH, C. S., XIE, L.-F., ZHANG, X.-Q., CHEN, L.-Q., YANG, W.-C. & YE, D. 2005. Overexpression of TAPETUM DETERMINANT1 alters the cell fates in the Arabidopsis carpel and tapetum via genetic interaction with excess microsporocytes1/extra sporogenous cells. *Plant Physiology*, 139, 186-91.
- YANG, Z. 2008. Cell Polarity Signaling in Arabidopsis. *Cell and Developmental Biology*, 24, 551-575.
- YAO, C.-K., LIN, Y. Q., LY, C. V., OHYAMA, T., HAUETER, C. M., MOISEENKOVA-BELL, V. Y., WENSEL, T. G. & BELLEN, H. J. 2009. A synaptic vesicle-associated Ca²⁺ channel promotes endocytosis and couples exocytosis to endocytosis. *Cell*, 138, 947-60.
- YE, H., LI, L. & YIN, Y. 2011. Recent Advances in the Regulation of Brassinosteroid Signaling and Biosynthesis Pathways. *J Integr Plant Biol*, 53, 455-68.
- YEE, D. & GORING, D. R. 2009. The diversity of plant U-box E3 ubiquitin ligases: from upstream activators to downstream target substrates. *Journal of Experimental Botany*, 60, 1109-21.
- YOO, S.-D., CHO, Y.-H. & SHEEN, J. 2007. Arabidopsis mesophyll protoplasts: a versatile cell system for transient gene expression analysis. *Nat Protoc*, 2, 1565-1572.
- ZENG, W. & HE, S. Y. 2010. A prominent role of the flagellin receptor FLAGELLIN-SENSING2 in mediating stomatal response to Pseudomonas syringae pv tomato DC3000 in Arabidopsis. *Plant Physiol*, 153, 1188-98.
- ZHANG, S., SHI, Y., JIN, H., LIU, Z., ZHANG, L. & ZHANG, L. 2009. Covalent complexes of proteasome model with peptide aldehyde inhibitors MG132 and MG101: docking and molecular dynamics study. *J Mol Model*, 15, 1481-90.
- ZHANG, W., JEON, B. W. & ASSMANN, S. M. 2011. Heterotrimeric G-protein regulation of ROS signalling and calcium currents in Arabidopsis guard cells *J Exp Bot*, 62, 2371-9.
- ZHANG, Y. & XUE, Y. 2008. Molecular biology of S-RNase-based self-incompatibility. *Self-Incompatibility in Flowering Plants: Evolution, Diversity, and Mechanisms*.

- ZHAO, C., AVCI, U., GRANT, E. H., HAIGLER, C. H. & BEERS, E. P. 2008. XND1, a member of the NAC domain family in *Arabidopsis thaliana*, negatively regulates lignocellulose synthesis and programmed cell death in xylem. *The Plant Journal*, 53, 425-436.
- ZHAO, D.-Z., WANG, G.-F., SPEAL, B. & MA, H. 2002. The excess microsporocytes1 gene encodes a putative leucine-rich repeat receptor protein kinase that controls somatic and reproductive cell fates in the Arabidopsis anther. *Genes & Development*, 16, 2021-31.
- ZHAO, L., HUANG, J., ZHAO, Z., LI, Q., SIMS, T. L. & XUE, Y. 2010. The Skp1-like protein SSK1 is required for cross-pollen compatibility in S-RNase-based self-incompatibility. *The Plant Journal*, 62, 52-63.
- ZINKL, G. M., ZWIEBEL, B. I., GRIER, D. G. & PREUSS, D. 1999. Pollen-stigma adhesion in Arabidopsis: a species-specific interaction mediated by lipophilic molecules in the pollen exine. *Development*, 126, 5431-40.
- ZIPFEL, C., ROBATZEK, S., NAVARRO, L., OAKELEY, E. J., JONES, J. D. G., FELIX, G. & BOLLER, T. 2004. Bacterial disease resistance in Arabidopsis through flagellin perception. *Nature*, 428, 764-7.
- ZONIA, L. & MUNNIK, T. 2009. Uncovering hidden treasures in pollen tube growth mechanics. *Trends Plant Sci*, 14, 318-327.

APPENDIX I

Clustal W alignment of the PrpS₁, PrpS₃, PrpS₈ and Flower protein (CG6151). Identical amino acids are marked with “*”, conserved substitutions with “.” and semi-conserved substitutions with “.”. Underlined region of PrpS1 is the predicted extracellular domain; highlighted in yellow are the conserved amino acid residues, potentially involved in channel formation; highlighted in red are the glycines forming GxxxG motif also potentially involved in the channel formation. Clustal W source:

<http://www.ebi.ac.uk/Tools/clustalw2/index.html>

```
PrpS1      MPRSGSVVTLFQFVGGGLCTLLGVSVAIKAIFAQDYTLKDLIILIVLVALSIILGGPITLT 60
PrpS8      MPRHAIVVHVFQFLAGFVTLFGSALAIRTVISHPYTLQDLIIFILLFAIAVLVKGKYYITIT 60
PrpS3      MPRNRHAIYVFRFLAMFVTLFGVAFLVRKSHHALTWKDLTAFVVLIVLSVIGGGYVSLM 60
CG6151     -MSFAEKITGLLARPNQQDPIGPEQPWYLKYGSRLLGIVAAFFAILFGLWNVFS-IITLS 58
          :   :               :*                   : :*. : : . :::

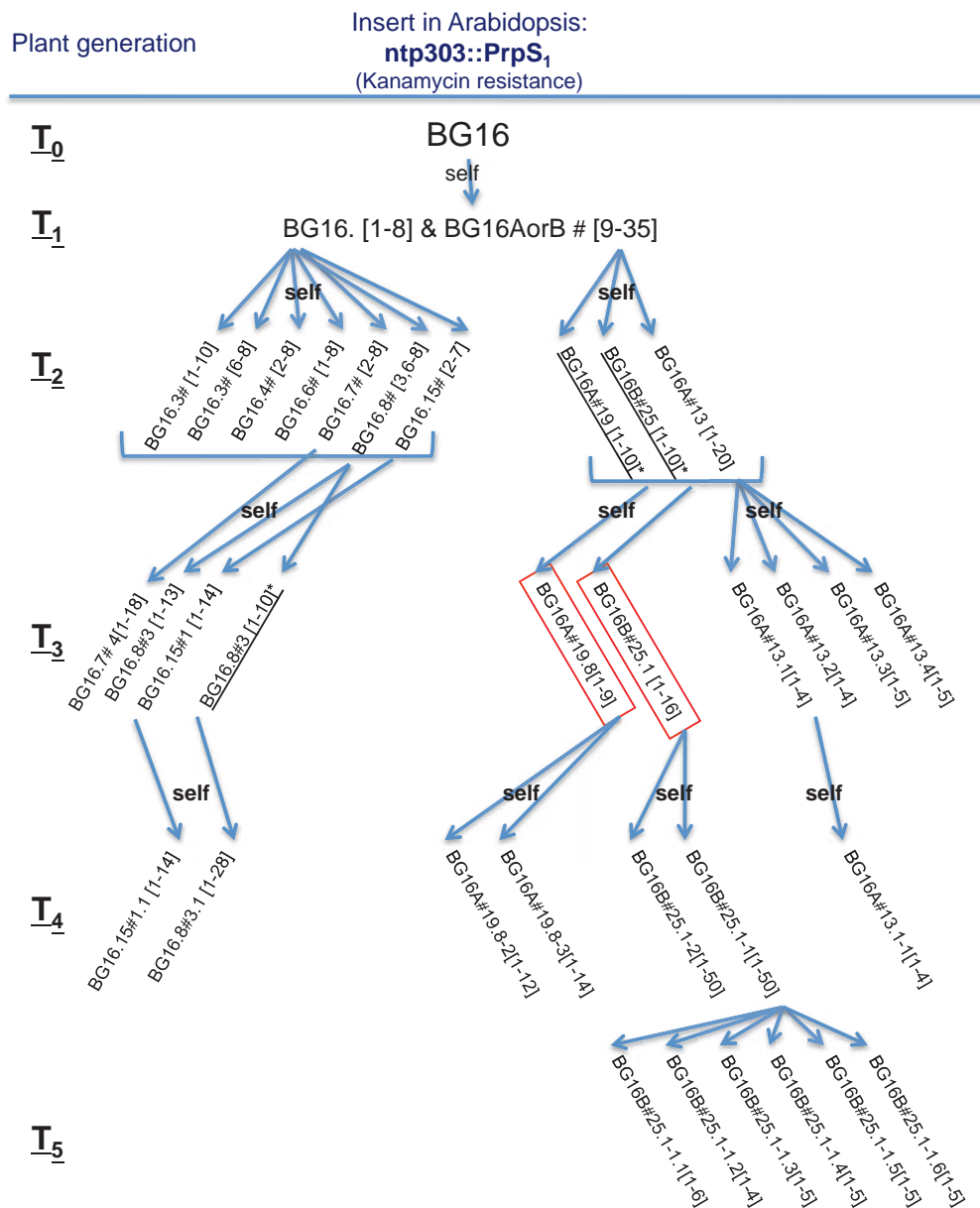
PrpS1      CVKLLGLVLHRLS-----FSEDQKVVVAFGTAAICDVLLVLPKNMLPMTIFSFLSSIMICV 115
PrpS8      YLKLLGWVLQHLT-----VTENQKVVVAFGTAVCDVFLVTTNMTFVTSICFLSSIMICV 115
PrpS3      YVQALRWLLQHLH-----VSENQKVVIAFGTTAICDVFLATHNMHATAALSFIALIMICV 115
CG6151     VSCLVAGILQMVAGFVVMLEAPCCFVCFGQVNEIAEKVESKPLYFRAGLYIAMAIPPII 118
          :  :*: :   . *   . : .** .   : . :   : : : *   :

PrpS1      VAVGWDCDR-SCMTEGFLVGFSGKLLLVYLIKQDFTFSLLCGSVLC LAVVAKFTEGKAEAT 174
PrpS8      VAAGWDRDR-SCMTECFLLICFGKLLLVNLIREDCTASVMYGSVLF LAIVAKFTE NAVGAT 174
PrpS3      VAIGWGRDR-SCMTEGFFVGFSGKLLLINLFSGNLPSALFTGIVLFLAVVAKLTECADEAT 174
CG6151     LCFGLASLFGSCLIFCTGVVYGMALG--KKASAEDMRAAAQQTFFGGNTPAQTNDRAGIV 176
          :. *      **: * : : * : *   .   .   . . . . * :

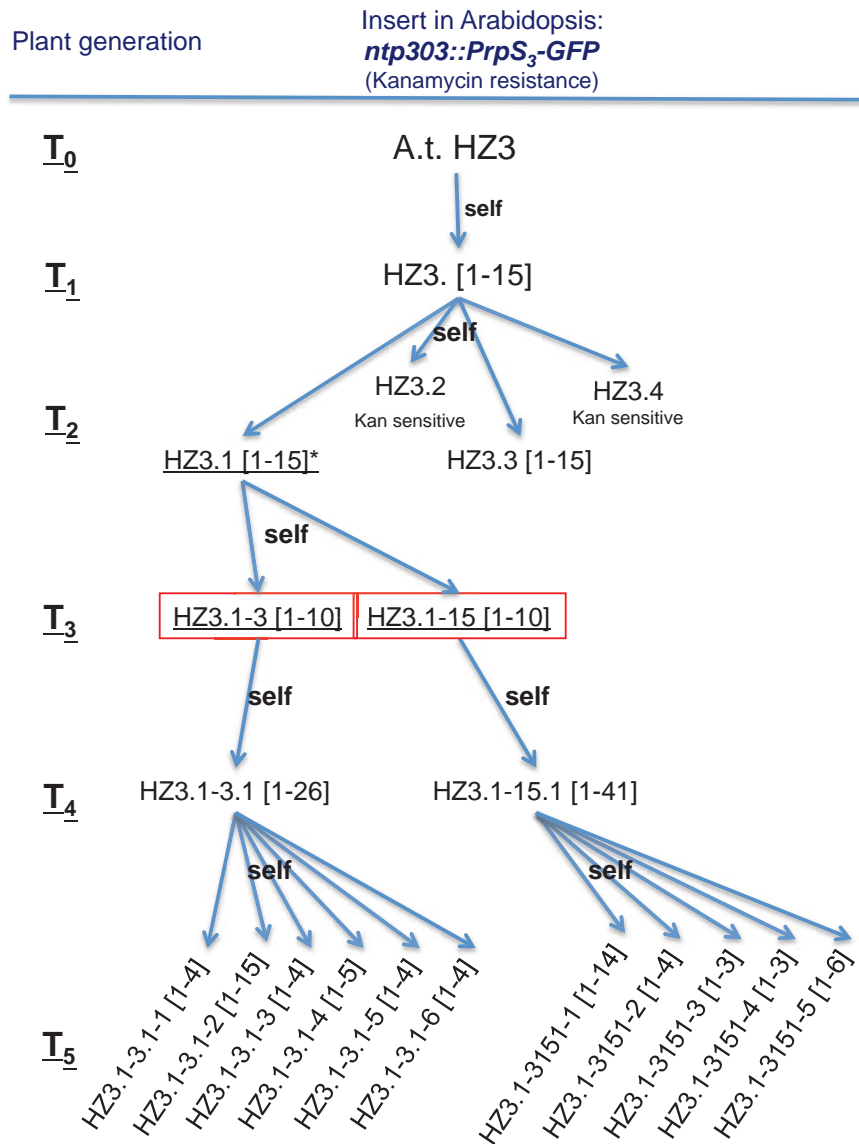
PrpS1      P-NPNLAGKADSPHLITQA 192
PrpS8      PLNPPIVGHEDSSHRSVEV 193
PrpS3      S-AARLVGNADSPCPNEA- 191
CG6151     N-NAQPPSFTGAVGTDSNV 194
          .   .   . :
```

APPENDIX II

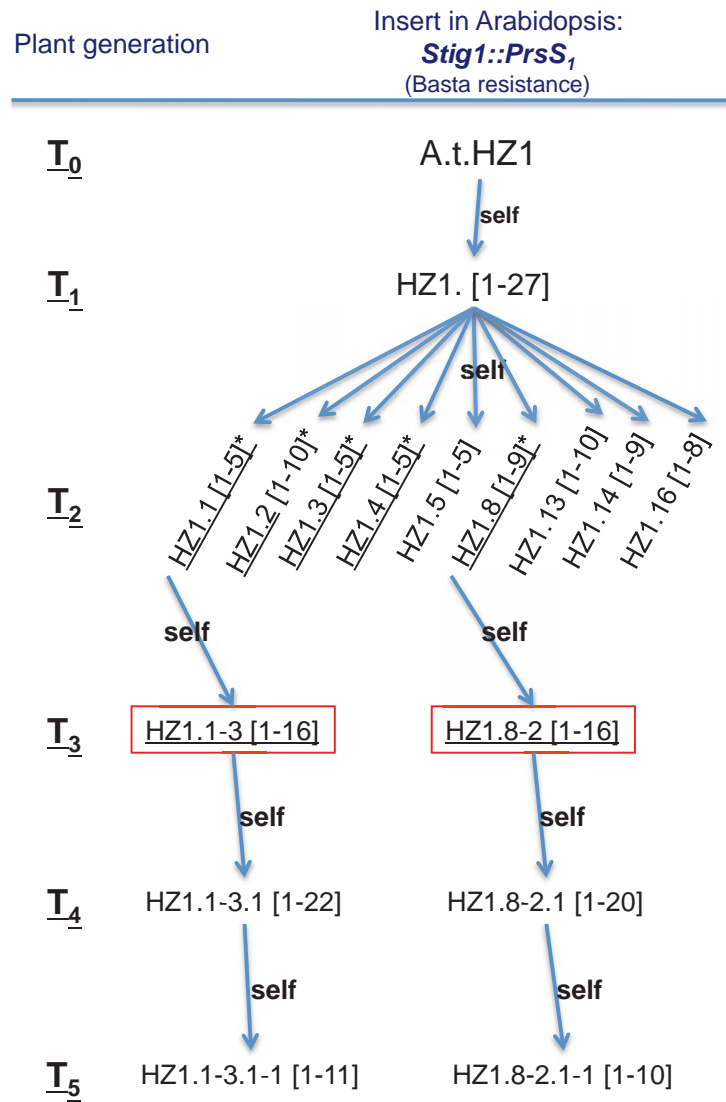
a) Family tree of the PrpS₁-GFP expressing *A.thaliana* line BG16. The underlined lines were analysed by RT-PCR and the lines outlined in red were identified as the highest expressing lines.



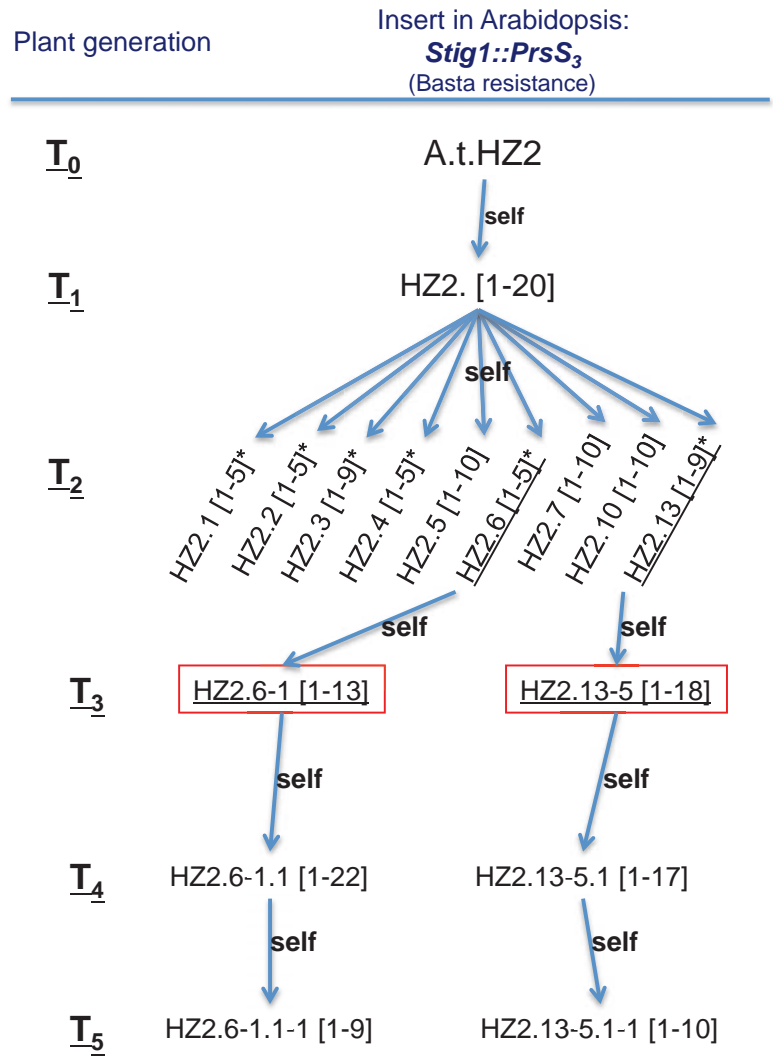
b) Family tree of the PrpS₃-GFP expressing *A.thaliana* line HZ3. The underlined lines were analysed by RT-PCR and the lines outlined in red were identified as the highest expressing lines.



c) Family tree of the PrsS₁ expressing *A.thaliana* line HZ1. The underlined lines were analysed by RT-PCR and the lines outlined in red were identified as the highest expressing lines.



d) Family tree of the PrsS₃ expressing *A.thaliana* line HZ2. The underlined lines were analysed by RT-PCR and the lines outlined in red were identified as the highest expressing lines.



APPENDIX III

Published papers

Poulter N. S., **Vatovec S.** and Franklin-Tong V. E. 2008. Microtubules are a target for self-incompatibility signaling in *Papaver* pollen. *Plant Physiol.*, 146: 1358-1367.

My contribution: Natalie Poulter carried out most of the studies. I carried out some of the experiments in collaboration doing my final year project for University of Ljubljana, Slovenia. I helped with caspase assays presented in the paper, tube length studies as well as western blot (**Figure 3**). I proof-read the manuscript.

Microtubules Are a Target for Self-Incompatibility Signaling in *Papaver* Pollen¹

Natalie S. Poulter, Sabina Vatovec, and Veronica E. Franklin-Tong*

School of Biosciences, University of Birmingham, Edgbaston, Birmingham B15 2TT, United Kingdom

Perception and integration of signals into responses is of crucial importance to cells. Both the actin and microtubule cytoskeleton are known to play a role in mediating diverse stimulus responses. Self-incompatibility (SI) is an important mechanism to prevent self-fertilization. SI in *Papaver rhoeas* triggers a Ca^{2+} -dependent signaling network to trigger programmed cell death (PCD), providing a neat way to inhibit and destroy incompatible pollen. We previously established that SI stimulates F-actin depolymerization and that altering actin dynamics can push pollen tubes into PCD. Very little is known about the role of microtubules in pollen tubes. Here, we investigated whether the pollen tube microtubule cytoskeleton is a target for the SI signals. We show that SI triggers very rapid apparent depolymerization of cortical microtubules, which, unlike actin, does not reorganize later. Actin depolymerization can trigger microtubule depolymerization but not vice versa. Moreover, although disruption of microtubule dynamics alone does not trigger PCD, alleviation of SI-induced PCD by taxol implicates a role for microtubule depolymerization in mediating PCD. Together, our data provide good evidence that SI signals target the microtubule cytoskeleton and suggest that signal integration between microfilaments and microtubules is required for triggering of PCD.

The plant cytoskeleton comprises actin microfilaments and tubulin microtubules that are highly dynamic through their interaction with various actin-binding proteins and microtubule-associated proteins (Erhardt and Shaw, 2006; Hussey et al., 2006). Both actin microfilaments and cortical microtubules play a key role in determining cell shape and growth, and recent work has provided valuable insights (Smith and Oppenheimer, 2005). There is now considerable evidence that the plant actin cytoskeleton plays a key role in modulating signal-response coupling, with many examples of actin mediating various biotic and abiotic responses (Staiger, 2000). Cortical microtubules are also involved in signal-response coupling. It has been shown that abiotic stimuli, such as gravity (Himmelspach et al., 1999), hormones (Shibaoka, 1994), freezing (Bartolo and Carter, 1991), and salt stress (Shoji et al., 2006), result in the reorientation or depolymerization of microtubules. Biotic interactions resulting in microtubule alterations also exist. Plant interactions with pathogenic fungi and symbiotic interactions with mycorrhizal fungi and rhizobia are known to stimulate microtubule reorganization (for review, see Wasteneys and Galway, 2003; Takemoto and Hardham, 2004).

Self-incompatibility (SI) is a genetically controlled system to prevent self-fertilization in flowering plants. A multi-allelic *S*-locus is responsible for specifying *S*-specific pollen rejection to allow discrimination between incompatible and compatible pollen. Interaction of pollen *S*- and pistil *S*-determinants that have matching alleles allows "self" (incompatible) pollen to be recognized and rejected, while compatible pollen is allowed to grow and set seed. In this way, SI provides an important mechanism to prevent inbreeding through specific recognition and rejection of incompatible pollen. Several different SI systems exist; they have quite distinct molecular and genetic control; thus, different mechanisms are involved in SI in different species (for review, see Takayama and Isogai, 2005; McClure and Franklin-Tong, 2006).

In *Papaver rhoeas*, the pistil part of the *S*-locus encodes small, approximately 15-kD proteins that act as signaling ligands named *S* proteins (Foote et al., 1994). Their interaction with incompatible pollen triggers *S*-specific increases of cytosolic-free calcium concentration ($[\text{Ca}^{2+}]_i$; Franklin-Tong et al., 1993). The SI-induced Ca^{2+} -dependent signaling network comprises several intracellular events in incompatible pollen, indicating quite complex networks of interconnected events involved in the SI response. Ca^{2+} -dependent phosphorylation of a cytosolic pollen soluble inorganic pyrophosphatase (sPPase), Pr-p26.1 (de Graaf et al., 2006), inhibits its sPPase activity. As sPPases are important enzymes for driving biosynthesis, they are crucial for cell growth, so SI, by targeting this enzyme, results in pollen tube inhibition. SI also triggers reorganization and depolymerization of the F-actin cytoskeleton (Geitmann et al., 2000; Snowman et al., 2002). As the actin cytoskeleton is required for pollen tube growth (Gibbon et al., 1999), this represents another

¹ This work was supported by the Biotechnology and Biological Sciences Research Council (to V.E.F.-T. and a studentship to N.S.P.). S.V. worked as an undergraduate project student from the University of Ljubljana, Slovenia.

* Corresponding author; e-mail v.e.franklin-tong@bham.ac.uk.

The author responsible for distribution of materials integral to the findings presented in this article in accordance with the policy described in the Instructions for Authors (www.plantphysiol.org) is: Veronica E. Franklin-Tong (v.e.franklin-tong@bham.ac.uk).

www.plantphysiol.org/cgi/doi/10.1104/pp.107.107052

mechanism to inhibit incompatible pollen tube growth. SI also triggers programmed cell death (PCD), involving several caspase-like activities (Thomas and Franklin-Tong, 2004; Bosch and Franklin-Tong, 2007). PCD is a conserved mechanism to get rid of unwanted cells and is used to sculpt tissues during development as well as in response to abiotic stress and pathogens (van Doorn and Woltering, 2005). SI activates PCD specifically in incompatible pollen, thereby preventing self-fertilization. Recent investigations revealed that alterations in actin dynamics can push pollen tubes into PCD (Thomas et al., 2006), and an SI-activated mitogen-activated protein kinase (Rudd et al., 1996) is implicated in signaling to PCD (Li et al., 2007). These data suggest that in *Papaver*, these components contribute to an integrated SI signaling network to achieve inhibition and death of incompatible pollen.

While the actin cytoskeleton is well established as being essential for tip growth in plant cells (Gibbon et al., 1999; Staiger, 2000), the role of the microtubule cytoskeleton is more variable, depending to some extent on the cell type. In some tip-growing plant cells, microtubule-disrupting drugs have no effect on tip growth; in others, they result in inhibition of growth, multiple growth initiation sites, or loss of directionality in root hairs (Bibikova et al., 1999) and pollen tubes (Anderhag et al., 2000; Gossot and Geitmann, 2007). However, it is well established that microtubules do not play an obvious role in regulating angiosperm pollen tube growth rate (Heslop-Harrison et al., 1988; Åström et al., 1995; Raudaskoski et al., 2001). Apart from data showing that they help organize the generative cell (GC) and vegetative nucleus (Raudaskoski et al., 2001; Laitinen et al., 2002), relatively little is known about their function (Cai and Cresti, 2006). As the actin cytoskeleton is known to play a role in SI, we speculatively explored a possible role for the microtubule cytoskeleton in SI-induced signaling. Here, we report that SI stimulates rapid and massive apparent microtubule depolymerization, demonstrating that the pollen microtubule cytoskeleton is an early target for SI signals. Our data implicate signal integration between the microfilament and microtubule cytoskeleton and suggest a role for microtubules in SI-induced PCD.

RESULTS

Microtubule Cytoskeleton Organization in Growing *Papaver* Pollen Tubes

The microtubule cytoskeleton organization in normally growing *P. rhoeas* pollen tubes, using immunolocalization and probing with α -tubulin (Fig. 1), has previously been described (Gossot and Geitmann, 2007). The microtubule arrangement is very similar to that described previously (Åström et al., 1995; Gossot and Geitmann, 2007). The tip region is relatively microtubule-free; behind this region are arrays of short, longitudinally organized microtubule bundles

(Fig. 1A). Further back, in the shank region, there are longer, more regularly organized longitudinal microtubule bundles (Fig. 1, A and B), which are mainly cortical (Fig. 1, B and C). Pollen tubes have a vegetative nucleus and a GC, which has a distinctive population of spindle-shaped GC microtubules (Fig. 1B).

SI Triggers Microtubule Depolymerization

To establish whether microtubules are a target for SI signaling, we examined the microtubule cytoskeleton using immunolocalization at various time points after incompatible SI induction (Fig. 2). Typical microtubule and microfilament organization was seen in control pollen tubes (Fig. 2, A and B). The microtubule cytoskeleton was rapidly altered after SI induction. As early as 1 min after SI, cortical microtubule bundles were virtually undetectable in incompatible pollen tubes; much weaker staining suggested that they had depolymerized (Fig. 2C). The GC spindle-shaped microtubules remained relatively intact at this time point (Fig. 2D). F-actin also dramatically reorganized by 1 min and accumulated in the tip, where it is not normally detected; many of the filament bundles had disappeared (Fig. 2E). At 3 min, the cortical microtubule bundles were virtually undetectable (Fig. 2F), and F-actin appeared disintegrated (Fig. 2G). At 30 min, cortical microtubules remained depolymerized (Fig. 2H), the GC spindle-shaped microtubules were still evident but disintegrating (Fig. 2I), and F-actin was aggregating (Fig. 2J). These data demonstrate that SI induces very rapid alterations to the cortical micro-

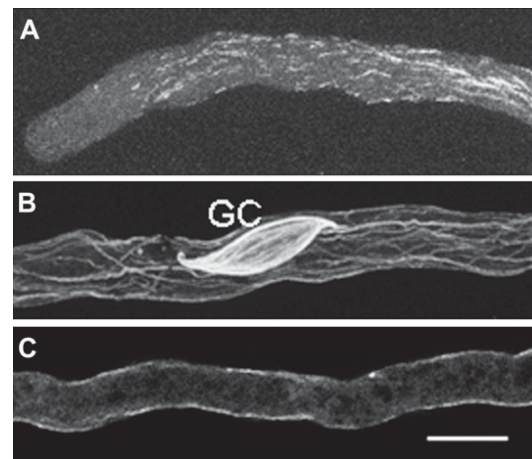


Figure 1. Microtubule organization in untreated *Papaver* pollen tubes. A, The apical region is relatively microtubule free; behind this is a region comprising shorter microtubule bundles, and behind this are longer arrays of cortical microtubule bundles. B, In the shank region, cortical microtubules are longitudinally arranged; the GC has a distinctive population of spindle-shaped microtubules. C, A single confocal optical section (0.5 μ m) shows that microtubules are primarily cortical. A and B, Full projections of confocal optical sections. Microtubules were detected using immunolocalization with anti- α -tubulin antibody clone B-5-1-2. Scale bar = 10 μ m.

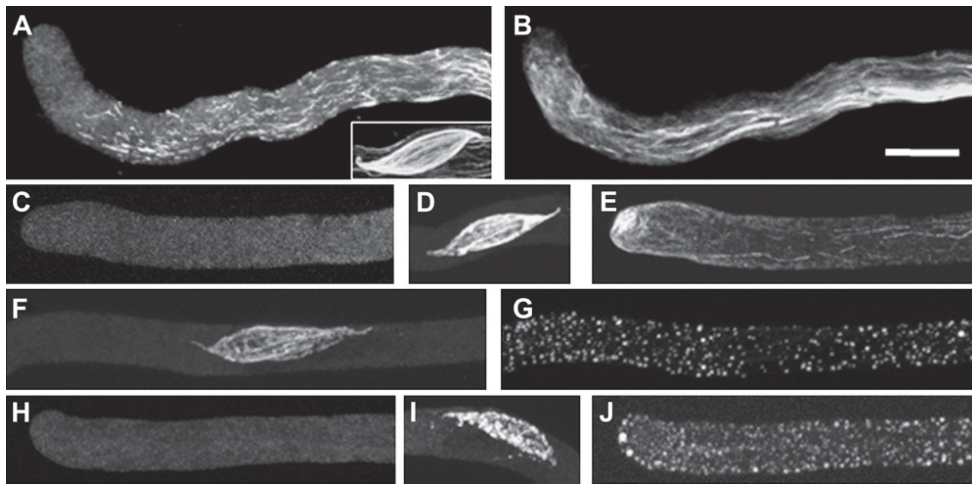


Figure 2. SI stimulates rapid apparent depolymerization of cortical microtubules coinciding with actin depolymerization. A, Cortical microtubules in an untreated pollen tube. Inset, GC microtubules. B, F-actin in an untreated pollen tube. C, At 1 min after SI induction, cortical microtubules are apparently virtually completely depolymerized. D, At 1 min after SI, GC microtubules are more or less intact. E, At 1 min after SI, F-actin is in the apical region; many F-actin bundles have disappeared. F, At 3 min after SI, cortical microtubules are undetectable; spindle-shaped microtubules show signs of disintegration. G, At 3 min after SI, F-actin has formed small punctate foci. H, At 30 min after SI induction, cortical microtubules are undetectable. I, At 30 min after SI induction, GC microtubules are further degraded. J, At 30 min after SI induction, F-actin comprises larger punctate foci. Microtubules were detected using immunolocalization with anti- α -tubulin; F-actin was colocalized using rhodamine-phalloidin. Images are full projections of confocal sections. Scale bar = 10 μ m.

bule cytoskeleton of incompatible pollen tubes, which appeared to be depolymerized. The spindle-shaped microtubules were much more stable and were still apparent at 60 min post-SI but were disintegrating. These comparisons between SI-induced microtubule and microfilament responses show that although both respond very rapidly, they are quite distinct responses.

Although the rapidity of the alterations to the microtubules argued against degradation of total tubulin and suggested tubulin depolymerization, we wished to establish whether this was the case. To address this question, we examined the overall levels of α -tubulin in SI-induced pollen tubes at various time points, using western blotting. The overall amount of α -tubulin in the pollen tubes remained virtually constant for at least 60 min after SI induction (Fig. 3), although cortical microtubules detected using immunolocalization disappeared within 1 min of SI induction. This strongly suggests that the SI-induced cortical microtubule disappearance is due to tubulin depolymerization rather than degradation.

Actin Depolymerization Results in Alterations to the Microtubule Cytoskeleton

Because SI stimulated rapid actin depolymerization (Snowman et al., 2002), we wondered whether this might be responsible for alterations to the microtubules. We used latrunculin B (LatB) to examine the effect of F-actin depolymerization on the pollen microtubule cytoskeleton. Pollen was treated with 1 μ M LatB for various time periods; we then imaged the effect of this treatment on both F-actin and microtu-

bule populations. These relatively high concentrations were employed, as we wished to mimic the SI effect of rapid, complete depolymerization within a couple of minutes as closely as possible (Thomas et al., 2006). Typical untreated control pollen tubes are shown in Figure 4, A to D. After 5 min treatment with 1 μ M LatB (Fig. 4, E–H), F-actin appeared fragmented, with a few short actin microfilament bundles remaining (Fig. 4, E and F). Although apical microtubule organization was altered by LatB treatment, the changes were not as observed for actin. Microtubules were present in the apical region and showed a distinctive random organization (Fig. 4G), but cortical microtubules in the shank appeared largely unaffected (Fig. 4H), as were the GC spindle-shaped microtubules (data not shown). Longer treatments with 1 μ M LatB (Fig. 4, I–L) resulted in depolymerized F-actin (Fig. 4, I and J) and loss of virtually all cortical microtubules in the apical region (Fig. 4K) and shank (Fig. 4L). These data show that actin depolymerization results in apparent depolymerization of cortical microtubules, confirming data from Gossot and Geitmann (2007). This provides evidence for signaling between these two cytoskeletal



Figure 3. SI does not trigger tubulin degradation. Western blot of extracts from untreated pollen tubes (UT) and extracts from SI-induced pollen tubes at 15, 30, and 60 min after SI, probed with anti- α -tubulin antibody clone B-5-1-2. Overall α -tubulin levels (equal loading of samples; arrowhead) did not significantly change.

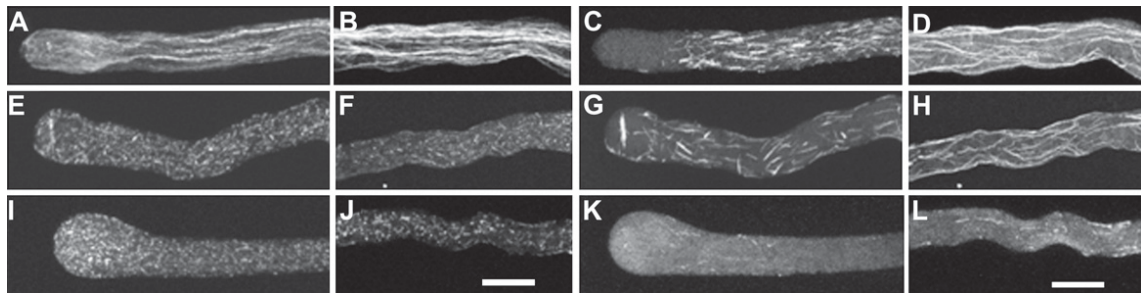


Figure 4. Actin depolymerization triggers changes in microtubule organization and apparent depolymerization. A to D, Typical untreated pollen tube cytoskeleton organization. A and B, F-actin; C and D, cortical microtubules. E to H, Pollen tubes treated with $1 \mu\text{M}$ LatB for 5 min. F-actin in the apical (E) and shank (F) region is fragmented. G and H, Cortical microtubules in the apical and mid-region are short and disorganized (G), while cortical microtubules in the shank region are relatively undisturbed (H). I to L, Pollen tubes treated with $1 \mu\text{M}$ LatB for 30 min. F-actin in the apical (I) and shank (J) region is extensively fragmented, indicating depolymerization. K, Microtubules in the apical and mid-region are virtually undetectable. L, Microtubules are virtually undetectable, with a few fragmented bundles remaining. Microtubules were detected using anti- α -tubulin; F-actin was colocalized using rhodamine-phalloidin. Images are full projections. Scale bars = $10 \mu\text{m}$.

components, though this does not necessarily involve direct interactions between actin and tubulin.

Actin Stabilization Prevents or Delays SI-Induced Microtubule Depolymerization

To investigate further whether actin depolymerization plays a role in the SI-induced apparent microtubule depolymerization, we stabilized F-actin using jasplakinolide (Jasp) and then induced SI. We reasoned that if actin depolymerization was important for microtubule depolymerization, stabilizing actin should prevent or delay this event. Untreated pollen tubes showed normal microtubule configurations (Fig. 5A); 30 min treatment with $0.5 \mu\text{M}$ Jasp, which causes bulbous tips due to actin stabilization/reorganization (Thomas et al., 2006), stimulated reorganization, but not depolymerization, of microtubules (Fig. 5B). After SI, microtubules were rapidly depolymerized by 1 to 3 min (see Fig. 2, C and F). Ten minutes after SI, microtubules were completely depolymerized (Fig. 5C), but with a pretreatment of $0.5 \mu\text{M}$ Jasp 30 min prior to SI induction, at 10 min post-SI significant remnants of microtubules remained (Fig. 5D). Thus, Jasp-mediated stabilization of F-actin alleviated or delayed SI-induced microtubule depolymerization, providing further evidence consistent with the notion that F-actin depolymerization signals to microtubule depolymerization during SI.

Microtubule Depolymerization Is Not Required for Actin Alterations

Because actin depolymerization results in microtubule depolymerization, this suggested cross talk between actin and tubulin. As the response was rapid, we wondered whether microtubules might signal to actin. We therefore examined the effect of microtubule depolymerization on the pollen tube actin cytoskeleton, using oryzalin to artificially depolymerize tubu-

lin. The relatively high concentrations used were to ensure that the SI effect of rapid depolymerization within a couple of minutes was mimicked as closely as possible. After 5 min treatment with $10 \mu\text{M}$ oryzalin, no cortical microtubules were evident (Fig. 6A); there was no detectable effect on the actin cytoskeleton (Fig. 6B). Even after 30 min treatment with oryzalin, when cortical microtubules were undetectable (Fig. 6C), F-actin organization appeared normal (Fig. 6D). To confirm that oryzalin did not affect actin, we measured pollen tubes, as actin depolymerization inhibits pollen tube growth (Gibbon et al., 1999). For pollen tubes treated with $10 \mu\text{M}$ oryzalin for 60 min, mean lengths were $293 \pm 10 \mu\text{m}$, compared with $314 \pm 11 \mu\text{m}$ for untreated controls ($n = 3$ independent experiments). These values were not significantly different from each other ($P = 0.156$, nonsignificant), establishing that oryzalin had no effect on actin. Our data demonstrate that microtubule depolymerization does not stimulate actin depolymerization in pollen tubes, confirming data from Gossot and Geitmann (2007). Because these high levels of oryzalin do not affect actin or growth, we can be reasonably sure that possible side-effects are not an issue. This suggests there is one-way cross talk from actin to tubulin cytoskeleton, but not vice versa.

We also investigated whether stabilizing microtubules with taxol might affect actin reorganization. Taxol inhibits microtubule dynamics, causing stabilization of microtubules (Blagosklonny and Fojo, 1999), and is effective in plant cells (Baskin et al., 1994; Collings et al., 1998). Taxol does not dramatically affect microtubule organization, but some bundling is generally observed (Collings et al., 1998). Taxol, as expected, did not stimulate any major alterations to the organization of either the microtubule (Fig. 7, A and B) or actin microfilament (Fig. 7, C and D) cytoskeleton of pollen tubes, but the microtubule bundles were slightly larger and brighter, suggesting stabilization. The concentrations of taxol used are in line with other studies (see, e.g. Collings et al., 1998). To confirm that

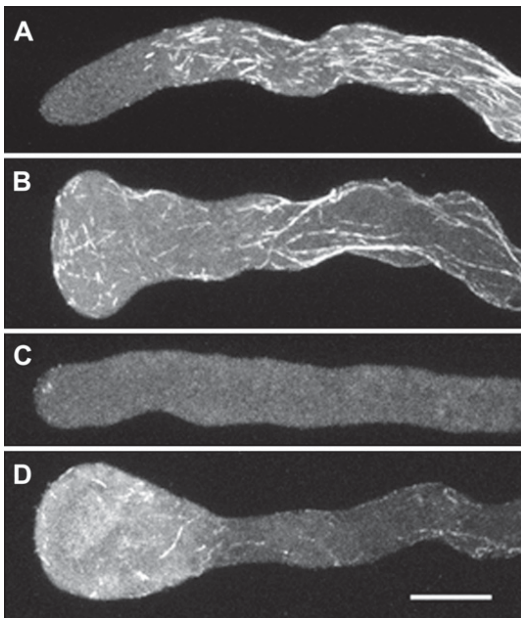


Figure 5. Actin stabilization by Jasp alleviates or delays SI-induced apparent microtubule depolymerization (A). Typical untreated pollen tube microtubule organization. B, Microtubule organization 30 min after Jasp treatment. C, Microtubules were completely depolymerized 10 min after SI. D, Microtubules were detectable after 30 min Jasp pretreatment followed by 10 min SI induction. Microtubules were detected with anti- α -tubulin. Images are full projections. Scale bar = 10 μ m.

taxol had no effect on the actin cytoskeleton, we measured pollen tubes after treatment with 5 and 10 μ M taxol for 1 h. The mean pollen tube lengths were $194.6 \pm 9.8 \mu$ m and $194.0 \pm 9.1 \mu$ m, respectively, compared to $190.0 \pm 8.1 \mu$ m for untreated controls ($n = 3$). Thus, taxol had no significant effect on pollen tube growth ($P = 0.717, 0.744$, respectively, nonsignificant), consistent with taxol not having an effect on the actin cytoskeleton. To investigate whether stabilizing microtubules affected the ability of actin to depolymerize, we pretreated pollen tubes with 5 μ M taxol for 30 min and then added 1 μ M LatB for 30 min (Fig. 7, E–H). Although the organization of the microtubules in the apical region was disturbed (which is expected, as LatB inhibits pollen tube growth), the shank microtubules appeared relatively normal (Fig. 7, E and F), but F-actin depolymerized as normal (Fig. 7, G and H). Thus, microtubule depolymerization, although it accompanies actin depolymerization, is not required for actin depolymerization in pollen tubes. This confirms our data suggesting one-way signaling from actin to tubulin cytoskeleton.

Disruption of Microtubule Dynamics Does Not Trigger PCD

We previously demonstrated that actin depolymerization or stabilization can trigger PCD in pollen tubes

(Thomas et al., 2006). Because SI also stimulated apparent microtubule depolymerization, we wondered whether microtubule depolymerization might also signal to PCD. We investigated this using oryzalin to depolymerize, or taxol to stabilize, pollen tube microtubules. Pollen tubes were treated with 10 μ M oryzalin or 5 μ M taxol and extracts tested for caspase-3-like activity using Ac-DEVD-AMC, a caspase-3 substrate, which we have used previously (Bosch and Franklin-Tong, 2007; Li et al., 2007). Untreated pollen tube extracts exhibited low DEVDase activity. The DEVDase activities in oryzalin- and taxol-treated pollen tube extracts were not significantly different from the untreated controls ($P = 0.9581$ and 0.6286 , respectively; $n = 4$). Thus, microtubule depolymerization or stabilization alone clearly does not trigger PCD in *Papaver* pollen.

SI-Induced PCD Requires Depolymerization of Microtubules to Progress

Although changes in microtubule dynamics alone are not sufficient to signal to PCD, we wondered whether tubulin depolymerization might be required in conjunction with actin depolymerization to allow progression into SI-induced PCD. As microtubule depolymerization accompanies actin depolymerization, this was an important point to establish. We investigated whether pollen tubes with stabilized microtubules prior to SI-induced actin depolymerization affected entry into PCD. Pollen tubes were pretreated with 5 μ M taxol, SI was induced, and extracts were

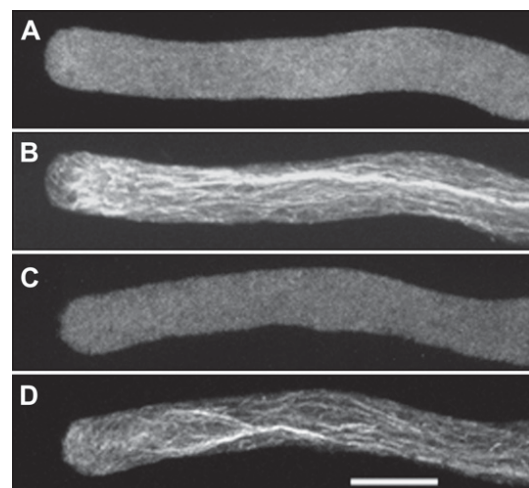


Figure 6. Microtubule depolymerization does not trigger alterations to the actin cytoskeleton. A and B, A 5-min treatment with 10 μ M oryzalin. A, Apparent complete depolymerization of cortical microtubules. B, No apparent effect on F-actin organization. C and D, A 30-min treatment with 10 μ M oryzalin. C, Cortical microtubules are apparently completely depolymerized. D, No apparent effect on F-actin organization. Microtubules were detected with anti- α -tubulin; F-actin was colocalized using rhodamine-phalloidin. Images are full projections. Scale bar = 10 μ m.

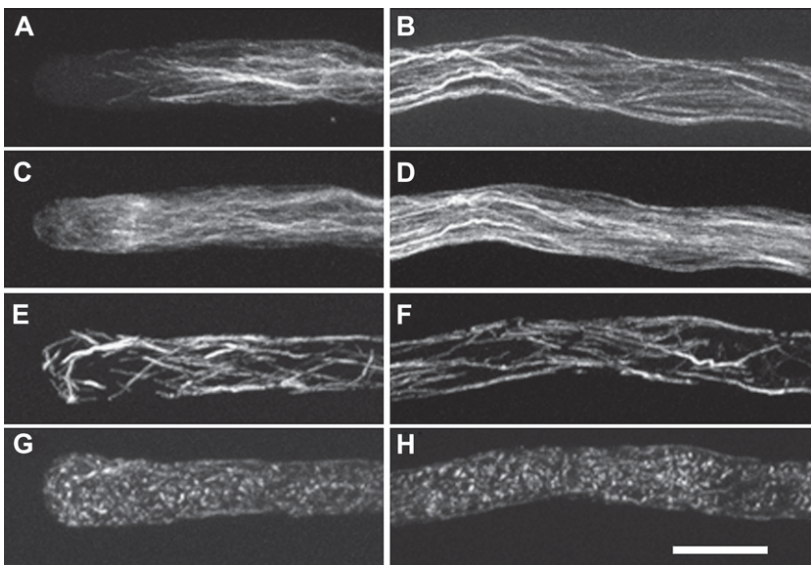


Figure 7. Microtubule depolymerization is not required for actin depolymerization. A to D, A 5- μM taxol treatment for 60 min. A and B, Cortical microtubule arrangement appears stabilized. C and D, F-actin organization was not significantly affected. E to H, Thirty-minute consecutive treatments of 5 μM taxol and 1 μM LatB. Microtubule organization in the tip was altered (E), but microtubules remained stabilized and intact (E and F). Actin microfilaments in the tip (G) and shank (H) were depolymerized. Microtubules were detected with anti- α -tubulin, F-actin with rhodamine-phalloidin. Images are confocal full optical projections. Scale bar = 10 μm .

assayed for DEVDase/caspase-3-like activity. Untreated pollen tube extracts exhibited low DEVDase activity, while SI induced high DEVDase activity (72.5% higher than untreated samples), which was significantly different from the controls ($P < 0.001$, ***, $n = 10$). In pollen tubes pretreated with taxol prior to SI induction, the level of DEVDase activity was significantly reduced; 41% lower compared to SI alone ($P = 0.0256$, *, $n = 10$). The reduction in DEVDase activity by taxol firmly implicates that microtubule depolymerization plays a role in mediating SI-induced PCD in addition to actin depolymerization. Moreover, when pollen tubes were pretreated with oryzalin for 30 min prior to SI induction, there was no significant difference in the DEVDase activity compared with SI-induced samples ($P = 0.7079$; $n = 5$). Together with the results from the taxol treatment, this is consistent with the idea that microtubule depolymerization is involved in SI-induced PCD, but suggests that an optimal threshold level of caspase activation is already achieved by SI-induced actin depolymerization.

In summary, our data provide good evidence that SI targets the microtubule cytoskeleton and implicate signal integration between microfilament and microtubule cytoskeleton. They reveal that SI-induced microtubule disruption is very different from that of actin. Altering microtubule dynamics did not stimulate F-actin depolymerization, suggesting one-way signaling from actin to microtubules. While actin microfilament depolymerization is sufficient to trigger PCD in pollen tubes via activation of a caspase-3-like/DEVDase activity, microtubule depolymerization alone is not. However, stabilization of microtubules reduced SI-induced caspase-like activity, suggesting that microtubule depolymerization, although on its own is insufficient to trigger PCD, is not just a consequence of SI signaling but is required for SI-induced PCD to progress.

DISCUSSION

Temporal Dynamics of the SI-Mediated Microtubule Alterations

Here, we show that in *Papaver*, although like other angiosperm pollen tubes, microtubules do not play an obvious role in regulating pollen tube growth rate (Heslop-Harrison et al., 1988; Raudaskoski et al., 2001), they are clearly responding to SI signals. Moreover, as our data demonstrate that the cortical microtubule cytoskeleton is a very early target for SI signals, it suggests that these alterations are not just a consequence of events but are likely to play a role in mediating SI. SI induces very rapid alterations to the cortical microtubule cytoskeleton, which are apparently depolymerized within approximately 1 min. Although both microtubule and microfilament SI-induced responses are very rapid, they are quite distinct responses. In contrast to F-actin, which also depolymerizes very rapidly, the microtubules remain depolymerized, while F-actin reorganizes and aggregates into punctate foci later.

One problem with fixation and such rapid responses is that it is difficult to establish exactly how rapid these changes to the cytoskeleton are and how they interrelate. Our data, and those of Gossot and Geitmann (2007) using LatB to artificially trigger actin depolymerization, show consequent apparent microtubule depolymerization, suggesting that SI-induced actin depolymerization triggers microtubule depolymerization. As stabilizing actin using Jasp prevents complete microtubule depolymerization, this further suggests a causal link. However, because of their rapidity, it is difficult to ascertain the order of these events definitively using fixation and immunolocalization. Live-cell imaging of microtubule- and microfilament-localized GFP fusion proteins would help establish the timing and nature of cytoskeletal organization and dynamics.

This would aid elucidation of the relationship between the actin and microtubule networks, especially during these early, rapid responses; we will address this in future studies.

Signal-Mediated Cortical Microtubule Reorganization/Depolymerization

Because cortical microtubules are intimately associated with the plasma membrane, where numerous receptors reside, they are implicated as targets of signaling networks (Gilroy and Trewavas, 2001; Wasteneys and Galway, 2003). Our data contribute to the evidence for this, demonstrating that the *Papaver* pollen tube microtubules are an early target of the SI-signaling network. Here, we have shown that a specific recombinant protein stimulus, involved in a biologically relevant phenomenon, has a very distinctive effect on pollen tube microtubules. The SI-induced apparent microtubule depolymerization response is extremely rapid and dramatic, far more so than any physiological response previously reported in a plant cell, to our knowledge.

Microtubule reorganization and/or apparent depolymerization occurs in response to specific abiotic stimuli (Bartolo and Carter, 1991; Himmelsbach et al., 1999; Shoji et al., 2006). Several examples of the microtubule cytoskeleton alterations in response to biotic stimuli, such as infection by pathogenic fungi or symbiotic interactions with mycorrhiza or rhizobia, exist (for review, see Takemoto and Hardham, 2004). These interactions generally involve reorganization and/or focusing of the microtubule cytoskeleton around the infecting organism. However, rapid apparent depolymerization of microtubules has also been reported, for example, in parsley (*Petroselinum crispum*)- and soybean (*Glycine max*)-*Phytophthora* interactions and in elicitor-treated tobacco (*Nicotiana tabacum*) cells (Gross et al., 1993; Binet et al., 2001; Cahill et al., 2002). Nod factor signaling also stimulates rapid localized apparent depolymerization of microtubules in root hairs and later increases in microtubule arrays (Timmers et al., 1999; Weerasinghe et al., 2003). Thus, biotic interactions involve specific alterations to the microtubule cytoskeleton (for review, see Takemoto and Hardham, 2004). Our data provide evidence for signaling to the microtubule cytoskeleton from another physiologically relevant system.

Microtubule Depolymerization Plays a Functional Role in SI-Mediated PCD

We previously showed that stabilizing F-actin using Jasp partially alleviates SI-induced PCD (Thomas et al., 2006) to about the same extent as taxol in this study. Although we did not know it at the time, actin depolymerization also stimulates microtubule depolymerization. Thus, our finding that stabilization of actin by Jasp also partially stabilizes microtubules implicates a role for microtubule depolymerization in mediating

PCD. We provide a simple model outlining our understanding of the cytoskeletal events triggered by SI in order to clarify the relationship between microfilaments and microtubules (Fig. 8). Although microtubules are rapidly depolymerized by SI induction, microtubule depolymerization alone does not trigger PCD in pollen tubes. This is in contrast to actin depolymerization, which plays a key role in initiating PCD in pollen (Thomas et al., 2006). Despite this, stabilization of microtubules using taxol alleviates SI-induced PCD, suggesting that microtubules play a role in mediating PCD. Microtubule depolymerization, which we and others (Gossot and Geitmann, 2007) have shown occurs as a consequence of actin depolymerization, is effectively reduced by taxol. As we show here that taxol does not inhibit pollen tube growth, SI-induced actin depolymerization should progress normally in the presence of taxol. Thus, normal levels of SI-induced caspase induction should be triggered in the presence of taxol if microtubules play no role and are depolymerized merely as a consequence of SI-induced actin depolymerization. However, as taxol alleviates PCD, this clearly demonstrates that preventing microtubule depolymerization is important for progression of PCD (Fig. 8). This strongly suggests that the microtubules are not just onlookers, but that they play a role in mediating caspase activation.

Microtubule reorganization triggered by pathogen infection hints at a possible microtubule involvement in PCD in plant cells. Our data are consistent with a model whereby microtubules, in concert with actin, somehow play a functional role in integrating signals involved in regulating PCD. However, a direct connection between microtubule reorganization and triggering of PCD remains to be elucidated.

Notably, the GC spindle-shaped microtubules were not dramatically affected by SI and remained relatively intact for a considerable time; these microtubules showed signs of disintegration but were still apparent at 60 min post-SI. This suggests that either the SI signals are specifically targeted to the cortical microtubules and/or that the GC-associated microtubule population is protected. Thus, it is the cortical microtubule population that is primarily affected and participates in this response. Interestingly, the GC appears to be a target for caspase-3-like/DEVDase activity 2 to 3 h after SI induction (Bosch and Franklin-Tong, 2007).

Evidence for Cross Talk between Actin and Tubulin

It is evident from our data that there is cross talk between microfilaments and microtubules in pollen tubes during SI. We have shown that SI triggers both actin depolymerization (Snowman et al., 2002) and apparent microtubule depolymerization. Moreover, depolymerizing actin with LatB triggers microtubule depolymerization, while depolymerizing microtubules with oryzalin has no effect on actin organization, as also previously shown by Gossot and Geitmann (2007). This suggests the actin depolymerization triggers microtu-

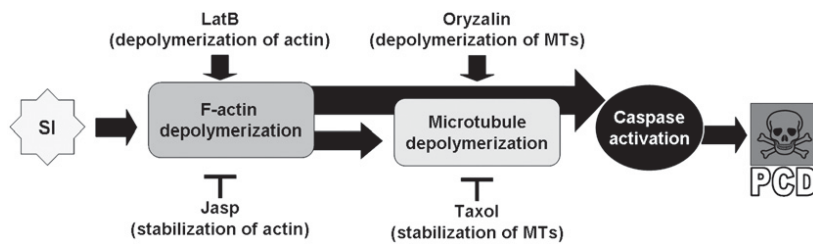


Figure 8. Model for integration of cytoskeletal events triggered by SI. SI triggers actin depolymerization, which is sufficient to trigger caspase activation and PCD (Thomas et al., 2006). LatB causes actin depolymerization, caspase activation, and PCD (Thomas et al., 2006). Treatment with Jasp after SI induction alleviated the extent of PCD (Thomas et al., 2006). Thus, partial prevention of actin depolymerization gives some protection from PCD. SI also triggers microtubule depolymerization (this study). Use of LatB showed that actin depolymerization also triggers microtubule depolymerization (Gossot and Geitmann, 2007; this study). This suggests that during SI, microtubule depolymerization is a consequence of actin depolymerization. Use of oryzalin showed that microtubule depolymerization on its own is not sufficient to trigger caspase activation and PCD (this study). This raises the question of whether microtubule depolymerization is actually required for PCD, or whether it is just a consequence of actin depolymerization. Use of taxol, which alleviated the extent of PCD, showed that preventing microtubule depolymerization is somehow involved in regulating PCD (this study). This implicates a functional role for both actin and tubulin in signaling to PCD.

bule depolymerization, but not vice versa, providing evidence for one-way signaling between these two cytoskeletal components in pollen tubes. As actin stabilization by Jasp delays or prevents microtubule depolymerization, this further suggests that actin influences microtubule polymerization status (Fig. 8).

Microtubules and actin microfilaments are often closely associated; in animal and yeast cells, there is no question that actin microfilament and microtubule cytoskeletons interact, and there is substantial evidence that this is also the case in plant cells. For example, transverse cortical microtubules and microfilaments in diffusely elongating cells can influence each other's organization (Collings and Allen, 2000). Drug-induced microtubule disassembly in Characean internodal cells (Foissner and Wasteneys, 2000) and root hairs (Tominaga et al., 1997) exacerbate the effects of actin-targeted drugs, suggesting that microtubule dynamics can influence actin dynamics. In fern cells (Kadota and Wada, 1992; Collings et al., 2006) and pollen tubes (Gossot and Geitmann, 2007), actin-depolymerizing drugs affect cortical microtubules. Thus, there is good evidence for signaling and interplay between microtubules and microfilaments, but the direction of the signaling varies. In SI, both actin depolymerization (Thomas et al., 2006) and microtubule depolymerization play a role in PCD, providing evidence for an integrated signaling network between these components.

Emerging data are beginning to provide some clues about how interactions between actin and tubulin are achieved. Identification of proteins bridging these interactions has confirmed functional interactions between microtubules and microfilaments in animals and fungi (for review, see Goode et al., 2000). In plants, proteins that interact with both microtubules and actin microfilaments are beginning to be identified (Igarashi et al., 2000; Preuss et al., 2004; Huang et al., 2007), providing the first firm evidence for how these two

dynamic cytoskeletal components are linked in plant cells. There is clearly much remaining to be explored in the future, and the SI-induced responses reported here appear to represent an excellent model system in which to examine interactions between microtubules and microfilaments.

MATERIALS AND METHODS

Pollen Treatments

Pollen of *Papaver rhoeas* was germinated and grown in vitro in liquid germination medium [0.01% H_3BO_3 , 0.01% KNO_3 , 0.01% $Mg(NO_3)_2 \cdot 6H_2O$, 0.036% $CaCl_2 \cdot 2H_2O$, and 13.5% Suc] as described previously (Snowman et al., 2002) at 25°C. Pollen was grown for 1 h before any treatments were applied.

For SI treatments, recombinant proteins were produced by cloning the nucleotide sequences specifying the mature peptide of the S_1 , S_3 , and S_8 alleles of the *S* gene (pPRS100, pPRS300, and pPRS800) into the expression vector pMS119 as described previously (Foote et al., 1994). Expression and purification of the proteins was performed as described by Kakeda et al. (1998). SI was induced by adding recombinant *S* proteins (final concentration $10 \mu g mL^{-1}$) to pollen that had been grown for 1 h in vitro (Snowman et al., 2002).

For the cytoskeleton drug treatments, $1 \mu M$ LatB, $0.5 \mu M$ Jasp (Calbiochem), 5 or $10 \mu M$ taxol, or $10 \mu M$ oryzalin (Sigma-Aldrich) was added to pollen tubes grown for 1 h. Controls comprised addition of dimethyl sulfoxide at a final concentration of 0.1% (v/v). For the drug-SI experiments, pollen tubes were subjected to a consecutive treatment of the relevant drug for 30 min, followed by the addition of incompatible *S* proteins for 5 h.

Immunolocalization

Pollen tubes were prefixed using the cross-linker 3-maleimidobenzoic acid *N*-hydroxysuccinimide ester (MBS; $400 \mu M$; Pierce) for 6 min at 20°C, followed by 2% formaldehyde (1 h, 4°C), as described by Thomas et al. (2006); we used 2% formaldehyde as a compromise. Actin preservation was indistinguishable from what we previously obtained using 4% formaldehyde following MBS (Geitmann et al., 2000). MBS has been reported to stop cytoplasmic streaming within seconds (Ketelaar and Emons, 2001). The treatment times indicated in the text are the time point after treatment that MBS was added. Cells were washed in actin-stabilizing buffer (100 mM PIPES, pH 6.8, 1 mM $MgCl_2$, 1 mM $CaCl_2$, 75 mM KCl) then in MES buffer (15 mM MES, pH 5.0), then incubated in 0.05% cellulose, 0.05% macerozyme in MES buffer containing 0.1 mM phenylmethylsulfonyl fluoride and 1% bovine serum albumin for 10 min. Washes in MES, then Tris-buffered saline (TBS), were followed by permeabilization in

0.1% Triton X-100/TBS for 10 min, and blocking in TBS/1% bovine serum albumin for 30 min.

Samples were incubated with anti- α -tubulin antibody (clone B-5-1-2; Sigma-Aldrich; 1:1,000 dilution) overnight at 4°C. They were washed in TBS, then incubated for 1.5 h at room temperature in anti-mouse fluorescein isothiocyanate antibody (1:300 dilution). Following TBS washes, rhodamine-phalloidin (66 nm) was added. Pollen tubes were mounted with 5 μ L of Vectashield (Vector Laboratories). Images were collected using a Bio-Rad Radiance 2000 laser-scanning system (50-mW argon laser, 488-nm line, and 1.5-mW HeNe laser, 543 nm) with a 60 \times plan-Apo 1.4 NA oil objective (Nikon). z-Series of 0.5- μ m optical slices were captured. Images were analyzed using ImageJ and archived as TIF files.

Protein Extraction and Western Blotting

SI was induced and pollen tubes collected by centrifugation in HEPES buffer (50 mM HEPES, pH 7.4, 10 mM NaCl, 0.1% CHAPS, 10 mM dithiothreitol, 1 mM EDTA, 10% glycerol) and samples snap-frozen in liquid N₂. Proteins were extracted by sonication (2 \times 10 s, 10 amps) and analyzed using SDS-PAGE and western blotting. Samples were measured using the Bio-Rad protein assay; equal amounts were loaded and checked by Ponceau staining of blots. Blots were probed with a 1:4,000 dilution of the monoclonal anti- α -tubulin antibody clone B-5-1-2 (Sigma-Aldrich), then probed with an anti-mouse alkaline phosphatase secondary antibody and detected using alkaline phosphatase.

Pollen Tube Length Measurements

Pollen tubes were grown for 1 h, then samples were treated as specified in the text, and pollen tubes fixed in 2% formaldehyde for 1 h, washed in TBS, and mounted on glass slides. Thus, before treatment, all mean pollen tube lengths were similar. Fixed pollen tubes were imaged using a Nikon Eclipse TE-300 microscope attached to a SenSys camera, using a Quips PathVysion image analysis system (Applied Imaging International). Final pollen tube lengths were measured (40 tubes for each of three independent treatments) using IPlab software. Lengths indicated are total lengths of the pollen tubes (i.e. 1 h pretreatment time plus treatment time with the relevant drug). Statistical analysis comprised a *t* test analysis.

Caspase Assays

PCD was assessed using a fluorogenic caspase-3/7-amino-4-trifluoromethyl coumarin substrate, Ac-DEVD-AMC, to measure caspase-like activity. Pollen tubes were subjected to treatments for 5 h and protein extracts made by grinding and sonicating pollen tubes in caspase extraction buffer (50 mM sodium acetate, 10 mM L-Cys, 10% [v/v] glycerol, and 0.1% [w/v] CHAPS, pH 6.0). Assays containing 10 μ g of protein extract at 1 μ g μ L⁻¹ and 50 μ M substrate were performed in caspase extraction buffer, pH 5.0. Release of fluorophore by cleavage was measured (excitation 380 nm, emission 460 nm) using a FLUOstar OPTIMA reader (BMG Labtechnologies) at 27°C for 5 h. Background relative fluorescent unit readings for control samples were subtracted from test samples. All assays were performed on at least four independent samples, each measured in duplicate. *P* values were calculated using a two-way ANOVA.

ACKNOWLEDGMENTS

We thank the horticultural staff for growing the plants and helping harvest material. Thanks to Tobias Baskin for helpful advice on tubulin antibodies, and to Harpal Pooni and Mike Kearsley for statistical advice.

Received August 8, 2007; accepted December 15, 2007; published January 11, 2008.

LITERATURE CITED

Anderhag P, Hepler PK, Lazzaro MD (2000) Microtubules and microfilaments are both responsible for pollen tube elongation in the conifer *Picea abies*. *Protoplasma* **214**: 141–157

- Åström H, Sorri O, Raudaskoski M (1995) Role of microtubules in the movement of the vegetative nucleus and generative cell in tobacco pollen tubes. *Sex Plant Reprod* **8**: 61–69
- Bartolo ME, Carter JV (1991) Microtubules in mesophyll cells of non-acclimated and cold-acclimated spinach: visualization and responses to freezing, low temperature, and dehydration. *Plant Physiol* **97**: 175–181
- Baskin TI, Wilson JE, Cork A, Williamson RE (1994) Morphology and microtubule organization in *Arabidopsis* roots exposed to oryzalin or taxol. *Plant Cell Physiol* **35**: 935–942
- Bibikova TN, Blancaflor EB, Gilroy S (1999) Microtubules regulate tip growth and orientation in root hairs of *Arabidopsis thaliana*. *Plant J* **17**: 657–665
- Binet MN, Humbert C, Lecourieux D, Vantard M, Pugin A (2001) Disruption of microtubular cytoskeleton induced by cryptogein, an elicitor of hypersensitive response in tobacco cells. *Plant Physiol* **125**: 564–572
- Blagosklonny MV, Fojo T (1999) Molecular effects of paclitaxel: myths and reality (a critical review). *Int J Cancer* **83**: 151–156
- Bosch M, Franklin-Tong VE (2007) Temporal and spatial activation of caspase-like enzymes induced by self-incompatibility in *Papaver* pollen. *Proc Natl Acad Sci USA* **104**: 18327–18332
- Cahill D, Rookes J, Michalczyk A, McDonald K, Drake A (2002) Microtubule dynamics in compatible and incompatible interactions of soybean hypocotyl cells with *Phytophthora sojae*. *Plant Pathol* **51**: 629–640
- Cai G, Cresti M (2006) The microtubule cytoskeleton in pollen tubes: structure and role in organelle trafficking. In R Malho, ed, *The Pollen Tube: A Cellular and Molecular Perspective*. Plant Cell Monographs. Springer, Berlin/Heidelberg, pp 157–175
- Collings D, Allen NS (2000) Cortical actin interacts with the plasma membrane and microtubules. In FB CJ Staiger, D Volkman, PW Barlow, eds, *Actin: A Dynamic Framework for Multiple Plant Cell Functions*. Kluwer Academic, Dordrecht, The Netherlands, pp 145–164
- Collings DA, Asada T, Allen NS, Shibaoka H (1998) Plasma membrane-associated actin in bright yellow 2 tobacco cells. Evidence for interaction with microtubules. *Plant Physiol* **118**: 917–928
- Collings DA, Lill AW, Himmelspach R, Wasteneys GO (2006) Hypersensitivity to cytoskeletal antagonists demonstrates microtubule-microfilament cross-talk in the control of root elongation in *Arabidopsis thaliana*. *New Phytol* **170**: 275–290
- de Graaf BHJ, Rudd JJ, Wheeler MJ, Perry RM, Bell EM, Osman K, Franklin FCH, Franklin-Tong VE (2006) Self-incompatibility in *Papaver* targets soluble inorganic pyrophosphatases in pollen. *Nature* **444**: 490–493
- Erhardt DW, Shaw SL (2006) Microtubule dynamics and organization in plant cortical array. *Annu Rev Plant Biol* **57**: 859–875
- Foissner I, Wasteneys GO (2000) Microtubule disassembly enhances reversible cytochalasin-dependent disruption of actin bundles in characean internodes. *Protoplasma* **214**: 33–44
- Foote HCC, Ride JP, Franklin-Tong VE, Walker EA, Lawrence MJ, Franklin FCH (1994) Cloning and expression of a distinctive class of self-incompatibility (S) gene from *Papaver rhoeas* L. *Proc Natl Acad Sci USA* **91**: 2265–2269
- Franklin-Tong VE, Ride JP, Read ND, Trewavas AJ, Franklin FCH (1993) The self-incompatibility response in *Papaver rhoeas* is mediated by cytosolic-free calcium. *Plant J* **4**: 163–177
- Geitmann A, Snowman BN, Emons AMC, Franklin-Tong VE (2000) Alterations in the actin cytoskeleton of pollen tubes are induced by the self-incompatibility reaction in *Papaver rhoeas*. *Plant Cell* **12**: 1239–1251
- Gibbon BC, Kovar DR, Staiger CJ (1999) Latrunculin B has different effects on pollen germination and tube growth. *Plant Cell* **11**: 2349–2363
- Gilroy S, Trewavas A (2001) Signal processing and transduction in plant cells: the end of the beginning? *Nat Rev Mol Cell Biol* **2**: 307–314
- Goode BL, Drubin DG, Barnes G (2000) Functional cooperation between the microtubule and actin cytoskeletons. *Curr Opin Cell Biol* **12**: 63–71
- Gossot O, Geitmann A (2007) Pollen tube growth: coping with mechanical obstacles involves the cytoskeleton. *Planta* **226**: 405–416
- Gross P, Julius C, Schmeltzer E, Hahlbrock K (1993) Translocation of cytoplasm and nucleus to fungal penetration sites is associated with depolymerisation of microtubules and defense gene activation in infected, cultured parsley cells. *EMBO J* **12**: 1735–1744
- Heslop-Harrison J, Heslop-Harrison Y, Cresti M, Tiezzi A, Moscatelli A (1988) Cytoskeletal elements, cell shaping and movement in the angiosperm pollen tube. *J Cell Sci* **91**: 49–60

- Himmelspach R, Wymer CL, Lloyd CW, Nick P (1999) Gravity-induced reorientation of cortical microtubules observed in vivo. *Plant J* **18**: 449–453
- Huang S, Jin L, Du J, Li H, Zhao Q, Ou G, Ao G, Yuan M (2007) SB401, a pollen-specific protein from *Solanum berthaultii*, binds to and bundles microtubules and F-actin. *Plant J* **51**: 406–418
- Hussey PJ, Ketelaar T, Deeks MJ (2006) Control of the actin cytoskeleton in plant cell growth. *Annu Rev Plant Biol* **57**: 109–125
- Igarashi H, Orii H, Mori H, Shimmen T, Sonobe S (2000) Isolation of a Novel 190 kDa Protein from tobacco BY-2 cells: possible involvement in the interaction between actin filaments and microtubules. *Plant Cell Physiol* **41**: 920–931
- Kadota A, Wada M (1992) The circular arrangement of cortical microtubule around the subapex of tip growing fern protonemata is sensitive to cytochalasin B. *Plant Cell Physiol* **33**: 99–102
- Kakeda K, Jordan ND, Conner A, Ride JP, Franklin-Tong VE, Franklin FCH (1998) Identification of residues in a hydrophilic loop of the *Papaver rhoeas* S protein that play a crucial role in recognition of incompatible pollen. *Plant Cell* **10**: 1723–1731
- Ketelaar T, Emons AMC (2001) The cytoskeleton in plant cell growth: lessons from root hairs. *New Phytol* **152**: 409–418
- Laitinen E, Nieminen KM, Vihinen H, Raudaskoski M (2002) Movement of generative cell and vegetative nucleus in tobacco pollen tubes is dependent on microtubule cytoskeleton but independent of the synthesis of callose plugs. *Sex Plant Reprod* **15**: 195–204
- Li S, Samaj J, Franklin-Tong VE (2007) A mitogen-activated protein kinase signals to programmed cell death induced by self-incompatibility in *Papaver* pollen. *Plant Physiol* **145**: 236–245
- McClure B, Franklin-Tong V (2006) Gametophytic self-incompatibility: understanding the cellular mechanisms involved in “self” pollen tube inhibition. *Planta* **224**: 233–245
- Preuss ML, Kovar DR, Lee YRJ, Staiger CJ, Delmer DP, Liu B (2004) A plant-specific kinesin binds to actin microfilaments and interacts with cortical microtubules in cotton fibers. *Plant Physiol* **136**: 3945–3955
- Raudaskoski M, Astrom H, Laitinen E (2001) Pollen tube cytoskeleton: structure and function. *J Plant Growth Regul* **20**: 113–130
- Rudd JJ, Franklin FCH, Lord JM, Franklin-Tong VE (1996) Increased phosphorylation of a 26-kD pollen protein is induced by the self-incompatibility response in *Papaver rhoeas*. *Plant Cell* **8**: 713–724
- Shibaoka H (1994) Plant hormone-induced changes in the orientation of cortical microtubules: alterations in the cross-linking between microtubules and the plasma membrane. *Annu Rev Plant Physiol Plant Mol Biol* **45**: 527–544
- Shoji T, Suzuki K, Abe T, Kaneko Y, Shi H, Zhu JK, Rus A, Hasegawa PM, Hashimoto T (2006) Salt stress affects cortical microtubule organization and helical growth in *Arabidopsis*. *Plant Cell Physiol* **47**: 1158–1168
- Smith LG, Oppenheimer DG (2005) Spatial control of cell expansion by the plant cytoskeleton. *Annu Rev Cell Dev Biol* **21**: 271–295
- Snowman BN, Kovar DR, Shevchenko G, Franklin-Tong VE, Staiger CJ (2002) Signal-mediated depolymerization of actin in pollen during the self-incompatibility response. *Plant Cell* **14**: 2613–2626
- Staiger CJ (2000) Signalling to the actin cytoskeleton in plants. *Annu Rev Plant Physiol Plant Mol Biol* **51**: 257–288
- Takayama S, Isogai A (2005) Self-incompatibility in plants. *Annu Rev Plant Biol* **56**: 467–489
- Takemoto D, Hardham AR (2004) The cytoskeleton as a regulator and target of biotic interactions in plants. *Plant Physiol* **136**: 3864–3876
- Thomas SG, Franklin-Tong VE (2004) Self-incompatibility triggers programmed cell death in *Papaver* pollen. *Nature* **429**: 305–309
- Thomas SG, Huang S, Li S, Staiger CJ, Franklin-Tong VE (2006) Actin depolymerization is sufficient to induce programmed cell death in self-incompatible pollen. *J Cell Biol* **174**: 221–229
- Timmers ACJ, Auriac MC, Truchet G (1999) Redefined analysis of early symbiotic steps of the *Rhizobium-Medicago* interaction in relationship with microtubule cytoskeleton rearrangements. *Development* **126**: 3617–3628
- Tominaga M, Morita K, Sonobe S, Yokota E, Shimmen T (1997) Microtubules regulate the organization of actin filaments at the cortical region in root hair cells of *Hydrocharis*. *Protoplasma* **199**: 83–92
- van Doorn WG, Woltering EJ (2005) Many ways to exit? Cell death categories in plants. *Trends Plant Sci* **10**: 117–122
- Wasteneys GO, Galway ME (2003) Remodelling the cytoskeleton for growth and form: an overview with some new views. *Annu Rev Plant Biol* **54**: 691–722
- Weerasinghe RR, Collings DA, Johannes E, Allen NS (2003) The distributional changes and role of microtubules in Nod factor challenged *Medicago sativa* root hairs. *Planta* **218**: 276–287

Wheeler M. J., De Graaf B. H. J., Hadjiosif N., Perry R. M., Poulter N. S., Osman K.,

Vatovec S., Harper A., Franklin F. C. H. and Franklin-Tong V. E. (2009)

Identification of the pollen self-incompatibility determinant in *Papaver rhoeas*.

Nature, 459: 992-995.

My contribution: I analysed the predicted transmembrane structure of the PrpS protein using various prediction programmes (**supplementary Figure 2**) and demonstrated, using western ligand-blotting, that a predicted extracellular domain interacts in an *S*-specific manner with the stigmatic PrsS protein (**Figure 2e**). I proof-read the manuscript.

Identification of the pollen self-incompatibility determinant in *Papaver rhoeas*

Michael J. Wheeler^{1*†}, Barend H. J. de Graaf^{1*†}, Natalie Hadjiosif^{1*}, Ruth M. Perry¹, Natalie S. Poulter¹, Kim Osman¹, Sabina Vatovec¹, Andrea Harper¹, F. Christopher H. Franklin¹ & Veronica E. Franklin-Tong¹

Higher plants produce seed through pollination, using specific interactions between pollen and pistil. Self-incompatibility is an important mechanism used in many species to prevent inbreeding; it is controlled by a multi-allelic *S* locus^{1,2}. ‘Self’ (incompatible) pollen is discriminated from ‘non-self’ (compatible) pollen by interaction of pollen and pistil *S* locus components, and is subsequently inhibited. In *Papaver rhoeas*, the pistil *S* locus product is a

the pollen component of the *S* locus on a cosmid clone comprising a 42-kilobase (kb) region at the *S*₁ locus.

Nucleotide sequencing and analysis identified a novel putative open reading frame (ORF) 457 base pairs (bp) from the *S*₁ pistil gene (Fig. 1a). Expression analysis using polymerase chain reaction with reverse transcription (RT-PCR) revealed that the ORF was specifically transcribed in pollen (Fig. 1b), appearing during anther

Bosch M., Poulter N. S., **Vatovec S.** and Franklin-Tong V. E. 2008. Initiation of programmed cell death in self-incompatibility: role for cytoskeleton modifications and several caspase-like activities. *Molecular Plant*, 1: 879-887.

My contribution: This paper was a review. Noni Franklin-Tong, Maurice Bosch and Natalie Poulter mainly wrote the manuscript. I proof-read the manuscript.

Initiation of Programmed Cell Death in Self-Incompatibility: Role for Cytoskeleton Modifications and Several Caspase-Like Activities

Maurice Bosch^{a,b}, Natalie S. Poulter^a, Sabina Vatovec^a and Veronica E. Franklin-Tong^{a,1}

^a School of Biosciences, University of Birmingham, Edgbaston, Birmingham. B15 2TT, UK

^b Present address: Institute of Biological, Environmental and Rural Sciences (IBERS), Aberystwyth University, Plas Gogerddan, Aberystwyth SY23 3EB, UK

ABSTRACT Programmed cell death (PCD) is an important and universal process regulating precise death of unwanted cells in eukaryotes. In plants, the existence of PCD has been firmly established for about a decade, and many components shown to be involved in apoptosis/PCD in mammalian systems are found in plant cells undergoing PCD. Here, we review work from our lab demonstrating the involvement of PCD in the self-incompatibility response in *Papaver rhoeas* pollen. This utilization of PCD as a consequence of a specific pollen–pistil interaction provides a very neat way to destroy unwanted ‘self’, but not ‘non-self’ pollen. We discuss recent data providing evidence for SI-induced activation of several caspase-like activities and suggest that an acidification of the cytosol may be a key turning point in the activation of caspase-like proteases executing PCD. We also review data showing the involvement of the actin and microtubule cytoskeletons as well as that of a MAPK in signalling to caspase-mediated PCD. Potential links between these various components in signalling to PCD are discussed. Together, this begins to build a picture of PCD in a single cell system, triggered by a receptor–ligand interaction.

Wheeler M. J., **Vatovec S.** and Franklin-Tong V. E. (2010) The pollen *S*-determinant in *Papaver*: comparisons with known plant receptors and protein ligand partners. *Journal of Experimental Botany*, 61: 2015-2025.

My contribution: This paper was a review containing some original data. I contributed original data demonstrating *S*-specific PrpS-PrsS binding using western ligand blotting (**Figure 3**). I also organized data into Figure 3 and wrote the figure legend. I did the proof-reading of the manuscript.

REVIEW PAPER

The pollen S-determinant in *Papaver*: comparisons with known plant receptors and protein ligand partners

Michael J. Wheeler[†], Sabina Vatovec and Veronica E. Franklin-Tong*

School of Biosciences, University of Birmingham, Edgbaston, Birmingham B15 2TT, UK

[†] Present address: Warwick HRI, Wellesbourne, Warwick CV35 9EF, UK.

* To whom correspondence should be addressed: E-mail: v.e.franklin-tong@bham.ac.uk

Received 5 November 2009; Revised 8 December 2009; Accepted 9 December 2009

Abstract

Cell–cell communication is vital to multicellular organisms and much of it is controlled by the interactions of secreted protein ligands (or other molecules) with cell surface receptors. In plants, receptor–ligand interactions are known to control phenomena as diverse as floral abscission, shoot apical meristem maintenance, wound response, and self-incompatibility (SI). SI, in which ‘self’ (incompatible) pollen is rejected, is a classic cell–cell recognition system. Genetic control of SI is maintained by an S-locus, in which male (pollen) and female (pistil) S-determinants are encoded. In *Papaver rhoeas*, PrsS proteins encoded by the pistil S-determinant interact with incompatible pollen to effect inhibition of pollen growth via a Ca²⁺-dependent signalling network, resulting in programmed cell death of ‘self’ pollen. Recent studies are described here that identified and characterized the pollen S-determinant of SI in *P. rhoeas*. Cloning of three alleles of a highly polymorphic pollen-expressed gene, PrpS, which is linked to pistil-expressed PrsS revealed that PrpS encodes a novel ~20 kDa transmembrane protein. Use of antisense oligodeoxynucleotides provided data showing that PrpS functions in SI and is the pollen S-determinant. Identification of PrpS represents a milestone in the SI field. The nature of PrpS suggests that it belongs to a novel class of ‘receptor’ proteins. This opens up new questions about plant ‘receptor’–ligand pairs, and PrpS-PrsS have been examined in the light of what is known about other receptors and their protein–ligand pairs in plants.

Key words: Cell–cell recognition, *Papaver rhoeas*, pollen S-determinant, pollen tube inhibition, PrpS, receptor, self-incompatibility, self-recognition.

De Graaf B.H.J. *, **Vatovec S.** *, Juárez-Díaz J.A. *, Zou H., Chai L., Kooblall K., Forbes T., Wilkins K.A., Franklin F.C.H. and Franklin-Tong V.E.

The *Papaver* self-incompatibility pollen *S*-determinant, PrpS, functions in *Arabidopsis thaliana*.

* - these authors contributed equally to this work

My contribution:

Barend de Graaf initiated the project, contributed the original idea for the manuscript, produced *A.thaliana* transgenic line expressing PrpS₁-GFP, carried out the experiments presented on Figure 1 and wrote the manuscript. Javier Juarez-Diaz helped me with the RT-PCR experiments (Figure 1 e), helped with preparation of samples for actin confocal imaging (Figure 3 a-j) and helped with the discussions for the manuscript. Huawen Zou produced *A.thaliana* transgenic line expressing PrpS₃-GFP. Katie Wilkins carried out imaging of pollen on the confocal microscope (Figure 3 a-j) and Lijun Chai prepared samples and analysed the actin cytoskeleton of the PrpS₃ expressing pollen (Figure 3 l). Kreepa Kooblall and Tom Forbes were the project students under my supervision. Kreepa Kooblall started the initial pollen tube inhibition studies on transgenic *A.thaliana* pollen expressing PrpS₁-GFP, while Tom Forbes started the initial actin cytoskeleton analysis in transgenic *A.thaliana* expressing PrpS₁-GFP. Chris Franklin contributed with counsel and discussions during the project. Noni Franklin-Tong managed the project, provided the guidance, wrote the paper and is the corresponding author.

I carried out the RT-PCR and segregation analysis of the transgenic *A.thaliana* lines (**Figure 1 e**), I carried out the experiment and statistical analysis of pollen tube inhibition of PrpS₁ and PrpS₃ expressing pollen (**Figure 2**) and pollen viability of PrpS₁ and PrpS₃ expressing

pollen (**Figure 4 a-e**). I produced samples for the confocal imaging of the actin cytoskeleton (**Figure 3 a-j**) and carried out the epifluorescence imaging, analysis and statistics of the actin cytoskeleton of the PrpS₁ expressing pollen (**Figure 3 k**). I proof-read the manuscript.

The *Papaver* Self-Incompatibility Pollen *S*-Determinant, *PrpS*, Functions in *Arabidopsis thaliana*

Barend H.J. de Graaf,^{1,2,5} Sabina Vatovec,^{1,5}
Javier Andrés Juárez-Díaz,^{1,5} Lijun Chai,¹ Kreepa Kooblall,^{1,3}
Katie A. Wilkins,¹ Huawen Zou,^{1,4} Thomas Forbes,¹
F. Christopher H. Franklin,^{1,6}
and Veronica E. Franklin-Tong^{1,6,*}

¹School of Biosciences, University of Birmingham, Edgbaston, Birmingham B15 2TT, UK

Summary

Many angiosperms use specific interactions between pollen and pistil proteins as “self” recognition and/or rejection mechanisms to prevent self-fertilization. Self-incompatibility (SI) is encoded by a multiallelic *S* locus, comprising pollen and pistil *S*-determinants [1, 2]. In *Papaver rhoeas*, cognate pistil and pollen *S*-determinants, PrpS, a pollen-expressed transmembrane protein, and PrsS, a pistil-expressed secreted protein [3, 4], interact to trigger a Ca²⁺-dependent signaling network [5–10], resulting in inhibition of pollen tube growth, cytoskeletal alterations [11–13], and programmed cell death (PCD) [14, 15] in incompatible pollen. We introduced the *PrpS* gene into *Arabidopsis thaliana*, a self-compatible model plant. Exposing transgenic *A. thaliana* pollen to recombinant *Papaver* PrsS protein triggered remarkably similar responses to those observed in incompatible *Papaver* pollen: *S*-specific inhibition and hallmark features of *Papaver* SI [11–15]. Our findings demonstrate that *Papaver PrpS* is functional in a species with no SI system that diverged ~140 million years ago [16]. This suggests that the *Papaver* SI system uses cellular targets that are, perhaps, common to all eudicots and that endogenous signaling components can be recruited to elicit a response that most likely never operated in this species. This will be of interest to biologists interested in the evolution of signaling networks in higher plants.

expression was observed (n = 300). Individual plants was analyzed, pollen s 100% for GFP-expression (n = 2,0 consistent with them being hemizy the insert; untransformed Col-0 pol centence (Figure 1C). PrpS-GFP locali plasma membrane in pollen tubes shown in *Papaver* pollen [4]. Expre transgenes in these lines was co transcripts were not detected in un (Figure 1E).

Expression of PrpS-GFP Is Sufficiently Induced *S*-Specific Inhibition of *A. thaliana*

To determine whether PrpS was functional in *A. thaliana*, we adapted the in vitro self-incompatibility assay used for *Papaver* SI [3]. Transgenic *A. thaliana* *AtPpS3* was grown in vitro and retested with PrsS proteins added. If PrpS functions in *A. thaliana*, the signaling network in *Arabidopsis*, PrpS-GFP should trigger *S*-specific pollen inhibition in *A. thaliana* pollen expressing PrpS-GFP. We tested whether this was the case (Figure 1G). Recombinant PrsS₁ did not affect pollen germination but reduced pollen germination of *A. thaliana* pollen by 42% (n = 300). When only pollen was assessed after addition of PrsS₁, no pollen germinated (Figures 1F and 1G, ***p < 0.001). The strong correlation of GFP expression and pollen inhibition demonstrates that PrsS₁ inhibits *A. thaliana* pollen germination by PrpS₁-GFP. This suggests that *Papaver PrpS* in *Arabidopsis* pollen is sufficient to inhibit pollen germination by PrsS₁. Using *Papaver* haplotype *S*₁*S*₈) confirmed that PrpS₁ is functional (Figure 1F). Addition of PrsS₁ partially reduced pollen germination (p = 0.022, n = 300), addition of both PrsS₁ and PrsS₈ resulted in complete inhibition (p = 0.009, n = 300).

We next tested lines *AtPpS1* and *AtPpS8* for PrpS-GFP expression for *S*-specific